

2017

Development of a conditionally-attenuated cytomegalovirus (CMV) vaccine vector platform, and initial investigations into use of CMV as a vaccine against pandemic influenza A virus

Hama Salih, Shirin

<http://hdl.handle.net/10026.1/9919>

<http://dx.doi.org/10.24382/701>

University of Plymouth

All content in PEARL is protected by copyright law. Author manuscripts are made available in accordance with publisher policies. Please cite only the published version using the details provided on the item record or document. In the absence of an open licence (e.g. Creative Commons), permissions for further reuse of content should be sought from the publisher or author.

Development of a conditionally-attenuated cytomegalovirus (CMV) vaccine vector platform, and initial investigations into use of CMV as a vaccine against pandemic influenza A virus

By

Shirin HamaSalih

A thesis submitted to Plymouth University
in fulfilment for the degree of

DOCTOR OF PHILOSOPHY

School of Biomedical and Healthcare Sciences
Peninsula Schools of Medicine and Dentistry

September 2017

Copyright Statement

This copy of the thesis has been supplied on condition that anyone who consults it is understood to recognise that its copyright rests with its author and that no quotation from the thesis and no information derived from it may be published without the author's prior consent.

Abstract

Cytomegalovirus (CMV)-based vectors are a promising vaccine platform with an ability to induce high levels of durable, immediate, effector memory T (T_{EM}) cell responses against their heterologous encoded pathogen target antigen. The primary focus of this thesis is centered on a hypothesis that targeting of essential CMV tegument proteins by using regulatable protein-destabilization is suitable as a conditional vaccine attenuation strategy. CMVs are generally benign, however in individuals whose immune systems are immature or weakened, CMV can be a significant pathogen causing substantial morbidity and mortality. Previous studies have shown that replication-defective versions of CMV made by conventional permanent deletion of essential genes are not compromised in terms of their immunogenicity. However, such non-conditional attenuation requires parallel development of complementing cell lines, which is technically difficult, expensive and not suitable for use in many situations and environments, in particular low and middle-income countries (LMICs). Recently, protein destabilizing domain (DD) technology has been developed that has the potential to be brought against this issue. DDs are conditionally unstable protein domains that can provide regulatable degradation of a desired protein by genetic fusion to the targeted protein. Addition of a small-molecule binding ligand stabilizes the DD, thereby increasing levels of the targeted protein in a rapid and dose-dependent manner. Using the murine CMV (MCMV) system, we hypothesized that fusion of a DD to essential tegument proteins of MCMV would be capable of regulating the stability of the tegument proteins resulting in generation of conditionally-attenuated MCMV vectors. Part one of this thesis details construction and *in vitro* characterization of recombinant MCMVs using this DD-based destabilization strategy, and identifies this approach as able to provide a means for production of CMV-based vaccines that differ in their levels of attenuation based on the specific tegument protein targeted.

The second part of the thesis is concerned with initial development of CMV as a vaccine vector against pandemic influenza A (IA) virus infection. IA virus is a respiratory pathogen that despite the availability of vaccines continues to have an enormous impact on population health and world economy. Standard seasonal (epidemic) IA vaccines provide only ‘homosubtypic’ immunity. The omnipresent potential for emergence of pandemic IA subtypes, for which the human population possesses no immunity, makes IA a major global health concern. The hypothesis being tested in these studies is that targeting of more conserved IA virus proteins with CD8⁺ T_{EM} cell-based immunity by using CMV-based vectors as a quintessential inducer of such ‘effector’ memory responses, will provide the desired heterotypic immunity capable of preventing pandemic IA. This initial study determined the capacity of a MCMV-based vaccine expressing the conserved IA proteins nucleoprotein (NP), polymerase (PA) and non-structural protein 2 (NS2) to induce immunity in mice as a strategy to prevent pandemic IA emergence.

DEDICATION

This thesis is dedicated to my Father`s soul, to my Mother, to my brothers and sisters, to my dearest Husband: Wuria and to my lovely kids: Dania and Ali for all their love, support and encouragement.

Acknowledgements

I would first of all like to thank my God, Allah, for getting me through all the difficulties. This thesis marks the end of my journey to obtain my PhD. Working for the Jarvis lab at the Plymouth University has been amazing learning experience. It gives me great opportunity and pleasure to express my heartfelt thanks to all those people who have contributed in so many different ways to the success of this PhD and made it unforgettable learning experience for me. First and foremost, I would like to thank Dr. Michael Jarvis, director of my study, for accepting me into his research lab despite my lack of experience in virology. I am deeply grateful for the opportunities he has given me. Michael taught me everything I know about managing lab work, scientific writing, oral presentation and scientific integrity. The successful completion of my thesis would not have been possible without his exceptional mentorship throughout the years. Thank you for your guidance, support, and for training me in your lab with your high standard scientific and technical expertise.

To my second supervisor Dr. John Moody: I cannot thank you enough for your support and guide, I could not have done this journey without you. You are one of the most generous, helpful and welcoming people I have ever met.

We gratefully acknowledge the Wandless lab for sharing destabilization domain protein and the University of Edinburgh and Rocky Mountain, Montana (United States of America) for performing animal studies.

I wish to express my deepest thankfulness to my beloved “Mum”, your prayer for me was what sustained me thus far. There was no one more instrumental in helping me through this journey than you. I am blessed to have you. You were, are and always will be a continuous source of unconditional love, tremendous support, encouragement and inspiration not only in my graduate study but in everyday life.

I would like to thank my husband “Dr. Wuria” you bore alone the responsibility for our family while I worked in the lab or in the office. Thank you for your love, patience, motivation and for always making sure that I am well fed and happy. Thank you for sharing this dream with me, I love you and this PhD is deservedly yours as it is mine.

I would also like to thank my kids “Dania & Ali” the angels of mine. Thanks for all of the hugs and kisses everyday as well as teaching me that time management is only a theory. I know PhD stole our special moments together, I apologise to you for working late hours, weekends and holidays during this journey. Please forgive me for ever having said “I am busy, I cannot listen now or I cannot read bed time story”. Thank you for being the smile, the hope and the greatest loves of my life. I wish to express my deepest thankfulness to my brothers and sisters and extended family in Kurdistan for their motivation and encouragement throughout my career.

I am also thankful to have met so many wonderful people along the way in which I have built great friend ships with. Thank you to my lab colleagues and office mate for providing coffee breaks, humour, supports, for listening and hugs when things were too stressful over the past few years. I would also like to express a warm gratitude for the wonderful staff in the Davy building for constantly being helpful, supportive and friendly in various ways, assisted me throughout my PhD journey. Thank you everyone, I will miss all of you guys. Last but not least I would like to express my sincere thanks to all the current and former members of the Jarvis lab for their support and encouragement specifically “Dr. Aisling” as she taught me most everything I know about molecular and virology technique. She provided me valuable suggestion and advice not just on experiments but on graduate school life in general. I cannot thank her enough.

List of Contents

Chapter One

Introduction

1.1 General background.....	28
1.1.1 Herpesviridae.....	28
1.1.2 Cytomegalovirus (CMV).....	30
1.1.2.1 Virion structure.....	31
1.1.2.1.1 Genome.....	31
1.1.2.1.2 Capsid.....	33
1.1.2.1.3 Envelope.....	34
1.1.2.1.4 Tegument.....	36
1.1.2.1.4.1 Lower matrix protein UL83 (pp65).....	37
1.1.2.1.4.2 The basic phosphoprotein UL32 (pp150).....	38
1.1.2.1.4.3 Upper matrix protein UL82 (pp71).....	41
1.1.2.1.4.4 The membrane-associated myristylated protein pp28 (UL99)	41
1.1.2.2 Virus life cycle.....	43
1.1.2.2.1 Viral entry.....	44
1.1.2.2.2 Viral gene expression.....	45
1.1.2.2.3 DNA replication.....	46
1.1.2.2.4 Virus assembly, maturation and egress.....	48
1.1.2.3 Pathogenesis of CMV.....	51
1.1.2.4 MCMV as a model for HCMV infection.....	53
1.2 CMV Mutagenesis.....	54
1.2.1 Generation of recombinant CMVs.....	54
1.2.1.1 Methods of mutagenesis prior to BAC-based technology.....	54
1.2.1.2 Methods of mutagenesis using bacterial artificial chromosome (BAC)-based technology.....	57
1.2.1.2.1 The BAC vector.....	58
1.2.1.2.2 BAC targeted mutagenesis by Red-mediated homologous recombination.....	62

1.2.2 Herpesviruses as a vaccine vector.....	63
1.2.2.1 Viral vectors.....	63
1.3 CMV Attenuation	67
1.3.1 CMVs as an attenuated vector platform.....	67
1.3.2 Conditional expression of essential genes and mutants of CMV.....	68
1.4 Influenza A Virus.....	73
1.4.1 Influenza and influenza viruses.....	73
1.4.2 IA virus virion structure.....	74
1.4.2.1 IA virus genome.....	75
1.4.2.2 IA virus classification.....	75
1.4.2.2.1 Hemagglutinin (HA).....	78
1.4.2.2.2 Neuraminidase (NA).....	78
1.4.2.2.3 Polymerase proteins.....	79
1.4.2.2.4 Matrix proteins (M1 and M2).....	80
1.4.2.2.5 Non-structural proteins	80
1.4.2.2.6 Nucleoprotein (NP)	82
1.4.3 Antigenic diversity of IA virus.....	83
1.4.3.1 Antigenic Drift.....	83
1.4.3.2 Antigenic Shift.....	85
1.4.4 IA virus pandemics.....	89
1.4.4.1 1918 ‘Spanish Influenza’ pandemic (H1N1).....	90
1.4.4.2 1957 ‘Asian Influenza’ pandemic (H2N2).....	91
1.4.4.3 1968 ‘Hong Kong’ pandemic (H3N2).....	91
1.4.4.4 1977 ‘Russian’ pandemic (H1N1) – re-emergence of a H1N1 strains.....	92
1.4.4.5 2009 pandemic (H1N1).....	92
1.4.5 Innate immune responses.....	94
1.4.5.1 Adaptive immune responses to IA virus infection.....	96
1.4.5.1.1 Antibody-mediated protection against IA infection.....	97
1.4.5.1.2 Cell-mediated protection against IA infection.....	98
1.4.5 Objectives of the thesis.....	104

Chapter Two

Materials and Methods	106
2.1 Maintenance of eukaryotic cell lines.....	106
2.1.1. Murine embryonic fibroblast (MEF) cell line	106
2.1.1.1 Sub-culturing of MEF cells.....	106
2.1.1.2. Storage of MEF cells	107
2.1.1.3 Reviving frozen cell stocks.....	107
2.1.2 Visual monitoring of cell monolayers.....	108
2.1.3 Cell quantitation.....	108
2.2 Bacteriology methods.....	109
2.2.1 Bacteria and plasmids.....	109
2.2.2 Culture and long-term storage of bacteria.....	110
2.2.3 Preparation of electrocompetent bacteria	111
2.2.4 Transformation of electrocompetent bacteria.....	111
2.3 Molecular Biology methods.....	113
2.3.1 Isolation and purification of nucleic acids.....	113
2.3.1.1 Isolation of plasmid DNA (Mini preps)	113
2.3.1.2. Isolation of BAC DNA from bacteria (BAC preps) using Alkaline Lysis.....	114
2.3.1.3 Isolation of viral DNA from virus stocks.....	115
2.3.2 Quantitation of DNA.....	115
2.3.3 Polymerase chain reaction (PCR).....	116
2.3.3.1 PCR primer design and preparation.....	116
2.3.3.2 Standard PCR.....	116
2.3.4 Restriction enzyme analysis of BAC DNA.....	120
2.3.5 Agarose gel electrophoresis	120
2.3.6. Agarose gel electrophoresis DNA purification.....	121
2.3.7 Spin-column DNA purification	122
2.3.8 Sequencing	122
2.4 Cloning.....	123

2.4.1 Preparation of insert and vector.....	123
2.4.2 Digestion of DNA with restriction enzymes.....	124
2.4.3 Ligation of DNA.....	124
2.4.4 Transformation of <i>E. coli</i> with DNA plasmids.....	124
2.5. Mutagenesis of MCMV BACs	125
2.5.1 Mutagenesis of MCMV BACs by using E/T homologous recombination.....	125
2.5.1.1 Preparation of DNA recombinant fragment for recombineering.....	126
2.5.1.2 Recombineering of the MCMV BAC Genome.....	128
2.5.1.3 Removal of the FRT-flanked selection marker.....	129
2.5.2 Mutagenesis of MCMV BAC plasmid using Galk recombination.....	130
2.5.2.1 Insertion of MCMV BAC into SW105 bacterial strain.....	131
2.5.2.2 Preparation of galK cassette.....	131
2.5.2.3 Electroporation of the galK cassette into electro-competent SW105 bacteria and positive selection.....	133
2.5.2.4 Electroporation of the DNA cassette into electrocompetent SW105 bacteria for reversion of galK followed by selection on DOG plates.....	134
2.6 Virology.....	134
2.6.1 Virology Methods.....	134
2.6.1.1 Reconstitution of viral progeny from recombinant MCMV BAC DNA in MEF cells.....	134
2.6.1.2 Reconstitution of viral progeny from recombinant MCMV BAC DNA in MEF cells in the presence of trimethoprim (TMP)	136
2.6.1.3 Removal of the BAC cassette from reconstituted MCMV.....	136
2.6.1.4 Preparation of virus seed stocks.....	137
2.6.1.5 Production of High Titre MCMV Virus Stocks.....	137
2.6.1.6 Titration of virus by TCID ₅₀ Limiting Dilution (median tissue culture infectious dose) assay.....	138
2.6.1.7 Virus titration using a plaque assay.....	138
2.6.1.8 Virus growth curve kinetics.....	139
2.7 Analysis of MCMV proteins.....	139
2.7.1 SDS-PAGE.....	139

2.7.2 Western blotting analysis.....	140
2.7.2.1 Transfer.....	141
2.7.2.2 Immunodetection.....	141
2.7.2.3 Membrane Stripping.....	141
2.8 Animal models and vaccination.....	142
2.8.1 T cell analysis by ICS.....	143
2.9 Statistics.....	145

Chapter Three

Development of a conditionally-attenuated cytomegalovirus (CMV) vaccine vector platform

3.1 Introduction.....	147
3.2 Results.....	150
3.2.1 Cloning of MCMV recombinants conditionally attenuated by genetic fusion of ecDHFR to genes encoding pp150 or pp28 tegument proteins.....	151
3.2.1.1 Cloning of ‘suicide’ plasmid containing ecDHFR for use as PCR template in construction of MCMV recombinants.....	154
3.2.1.1.1 Cloning of E134G and Y100I into pOriFRT(wt)-ecDHFR plasmid.....	159
3.2.1.1.1.1 Restriction digestion analysis of recombinant plasmid pOriFRT(wt)-E134G/Y100I.....	162
3.2.1.1.1.2 Sequence analysis of pOriFRT(wt)-ecDHFR(E134G) and (Y100I) template plasmids....	164
3.2.1.1.2 Cloning of F140P into pOriFRT(wt)-ecDHFR plasmid.....	167
3.2.1.1.2.1 Restriction digest analysis of recombinant pOriFRT(wt)-ecDHFR(F140P) plasmid	170
3.2.1.1.2.2 Sequencing analysis of pOriFRT(wt)-ecDHFR(F140P) template plasmid.....	171
3.2.2 Construction of recombinant MCMV BAC clones carrying the ecDHFR-tagged to essential tegument protein M32 (pp150) or M99 (pp28).....	173
3.2.2.1 Construction of conditionally replication-defective MCMV-pp150-E134G/Y100I vector by E/T homologous recombination.....	175
3.2.2.1.1 Generation of PCR fragments with flanking viral homologies to pp150 (N-terminus).....	176
3.2.2.1.2 Construction of recombinant MCMV-pp150 based vector using E/T- based linear recombination.....	180
3.2.2.1.3 Restriction digestion of mutant BAC DNA to ensure intact genome.....	182
3.2.2.1.4 Kan ^R cassette excision from recombinant MCMV-pp150-E134G/Y100I BACs.....	184

3.2.2.2 Construction of conditionally replication-defective MCMV-pp150/pp28-F140P vectors by Red E/T homologous recombination.....	185
3.2.2.2.1 Generation of PCR fragments with flanking viral homologies to pp150/pp28.....	186
3.2.2.2.2 Construction of recombinant MCMV-pp150/pp28 based vectors using E/T based linear recombination	190
3.2.2.2.3 Restriction digestion of mutant BAC DNA to ensure intact genome.....	191
3.2.2.2.4 Kan ^R cassette excision from recombinant MCMV-pp150/pp28-F140P BACs.....	194
3.2.3 Reconstitution of MCMV-pp150/pp28-F140P recombinant viruses.....	202
3.2.3.1 Preparation of seed stock from recombinant MCMV-pp150/pp28-F140P viruses in the presence of TMP.....	204
3.2.3.2 Preparation of concentrated virus stocks in the presence of TMP.....	204
3.2.3.3 Confirmation of the absence of MCMV-WT from recombinant MCMV-pp150/pp28-F140P.....	207
3.2.4 Characterisation of recombinant MCMV-pp150/pp28-F140P virus in vitro	211
3.2.4.1. Replication of MCMV-pp150/pp28-F140P at differing concentration of TMP.....	211
3.2.4.1.1 Confirmation that F140P fused to MCMV-pp150/pp28 at the different concentration of TMP.....	217
3.2.4.1.1.1 PCR analysis of recombinant MCMV-pp150/pp28-F140P vectors.....	217
3.2.4.1.1.2 Sequence confirmation of recombinant MCMV-pp150/pp28-F140P at a different concentration of TMP.....	219
3.2.4.2 Dynamics of pp150 or pp28 stability were analysed during infection.....	224
3.2.4.3 Characterisation of the recombinant MCMV-pp150/pp28-F140P viruses phenotypes.....	231
3.2.4.3.1 Mutant MCMV-pp150F140P has wild-type properties in MEF fibroblast cells in the presence of TMP, but shows intermediate attenuated growth in the absence of TMP.....	232
3.2.4.3.2 Recombinant MCMV-pp28-F140P growth properties in MEF fibroblast cells in the presence or absence of TMP.....	236
3.2.4.4 Recombinant MCMV-pp28-F140P that grew in the MEF cells in the absence of TMP could not cause secondary infection.....	243
3.3 Discussion.....	246

Chapter Four

CD8⁺ T cell targeting of conserved IA virus structural proteins using CMV-based vectors to elicits homo and heterosubtypic immunity

4.1 Introduction.....	260
4.2 Results.....	261
4.2.1 Cloning of MCMV-IA-based vectors.....	261
4.2.1.1 PCR fragments with flanking viral homologies to IE2 were generated.....	263
4.2.1.2 Construction of recombinant MCMV-IA (NP, PA and NS2) based vector using E/T-based linear recombination.....	265
4.2.1.3 Restriction digestion analysis of recombinant BAC DNA.....	267
4.2.1.4 Excision of the Kan ^R cassette from recombinant MCMV-IA (NP, PA and NS2) BAC DNA.....	269
4.2.1.5 Reconstitution of recombinant MCMV-IA (NP, PA, and NS2) virus.....	277
4.2.1.6 Removal of BAC cassette from recombinant MCMV-IA viruses.....	278
4.2.1.7 Preparation of recombinant MCMV-IA virus seed stocks.....	279
4.2.1.8 Preparation of concentrated virus stocks from seed stock	279
4.2.1.9 Recombinant MCMV-IA viruses show comparable replication to MCMV-WT virus.....	285
4.2.2 Induction of CD8 ⁺ T cell responses using recombinant MCMV-IA virus vectors.....	288
4.2.3 Construction of recombinant MCMV-IA-NP within a different MCMV-WT background MCMV-WT (F5).....	299
4.2.3.1 Expression of IE2 protein in the recombinant MCMV-IA vectors.....	311
4.3 Discussion.....	314

Chapter Five

Conclusions And Future Direction

5.1 Development of a conditionally-attenuated CMV vaccine vector platform.....	324
5.2 An initial investigation into use of MCMV as a vaccine against pandemic IA virus.....	327

LIST OF FIGURES

Chapter One

Figure 1.1 Structure of CMV virion.....	30
Figure 1.2 Schematic of CMV genome organization.....	33
Figure 1.3 Function of the tegument proteins (pp150 and pp28).....	40
Figure 1.4 Schematic diagram of HCMV pp28.....	43
Figure 1.5 CMV life cycle	50
Figure 1.6 A general method of destabilization domain strategy.....	70
Figure 1.7. Schematic showing the structure of the IA virion.....	75
Figure 1.8 EM of purified IA virions.....	75
Figure 1.9 Schematic of antigenic drift.....	84
Figure 1.10 Schematic diagram of antigenic shift.....	87
Figure 1.11 Pigs act as a mixing vessel for IA viruses.....	88

Chapter Two

Figure 2.1 Schematic of E/T (Red) homologous recombination	127
Figure 2.2 Schematic representation of the galK recombination.....	132
Figure 2.3 Schematic showing MCMV/IA vaccinated mouse groups.....	143

Chapter Three

Figure 3.1 Schematic showing the DD strategy.....	152
Figure 3.2 A flow-chart showing cloning ecDHFR into the pOriFRT(wt) vector.....	153
Figure 3.3 A flow-chart of construction of the recombinant MCMV vector vaccine.....	155
Figure 3.4 Schematic illustrating cloning of ecDHFR (E134G) domain to the pOriFRT(wt) vector.....	156
Figure 3.5 Schematic illustrating cloning of ecDHFR (Y100I) domain to the pOriFRT(wt) vector.....	158
Figure 3.6 DNA gel showing PCR amplification of ecDHFR.....	160
Figure 3.7 Gel electrophoresis showing SacI and XmaI digestion of PCR product and pOriFRT(wt).....	161
Figure 3.8 Restriction enzyme screening of pOriFRT(wt)-ecDHFR(E134G) clones.....	163

Figure 3.9 Restriction enzyme screening of pOriFRT(wt)-ecDHFR(Y100I) clones.....	163
Figure 3.10 Confirmation of ecDHFR (E13G) cloned into the pOriFRT(wt) plasmid via Sanger sequencing.....	165
Figure 3.11 Confirmation of ecDHFR (Y100I) cloned into the pOriFRT(wt) plasmid via Sanger sequencing.....	166
Figure 3.12 Schematic illustrating cloning of ecDHFR (F140P) domain to the pOriFRT(wt) vector.....	168
Figure 3.13 DNA gel showing PCR amplification of ecDHFR (F140P) domain from AcGFP-DHFR-F140P.....	169
Figure 3.14 Gel electrophoresis showing SacI and XmaI digestion of PCR product and pOriFRT(wt) plasmid during cloning of pOriFRT(wt)-ecDHFR (F140P).....	170
Figure 3.15 Restriction enzyme screening of pOriFRT(wt)-ecDHFR(F140P) clones.....	171
Figure 3.16 Confirmation of ecDHFR (F140P) cloned into the pOriFRT(wt) plasmid	172
Figure 3.17 Schematic illustration of the conditionally replication-defective MCMV vaccine	174
Figure 3.18 Schematic illustrations of the conditionally replication-defective MCMV-PP150-E134G/Y100I vectors using DD strategy.....	176
Figure 3.19 Recombinogenic PCR fragments used for construction of the recombinant MCMV-pp150-E134G	178
Figure 3.20 Recombinogenic PCR fragments used for construction of the recombinant MCMV-pp150-Y100I.....	179
Figure 3.21 Schematic illustrating the construction of MCMV-pp150-ecDHFR (E134G/Y100I).....	181
Figure 3.22 Characterization of the recombinant MCMV-pp150-E134G/Y100I BAC genome using EcoRI.....	183
Figure 3.23 Schematic illustration of the conditionally replication-defective MCMV-PP150-F140P vector	185
Figure 3.24 Schematic illustration of the conditionally replication-defective MCMV-PP28-F140P vector	186
Figure 3.25 PCR recombination fragments used for construction of the recombinant MCMV-pp150-F140P vaccine	188
Figure 3.26 PCR recombination fragments used for construction of the recombinant MCMV-pp28-F140 vaccine	189
Figure 3.27 Schematic illustrating the construction of MCMV-pp150/pp28-ecDHFR (F140P) vectors.....	191
Figure 3.28 Characterization of recombinant MCMV-pp150-F140P BACs by using EcoRI.....	192
Figure 3.29 Characterization of recombinant MCMV-pp28-F140P BACs, by using EcoRI.....	193

Figure 3.30 Confirmation of Kan ^R marker removal from MCMV-pp150-F140P.....	195
Figure 3.31 Confirmation of Kan ^R marker removal from MCMV-pp28-F140P	195
Figure 3.32 Characterization of the recombinant (post-FLP) MCMV-pp150-F140P BAC genome using EcoRI	198
Figure 3.33 Characterization of the recombinant (post-FLP) MCMV-pp28-F140P BAC genome using EcoRI	199
Figure 3.34 Confirmation of MCMV-pp150-F140P BAC genome via Sanger DNA sequencing.....	200
Figure 3.35 Confirmation of MCMV-pp28-F140P BAC genome via Sanger DNA sequencing.....	201
Figure 3.36 Titration of Concentrated stocks in the present or absence of TMP by TCID50.....	206
Figure 3.37 Titration of Concentrated stocks in the present or absence of TMP by TCID50	206
Figure 3.38 Confirming presence of F140P domain in MCMV-pp150-F140P virus by PCR.....	208
Figure 3.39 Confirming presence of F140P domain in MCMV-pp28-F140P virus by PCR.....	208
Figure 3.40 Conformation of ecDHFR (F140P) within MCMV-pp150-F140P virus genome.....	209
Figure 3.41 Conformation of ecDHFR (F140P) within MCMV-pp28-F140P virus genome.....	210
Figure 3.42 Image of dose-dependent regulation of the recombinant MCMV-pp150-F140P.....	213
Figure 3.43 Image of dose-dependent regulation of the recombinant MCMV-pp28-F140P.....	213
Figure 3.44 Dose-dependent regulation of the recombinant MCMV-pp150-F140P replication by ligand-TMP.....	215
Figure 3.45 Dose-dependent regulation of the recombinant MCMV-pp28-F140P replication by ligand-TMP.....	216
Figure 3.46 PCR screening of recombinant MCMV-pp150-F140P mutant virus maintained at different concentration of TMP.....	218
Figure 3.47 PCR screening of recombinant MCMV-pp28-F140P mutant virus maintained at different concentration of TMP.....	218
Figure 3.48 Sequence conformation of recombinant MCMV-pp150-F140P vector.....	221
Figure 3.49 Sequence conformation of recombinant MCMV-pp28-F140P vector	223
Figure 3.50 Schematic illustration of the pp150 or pp28 stability in the presence of TMP.....	226
Figure 3.51 Schematic illustration of the pp150 or pp28 stability in the absence of TMP.....	226
Figure 3.52 Dynamics of pp150 or pp28 stability were analysed during infection in the presence of TMP.....	228
Figure 3.53 Dynamics of pp150 or pp28 stability were analysed during infection in the absence of TMP.....	230

Figure 3.54 Replication of recombinant MCMV-pp150-F140P viruses in the presence or absence of TMP.....	235
Figure 3.55 Replication of recombinant MCMV-pp28-F140P virus compared to its parental MCMV-WT virus in the presence or absence of TMP.....	240
Figure 3.56 Replication of recombinant MCMV-pp28-F140P virus compared to its parental MCMV-WT virus in the presence or absence of TMP using standard plaque assay.....	242
Figure 3.50 Secondary infection of the recombinant MCMV-pp28-F140P in the absence of TMP.....	244

Chapter Four

Figure 4.1 Schematic illustration of MCMV-IA constructs.....	262
Figure 4.2 Recombination PCR fragments used for construction of three MCMV-IA vectors	264
Figure 4.3 Schematic illustrating the construction of MCMV-IA vectors.....	266
Figure 4.4 Characterization of the recombinant MCMV-IA BAC genome using <i>EcoRI</i>	268
Figure 4.5 Characterization of recombinant post-FLP MCMV-IA BAC genomes using <i>EcoRI</i>	271
Figure 4.6 Confirmation of excision of the Kan ^R marker.....	273
Figure 4.7 Confirmation of IA epitope within MCMV-IA BACs via Sanger sequencing.....	276
Figure 4.8 Confirming excision of BAC cassette from reconstituted MCMV-IA-(NP, PA or NS2) genome by PCR.....	278
Figure 4.9 Confirming presence of IA epitopes in MCMV-IA viruses genome by PCR.....	281
Figure 4.10 Confirmation of IA epitope within MCMV-IA virus genome by Sanger DNA sequencing.....	284
Figure 4.11 Replication of recombinant MCMV-IA vectors compared to its parental MCMV-WT (FWT) virus.....	287
Figure 4.12 Schematic showing MCV-IA vaccinated mouse groups.....	290
Figure 4.13 T cells responses at week 7/8 following vaccination with MCMV-IA (NP+PA+NS2) vector.....	292
Figure 4.14 Kinetic analysis of T cells responses to MCMV-IA-(NP+PA+NS2) at week 7/8.....	293
Figure 4.15 MCMV-IA-(NP+PA+NS2) induce low level of IA-specific T cell response in C57BL/6 mice at week 7/8.....	294
Figure 4.16 T cells responses at week 12 following vaccination with MCMV-IA (NP+PA+NS2).....	296
Figure 4.17 Kinetic analysis of T cells responses to MCMV-IA-(NP+PA+NS2) at week 12.....	297
Figure 4.18 T cells responses at week 12 following vaccination with MCMV-IA (NP+PA+NS2).....	298
Figure 4.19 Schematic illustration of MCMV-IA-NP (F5) constructs	300
Figure 4.20 Recombination PCR fragments used for construction of MCMV-IA-NP (F5) vaccine.....	301
Figure 4.21 Characterization of recombinant MCMV-IA-NP (F5) BAC genome using <i>EcoRI</i>	303

Figure 4.22 Confirming excision of Kan ^R marker from MCMV-IA-NP(F5) BAC.....	304
Figure 4.23 Confirmation of IA epitope within MCMV-IA-NP (F5) BACs via Sanger sequencing.....	305
Figure 4.24 Confirming presence of NP epitope in MCMV-IA-NP (F5) virus genome by PCR.....	307
Figure 4.25 Confirmation of NP epitope within MCMV-IA-NP (F5) virus genome	308
Figure 4.26 Replication of recombinant MCMV-IA-NP (F5) virus compared to its parental MCMV-WT (F5) virus.....	310
Figure 4.27 Replication of recombinant MCMV-IA-NP (F5) virus compared to its parental MCMV-WT (F5) and MCMV-EBOV-NP (5A1) virus.....	311
Figure 4.28 Replication of recombinant MCMV-IA-NP (F5) virus compared to its parental MCMV-WT	311
Figure 4.29 Analysis of IE2 expression of recombinant MCMV and parental wild-type via Western blot	312

LIST OF TABLES

Chapter One

Table 1.1 Human diseases caused by Herpesviridae members.....	52
Table 1.2 BAC-cloned human herpesviruses.....	60
Table 1.3 BAC-cloned animal herpesviruses.....	61
Table 1.4 Destabilization domain strategy used for regulate proteins of CMV.....	72
Table 1.5 IA virus genome segments and encoded proteins.....	76
Table 1.6 Pandemic outbreaks and mortality associated with IA virus.....	90

Chapter Two

Table 2.1: Plasmids, BACs and bacterial strains.....	112
Table 2.2: Primers for generating and sequencing MCMV influenza recombinants.....	117
Table 2.3: Primers used for cloning and sequencing MCMV-ecDHFR recombinants using galK strategy.....	118
Table 2.4: Primers used for cloning and sequencing MCMV-ecDHFR recombinants	118
Table 2.5: Primers used for generating and sequencing MCMV-IE recombinants.....	119
Table 2.6: Primers used for generating and sequencing MCMV-pp150 recombinants.....	119
Table 2.7: Primers used for generating and sequencing MCMV-pp28 recombinants.....	119

Chapter Three

Table 3.1 Characteristics of ec-DHFR DDs.....	152
Table 3.2 Numbers of recombinant MCMV-pp150-(E134G or Y100I) BACs.....	180
Table 3.3 Analysis of MCMV BAC clones following excision of Kan cassette.....	184
Table 3.4 Number of recombinant MCMV-pp150/pp28-F140P BAC clones	191
Table 3.5 Analysis of recombinant MCMV BAC clones following excision of Kan.....	195
Table 3.6 Reconstitution of recombinant MCMV-pp150/pp28-F140P BAC clones.....	203
Table 3.7 Number of MCMV-pp150/pp28-F140P plaques	212
Table 3.8 TMP concentration (0, 1, 5, 10, 50, 100 μ M) and P values	215

Table 3.9 TMP concentration (0, 1, 5, 10, 50, 100 μ M) and P values	216
Table 3.10 Mean plaque counts of mutant MCMV-pp28-F140P virus at day five post infection.....	245

Chapter Four

Table 4.1 Number of recombinant MCMV-IA (NP, PA or NS2) BAC clones following E/T recombination.....	266
Table 4.2 Analysis of recombinant MCMV BAC clones following excision of Kan ^R	269
Table 4.3 Plaque numbers of recombinant MCMV-IA (NP, PA, and NS2).....	277
Table 4.4 Titres of MCMV-WT and the recombinant MCMV-IA virus vectors stocks.....	280
Table 4.5 Influenza A and MCMV H2 ^b - restricted peptides.....	289
Table 4.6 Numbers of recombinant MCMV-IA-NP (F5) BAC clones	302
Table 4.7 Analysis of MCMV BAC clones following excision of Kan cassette.....	304
Table 4.8 Reconstitution of recombinant MCMV-IA -NP BAC clones in the MEFs.....	306
Table 4.9 Titres of MCMV-WT and the recombinant MCMV-IA virus vectors stocks.....	307

Author's Declaration

At no time during the registration for the degree of Doctor of Philosophy has the author been registered for any other University award without prior agreement of the Graduate Committee.

Work submitted for this research degree at the Plymouth University has not formed part of any other degree either at Plymouth University or at another establishment.

Word count of main body of thesis: 75,000

Signed

Date

Abbreviations used in this study

Aa	amino acid
Ab	antibody
APC	Antigen presenting cell
BAC	Bacterial artificial chromosome
BFA	Brefeldin A
Bp	Base pairs
C	Carboxyl (-terminal end of protein)
°C	temperature in degrees Celsius
CMV	Cytomegalovirus
CTL	Cytotoxic T-lymphocytes
CPE	Cytopathic Effect
dH ₂ O	distilled water
DD	Destabilization domain
DMEM	Dulbecco's modified Eagles medium
DMSO	Dimethyl sulphoxide
DNA	deoxyribonucleic acid
dpi	days post infection
<i>E.coli</i>	<i>Escherichia coli</i>
ecDHFR	Escherichia coli dihydrofolate reductase
EDTA	Ethylenediaminetetra-acetic acid
ER	Endoplasmic reticulum
Flu	influenza
FLP	Flippase
FRT	Flippase Recombination Target

HA	Haemagglutinin
HCMV	Human cytomegalovirus
HEPES	N-2-hydroxyethylpiperazine-N ² -2-ethansulfonic acid
hpi	Hours post infection
IA	Influenza A
IE	Immediate early
IFN	Interferon
i.p.	Intraperitoneally
i.v.	Intravenously
IL	Interleukin
Kbp	Kilobase pairs
l	litter
L	Late
LB	Luria-Bertani broth
MCMV	Mouse cytomegalovirus
mCP	Minor Capsid protein
MCP	Major Capsid protein
MEF	Mouse embryo fibroblasts
MgCl ₂	Magnesium chloride
MHC	Major Histocompatibility Complex
MOI	Multiplicity of infection
N	amino (-terminal of protein)
NaCl	Sodium chloride
Nt	Nucleotide
ORF	Open reading frame

PAMP	Pathogen-associated molecular patterns
PAGE	Polyacrylamide Gel Electrophoresis
PBM	Peripheral blood monocytes
PBS	Phosphate buffered saline
PBST	phosphate buffered saline+Tween 20
PCR	Polymerase chain reaction
PFU	Plaque forming units
P.i.	Post infection
ROI	Region of interest
RT	Room temperature
rpm	Revolutions per minute
SD	Standard deviation
SDS	Sodium Dodecyl Sulfate
TAE	Tris acetate EDTA buffer
TE	Tris-HCl/EDTA
TEMED	N'-N'-N'-N'-tetramethylethylenediamine
TCID50	50% Tissue Culture Infective Dose
T _{CM}	Central memory T-cell
TCR	T cell receptor
T _{EM}	Effector memory T-cell
Th	T helper cells
TLRs	Toll-like receptors
TMP	Trimethoprim
TNF	Tumour necrosis factor
Tween 20	Polyoxyethylene-sorbitanmonolaurate

UL	Unique long
US	Unique short
UV	ultra-violet
v/v	volume per volume
wt	Wild type
w/v	Weight per volume
μg	microgram
μl	microliter
μM	micromolar
3'	Three prime end of DNA sequences
5'	Five prime end of DNA sequences

Chapter One:

Introduction

1.1 General Background

1.1.1 Herpesviridae

Herpesviruses are a significant cause of human disease worldwide and are among the most widespread and successful viral microbes across the entire animal kingdom. The herpesvirus family is a group of over 100 viruses that infect a variety of animal species including birds, mammals, fish and reptiles. It is believed that mammalian herpesviruses arose from a common ancestral virus at least 80 million years ago (McGeoch *et al.*, 1995) with non-mammalian herpesviruses having diverged from this common lineage 120 million years earlier (Davison, 1993).

Herpesviruses are large DNA viruses, ranging in size from approximately 130 to 250 nm in diameter. They possess a large linear double-stranded DNA genome (127-290 kb) enclosed within a T=16 icosahedral capsid, which is then surrounded by an amorphous tegument layer. The tegument layer is proteinaceous in nature, being comprised of over fourteen different virus-derived proteins as well as a number of cellular proteins (Varnum *et al.*, 2004). The tegumented capsid is then surrounded by a lipid envelope containing membrane-associated proteins (Varnum *et al.*, 2004; Figure 1.1).

Herpesvirus family members share additional common features. These include host range restriction, nuclear-localized replication (both in terms of DNA replication and genome encapsulation) and establishment of persistent life-long infection within their respective host (Pellet & Roizman, 2007). Following an initial lytic acute replication, life-long infection is characterized by the virus entering a latent phase with minimal virus gene transcriptional activity (Davison, 2002). Sites of latency vary depending on the particular mammalian herpesvirus subfamily (see below). In healthy, immunocompetent individuals herpesvirus infection may remain asymptomatic for long periods, even for life. However, reactivation of

latent virus can occur during periods of stress and immunosuppression, leading to conditions ranging in severity from recurrent cold-sores to herpes stromal keratitis, the leading cause of herpes simplex virus (HSV) blindness in the western world (Crough & Khanna, 2009).

Herpesviruses are divided into three subfamilies: alpha-, beta-, and gamma-herpesviruses. Alpha-herpesviruses are neurotropic (Slater *et al.*, 1994). They demonstrate variability in host range, have a short reproductive cycle in infected hosts, and grow rapidly in cell culture. They also have the ability to establish latent infection in sensory ganglia. There are 3 human alpha-herpesviruses. HSV-1 and -2 are responsible for cold-sores and genital herpes, respectively. Varicella zoster virus (VZV) is the causative agent of chickenpox and shingles (Arbuckle *et al.*, 2010; Kondo & Mocarski, 1994; Wang *et al.*, 2005; Young & Murray, 2003).

Beta-herpesviruses have more a highly restricted host range, longer reproductive cycles, and grow more slowly in cell culture than alpha-herpesviruses. Members of the beta-herpesvirus subfamily include human cytomegalovirus (CMV; HCMV), human herpesvirus-6A and -6B and human herpesvirus-7. CMV derives its name from the enlargement of infected cells (cytomegaly) observed during infection. During latency, main sites of virus persistence are myeloid-derived cells (i.e., CD34⁺ stem cells), salivary glands and kidney cells. Gamma-herpesvirus subfamily members have a similarly restricted host range and establish latency in lymphoid tissue. Viral replication is generally restricted to either T or B cells and includes well known human pathogens such as Kaposi's sarcoma-associated herpes virus (KSHV) and Epstein-Barr virus (EBV).

This thesis focuses on the CMV beta-herpesvirus, which is discussed in more detail below.

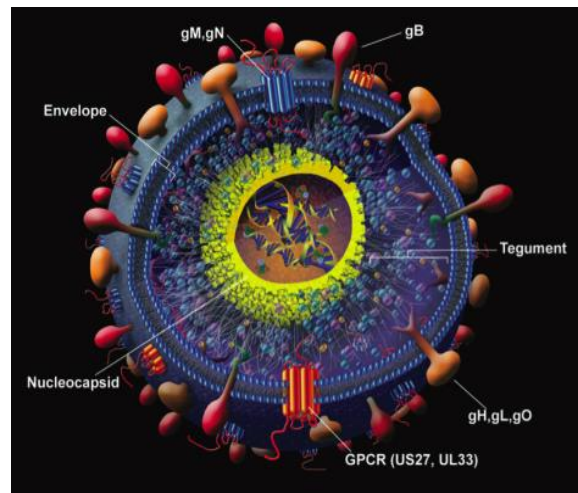


Figure 1.1 Structure of CMV virion. The double-stranded (ds) DNA viral genome is contained within an icosahedral viral capsid surrounded by a proteinaceous tegument layer. The tegumented capsid is in turn surrounded by a lipid bilayer membrane envelope studded with virally encoded glycoproteins. Reprinted from (Streblow *et al.*, 2006).

1.1.2 Cytomegalovirus (CMV)

CMVs are present in a wide range of mammalian hosts, including human, primate, and rodents (Roizman & Pellett, 2001). However, CMVs are highly species-restricted, with no cross-species infection having been identified even between closely evolutionarily related mammalian species. A typical consequence of CMV infection *in vitro* as well as *in vivo* is enlargement of the infected cell (cytomegaly) and the presence of inclusions in the nucleus called owl's eyes (Wallace *et al.*, 1956). The CMV genome encodes more than 200 proteins, many of which are of unknown function. Many of these proteins are not essential for the viral growth *in vitro*, but are believed to have an important role *in vivo* by modulation of the host environment (Mocarski, 2002). HCMV is the best studied of the CMVs in terms of pathogenesis, and is a major human pathogen that infects a large proportion of the human population. Generally HCMV produces subclinical infection in healthy people with normal immune systems.

1.1.2.1 Virion structure

The CMV virion consists of a highly ordered icosahedral nucleocapsid of about 130 nm in diameter containing a linear viral ds-DNA genome of approximately 230 kilobases (kb). This genome size is on the larger end of herpesviruses, with genomes of alpha- and gamma-herpesviruses generally being smaller in size (>120 kb). The CMV capsid is surrounded by a lipid bilayer envelope carrying various viral glycoproteins that are responsible for viral attachment and entry into host cells. Similar to all herpesviruses, CMVs also have a large amorphous proteinaceous layer between the capsid and the envelope called the tegument. Currently at least 30 viral tegument proteins are known to be present within the CMV virion (Kalejta, 2008). Upon viral entry, tegument proteins are introduced into the cell and perform critical functions during the viral life cycle. The following sections will look at each virus structural element in detail.

1.1.2.1.1 Genome

The HCMV DNA genome is 230 kb in size. Although early studies suggested a protein coding capacity in the order of 100 to 200 proteins, more recent ribosome profiling studies have identified over 750 translated open reading frames (ORFs). This makes HCMV one of the most complex viral pathogens known to infect humans (Stern-Ginossar *et al.*, 2012). The HCMV genome, like those of other members of the primate beta-herpesvirus subfamily is organised into two unique regions: the unique long (U_L) and unique short (U_S) regions (Figure 1.2; Mocarski *et al.*, 2013). Each unique region is flanked by terminal repeat components (TR_L or TR_S) of approximately 300 to 600 bp. This terminal component is repeated in an inverted orientation at the other end of the unique region (called IR_L or IR_S), and gives rise to general organization of the HCMV genome as $TR_L-U_L-IR_L-IR_S-U_S-TR_S$ (Cha *et al.*, 1996; Tamashiro & Spector, 1986). CMV replication generates equimolar

populations of four isomers of the genome (Kilpatrick & Huang, 1977). These isomers have the same DNA sequence but differ in orientation and position of the UL and US segments (Kilpatrick & Huang, 1977). Within the virion the ds-DNA genome is maintained as a linear molecule, which then undergoes circularization within the nucleus shortly after infection. Studies have shown that the circular isomeric form of the HCMV genome even in the form of a bacterial artificial chromosome (BAC) (discussed in detail below) is infectious (Borst *et al.*, 1999).

Genomes of other CMVs show some variation on the theme of unique regions flanked by repeats. Chimpanzee CMV (CCMV), being the only other CMV from apes to have been fully sequenced, is comparable to HCMV with two unique regions (U_L and U_S) flanked by direct repeats (Davison *et al.*, 2003). Rat CMV (RCMV) (Maastricht strain) has a small terminal repeat of 504 bp that lacks the internal repeat sequence (Vink, Beuken & Bruggeman, 1996). The laboratory-passaged MCMV (Smith strain) was the first complete MCMV genome to be sequenced. Using whole-genome shotgun sub-cloning followed by Sanger sequencing of virion-associated DNA, the MCMV Smith strain genome was shown to consist of 230,278 bp arranged with a small terminal repeat (31 bp) and several short internal repeats (Rawlinson, Farrell & Barrell, 1996). It was indicated that the MCMV genome encodes approximately 170 ORFs, but based on the recent study of HCMV by Stern-Ginossar *et al.* (2012), it would appear that this number may be increased substantially upwards.

Comparison of HCMV and MCMV DNA content show similarities in both distribution and level of G+C (58% and 58.7%, respectively); (Rawlinson, Farrell & Barrell, 1996). Substantial sequence variation has been observed between different strains of HCMV. However, genomic sequencing of an additional laboratory strain of MCMV (strain K181) identified relatively high MCMV genome conservation. More recently, Smith *et al.* (2008) showed that there were also no major deletions or insertions in the genome of multiple recent

MCMV field strain isolates with genome size being similarly highly conserved (Smith *et al.*, 2008). More subtle differences in sequence, particularly at the genomic termini were observed, however, which did impact *in vivo* replication of the viruses.

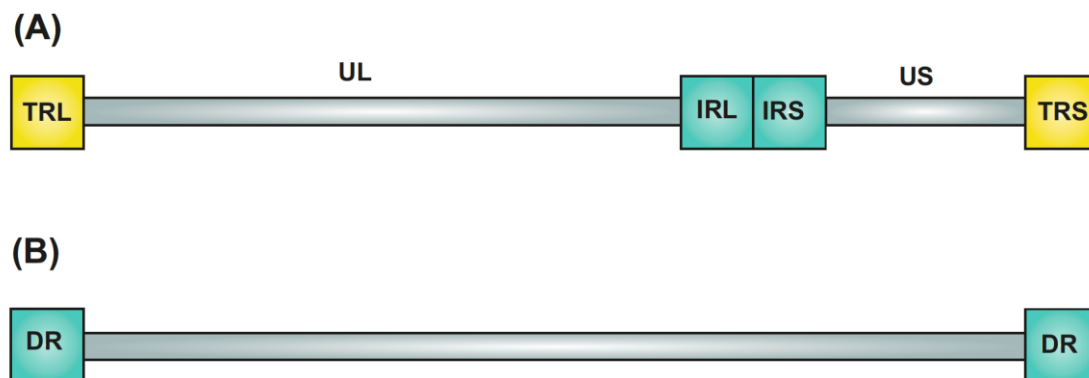


Figure 1.2 Schematic of CMV genome organization. (A) The HCMV genome consists of the unique long sequence (UL), flanked by terminal repeat long (TRL) and inverted repeat long (IRL). The unique short sequence (US) is flanked by terminal repeat short (TRS) and inverted repeat short (IRS). (B) The MCMV genome consists of a single unique sequence with two terminal direct repeats (DR); (Mocarski *et al.*, 2013; Rawlinson, Farrell & Barrell, 1996).

1.1.2.1.2 Capsid

The capsid (also called nucleocapsid) packages and protects the viral genome. Cryo-electron microscopy (EM) and image reconstruction has been used to determine the structure of the CMV capsid (Dai *et al.*, 2008; Yu *et al.*, 2011). These studies show the CMV capsid to have an icosahedral lattice geometry structure with each icosahedron consisting of hexamer-pentamer clusters (Butcher *et al.*, 1998). The major structural subunit of the capsid is the capsomere, which is comprised of hexons at the faces and pentons at the vertices organised with a triangulation number of 16 ($T = 16$). The hexon capsomeres form the 150 subunits of

each icosahedral face, and the penton capsomeres form the 12 icosahedral face vertices. The CMV capsid is composed of four structural proteins: major capsid protein (MCP, encoded by *UL86* and *M86* in HCMV and MCMV, respectively), minor capsid protein (mCP, encoded by *UL85* and *M85*), minor capsid-binding protein (mC-BP encoded by *UL46* and *M46*) and smallest capsid protein (SCP, encoded by *UL48A* and *M48.2*); (Gibson *et al.*, 1996; Sedarati & Rosenthal, 1988). All 150 hexon capsomeres are composed of MCP and SCP, while the majority of the penton capsomeres consist of pentamers of MCP. Both types of capsomeres are linked together by mC-BP and mCP triplexes that are required for the stabilization of the capsid structure (Dai *et al.*, 2013; Trus *et al.*, 2001).

1.1.2.1.3 Envelope

CMV virions have a phospholipid bilayer envelope that contains viral glycoproteins as well as cellular proteins derived from the host. In the current 'Envelopment, De-envelopment, Re-envelopment' model initial herpesvirus envelopment takes place at the inner nuclear membrane. Following de-envelopment from the cisternae of endoplasmic reticulum (ER) to release the capsid into the cytosol, final envelopment and acquisition of the mature virion envelope occurs in endosomal *trans*-Golgi network (TGN) regions (Eggers *et al.*, 1992; Gibson *et al.*, 1996). The role of lipid components acquired during envelopment in stabilizing virion structure and maintaining the integrity of the viral envelope has not been determined. CMV also acquires host cellular proteins during envelopment. These proteins include CD55 and CD59, β -microglobulin and annexin II (Grundy, McKEATING & Griffiths, 1987; Grundy *et al.*, 1987; Wright *et al.*, 1995). It has been suggested that these proteins may play a role in modulating virus attachment or host cellular responses (Boehme *et al.*, 2004; Compton *et al.*, 2003).

The virus-encoded glycoproteins present within the HCMV envelope are generally conserved between different CMVs. These glycoproteins are essential for initiation of virus-host attachment, virus entry and cell-to-cell virus transmission. Over 50 distinct virion encoded glycoproteins are thought to be present within the HCMV particle, although the majority have not been studied in any detail. Three major glycoprotein complexes have been identified: homodimers of glycoprotein B (gB, encoded by UL55); heterodimers of glycoprotein M (gM, UL100) and glycoprotein N (gN, UL73); and heterotrimers of glycoprotein H (gH, UL75), glycoprotein L (gL, UL15) and either glycoprotein O (gO, UL74) or glycoproteins encoded by UL128, UL130 and UL131A (Huber & Compton, 1998; Huber & Compton, 1999; Jarvis & Nelson, 2007; Mach *et al.*, 2000).

The gB is a type I integral membrane protein that forms a homodimeric glycoprotein complex termed gCI. This gCI complex binds to heparan sulfate proteoglycans facilitating both entry into host cells and cell-to-cell spread of infection. The gM/gN complex is the most abundant component of the viral envelope, and has a role in virus entry and membrane fusion through formation of a gM/gN disulphide-linked dimer which also exhibits heparin-binding activity (Kari & Gehrz, 1992; Mach *et al.*, 2000). The gH/gL proteins together with gO are required for viral entry into fibroblasts through mediating fusion of viral and host cell membrane (Spaete *et al.*, 1993). A gH/gL/pUL128/pUL130/pUL131A is required for viral entry into non-fibroblast cells, including endothelial, epithelial and dendritic cells (for review, see: (Jarvis & Nelson, 2007). The genes encoding these core glycoproteins (with the exception for the cell tropism related gO, pUL128/pUL130/pUL131A) are all essential for virus replication (Mach *et al.*, 2000; Varnum *et al.*, 2004).

1.1.2.1.4 Tegument

The tegument layer of CMV occupies the space between the outer lipid membrane and the icosahedral protein capsid containing the viral genomic ds-DNA (Kalejta, 2008). The tegument layer is unique to herpesviruses. It contains approximately 30 virus-encoded proteins (Roizman & Sears, 2001), thereby accounting for more than half of the seventy-one viral proteins that are found in infectious HCMV virions (Kalejta, 2008; Varnum *et al.*, 2004). Given a capsid size of 125 nm within a 220 nm virion, the tegument represents a significant aspect of the virion space-representing approximately 40% of the virion protein mass (Gibson, 1996). The tegument layer appears largely unstructured by EM, although some structure is observed in regions associate with binding of tegument to the capsid. Tegument proteins are delivered to cells at the very start of the infection process following fusion of the virus envelope with cellular membranes, and thereby have the potential to modulate the cellular environment even prior to the onset of viral gene expression (Kalejta, 2008).

Following release into the cytoplasm, tegument proteins play an important role in multiple stages of the viral life cycle, which starts by facilitating release of viral DNA from disassembling capsids. The capacity for tegument to function immediately after infection without requiring *de novo* gene expression has presumably evolved due to the significant advantage it provides to the virus. Other important functions associated with the tegument are modulation of gene expression, immune evasion, and assembly and egress. Most tegument protein are phosphorylated, but the physiological significance of this phosphorylation remains largely unexplored. The four most abundant tegument proteins are lower matrix protein, pp65 (UL83, M83), basic phosphoprotein pp150 (UL32, M32), upper matrix protein pp71 (UL82, M82) and membrane-associated myristylated protein pp28 (UL99, M99) (Baxter & Gibson, 2001; Gibson, 1996; Kalejta, 2008; Sanchez *et al.*, 2000).

1.1.2.1.4.1 Lower matrix protein UL83 (pp65)

The pp65 protein encoded by UL83 is the most abundant of the tegument proteins accounting for >15% of the virion protein mass (Gibson, 1996; Varnum *et al.*, 2004). The UL83 gene is expressed with L kinetics, however due to the presence within the incoming virion, pp65 rapidly accumulates within the cell following infection. Early during infection, pp65 is localized within the nucleus of infected cells, but in the late phase the protein redistributes predominantly to the cytoplasm (Kalejta, 2008). UL83 is not essential for virus replication, as UL83 deletion does not significantly impair the growth of virus in fibroblasts (Schmolke *et al.*, 1995). However, UL83 deleted HCMV is unable to make a virus-like particle called a ‘dense body’, one of three viral particle types (virions and non-infectious enveloped particles being the other two) that are observed during normal HCMV infection (Irmiere & Gibson, 1983).

A number of studies have shown pp65 to play an important role in protecting HCMV-infected cells from being destroyed by the immune system by inhibiting activation of multiple components of the host immune system (Arnon, Markel & Mandelboim, 2006). Pp65 has been shown to inhibit natural killer (NK) cell cytotoxic activity by binding to the activating receptor NKp30 and acting as an antagonistic ligand. In this capacity pp65 interferes with the ability of NKp30 to cross-talk between other NK cells, as well as preventing NK cell-mediated killing of infected cells (Arnon *et al.*, 2005; Arnon, Markel & Mandelboim, 2006). Pp65 has also been shown to inhibit the induction of host interferon responses (Abate, Watanabe & Mocarski, 2004) based on the observation of elevated level of expression of interferon-stimulated genes in cells infected with a recombinant virus lacking the pp65 protein (Abate, Watanabe & Mocarski, 2004). In regards to the adaptive immune response, pp65 was found to block the ability of MHC class I to present the viral immediate-early (IE) protein by phosphorylation of the IE protein (Gilbert *et al.*, 1996).

The kinase activity of pp65 is also involved in mediating degradation of the alpha chain in the HLA-DR MHC class II cell surface receptor by inducing the accumulation of HLA class II molecules within the lysosome (Odeberg *et al.*, 2003).

1.1.2.1.4.2 The basic phosphoprotein UL32 (pp150)

The pp150 basic phosphoprotein is the product of the UL32 gene of HCMV and is expressed with L kinetics. Pp150 is the second most abundant tegument protein after pp65 comprising approximately 10% of the virion mass (Gibson, 1996; Varnum *et al.*, 2004). Orthologues of UL32 are found in other beta-herpesviruses, including: MCMV, rat CMV, chimpanzee CMV, HHV-6, and HHV-7. However, UL32 orthologues are not found in either alpha- or gamma-herpesviruses (Adler, Nigro & Pereira, 2007). The pp150 molecule undergoes substantial post-translational modification by glycosylation and phosphorylation, which increases the molecular mass from an estimated 113 kDa to a mass of 150 kDa for pp150 within the virion (Jahn *et al.*, 1987; Roby & Gibson, 1986). Pp150 is found within non-infectious enveloped particles, cytoplasmic nucleocapsids and virions, but is not present in immature nuclear-localized capsids (Gibson & Irmiere, 1983; Irmiere & Gibson, 1983).

Protein sequence alignment of pp150 orthologues from other beta-herpesviruses shows an overall similarity of 17%, with the highest level of conservation occurring within the amino terminal ~300 amino acids (aa), suggesting a functional conservation of this region (Baxter & Gibson, 2001). Conserved regions 1 and 2 (CR1 and CR2) (L52 to Y62 and N201-L209, respectively) are two highly conserved N-terminal motifs present with the N-terminal region. Pp150 contacts the capsids through the end of the capsomeres or the triplex subunits that interlink them (Chen *et al.*, 1999; Trus *et al.*, 1999). Pp150 is also known to bind to the HCMV capsids through the N-terminal one-third of the molecule. This interaction with the

capsid is consistent with a role of pp150 in virus assembly (see below) (Baxter & Gibson, 2001). An additional cluster of four conserved cysteine (Cy_s-X₇-Cy_s-X₉-Cy_s-X₇-Cy_s) are found in primate CMVs near the CR2 region (Baxter & Gibson, 2001). Pp150 is modified by the attachment of O-linked N-acetyl glucose amine (a unique posttranslational glycosylation of nuclear and cytosolic proteins) at two serine residues (Serine-921 and Serine- 952) near the carboxyl terminus. However, mutation of either of these serines individually does not inhibit pp150 function (AuCoin *et al.*, 2006; Greis, Gibson & Hart, 1994).

Pp150 is essential for production of infectious virus since deletion of the UL32 ORF leads to a complete loss of productive virus replication (Tandon & Mocarski, 2008). The critical role of the CR motifs has also been shown as mutational CR inactivation (N201A and G207A) similarly prevents virus replication. In the absence of pp150, nucleocapsids were shown to accumulate in a juxtannuclear structure called the viral assembly compartment (AC), but failed to proceed further to vesicular transport associated with virion release (Tandon & Mocarski, 2008). These findings confirmed and expanded on results from earlier studies using a recombinant HCMV expressing pp150 tagged at its carboxyl terminus with enhanced green fluorescent protein (pp150-EGFP), which had similarly suggested a role for pp150 in late stages of virus assembly. In these earlier studies pp150 was shown to localize to the nucleus at early times of infection, but was then found primarily in the cytoplasm at later times. The pp150 protein was also shown to have near perfect co-localization with pUL86 (MCP), suggesting that viral particles in the nucleus acquired the tegument protein pp150 during budding at the nuclear membrane (Sampaio *et al.*, 2005), although other researchers had reported exclusive localization of pp150 to the cytoplasm (Sanchez *et al.*, 2000).

Consistent with a cytoplasmic assembly role, pp150 co-localizes at the AC with other tegument proteins including pp65 and pp28 (see below), envelope glycoproteins gB, gH and gM/gN, and with markers of the distal secretory pathway (Sanchez *et al.*, 2000).

Additional studies support this role for pp150 in late (cytoplasmic) stages of virus assembly (AuCoin *et al.*, 2006; Meyer *et al.*, 1997; Tandon & Mocarski, 2008; Yu, Silva & Shenk, 2003; Zipeto *et al.*, 1993); (Figure 1.3). Aside from its functional role, pp150 is a highly immunogenic protein eliciting a strong humoral immune response during both latent and reactivated viral infection in CMV positive individuals (Greijer *et al.*, 1999; Landini *et al.*, 1991). It is an immune-dominant target of the host cellular response against HCMV (Gyulai *et al.*, 2000; Riddell *et al.*, 1991) and represents a major target of human MHC-restricted cytotoxic T cells following HCMV infection (Elkington *et al.*, 2003; Gyulai *et al.*, 2000).

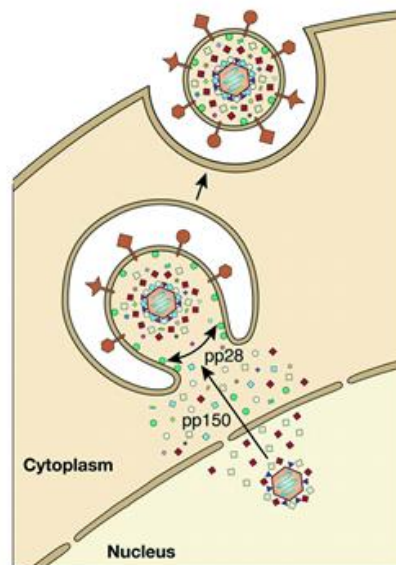


Figure 1.3 Function of the tegument proteins (pp150 and pp28). For the detail of the tegument protein functions see (Section 1.1.1.4). Re-printed from (Kalejta, 2008).

1.1.2.1.4.3 Upper matrix protein UL82 (pp71)

The pp71 tegument protein, encoded by the UL82 gene, is expressed with E-L kinetics (Kalejta, 2008). Pp71 localizes to the nucleus in both UL82 transfected and HCMV-infected cells (Smith, Kosuri & Kerry, 2014). It has been shown that transfection of pp71 into cultured cells lead to increased infectivity of the viral genomic DNA (Baldick *et al.*, 1997). As reviewed in Kalejta (2008) rather being essential, pp71 is required for *efficient* virus replication. The main function of pp71 is as a transcriptional activator that enhances IE gene expression within infected cells (Liu & Stinski, 1992). Pp71 is also believed to be important for initiation of tegument assembly and interacts directly with newly assembled capsids (Trus *et al.*, 1999). Pp71 has been shown to possess an immune evasion function by preventing cell surface expression of MHC class I through a delay in transport from the ER (Trgovcich *et al.*, 2006).

1.1.2.1.4.4 The membrane-associated myristylated protein pp28 (UL99)

The UL99 encoded tegument protein pp28 is 190 amino acids in length with a predicted molecular weight of 28 kDa. As a true late (L) gene (see below), the expression of UL99 is completely dependent on the onset of viral DNA replication and pp28 does not accumulate within infected cells until late times of infection (Phillips & Bresnahan, 2012; Silva *et al.*, 2003; Wing & Huang, 1995). Pp28 localizes in the cytoplasm in both transfected and HCMV infected cells. This localization is dependent on myristoylation of glycine 2 at the amino-terminus of the pp28 protein (Sanchez, Sztul & Britt, 2000). Myristoylation mediates insertion of the pp28 protein into cytoplasmic membranes associated with the cellular secretory pathway. This association appears to be critical for virus morphogenesis as a HCMV recombinant encoding a mutation that blocked myristoylation (G2A) resulted in

localization of the mutant pp28 to the nucleus and a failure to produce infectious virus (Britt *et al.*, 2004).

During HCMV infection, pp28 co-localizes and accumulates with other tegument proteins (pp150, pp65) and envelope glycoproteins (gB, gH and gP65) at the AC, with its co-localization appearing to be required for production of infectious virus (Seo & Britt, 2006) (Kalejta, 2008). Multiple studies have shown pp28 to be essential for virus replication, due to its role in late (cytoplasmic) steps of virus assembly (Britt *et al.*, 2004; Silva *et al.*, 2003). Consistent with this assembly function, phenotypic characterization of pp28-deleted viruses show that early events of viral replication including entry, gene expression and viral genome synthesis all appear to be normal. In contrast, in the absence of pp28 tegument proteins results in accumulation of non-enveloped capsids in the cytoplasm at late times of infection, which fail to associate with the AC (Silva *et al.*, 2003).

Fine-mapping studies showed the 61 N-terminal amino acids (aa) to be sufficient for wild type (WT) virus replication (Jones & Lee, 2004; Seo & Britt, 2006), with the first 50 amino acids also supporting viral replication, although with delayed kinetics and at decreased levels (Seo & Britt, 2006). Impaired replication corresponded to inefficient retention of pp28 mutants at the AC consistent and a defect in virion envelopment (Seo & Britt, 2006; Seo & Britt, 2007). These studies also showed that an acidic region of pp28 located between aa 44 and 59 and a region between aa 34 to 43 are required for normal localization of pp28 to the AC (Figure 1.3). The acidic region was shown to function in a context dependent manner, with pp28 accumulation at the AC being eliminated by relocalization of the acidic cluster to the carboxyl terminus of the pp28 protein (Seo & Britt, 2006). Together, these studies show pp28 to be essential for late (cytoplasmic) stages of CMV assembly. Interestingly, this is a similarity pp28 appears to share with pp150, wherein for both molecules the N-terminal region appears to play the more critical role.



Figure 1.4 Schematic diagram of HCMV pp28. The 190 aa pp28 protein contains a myristoylation sites at glycine 2 (G_2), an acidic domain located between aa 44-59 at the amino terminus and region located between aa 34-43, which are essential for pp28 function and replication of the virus.

1.1.2.2 Virus life cycle

To initiate infection, all viruses must deliver their genome into host cell (Figure 1.5). As an enveloped virus, HCMV entry requires the use of virus envelope proteins to facilitate adherence to the cell surface and fusion between the cellular membrane and the virus envelope. Fusion results in the transport of virion components into the cytoplasm, which is followed by transport of the capsid to the nucleus. The viral genome is then delivered to the nucleus through the nuclear pore (Smith & de Harven, 1974). The viral genome is used as a template for viral gene transcription leading ultimately to production of viral proteins, many of which are responsible for co-opting the cellular machinery and inhibiting the host immune response. This is followed by production of proteins involved in virus DNA replication at E early times. Later times of infection are concerned with virion assembly and egress (for review see: (Mocarski *et al.*, 2013). The entire replication process will be described in detail in the following sections.

1.1.2.2.1 Viral entry

During infection of the human host, HCMV productively replicates in many different cell types, including: fibroblast, epithelial, endothelial, monocyte-derived macrophage, smooth muscle, hepatocyte, stromal, and neuronal cells (Plachter, Sinzger & Jahn, 1996; Sinzger *et al.*, 2000). However, HCMV displays a relatively restricted cell tropism *in vitro*. Fibroblasts are the most commonly used cell type for CMV isolation and propagation in culture. HCMV appears able enter most cell types, with the restriction to full productive replication being associated with a post-penetration block in virus gene expression (Sinzger *et al.*, 2000). HCMV attachment and entry into fibroblasts is rapid and efficient, and occurs at neutral pH through direct fusion of the viral envelope with the plasma membrane (Compton, Nepomuceno & Nowlin, 1992). In other cell types like epithelial and endothelial cells, the virus enters via receptor-mediated endocytosis requiring low pH (Ryckman *et al.*, 2006). Although the complete repertoire of cellular receptors involved in mediating HCMV entry remain to be defined, the broad cellular tropism of the virus indicates that these receptor(s) are widely distributed across diverse cell types. The initial step in HCMV entry involves binding of gB to heparin sulphate proteoglycans present on the host cell surface, which is followed by subsequent interaction of gB with its non-heparin receptor resulting in a more stable binding state (Compton, Nowlin & Cooper, 1993). Platelet derived growth factor alpha (PDGFR-alpha) and epidermal growth factor (EGFR) receptors have been identified as two non-heparin gB binding receptors (Soroceanu, Akhavan & Cobbs, 2008).

Fusion of the viral envelope with the host cell membrane results in entry of the tegumented nucleocapsid into the cytoplasm. Tegument proteins facilitate transport the capsid to the nuclear pore through utilization of the cytosolic organelle transport network involving microtubules (Sinzger *et al.*, 2000). DNA is then released from the nucleocapsid and enters the nucleus through the nuclear pore complex. Tegument proteins pUL47 and pUL48, which

form a pUL47/pUL48 complex, appear to play a vital role in transporting capsids to the nucleus and possibly transporting the viral DNA into the nucleus. Mutant viruses lacking pUL47 have a delayed onset of IE gene expression and are less infectious compared to WT virus. Other studies suggest that the pp150 tegument protein may also be involved in this process. Nocodazole (a drug causing microtubule depolymerisation) is associated with diffuse cytoplasmic redistribution of pp150 throughout the cytoplasm, and was shown to prevent delivery of HCMV DNA to the nucleus and to block IE gene expression (Ogawa-Goto *et al.*, 2003). Once in the nucleus, DNA is circularized either by recombination between the repeat sequence at the terminal ends of the genome or by direct ligation of two ends of the genome (Mocarski *et al.*, 2013). The circularized DNA is localized near nuclear structures called nuclear domain 10 (ND10), where virus gene transcription occurs (Ahn, Jang & Hayward, 1999). Residual empty capsids remain at the cytoplasmic side of nuclear pores for several hours before disintegrating (Peng *et al.*, 2010).

1.1.2.2.2 Viral gene expression

Transcription of all herpesvirus genes, including those of CMV, occurs in the nucleus using host cell RNA-polymerase II and associated basal transcription machinery (Fortunato *et al.*, 2000). CMV gene expression can be classified into three major kinetic phases based on time of expression and sensitivity to inhibitors of protein translation and viral DNA synthesis. The three kinetic classes are: immediate-early (IE or α), early (E or β) and late (L or γ) genes (Fortunato *et al.*, 2000). IE genes are expressed immediately following virus entry. IE gene products regulate viral and cellular gene expression in order to optimize the cellular environment for virus genome replication, and are required to initiate the regulatory cascade that leads to appropriate expression of E genes.

Expression of E genes is dependent on the expression and availability of IE gene products, but does not require viral DNA synthesis. E genes can be divided into two subclasses β_1 (true-E) and β_2 (E-L) depending on time of expression. E gene products mostly encode non-structural proteins (for example, proteins involved in virus DNA genome replication such as viral DNA polymerase; UL54). Proteins involved in immune evasion such as the MHC down-modulators, US2 and US11 are also expressed at this time (Jones & Sun, 1997; Wiertz *et al.*, 1996).

L genes (γ phase) genes are similarly divided into two classes: γ_1 (partial-L) and γ_2 (true-L), with expression of γ_1 genes being amplified by viral DNA replication. The γ_1 genes are transcribed at low levels before DNA replication, which are then stimulated several fold following DNA replication. Expression of γ_2 genes is completely dependent on viral DNA replication. Examples of L genes include structural proteins and tegument proteins encoded by UL32 (PP150), UL94 (M94) and UL99 (pp28), which are all essential for late events of virion assembly and morphogenesis in the cytoplasm (see above) (AuCoin *et al.*, 2006; Silva *et al.*, 2003; Wing, Lee & Huang, 1996).

1.1.2.2.3 DNA replication

Replication of all herpesviruses occurs in the nucleus. Within 4 hours post-infection (hpi), the incoming linear HCMV DNA genome circularizes within the nucleus. For HCMV, DNA genome replication then occurs at between 14 to 24 hpi, and release of virus progeny starts from 36 hpi onwards. The peak of virus production occurs from between 60 to 80 hpi (yielding ~1000 copies of viral genome per infected cell); (Hertel & Mocarski, 2004). HCMV DNA synthesis requires a conserved set of six virus encoded replication fork proteins that together direct synthesis of the viral genome during productive lytic infection. The replication

fork proteins are as follows: DNA polymerase (encoded by UL54 and M54 for HCMV and MCMV, respectively), polymerase accessory enzyme (UL44/M44), single stranded (ss) DNA-binding protein (UL57/M57), and proteins of the heterodimeric helicase-primase (HP) complex (UL70/M70; UL120/M120) and the ATPase (helicase) subunit (UL105/M105) (McMahon & Anders, 2002; Rawlinson, Farrell & Barrell, 1996).

The DNA polymerase enzyme consists of pUL44 and pUL54. The pUL44 protein increases the processivity of DNA polymerase, which is essential for DNA replication. In addition to a 5' to 3' DNA synthesis function, DNA polymerase also contains a 3' to 5' endonuclease activity enabling 'proof-reading' of the large DNA genome. This HP complex has DNA-dependent ATPase, primase and helicase activities. Following unwinding of the heteroduplex genome DNA, the HP complex produces RNA oligonucleotides to prime polymerase elongation on the lagging DNA strand. As HCMV does not encode the necessary biosynthetic machinery for nucleotide biosynthesis, all dNTPs required for replication of the viral genome must be supplied by the host cell (Chee *et al.*, 1990). HCMV stimulates cellular transcription, translation and up-regulation of proteins involved in the biosynthesis of DNA precursors (Estes & Huang, 1977; Song & Stinski, 2002). At the same time, host cell DNA replication is prevented by a virus-induced block in progression of cell cycle (Fortunato *et al.*, 2000). Together, this HCMV-mediated regulation of the cell produces an environment rich in the necessary precursors for replication of the viral genome, whilst reducing competition of the host DNA replication machinery for replication of its own cellular DNA – a perfect parasite. Within the nucleus, HCMV DNA replication occurs in a structure called the 'replication compartment'. These structures are induced by the virus and then serve as sites for accumulation of proteins involved in viral genome replication (Wilkinson & Weller, 2003). Replication compartments initially form at the site of cellular ND10 nuclear bodies, which

are also the location at which the circular viral DNA genome localizes following release from the incoming nucleocapsid.

Within the herpesvirus genome, lytic DNA replication initiates at a specific site called the origin of DNA/lytic replication (ori-Lyt). Some herpesviruses, including beta-herpesviruses such as CMV have a single ori-Lyt , whilst others have two (EBV and VZV) or even three ori-Lyt sites (HSV-1 and HSV-2) (Roizman & Pellett, 2001). Following initiation at the ori-Lyt site, most evidence supports viral DNA replication occurring through a rolling circle (theta θ -based) mechanism similar to bacteriophage, with viral DNA synthesis resulting in the production of the large head-to-tail genome concatemers (Zhu *et al.*, 1998). These concatamers are then believed to serve as the substrate for the cleavage/packaging into newly synthesized capsid with unit length genome.

1.1.2.2.4 Virus assembly, maturation and egress

Capsid assembly and viral DNA packaging takes place in the nucleus of infected cells, with the assembly pathway being highly conserved across all herpesviruses (Kalejta, 2008). Following their synthesis in the cytoplasm, nucleocapsid proteins in the form of preassembled intermediates (see below) are translocated into the nucleus and accumulate as nuclear inclusion bodies, which give rise to the characteristic 'owl's eye' appearance of CMV infected cells. One preassembled capsid intermediate involves the viral major capsid protein (MC; pUL86) with the precursor of capsid assembly (scaffold) protein (pAP, pUL80.5) and proteinase precursor (pPR, pUL80a); (Fons *et al.*, 1986). A second intermediate consists of minor capsid protein (mCP; pUL85) together with mCP-binding protein (mCBP; pUL46) interacting to form triplexes. Following their translocation into the nucleus, these two intermediates undergo assembly into procapsids.

Immature procapsids undergo maturation via proteolytic cleavage of an associated scaffolding protein resulting in formation of B capsids. B capsids are then ready for packaging of viral DNA through a capsid pore and maturation into infectious C capsid with concomitant removal of the scaffolding protein (Oien *et al.*, 1997; Wood *et al.*, 1997). Cleavage of the scaffolding protein uses ATP to provide the necessary energy for encapsulation of the DNA within B capsids. This is followed by cleavage of the genome concatamer, following packaging of exactly one genome unit length, resulting in formation of mature C capsid. The mechanism by which HCMV DNA achieves the packaging of precisely one full unit length of genome per capsid is not completely understood.

Following C capsid formation, non-structural proteins, including those of the tegument control a complex two-stage Envelopment/De-envelopment/Re-envelopment process that precedes release of mature virions from the cell by exocytosis. Our understanding of this complex process is based primarily on studies using MCMV and HSV. The first step involves localization of C capsids to thickened concave patches in the inner nuclear membrane, which is then followed by budding of the capsid into the perinuclear cisternae of the ER (Gibson, 1996; Gibson *et al.*, 1996). The interaction of the virally encoded pUL53 with pUL50 proteins (along with other viral proteins) is essential for this initial localization of C capsids to the nuclear membrane, and appears to occur concurrently with capsid maturation (Lötzerich, Ruzsics & Koszinowski, 2006).

Following primary envelopment, de-envelopment delivers nucleocapsid into the cytoplasm for final assembly of the mature infectious enveloped virion at the assembly compartment (AC). The AC is a stable virus-induced structure composed of vesicles derived from the cellular secretory compartment. Virus proteins, including those present within the mature virion envelope, traffic to the AC and accumulate at the site. Most tegument proteins become associated with nucleocapsids during the final cytoplasmic phase of assembly at the AC.

However, some tegument proteins are also believed to become associated with the nucleocapsid during nuclear egress (Sanchez *et al.*, 1998; Tooze *et al.*, 1993). Host and viral kinases/phosphatases also contribute to the nuclear egress process (Steen *et al.*, 2000).

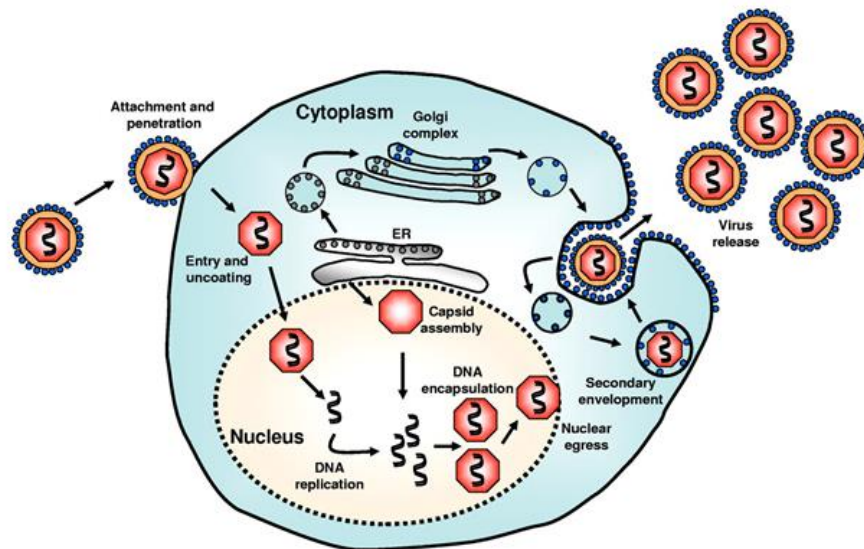


Figure 1.5 CMV life cycle. Virus enters host cells either through direct fusion or through the endocytic pathway depending on cell type. Virus attaches to cells through interaction of viral glycoproteins (including gB and gH) with heparin sulphate and other specific cell surface receptor(s). Fusion of the viral envelope with the cellular membrane releases nucleocapsid into the cytoplasm. The nucleocapsid is translocated to the nucleus, where viral DNA is released. Expression of IE gene triggers E expression, which is required for viral DNA replication. Virus DNA replication leads to the initiation of L gene transcription. Viral L genes encode proteins involved in DNA packaging and capsid assembly. Following its nuclear assembly, nucleocapsid enters the cytoplasm via a primary envelopment and then de-envelopment at the nuclear and then ER membranes. This is followed by final envelopment at the AC in the cytoplasm. The mature virus particles are then released by exocytosis at the plasma membrane, reprinted from (Crough & Khanna, 2009).

1.1.2.3 Pathogenesis of CMV

CMV is a widespread pathogen that infects between 40 to 100% of the population depending on age as well as location and socioeconomic status (Mocarski *et al.*, 2013; Pass, 2001; Selinsky *et al.*, 2005). After primary infection, virus is shed for weeks or months in bodily fluids including: tears, saliva, urine, semen and vertical secretions. HCMV is transmitted through direct contact with infected fluids and frequently occurs in the context of the childcare setting or during sexual contact. An additional route is through vertical transmission from mother to child during birth, via breast milk, or through the placenta during pregnancy (Pass, 2001). It is believed that these routes of vertical transmission play an important role in maintenance of CMV within the human population. Similar to all herpesviruses, HCMV has the ability to reactivate throughout the life of the host.

HCMV infection in healthy (immunocompetent) individuals is generally asymptomatic as the virus is controlled by the adaptive immune response. However, HCMV infection can cause life-threatening disease in immunocompromised individuals such as newborn infants, patients undergoing bone marrow or solid organ transplantation, and HIV infected individuals (Fowler *et al.*, 1992; Patrone *et al.*, 2003; Selik, Chu & Ward, 1995). In immunocompetent people symptoms are mild and include headache, malaise, fatigue, high fever, swollen lymph glands and rash. However, the clinical scenario is very different in the immunosuppressed. HCMV represents the most common viral cause of congenital infection and the leading viral cause of birth defects and brain damage in industrialized countries (Patrone *et al.*, 2003). Birth defects range from deafness and mental retardation to fatal disease that includes pneumonia, encephalitis, hepatitis, and hydrops fetalis (a fatal congenital condition that eventually leads to heart failure) Table 1.1. HCMV has also been implicated in proliferative and inflammatory diseases, including cancer and atherosclerosis (Shen *et al.*, 2004; Söderberg - Nauclér, 2006). The severity of medical problems associated with HCMV in

these vulnerable populations underlies the necessity for developing means for attenuation of HCMV-based vaccines, such that the attractive immunological characteristics (see below) can be safely exploited in all populations regardless of immune status.

Table 1.1 Human diseases caused by Herpesviridae members.

Subfamily/ viruses	Disease
<i>Alphaherpesviruses</i>	
Herpes simplex virus type 1	Skin sores, labial ocular lesions, encephalitis and conjunctivitis
Herpes simplex virus type 2	Genital lesions
Varicella-zoster virus	Chicken pox and Shingles
<i>Betaherpesviruses</i>	
	I. In immunocompetent individuals
	Enteritis, Infectious mononucleosis, Thrombocytopenia, severe anaemia and rarely encephalitis
	II. Congenital CMV
Human herpesvirus 5	Birth defects including mental retardation, vision & hearing loss
	III. In Immunocompromised individuals
	Lymphadenopathy, hepatitis, thrombocytopenia, nephritis, pneumonitis, gastrointestinal invasion and rarely encephalitis in transplant patients and vision loss and retinitis in AIDS patients
Human herpesvirus 6	Skin condition in infants called Exanthema subitum or Rosella infantum
Human herpesvirus 7	Skin condition in infants called Exanthema subitum or Rosella infantum
<i>Gammaherpesviruses</i>	
Epstein-Bar virus	Infectious mononucleosis associated with two rare forms of cancer: Nasopharyngeal carcinoma and Burkitt's lymphoma
Kaposi sarcoma-associated herpesvirus	Associated with Kaposi's sarcoma

1.1.2.4 MCMV as a model for HCMV infection

The strict host specificity of CMV means that HCMV can only be studied in humans. This has limited our understanding of many aspects of HCMV biology to extrapolation of findings from tissue culture using cells originated from humans. Empirical investigations of CMV *in vivo* are performed using related species-specific CMVs in their respective animal host. Murine CMV (MCMV) is a CMV of mice that provides a tractable *in vivo* model to investigate aspects of CMV biology, including persistence, latency and immunology with the hope of gaining insight into HCMV infection in humans. Many of the studies developing CMV as a vaccine vector platform have also been, at least initially for proof-of-concept, performed using recombinant MCMVs in mice (Morley, Ertl & Sweet, 2002; Tierney *et al.*, 2012; Tsuda *et al.*, 2011).

MCMV and HCMV share 80 conserved ORFs representing ~45% sequence identity between the two viruses (Rawlinson, Farrell & Barrell, 1996). MCMV is also similar to HCMV in term of kinetics of gene expression, course of infection, and associated pathology and host immune response to CMV infection. Infection of mice with MCMV is also believed to be similar to HCMV infection of humans in terms of the different stages of infection, but this has been more clearly defined in the experimental MCMV model. In this model, CMV infection can be divided into three temporally distinct stages: i) acute infection of central visceral organs, ii) persistent infection of salivary glands for several weeks, and iii) establishment of virus latency stage for the life of the host (Lu *et al.*, 2006).

The pathological outcomes of MCMV infection in mice resemble those of HCMV in humans during acute and persistent infection and during reactivation from latency after immune suppression. MCMV can cause severe infections or lethality (Krpmotic *et al.*, 2003) in immunologically immature or immunocompromised mice, whereas in immunocompetent

mice the virus can be re-activated from latency by immunosuppression (Sweet, 1999). However, a notable difference between the two viruses in their respective host species is that MCMV cannot be transmitted transplacentally to cause congenital defects in new born pups, which is due to differences in placental structure between rodents and primates. Nonetheless, the genetic and pathological similarities between these two viruses make the use of MCMV in mice an invaluable model for HCMV in humans, including for the development of CMV-based vaccines.

1.2 CMV Mutagenesis

1.2.1 Generation of recombinant CMVs

Functional characterization of viral genes by generating virus mutants has been important for the advance of many different areas of CMV research. The ability to construct recombinant CMVs expressing heterologous pathogen target antigens has similarly enabled translational studies towards the development of CMV-based vaccines.

1.2.1.1 Methods of mutagenesis prior to BAC-based technology

Mutagenesis of the herpesvirus genome has shown considerable technology-driven advances over the past 40 years. Compared to the relatively straightforward molecular manipulation of many viruses, the large genome combined with relatively slow growth of CMV in culture have been the main technological issues to be overcome for genetic manipulation of CMV. More than forty years ago a classical genetic approach using chemical-based mutagenesis was used to introduce random mutations into the herpesvirus genome for production of temperature-sensitive mutants, via point mutations, deletions or insertions (Brune, Messerle & Koszinowski, 2000). In spite of the large number of mutants generated by this technique, definitive identification of specific mutation(s) responsible for observed phenotypes and

exclusion of second site mutations were an inherent problem of such non-targeted mutagenic approaches (Sweet *et al.*, 2007).

Generation of the first recombinant herpesvirus using site-directed mutagenesis was reported in the early 1980s, by using homologous recombination performed in permissive eukaryotic cells (Mocarski, Post & Roizman, 1980). Homologous recombination was initially used for introduction of mutations into individual genes of HSV, and then later adapted for other members of herpesvirus family, including CMV (Manning & Mocarski, 1988; Spaete & Mocarski, 1987). In this method, the mutation together with a selectable genetic marker is introduced into the target gene via the eukaryotic cellular recombination machinery. Homologous recombination utilizes a ubiquitous cellular pathway that is essential for many cellular processes, including maintenance of genomic integrity, segregation of chromosomes during meiosis, and rescue of stalled or collapsed replication forks as well as a function in telomere maintenance. Homologous recombination provides a means for repair of DNA double stranded breaks which occur either during DNA replication or following DNA damage by external factors such as irradiation (Heyer, 2006; Hunter, 2007; Muyrers *et al.*, 2000).

The main disadvantage of this method is that selection procedures to purify recombinant viruses from WT virus are required. Since WT is over-represented in the resulting virus pool these procedures are generally laborious (especially for a slow growing virus such as CMV) requiring multiple rounds of selection. As selection is dependent on replication of the virus, isolation of recombinant viruses can be difficult if the mutation results in severe growth defects. Furthermore, completely replication-defective 'null' mutants of genes essential for viral growth can only be produced with parallel creation of complementing cell lines that provide the essential gene product in *trans* (DeLuca, McCarthy & Schaffer, 1985). Such cell

lines are notoriously difficult to produce, especially as many of the viral proteins will have cellular toxicity associated with their stable expression in cells.

Almost a decade later a methodology based on use of overlapping cosmid clones was developed that overcame some of the problems associated with WT virus (Van Zijl *et al.*, 1988). In this system, viral genomes were sub cloned into *E. coli* and maintained as a set of overlapping cosmid clones. Genetic mutations were then introduced into the single respective cosmid clone containing the herpesvirus gene being targeted. Recombinant viruses are reconstituted by cotransfection of permissive eukaryotic cells with the mutated clone, together with the remaining cosmid set. The main advantage of this approach was that the introduction of markers and selection against non-recombinant WT virus was not required as only recombinant virus is reconstituted (Brune, Messerle & Koszinowski, 2000).

However, the overlapping cosmid system still has several disadvantages including the difficulty of finding unique restriction sites within the large cosmids to use for genetic manipulation. Reconstitution of the viral genome in cell culture also required many recombination events to reassemble the entire full-length genome, which could lead to acquisition of unwanted 'off-target' mutations. Maintenance of the genetic stability of the cosmid clones also proved difficult, especially in those cosmids containing viral containing multiple repeat elements known to be susceptible to deletion or rearrangements. Finally, construction of the necessary reverting viruses needed to confirm that the observed phenotype in the recombinant virus is not due to an unwanted mutation elsewhere in the genome, was difficult with the cosmid-based technology.

1.2.1.2 Methods of mutagenesis using bacterial artificial chromosome (BAC)-based technology

The development of BAC-based technology for genetic manipulation of herpesvirus genome in the late 1990s, whereby the viral genome is maintained as an infectious BAC within *Escherichia coli* (*E.coli*), was a watershed moment for the CMV field (Messerle *et al.*, 1997) (Messerle *et al.*, 1997). BACs are DNA constructs based on the fertility (F) factor plasmid of *E. coli* (Shizuya *et al.*, 1992). The size of herpesvirus genomes, which range in size from 125-240 kb exceeds the cloning capacity of an individual plasmid or cosmid which can incorporate up to 10 or 30 kb of DNA, respectively (Warden, Tang & Zhu, 2010). Yeast artificial chromosomes (YACs) are able to carry larger regions of DNA (>2000 kb). However, YACs are not ideally suited to cloning of herpesvirus genomes as they are prone to undesired genomic rearrangements, especially between repetitive sequences as frequently occur in these viruses (Monaco & Larin, 1994; Ramsay, 1994). In contrast, F plasmids were shown to be capable of propagating mammalian DNA inserts with significantly higher stability (Kim *et al.*, 1992). Using the BAC technology, large DNA fragments from varied genomic sources can be maintained as a genetically stable F plasmid. This single foreign DNA source is then amenable to genetic manipulation by using bacterial-based genetic methodology (Shizuya *et al.*, 1992).

The demonstrated ability of F plasmids to stably maintain eukaryotic DNA fragments >300 kilobases (kb) (Shizuya *et al.*, 1992) led to the first adaptation of this system for the maintenance of herpesvirus genomes in the form of MCMV (Messerle *et al.*, 1997). This novel technique has subsequently proved to be an invaluable tool for the manipulation of multiple different herpesvirus genomes (including HCMV and rhesus CMV) (Chang & Barry, 2003; Messerle *et al.*, 1997; Redwood *et al.*, 2005). Infectious CMV virus is reconstituted by transfection of purified BAC DNA containing the entire herpesvirus genome sequence into permissive eukaryotic cells (Messerle *et al.*, 1997). Since the CMV genome is maintained in

bacteria without the requirement for virus replication, a significant advantage of BAC-based technology over earlier systems was that mutations could be introduced into any viral gene, including null mutations into essential genes (Messerle *et al.*, 1997; Wagner *et al.*, 1999).

1.2.1.2.1 The BAC vector

Cloning the herpesvirus genome as a BAC requires the BAC cassette sequence to be inserted into the viral genome (using homologous recombination in eukaryotic cells; see above (Warden, Tang & Zhu, 2010)). A typical BAC cassette is approximately 8 kb in size and contains all the genetic components required for maintenance of the BAC within bacteria, including an origin of replication (*oriS*) and replication gene (*repE*) involved in monitoring replication of the F plasmid. The BAC cassette also contains *ParA* and *ParB* genes that control the rate of replication so that the number of copies is limited to one or two copies in the bacterial cell (Shizuya *et al.*, 1992). This ability to maintain the BAC at low copy appears critical for stability as it reduces the opportunity for recombination. The cassette also contains a selectable antibiotic resistance gene, most commonly chloramphenicol in order to select the bacterial colonies containing the BAC.

For insertion of the BAC cassette into the viral genome the cassette is flanked by 0.5 to 1 kb of homologous sequence to the site of desired insertion within the CMV genome, which is generally a non-essential region of the virus which selected to avoid growth defects in the virus (Messerle *et al.*, 1997; Warden, Tang & Zhu, 2010). Transfection of the homology-flanked BAC cassette into CMV infected cells then results in formation of recombinant viruses containing the BAC cassette as a consequence of homologous recombination.

F plasmids must be circularized in order to replicate and be stably maintained within bacteria as an artificial chromosome. This necessitates isolation of the herpesvirus genome containing

the BAC cassette only after circularization of the viral genome, which occurs for HCMV within approximately 4 hpi (see above). This procedure relies on adaptation of a protocol developed by Hirt (1967) for the isolation of small circular DNA molecules from eukaryotic cells (Eizuru, Inagawa & Minamishima, 1984). The isolated circular viral DNA is then transformed into a suitable *E. coli* strain (DH10B or DH5 α) where the CMV BAC can be propagated and genetically modified. Bacterial genetic engineering can now be brought to bear against the generation of targeted mutations in the viral genome.

Infectious recombinant virus is reconstituted by transfection of the genetically modified virus BAC DNA into a suitable permissive eukaryotic cell lines (Warden, Tang & Zhu, 2010). In the past years, multiple herpesviruses have been cloned as infectious herpesvirus BACs (Tables 1.2 and 1.3). Among those listed is MCMV (Smith strain; Messerle *et al.*, 1997), which is relevant to the studies of this dissertation. The availability of herpesvirus genomes cloned as BACs allows modification of the viral genome and opens the way for myriad applications, such as using these cloned viruses as vehicles for development as vaccine and gene therapy platforms.

Table 1.2 BAC-cloned human herpesviruses

BAC-based human herpesvirus name	Representative studies
Herpes Simplex Virus-1 (HSV-1)	(Horsburgh <i>et al.</i> , 1999)
Herpes Simplex Virus-2 (HSV-2)	(Meseda <i>et al.</i> , 2004)
Varicella Zoster Virus (VZV)	(Nagaike <i>et al.</i> , 2004)
Epstein-Barr Virus (EBV)	(Delecluse <i>et al.</i> , 1998)
Cytomegalovirus (CMV)	(Borst <i>et al.</i> , 1999; Hahn <i>et al.</i> , 2003; Murphy <i>et al.</i> , 2003)
Human Herpesvirus 6 (HHV-6)	(Borenstein & Frenkel, 2009)
Kaposi's Sarcoma-Associated Herpesvirus (KSHV)	(Zhou <i>et al.</i> , 2002)

Table 1.3 BAC-cloned animal herpesviruses

BAC-based animal herpesvirus name	Representative studies
Bovine Herpesvirus Type I (BHV-1)	(Mahony <i>et al.</i> , 2002; Trapp <i>et al.</i> , 2003)
Bovine Herpesvirus Type 4 (BoHV-4)	(Gillet <i>et al.</i> , 2005)
Equine Herpesvirus Type I (EHV-1)	(Rudolph, O'CALLAGHAN & Osterrieder, 2002)
Feline Herpesvirus Type I (FHV-1)	(Tai <i>et al.</i> , 2010)
Guinea Pig Cytomegalovirus (GPCMV)	(McGregor & Schleiss, 2001)
Herpesvirus Saimiri (HVS)	(White, Calderwood & Whitehouse, 2003)
Koi Herpesvirus (KHV)	(Costes <i>et al.</i> , 2008)
Marek's Disease Virus (MDV)	(Schumacher <i>et al.</i> , 2000)
Murine Cytomegalovirus (MCMV)	(Bubeck <i>et al.</i> , 2004; Messerle <i>et al.</i> , 1997) (Brune <i>et al.</i> , 1999)
Murine Gammaherpesvirus 68 (MHV-68)	(Adler <i>et al.</i> , 2000)
Pseudorabies Virus (PRV)	(Smith & Enquist, 1999)
Rhesus Cytomegalovirus (RhCMV)	(Chang & Barry, 2003)
Rhesus Rhadinovirus (RRV)	(Estep <i>et al.</i> , 2007)
Herpesvirus of Turkeys (HVT)	(Baigent <i>et al.</i> , 2006)

1.2.1.2.2 BAC targeted mutagenesis by Red-mediated homologous recombination

Although BAC cloning of herpesvirus genomes was a major technical advance, the genetic manipulation of these BACs still proved cumbersome. Initial methodologies were based on the RecA recombination system of bacteria and utilized sequential cycles of positive and negative selection with an antibiotic and the SacB marker, respectively. Following selection of clones containing the desired mutation based on antibiotic resistance, the SacB gene was then used as a negative marker to remove both itself as well as the antibiotic gene, thereby leaving only the desired mutation in an otherwise WT genome. SacB encodes a protein called levansucrase, which catalyses the polymerization of fructosyl group in sucrose to form a lethal substance called levan which is toxic to *E. coli* (Bramucci & Nagarajan, 1996; Lepesant *et al.*, 1972; Wagner, Ruzsics & Koszinowski, 2002). However, the propensity for SacB inactivation, which would confer on a clone the ability to grow in the presence of sucrose without removal of the antibiotic resistance marker or the (now inactivated) SacB gene, was a major problem with this system.

In late 1990, a one-step mutagenesis strategy called E/T cloning was developed that was to revolutionize genetic manipulation of herpesvirus BACs (Zhang *et al.*, 1998). This method uses the recombination functions of recombination proteins either *recE* and *recT* genes from prophage Rac or *red α* and *red β* genes from bacteriophage λ (Muyrers *et al.*, 1999; Zhang *et al.*, 1998), or a defective lambda prophage (Lee *et al.*, 2001; Yu *et al.*, 2000). The γ Red-encoded *exo*, *bet*, and *gam* are required for mediated recombination of short (>40 bp) homologous regions at both ends of the linear DNA fragment carrying the desired mutation, therefore allowing insertion of the linear DNA fragment at any site within the CMV BAC (Ruzsics & Koszinowski, 2008). The *exo* gene product encodes a 5'-3' exonuclease activity which produces 3' overhangs from introduced ds-DNA targeting cassettes. The *bet* gene product is a ss-DNA binding protein that binds to the 3' overhang and promotes

recombination between the ds-DNA targeting cassette and regions of identical sequence within the BAC. At the same time, the *gam* gene function, prevents the degradation of linear DNA fragments by E.coli RecBCD exonuclease through inhibition of RecBCD.

A notable advantage of E/T recombination over the earlier RecA-based system was the need for homologous sequences of only 40 bp compared to >1000 bp (of homology flanking the site targeted) for Rec A-based mutagenesis (Muyrers *et al.*, 1999; Wagner, Ruzsics & Koszinowski, 2002). The homology sequences can also be freely selected, since the E/T recombination system does not require the presence of restriction enzyme recognition sites for cloning or excision of the targeted DNA sequence. Due to the short stretch of homology required for targeting, linear DNA fragments can also be generated by polymerase chain reaction (PCR) (Adler, Messerle & Koszinowski, 2003; Wagner, Ruzsics & Koszinowski, 2002; Zhang *et al.*, 1998). Following mutagenesis the marker gene can be removed by flanking the antibiotic resistance marker with short (34 bp) recombination sequence recognition sequences such as with FRT (FLP recognition target) or *LoxP* (locus of crossing over P1 phage) sites (Zhang *et al.*, 1998).

1.2.2 Herpesviruses as a vaccine vector

1.2.2.1 Viral vectors

The basic aim of viral vaccines is to elicit a protective host immune response while avoiding disease from the vaccine itself. These delivery systems express the antigens within the cells of the vaccinated individual *in situ* thereby eliciting a strong immune response, but are removed from the deleterious effects of the pathogen. A number of different virus-based vaccine vector platforms are being developed. These platforms differ in a variety of characteristics, such as their level of persistence in the host, cellular tropism, carrying capacity for heterologous genetic material and quality and magnitude of associated immune

responses (Skenderi & Jonjić, 2012). Virus-based vaccines have advantages compared to other vaccine modalities in that they are able to activate both CD8⁺ and CD4⁺ T cell responses, which are essential both for control of intracellular pathogens via direct killing of infected cells, but also for induction of robust antibody responses (Liu, 2010a). The ability of viral vectors to induce CD8⁺ T cells enables targeting of pathogen proteins or epitopes not normally exposed to antibodies, which are commonly more conserved regions. It is hypothesized that this capacity may be especially important for vaccination against highly divergent microbes like influenza A (IA) virus (Osterhaus, Fouchier & Rimmelzwaan, 2011).

Traditionally, viral vaccine vectors are unable to establish a persistent infection within the vaccinated individual, being either completely replication defective or at most only able to establish an acute, limited infection cycle. These conventional vaccines, which still express their target antigen intracellularly, are able to stimulate cellular immune response (both CD4⁺ and CD8⁺ T cells) and humoral immune responses without causing diseases. Although these classical vaccines have been successful for controlling some diseases (e.g. smallpox, yellow fever, measles, rubella and a number of other viral diseases), they have not been successful for more difficult to control pathogens such as HSV and human immunodeficiency virus.

CMV has recently been developed as an innovative vaccine platform that may have considerable advantages over other existing virus-based vector vaccine systems. CMV is one of the most immunogenic viruses known (Sylwester *et al.*, 2005) inducing a high immune response enriched for effector memory T- cells, T_{EM} (Hansen *et al.*, 2009), which commonly exceed 10% of the memory population for both CD4⁺ and CD8⁺ compartments (Sylwester *et al.*, 2005). T_{EM} cells are a subtype of memory CD8⁺ T cells, which tend to localize in peripheral and lymphoid tissue and are functionally primed for immediate defence at entry sites of the pathogen (Roberts, Ely & Woodland, 2005). This is because T_{EM} are resident in

the lung airway and other similar effector tissue sites, so have the ability to mediate early control of a secondary virus infection (Roberts, Ely & Woodland, 2005).

Several studies have shown CMV vectors to be effective at inducing protective immunity against different pathogens and pathogen associated toxins, including tetanus (Tierney *et al.*, 2012), highly virulent Ebola virus (Marzi *et al.*, 2016; Tsuda *et al.*, 2011) and simian immunodeficiency (SIV) virus (Hansen *et al.*, 2011; Hansen *et al.*, 2009). The efficacy of a CMV-based vaccine was initially demonstrated by the ability of RhCMV-based vectors expressing SIV target antigens to induce immunity against SIV in rhesus macaques (Hansen *et al.*, 2009). Approximately half of vaccinated animals resisted establishment of chronic SIV systemic infection, and T_{EM} based CD8⁺ T cells appeared to play a primary role in mediating this protection (Hansen *et al.*, 2011; Hansen *et al.*, 2009). Comparison with rhesus macaques vaccinated with a conventional recombinant adenovirus (Ad5) vaccine, which induces a primarily central memory T cell (T_{CM}) response, suggested that the ability of the RhCMV/SIV vaccine to maintain an SIV-specific T_{EM} response in these sites corresponded with its ability to stringently control the highly pathogenic SIV infections early after mucosal challenge (Hansen *et al.*, 2011).

MCMV-based vaccines have also been shown to induce protective immunity against a variety of pathogens. In a series of studies, expression of a single CD8⁺ T cell epitope of the Ebola virus nucleoprotein was shown to protect against infection with this highly virulent human pathogen (Tsuda *et al.*, 2011; Tsuda *et al.*, 2015). These studies also reemphasized the unique characteristics of the immune response against the Ebola virus antigen, with the expansion (inflation) of the NP-specific CD8⁺ T cell response over time. Inflation is a unique characteristic of CMV-induced immune responses characterized by the continuous accumulation of a large number of virus-specific CD8⁺ T cells in the blood (Karrer *et al.*,

2004), corresponding with maturation of a stable T_{EM} (memory) response with immediate effector function at mucosal epithelial effector sites which persists for life.

Most previous studies have focused on the T cell responses induced by CMV vectors. However, a number of studies indicate that CMV vectors may also be able to induce significant antibody responses against their encoded target antigen. A MCMV-based vaccine platform, encoding the tetanus toxin fragment C, induced sustained levels of protective antibodies essentially for the life of the mouse, following only a single dose of vaccination (Tierney *et al.*, 2012). A more recent study demonstrated the ability of a RhCMV-based vaccine expressing the full-length Ebola virus GP to protect against a lethal Ebola virus challenge. Interestingly, vaccination induced high levels of GP-specific antibodies with no detectable GP-directed T cell response, which corresponded to control of GP expression by the endogenous RhCMV Rh112 promoter expressed with L kinetics (Marzi *et al.*, 2016). In summary, CMV may be considered a unique vaccine vector platform due to its ability to elicit high levels of T_{EM} CD8⁺ T cell responses. Recent studies also suggest that the vector can be genetically engineered towards production of antibodies as well as T cells.

In this thesis, the MCMV mouse model is used for initial investigations into development of CMV as a vaccine platform. Studies detailed in Chapter 3 of this thesis use MCMV to examine the ability of a destabilization domain strategy to generate a conditionally replication-defective MCMV vaccine vector that can be produced *in vitro*, but will be attenuated *in vivo*. Chapter 4 is concerned with the initial development of a MCMV-based vector expressing internal conserved proteins of IA virus towards development of a universal IA vaccine.

1.3 CMV Attenuation

1.3.1 CMVs as an attenuated vector platform

Apart from their attractive immunological characteristics, fully replicating viral vectors such as CMV also have a number of potential disadvantages; a main one being the concern associated with *in vivo* gain-in virulence and diminished vaccine safety profile. Due to the pressure of selection on the replicating vector, stability of the heterologous target antigen may also be a concern if there is any selective disadvantage associated with expression of the target antigen gene. Viral vectors may also become virulence through recombination with endogenous viruses (Liu, 2010b)- albeit this is less of a concern for benign vectors like CMV. These concerns have led to the development of means of attenuating replicating viral vectors to improve their safety profile.

Initial attenuation strategies relied on repeated passage under suboptimal conditions in either cultured cells or non-host animal species. These approaches have proven to be an effective means for attenuation of both virus as well as bacterial based vaccines. However, there are a number of safety concerns associated with the use of this approach, the main one being the inability to clearly define the mutation(s) responsible for the attenuation as well as the possibility for reversion of the vaccine to WT virulence-in large part because the nature of the attenuating mutation is not known (Lauring, Jones & Andino, 2010).

Development of methodology for genetic manipulation of microbial genomes has enabled identification of many genes essential for viral replication and assembly through deletion or mutation of these genes. This knowledge has enabled targeted attenuation in which the attenuating mutation is clearly defined. Permanent inactivation of targeted genes requires propagation of the attenuated vector on a complementing cell line that expresses the missing viral gene(s) allowing viral replication. In the vaccine recipient, the virus is however unable to produce virus progeny, but viral genes are still expressed within the infected cells inducing

a strong immune response (Dudek & Knipe, 2006). The first use of a replication-defective virus as a vaccine was a HSV-1 strain with a deletion of a gene (ICP8; the major DNA-binding protein) essential for genome replication, which was shown to protect mice from HSV-1 infection (Nguyen, Knipe & Finberg, 1992). This virus induced a protective immune response similar to its replication-competent parental virus (Morrison & Knipe, 1996).

A main advantage of a replication-defective vaccine is the high level of safety that results from permanent genetic inactivation of the essential gene. However, the requirement for complementing cells to support growth of null mutants can be difficult to achieve, since the expression pattern of the essential gene is important for their function and because exogenous promoters often fail to reproduce the appropriate regulation observed with endogenous promoters (Pan *et al.*, 2016). This is expected to be an even greater concern for vaccine platforms with complex gene expression profiles such as herpesviruses, which is reflected by the small number of complementing cell lines that have been established for herpesvirus null mutants. This is further complicated for the β - and γ - herpesvirus subfamilies, as many of these viruses can only be propagated on primary cell cultures (Borst *et al.*, 2008; Mocarski *et al.*, 1996; Silva *et al.*, 2003).

1.3.2 Conditional expression of essential genes and mutants of CMV

An alternative strategy to deletion mutagenesis that avoids the need for *trans*-complementation is conditional expression of the essential gene being targeted. Conditional gene expression was initially used for the study of virus gene function. The first generation of conditionally-attenuated herpesviruses were temperature sensitive (*ts*) mutants, where they were shown to be often superior to null mutants in identifying viral functions (Whitley, Kimberlin & Roizman, 1998). Most of the *ts* mutants described are alpha-herpesviruses

(Schaffer *et al.*, 1973). Propagation of conditional beta-herpesvirus mutants by selection of a *ts* allele is technically more difficult, presumably due to the slower replication of the virus (Akel & Sweet, 1993), with generation of only a single HCMV *ts* mutant (UL122 gene) (Heider, Bresnahan & Shenk, 2002). More recent approaches have focused on conditional regulation of gene transcription. These have included tetracycline-regulated transactivation systems (Furth *et al.*, 1994). These systems have proved invaluable for elucidation of CMV gene function particularly in the MCMV model (Rupp *et al.*, 2005).

Recently, a novel strategy was established for conditional regulation of proteins at the level of protein stability. This strategy is based on fusion of targeted essential virus proteins to a small metastable protein domain (called a destabilization domain, DD), which results in stability of the targeted protein becoming dependent on the presence of a small molecule ligand (Banaszynski *et al.*, 2006). Two DD systems are currently in use, which are based on either rapamycin-binding protein (FKBP), or *E. coli* dihydrofolate reductase (ecDHFR). Both DD systems were engineered to be metabolically unstable in the absence of their high affinity, cell-permeable small ligands, Shield-1 or trimethoprim (TMP), respectively. The instability of the DD fused target protein results from degradation by the cellular proteasome. The addition of a ligand stabilizes the DD restoring their biological function in a rapid, reversible and ligand dose dependent manner (Figure 1.6; Banaszynski *et al.*, 2006; Iwamoto *et al.*, 2010).

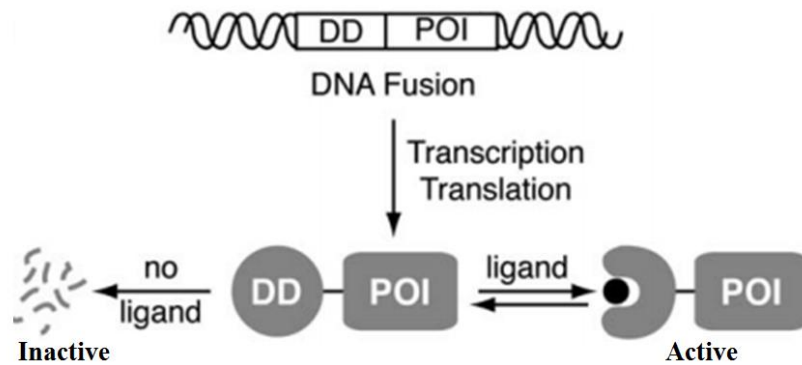


Figure 1.6 A general method of destabilization domain strategy. Destabilization domain (DD) protein fused genetically to a protein of interest (POI), the fusion results in degradation of the entire fusion protein. In the presence of a small synthetic ligand, the fusion protein is stabilized and protected from degradation, whereas the lack of ligand results in degradation of the fusion protein. Adopted from (Banaszynski *et al.*, 2006).

A 2009 study demonstrated the ability of a DD strategy to generate conditionally replicating CMV mutants using the dFKBP/Shield-1 system (Glaß *et al.*, 2009). The dFKBP was fused to three essential CMV genes: major IE protein of MCMV and HCMV and two uncharacterized essential proteins of HCMV, pUL51 and pUL77. The dFKBP was added to the N-terminal of the respective proteins since it had been reported that N-terminus DD fusion resulted in better control of protein levels than fusion of the C-terminus (Banaszynski *et al.*, 2006). Introduction by transfection of the recombinant MCMV BAC DNAs into permissive fibroblasts in the presence of shield-1 enabled virus reconstitution for all of the mutant viruses except the DD-destabilized pUL77 mutant. This suggested that fusion to the N-terminus may have interfered with an essential function of pUL77, which was supported by the ability to recover infectious virus in the presence of Shield-1 when the dFKBP DD domain was instead fused to the C-terminus of pUL77. For efficient complementation

concentrations of ligand were required that differed depending on the essential protein being targeted. Reversibility of this conditional attenuation system was also shown by withdrawal or addition of Shield-1 (Glaß *et al.*, 2009).

The ecDHFR-based system based on a mutant *E. coli* dihydrofolate reductase and its commercially available trimethoprim (TMP) as a stabilizing ligand was subsequently developed by the same laboratory as the FKBP/Shield-1 system (Iwamoto *et al.*, 2010). A major advantage was one of cost of the DD stabilizing ligand (TMP), which had essentially limited the FKBP/Shield-1 system to *in vitro* and small animal studies. The ecDHFR is a 159 aa-residue enzyme that reduces dihydrofolic acid to tetrahydrofolate acid, which is essential as a methyl group donor for several steps in prokaryotic primary metabolism (Schnell, Dyson & Wright, 2004).

As a DD, ecDHFR possesses desired characteristics including, low protein level in the absence of TMP (i.e. low basal stability), robust and predictable dose-response behaviour, large dynamic range and rapid kinetics of degradation (Iwamoto *et al.*, 2010). TMP is a well-characterised drug that is commercially available, inexpensive and possesses good pharmacological characteristics. TMP is used mainly in the treatment of urinary tract infection through its effect on ecDHFR activity. TMP is one of the most widely used antibiotics since it binds with higher affinity (>60,000 times) to bacterial rather than human DHFR and as a result inhibits bacterial DHFR far more potently than mammalian DHFR (Matthews *et al.*, 1985). These attractive pharmacological properties of TMP and commercial availability coupled with the specificity of the ecDHFR-TMP interaction and low cost makes this destabilized protein-ligand pair ideal for development as a DD strategy.

DD-based strategies have been shown to work successfully in multiple *in vivo* studies in mice (Banaszynski *et al.*, 2008). DD system have also been used in other organisms, including:

Plasmodium falciparum (Dvorin *et al.*, 2010; Muralidharan *et al.*, 2011; Russo *et al.*, 2009), *Toxoplasma gondii* (Herm-Götz *et al.*, 2007) and also applied to conditionally regulate protein expression levels in *Caenorhabditis elegans* (Cho *et al.*, 2013). Although, the DD-ligand system has successfully been applied to regulate many proteins of CMV (Table 1.4), it has been shown in (at least one study) that the strategy may not be applicable to all virus proteins (Fehr & Yu, 2011). In the current study, we analysed the applicability of the replication defective technology to generate conditionally replicating MCMV mutants, whose growth is dependent on the ligand TMP, by fusing the ecDHFR domain protein to two essential tegument proteins of MCMV: pp150 and pp28.

Table 1.4 Destabilization domain strategy used to regulate proteins of CMV

ORF	Gene properties	Reference
IE1/IE2	Multifunctional essential proteins	(Glaß <i>et al.</i>, 2009)
IE1/IE3	Multifunctional essential proteins	(Glaß <i>et al.</i>, 2009)
pUL77	Participate in CMV genome cleavage and packaging	(Glaß <i>et al.</i>, 2009)
pUL117	Is required to block host DNA synthesis during HCMV infection	(Qian <i>et al.</i>, 2010)
UL96	Preserves the integrity of PP150-associated nucleocapsids during translocation from the nucleous to the cytoplasm	(Tandon & Mocarski, 2011)
pUL79	Promote the accumulation of late viral transcripts following HCMV DNA replication	(Perng <i>et al.</i>, 2011)
pUL51	Essential for viral genome cleavage-packaging	(Borst <i>et al.</i>, 2013) (Glaß <i>et al.</i>, 2009)
UL48	Has role in intracellular capsid transport and has deubiquiting enzyme activity	(Das <i>et al.</i>, 2014)
UL94	Essential for cytoplasmic egress and binds to ss-DNA	(Das <i>et al.</i>, 2014)
UL103	May have a role in viral replication, controls virions and dense body egress	(Das <i>et al.</i>, 2014)

1.4 Influenza A Virus

1.4.1 Influenza and influenza viruses

Influenza (flu) in humans is an acute, highly contagious respiratory illness that mainly affects the respiratory tract (i.e. the bronchi, throat and nose; (Kreijtz, Fouchier & Rimmelzwaan, 2011). Flu is characterised by muscle pain, sudden onset of fever, headache, severe malaise with a sore throat, nasal inflammation and non-productive cough (Lamb, Krug & Knipe, 2001). Influenza is caused primarily by the influenza A (IA) virus. During seasonal epidemics, IA viruses are responsible for 3-5 million cases of severe infections worldwide (Subbarao, Murphy & Fauci, 2006). Although most people recover from IA virus infection within 1-2 weeks without requiring medical treatment, infection can result in pneumonia, hospitalisation and death in the elderly, very young or chronically ill people (Lamb, Krug & Knipe, 2001).

IA virus continue to have a major worldwide impact on humans health, with seasonal IA viruses alone causing 250,000-500,000 deaths worldwide annually (Drape *et al.*, 2006; Razuri *et al.*, 2012).

There are three genera of influenza virus: type A, B and C all belonging to the *Orthomyxoviridae* family, which is a group of enveloped negative-sense, ss-RNA viruses with a segmented genome (Palese & Shaw, 2007). Influenza viruses can be characterized based on morphological features, sequence variability in surface glycoproteins, antigenic differences, protein-encoding mechanisms and number of RNA segments (Lamb, Krug & Knipe, 2001; Zambon, 1999). IA virus has a broad host range and naturally infects a variety of birds and mammals including humans, horses, pigs and sea mammals. The natural reservoir for IA viruses is aquatic birds (Webster *et al.*, 1992). Influenza B (IB) and C (IC) viruses in contrast are normally found only in humans (Lamb, Krug & Knipe, 2001). This difference in breadth of species tropism is the main reason for only IA viruses being able to

cause pandemic disease. As IB and IC only infect humans, and thus can never evolve outside of the human population, most humans will have some level of immunity against these viruses (Gioia *et al.*, 2008). This is not the case for IA, which is maintained and can evolve remotely from the human population, only to be reintroduced without warning into a potentially immunologically naïve population.

1.4.2 IA virus virion structure

The IA virus particle has a typical diameter of 80-160 nm, surrounded by a lipid bilayer envelope that is derived from the host cell membrane during the budding process (Figure 1.7). The IA virus particle is coated with two surface glycoproteins: hemagglutinin (HA) and neuraminidase (NA) protruding from the lipid bilayer in an approximate ratio of 4:1. Laver & Valentine, 1969 were first to describe that the surface spikes visible by EM were the HA and NA proteins (Figure 1.8). Also embedded within the viral envelope is the integral membrane matrix 2 protein (M2). M2 overlays matrix 1 (M1) protein that encloses the virion core and structurally supports the particle.

The virion particle is pleomorphic in shape, ranging from spherical to filamentous depending on the viral strain and cell-type used for propagation (Lee & Saif, 2009; Noda & Kawaoka, 2010). The filamentous form was first described in 1949 (Chu, Dawson & Elford, 1949). EM analysis of lung tissue from a patient who died as a result of 2009 H1N1 pandemic flu, (Swine-Origin strain) revealed a similar filamentous shape of virus particles (Rossman & Lamb, 2011).

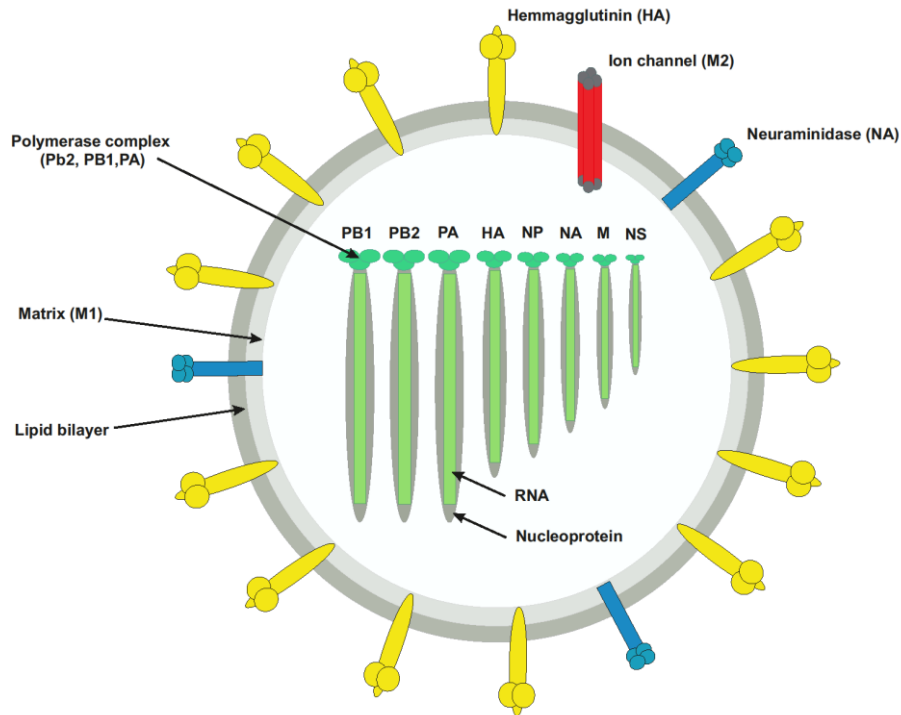


Figure1.7. Schematic showing the structure of the IA virion. The genome of the IA virus consists of eight ss-RNA segments. The virion envelope contains two surface glycoproteins: HA and NA. The integral M2 protein is also located within the envelope, where the protein functions as an ion channel. The M1 protein is located immediately underneath the virus envelope and interacts with both the surface proteins and the ribonucleoprotein (RNP) complex. The RNP complex comprised of PB1, PB2 and PA, together form the RNA polymerase. The non-structural NEP/NS2 protein is also localized within the virion, whereas NS1 is found only in infected cells. Adapted from (Lee & Saif, 2009).

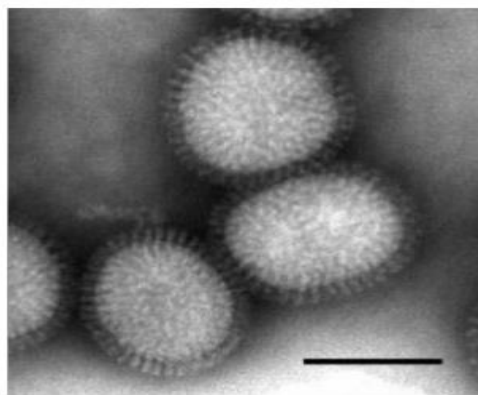


Figure 1.8 EM of purified IA virions. Virions are covered with spikes composed of HA and NA (Bar; 100 nm). Printed from (Noda & Kawaoka, 2010).

1.4.2.1 IA virus genome

The 13,600 nt genome of influenza virus is organised into eight segments of negative-sense ss-RNA. Segments are numbered based in order of decreasing length. Each RNA segment is surrounded by nucleoprotein (NP) forming a flexible rod-shaped ribonucleoprotein (RNP) that contains one copy of the trimeric polymerase (PB1, PB2, and PA) complex, which is essential for IA virus replication (Digard *et al.*, 1999). The eight genome segments of IA virus are known to encode at least 12 proteins: segment 1 (PB2), segment 2 (PB1 and PB1-F2), segment 3 (PA), segment 4 (HA), segment 5 (NP), segment 6 (NA), segment 7 (M1 and M2) and segment 8 (NS1 and NS2; Chen *et al.*, 2001; Samji, 2009; Wise *et al.*, 2009). Recently, two more new proteins (PA-X and M42) were discovered being translated from segments 3 and 7, respectively (Jagger *et al.*, 2012; Wise *et al.*, 2012). Table 1.5 summarises the function of protein (s) encoded by each segment.

1.4.1.1.3 IA virus classification

Influenza A viruses are classified antigenically based on antigenic distinct HA and NA serotypes found on the virion surface. Currently, 18 different HA serotypes (H1-H18) and 11 different NA serotypes (N1-N11) have been identified (Hampson & Mackenzie, 2006). Among these serotypes, 16 HA (H1-H16) and 9 NA (N1-N9) have been shown to circulate in waterfowl, with the remaining two (H17 and 18; and N10 and N11) having been isolated from bats (Tong *et al.*, 2012). Human IA viruses have been limited to only H1, H2 and H3, and N1 and N2 (Gioia *et al.*, 2008). Individual IA virus strains are classified by using a systematic nomenclature based on genus, animal species of isolation (except for humans), geographic location of isolation, isolate number, year of isolation, and HA and NA serotype. For example, A/Duck/Ukraine/1/63 (H3N8) is the first of a strain of a H3N8 type A influenza virus isolated from a duck in the Ukraine in 1963.

AI viruses can also be classified phylogenetically into two groups of viruses: Group 1 and Group 2 (Chen & Deng, 2009). Group 1 includes H1, H2, H5, H6, H8, H9, H11, H12, H13 and H16; whereas group 2 includes H3, H4, H7, H10, H14 and H15 (Ellebedy & Ahmed, 2012). Each group shares a region of sequence conservation in the stem region of the HA protein (see below) which contains the antibody binding site and is conserved amongst many IA viruses. As a consequence of genetic (segmental) reassortment (called antigenic shift; see below), IA viruses with new combinations of HA and NA serotypes have been generated over time. In recent years, avian influenza strains H5N1, H7N7 and H9N2 have been transmitted to humans, with disease but only limited human-to-human spread.

Table 1.5 IA virus genome segments and encoded proteins (Bouvier & Palese, 2008; Wise *et al.*, 2009).

RNA Segment	Encoded Protein(s)	Protein Function
1	PB2	Polymerase Subunit, mRNA cap recognition
2	PB1 PB1-F2 PB1-N40	Polymerase Subunit, RNA elongation Pro-apoptotic activity Polymerase complex interaction
3	PA PA-X	Polymerase Subunit, Endonuclease activity Modulates the host response & viral virulence
4	HA	Major surface glycoprotein, receptor binding & fusion activity
5	NP	RNA binding protein, nuclear import regulation
6	NA	Minor surface glycoprotein, sialidase activity, virus release
7	M1 M2 M42	RNA nuclear export regulation, viral budding & assembly Ion channel for controlling pH, virus uncoating & assembly Replaces M2 function in M2-null viruses
8	NS1 NEP/NS2	Interferon antagonist protein & regulation of host gene expression Nuclear Export of RNP

1.4.1.1.3.1 Hemagglutinin (HA)

HA represents the major surface antigen of the IA virus (McHardy & Adams, 2009). The HA glycoprotein is assembled as a homo-trimeric spike of non-covalently linked monomers in the ER (Bosch *et al.*, 1981). HA is initially produced as a single polypeptide (HA0) that is cleaved into two disulphide-linked subunits (HA1 and HA2). Depending on the IA virus strain (and HA proteolytic cleavage motif), cleavage of HA0 is carried out either by trypsin (a tissue-specific protease) or by the ubiquitously distributed furin protease (Bosch *et al.*, 1979). The capacity for furin cleavage is responsible for the highly pathogenic (HPAI) phenotype in domestic fowl since it enables proteolytic activation of HA systemically (Horimoto & Kawaoka, 1994).

HA is essential for the virus entry of the host cell. HA mediates virus attachment to the host cell by binding to sialic acid containing receptors on the host cell membrane. HA then mediates fusion between the virus membrane and endocytic vesicles following a major pH-dependent conformational change of HA associated with exposure of the HA fusion peptide. This fusion event results in release of the viral RNP with its associated genome into the host cell cytoplasm. HA also serves as the main target of the host immune system. As a surface antigen, HA is under constant immune selection pressure from neutralizing antibodies following exposure to the influenza virus, either by natural infection or by seasonal epidemic vaccination (Both *et al.*, 1983).

1.4.1.1.3.2 Neuraminidase (NA)

NA is the second major surface glycoprotein of the IA virus (Webster *et al.*, 1992). The NA protein is folded in the ER followed by oligomerization to form almost mushroom-shaped trimeric protein molecules. As a type II protein, the N-terminal stalk of NA protein is

embedded in the viral envelope, whilst the box-shaped head contains enzymatic activity to catalyse the cleavage of sialic acid from cellular proteins within the secretory pathway (Gottschalk, 1957). This function is critical for the release of virus progeny during the viral replication cycle, as it enables virion escape from the host cell, which would otherwise be retained by the binding of HA to sialic residues of the host membrane proteins (Lee *et al.*, 2014). NA also prevents virus self-aggregation, and although the NA does not have any direct role in the attachment of viruses to host cells, it facilitates virus access to the epithelial cells by removing mucins (Liu *et al.*, 1995; Palese *et al.*, 1974).

1.4.1.1.3.3 Polymerase proteins

The PB1, PB2 and PA proteins together form the RNA polymerase complex of the IA virus, which is essential for virus replication as it provides the RNA-dependent RNA polymerase (RdRp) activity (Akkina, 1990; Ghanem *et al.*, 2007). The proteins within this complex are named on the basis of the isoelectric properties of each protein. PB1 and PB2 are basic proteins while PA is an acidic protein. PB1 is the first basic subunit of the polymerase complex. It serves as a scaffold for binding of the other two polymerase complex subunits as well as the NP protein (Ghanem *et al.*, 2007; Liu *et al.*, 1995). As a catalytically active subunit of the RdRp complex, PB1 plays a key role in the initiation and elongation of mRNA, complementary RNA (cRNA) and genomic RNA (Nakagawa, Oda & Nakada, 1996; Ulmanen, Broni & Krug, 1981). For initiation of viral mRNA synthesis PB1, together with PB2 and PA (see below), generate capped RNA primers by endonucleolytic cleavage ‘cap-stealing’ using cellular mRNA as the substrate. These host cell derived primers are then used to prime viral RNA synthesis (Li, Rao & Krug, 2001).

PB2 is the second basic subunit of polymerase complex. The main function of the PB2 is to recognise and bind to the 5`-cap structure of host cell pre-mRNA, which in then later cleaved

during ‘cap-stealing’. PA is the third and only acidic subunit of the RdRp complex. The PA endonuclease cleaves 10-13 nucleotides from the PB2-bound host pre-mRNA (Cheung & Poon, 2007; Dias *et al.*, 2009; Li, Rao & Krug, 2001). PA is also essential for efficient accumulation of PB1 in the nucleus (Fodor & Smith, 2004). PA has also been shown to be involved in various aspects of viral transcription and replication. However, its exact roles in viral transcription and replication are still poorly defined (Digard, Blok & Inglis, 1989; Fodor *et al.*, 2002; Sanz-Ezquerro *et al.*, 1995).

1.4.1.1.3.4 Matrix proteins (M1 and M2)

Segment 7 encodes two viral structural proteins: M1 and M2. M1 is the most abundant protein in the virion. M1 lies beneath the virion envelope forming a shell around the virion nucleocapsid. M1 binds to the RNP complex to facilitate its nuclear to cytoplasmic transport (Bui *et al.*, 2000; Ye *et al.*, 1987). It has been suggested that M1 also interacts with HA and NA through their cytoplasmic tails (Enami & Enami, 1996). M2 is a tetrameric transmembrane protein that functions as an ion channel to regulate pH (Lamb, Zebedee & Richardson, 1985). Following virus entry into the host cell, M2 allows acidification of the interior of the virus from the acidified endosomes, which leads to critical conformational changes necessary for virus uncoating (Holsinger *et al.*, 1994). M2 also plays an essential role in facilitating virus egress in later stages of the replication cycle (Roberts *et al.*, 2013).

1.4.1.1.3.5 Non-structural proteins

Segment 8 is the smallest gene segment and encodes for two non-structural proteins NS1 and NS2. Although NS1 is not incorporated into the virion, the protein is abundantly present in the nucleus of infected cells (Paterson & Fodor, 2012). NS1 interacts with a variety of

cellular proteins and plays an essential role in the pathogenesis and replication of the IA virus. NS1 possesses regulatory functions controlling both mRNA splicing and translation (Fortes, Beloso & Ortin, 1994; Qiu, Nemeroff & Krug, 1995), as well as promoting translation of viral mRNA (Garfinkel & Katze, 1993). It is also involved in inhibition of cellular innate antiviral pathways (Min & Krug, 2006; Wang *et al.*, 2002), and has been shown to inhibit maturation and migration of dendritic cells leading to dysfunctional T cell stimulation and cytokine production (Fouchier *et al.*, 2005). NS1 can be divided into two distinct functional domains. Consistent with its function in modulating innate immune pathways, the N-terminal of NS1 is an RNA binding domain consisting of aa residues 1-73 that has been shown to bind with low affinity to RNA molecules *in vitro* in a sequence *independent* manner (Chien *et al.*, 2004; Qian *et al.*, 1995). C-terminal residues 74-230 bind cellular host proteins, which also aids in stabilization of the RNA-binding domain (Wang *et al.*, 2002).

NS2 (nuclear export protein; NEP), is expressed from an alternatively spliced mRNA. The NS2 protein is incorporated in a phosphorylated form into the IA virion (Richardson & Akkina, 1991). NS2 protein has been shown to perform many important biological functions during IA virus replication. In association with M1, NS2 facilitates the transport of the viral RNA complex from the nucleus to the cytoplasm (Robb *et al.*, 2009). The N-terminus of the NS2 contains an HIV-1Rev-like nuclear export signal (NES) that interacts with cellular nucleoproteins, and can mediate nuclear export (Paragas *et al.*, 2001). In addition to nuclear export function, NS2 also plays a critical role in the regulation of viral RNA transcription and replication (Robb *et al.*, 2009). NS2 is involved in the viral budding process via an interaction with cellular ATPase (Gorai *et al.*, 2012).

1.4.1.1.3.6 Nucleoprotein (NP)

NP is the highly conserved and the second most abundant protein of virion (Webster *et al.*, 1992). Following synthesis and post-translational phosphorylation, NP is transported into the nucleus to where it binds to newly synthesised viral RNA to provide structural organization to the RNA complex (Portela & Digard, 2002; Wu, Sun & Panté, 2007). NP interacts with cellular proteins such as: importin- α , F-actin and CRM1, consistent with a role in nuclear to cytoplasmic transport of RNP complexes (Digard *et al.*, 1999; Elton *et al.*, 2001; O'Neill & Palese, 1995). Genetic and biochemical studies have shown that NP also plays a critical role in switching RNA synthesis from the transcription mode to the replication mode. In both *in vitro* and *in vivo* studies NP was shown to be essential for the switch to the replication mode (Krug *et al.*, 1989). NP also interacts with other cellular (BAT/UAP56 and MX) (Momose *et al.*, 2001; Turan *et al.*, 2004) and viral (PB1, PB2 and M1 proteins) (Biswas, Boutz & Nayak, 1998; Elton *et al.*, 1999). The interaction between NP and M1 was suggested to play an important role in the budding process of the IA virus particle (Avalos, Yu & Nayak, 1997).

Interestingly, NP-specific antibodies were recently shown to provide protection in mice (Carragher *et al.*, 2008; LaMere *et al.*, 2011b). Interestingly, vaccination with NP protein in adjuvant provided broad protection against diverse IA viruses by a mechanism involving NP-specific IgG, FcR and CD8⁺ T cells (LaMere *et al.*, 2011b). Due to the longevity of the NP-specific antibodies the cross-protective immunity provided was shown to persist over several months (LaMere *et al.*, 2011a). Since NP is a conserved influenza virus antigen and a major target for immune response especially cytotoxic T lymphocyte responses, it has been considered as a prime candidate for universal vaccines that generate cross-protective T cell responses (Berkhoff *et al.*, 2007) (see below).

1.4.2 Antigenic diversity of IA virus

Antigenic variation is a hallmark of the IA virus (Subbarao, Murphy & Fauci, 2006). This variation is due to both the segmented structure of the influenza virus genome enabling genomic reassortment, as well as the absence of a proof-reading mechanism leading to the accumulation of genetic errors incurred during genome replication (Zambon, 1999). These two sources of genetic variation, however, have markedly different outcomes: termed ‘antigenic shift’ and ‘antigenic drift’, respectively.

1.4.2.1 Antigenic Drift

IA viruses in their natural host reservoir (aquatic birds) appear to be in evolutionary stasis. However, in other hosts virus develops rapidly in response to the immune selection (Sandbulte *et al.*, 2011). As influenza strains develop continuously to avoid detection by host antibodies directed against the surface glycoproteins, frequent non-synonymous changes of amino acids occur as a result of mutation within HA, NA or both (Adams & Sandrock, 2010). The accumulation of these mutations is known as ‘antigenic drift’ as the original HA and NA serotypes are maintained (Figure 1.9). These mutations occur due to the absence of proof-reading ability in the influenza’s RNA polymerase complexes leading to replication errors on the order of 1×10^{-4} per replication cycle (Holland *et al.*, 1982). Mutations including deletion, insertion, and substitutions are the most important mechanisms for producing variation in IA viruses (Webster *et al.*, 1992). Accumulation of mutations at the antigenic sites of HA can result in these sites no longer being recognised and neutralised by the host immune system. This can cause transition of the virus from low to higher pathogenic forms (Adams & Sandrock, 2010). As a result of antigenic drift, IA viruses can escape from immune control and cause seasonal epidemic flu on an annual basis. Due to immune selection through the flu season, the original ‘matched’ seasonal vaccine may no longer be able to control the virus.

Hence, flu vaccines must be reformulated annually to achieve the best match possible between the circulating virus strains and the strains that use in the vaccine generation (Chen & Deng, 2009; Neumann, Noda & Kawaoka, 2009).

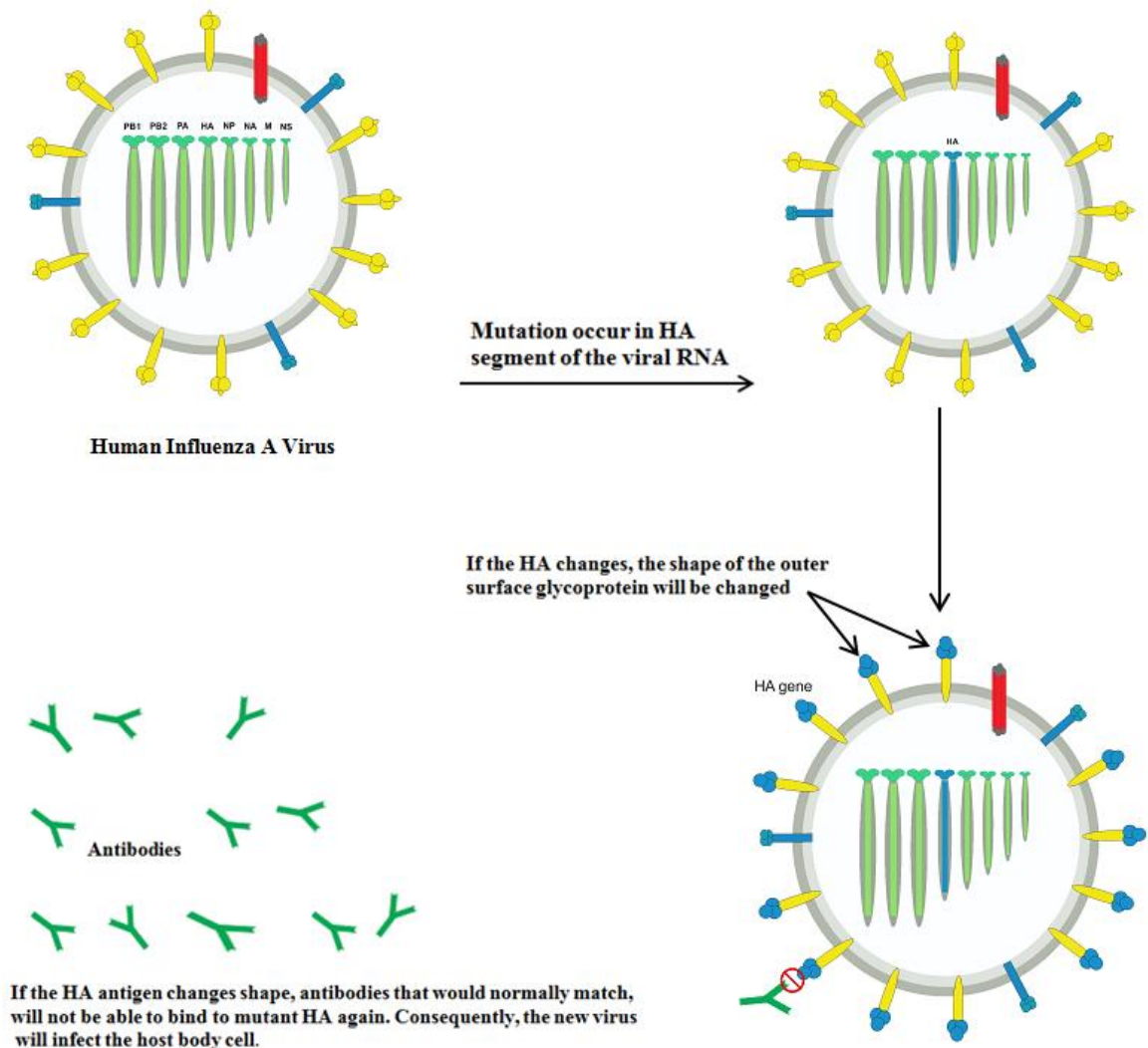


Figure 1.9 Schematic of antigenic drift. The antigenic drift process occurs when non-synonymous mutation occurs in the genes encoding HA. These changes enable escape from the host immune system due to the neutralizing antibodies being able to recognize the new mutant form of the HA protein.

1.4.2.2 Antigenic Shift

The second form of antigenic variation is antigenic shift. This is a major change in antigenicity of the virus associated with the introduction of novel viruses into an immunologically naïve population (Zambon, 1999). The segmented nature of the IA genome means that reassortment between two different IA viruses can occur, which is the driver of antigenic shift. Pandemic flu can arise when such reassortment results in the acquisition by an IA virus of new HA subtype (with or without NA) for which the existing human population has no immunity (Figure 1.10; Subbarao, Murphy & Fauci, 2006). In contrast to antigenic drift, antigenic shift can produce new IA virus subtypes suddenly at unpredictable and irregular intervals (Roose, Fiers & Saelens, 2009; Webster *et al.*, 1992). Historically, such pandemic events have been shown to be rare, but are essentially guaranteed. The emerging pandemic IA virus can cause millions of flu related deaths (Zambon, 1999).

Pandemic IA viruses can arise by several different mechanisms. The first mechanism involves direct transmission of an avian or swine IA virus with a capacity for efficient human-to-human transmission into the human population. It is believed that the 1918 H1N1 ‘Spanish flu’ arose through such a mechanism involving the introduction of an avian IA virus into an immunologically naïve human population (Yuen *et al.*, 1998). A second mechanism involves reassortment of co-circulating human and animal IA viruses due to simultaneous infection of cells followed by emergence of a novel IA virus reassortant that still possesses substantial human adaptation. Both the 1957 and the 1968 pandemic outbreaks arose from reassortment between human and avian viruses (Kasowski, Garten & Bridges, 2011; Webster *et al.*, 1992).

Sialic acid chemistry has a significant impact on IA virus transmission and thereby pandemic flu potential. IA viruses have different affinities for the $\alpha 2,3$ or $\alpha 2,6$ sialic acid linkage. Human IA viruses have greater affinity for the $\alpha 2,6$ linkage, which is found in the epithelial

cells of respiratory tissue of humans; whereas avian viruses preferentially bind through $\alpha 2,3$ linkages found on the surface of avian epithelial cells (Peiris, De Jong & Guan, 2007). The $\alpha 2,3$ -linkages are also present in human epithelial cells, especially in the lower respiratory tract, although they are much less common than the $\alpha 2,6$ -linkages. This means that avian influenza virus can infect humans and cause disease. However, since they are only found in the lower respiratory tract, such $\alpha 2,3$ -linkage utilizing avian viruses will transmit poorly through the human population (Lee & Saif, 2009; Matrosovich *et al.*, 2004). In addition, Ito *et al.* (1998) proved that the respiratory tract of pigs contained both $\alpha 2, 3$ and $\alpha 2, 6$ linked sialic acids, indicating that pigs could be infected by both human and avian influenza virus strains potentially resulting in reassortant pandemic virus (Ito *et al.*, 1998).

Pigs have an important role in IA virus reassortment due to their ability to become infected with different types of IA virus (both human and avian viruses). They can thereby serve as a “mixing vessel” or an intermediate host. The reason that pigs are a susceptible host for both human and avian influenza virus is due to the presence of both $\alpha 2,3$ - and $\alpha 2,6$ -linked receptors on epithelial cells lining the pig trachea, which allows reassortment and productive replication of IA viruses (Brown, 2000; Figure 1.11). Such an event is believed to have occurred in 2009, where a swine origin (H1N1) virus strain originated from a triple reassortment, containing genes originated from avian, porcine and human viruses (Michaelis, Doerr & Cinatl Jr, 2009).

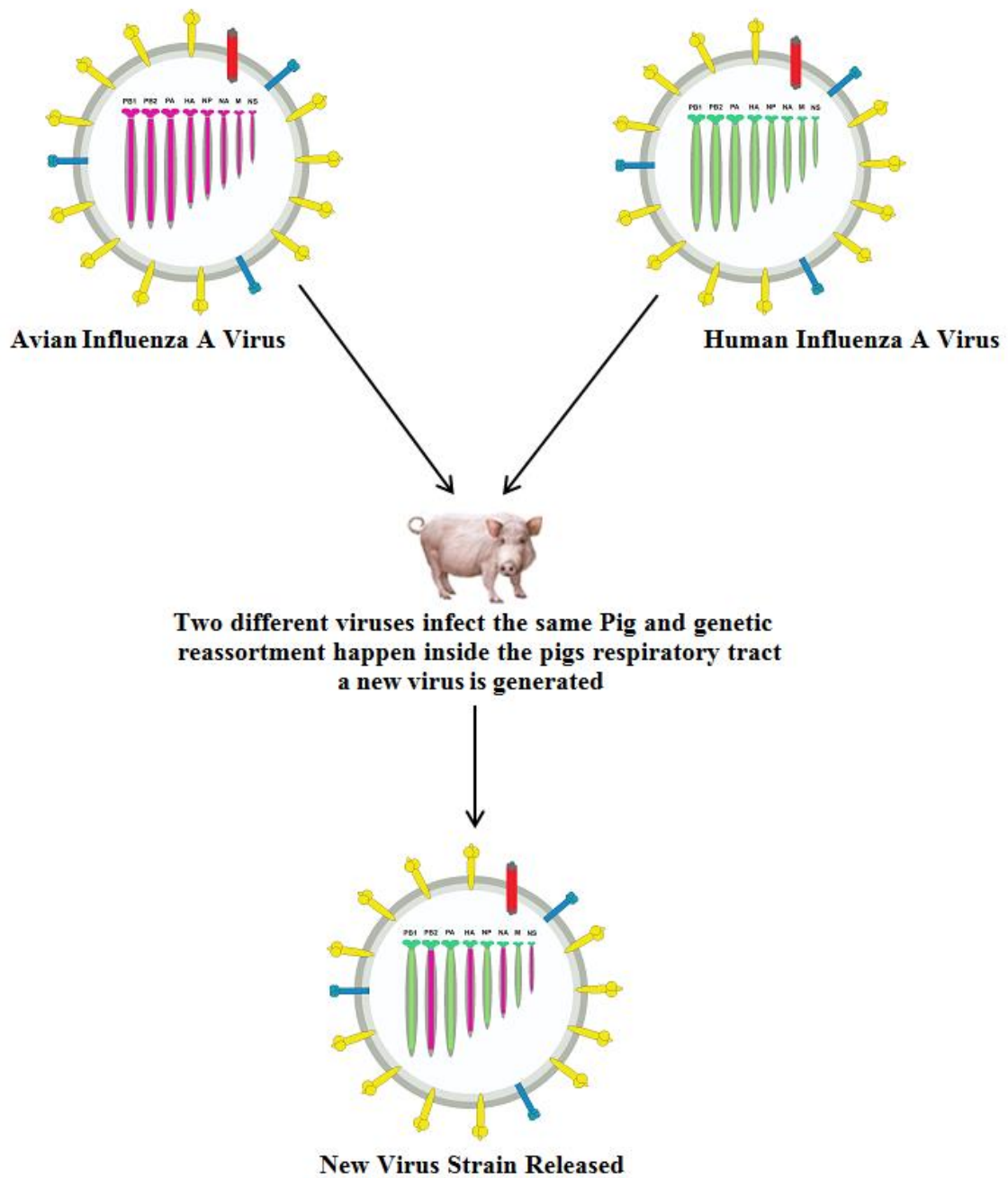


Figure 1.10 Schematic diagram of antigenic shift. Human and avian IA subtypes have ability to co-infect the pigs respiratory tract cells facilitating segmental reassortment and emergence of novel viruses with pandemic potential.

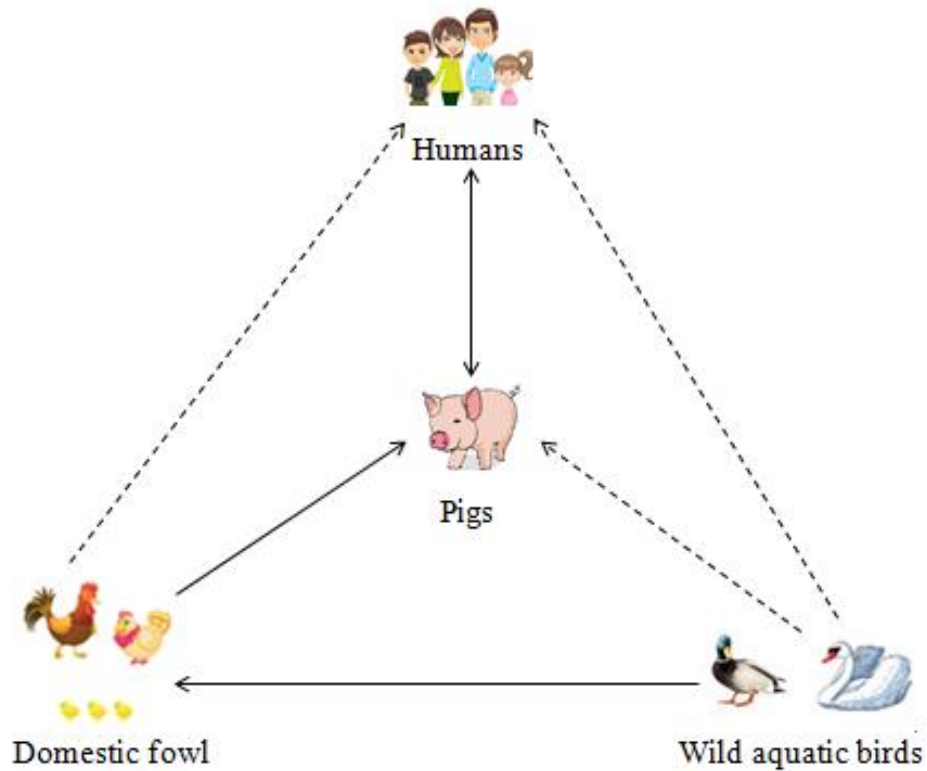


Figure 1.11 Pigs act as a mixing vessel for IA viruses. Wild aquatic birds are the natural reservoir for all influenza A viruses. IA viruses are frequently infect the domestic fowl from the natural reservoir of wild aquatic birds, and also infect pigs through frequent transmission from domestic fowl. Pigs can be frequently infected from domestic fowl and human. In pigs, the virus reassortment can occur between humans, avian and swine influenza A viruses. Influenza A virus from pigs can frequently infect humans. Transmission of influenza A viruses can be either occasional (dotted line), or frequent (solid lines). Adapted from (Ma, Kahn & Richt, 2009).

1.4.3 IA virus pandemics

Pandemics are defined as infectious outbreaks that affect large populations in a large geographic area, in a short period of time (Goldrick & Goetz, 2007). Pandemics can have a dramatic impact on world health and economy. The emergence of pandemic IA virus has been associated with the introduction and spread of an entirely new subtype with a new subset of genes, especially those coding for HA and NA, or re-emergence of a subtype that has not been in circulation for many years; in both cases the entire population is naïve and susceptible to infection (Roose, Fiers & Saelens, 2009). In general, the immune status and the exposure history of the human population will affect the severity and size of pandemics (Kreijtz *et al.*, 2008). A virus bearing a novel HA or NA has the ability to cause a pandemic if a number of criteria are met: (i) a large proportion of population lacks immunity (naïve) to the emerging IA virus, (ii) the IA virus is associated with significant human disease, (iii) the IA virus has the capacity to spread efficiently from person-to-person (Subbarao, Murphy & Fauci, 2006).

Based on phylogenetic studies of previous pandemic IA viruses, pathways to pandemic IA virus emergence are many and diverse. Pandemic AI viruses can emerge either by direct transfer from animal or avian sources to humans or following their reassortment with current circulating human strains. Alternatively, old pandemic strains may reappear as a new pandemic virus following their reintroduction years later into a now naïve human population (Kilbourne, 2006; Webster *et al.*, 1992). Seven IA pandemics have been reported during the past 200 years (Oxford, 2000). These are summarized in Table 1.6 and then discussed individually in more detail below.

Table 1.6 Pandemic outbreaks and mortality associated with IA virus. Adapted from (Morens, Taubenberger & Fauci, 2009; Oxford, 2000).

Year	Subtype	Deaths x10⁶	Country of origin
1889	H2N2	6	Europe
1898	H3N2	0.5	Europe
1918	H1N1	40	Europe
1957	H2N2	4	Asia
1968	H3N2	2	Asia
1977	H1N1	Not known	Asia
2009	H1N1	Not known	Mexico

1.4.3.1 1918 ‘Spanish Influenza’ pandemic (H1N1)

The largest pandemic was the H1N1 “Spanish flu” in 1918-1919. This strain caused the most destructive pandemic of the twentieth century, killing as many as 20 to 50 million people (Medina *et al.*, 2010; Taubenberger & Morens, 2010). All eight RNA segments of the IA virus associated with the Spanish flu were avian in origin (Taubenberger & Morens, 2010). HA, NA and PB1 proteins are in particular thought to have participated to the high pathogenicity the virus (Pappas *et al.*, 2008). Mortality was associated with an inversion of the normal ‘U’ shaped, being increased among young adults with 99% of deaths occurring in persons < 65 years of age (Kasowski, Garten & Bridges, 2011). This abnormal mortality distribution is thought to be a consequence of the cytokine storm induced by the 1918 pandemic virus strain, which would be greater in individuals with more competent immune responses. Consistent with this, recombinant IA virus expressing HA of pandemic Spanish H1N1 strain, was shown to induce a strong, macrophage-derived cytokine inflammatory response and was associated with severe haemorrhaging (Kobasa *et al.*, 2004). Secondary pneumonia is also believed to have played a critical role in the high mortality of pandemic

Spanish H1N1, as the virus encodes a PB1-F2 protein that promotes bacterial infection (McAuley *et al.*, 2007). The absence of antibiotics would also have been a further obvious complicating factor in promoting secondary bacterial complications.

1.4.3.2 1957 ‘Asian Influenza’ pandemic (H2N2)

The 1957-1958 pandemic “Asian flu” originated in the Southern Chinese Province of Guizhou in 1957. The virus originated by genetic reassortment between a human and avian IA virus (Oxford, 2000). HA (H2), NA (N2) and PB1 genes were of the avian virus origin, with the remaining genes coming from the circulating human H1N1 IA virus. Although the virus was not particularly pathogenic, the lack of any immunity in the human population to the HA2 and NA2 subtypes present in the emerging virus contributed to severity of the pandemic. The pandemic was associated with widespread illness and approximately two-million deaths with infection rates highest in 5 to 19 year-olds (Goldrick & Goetz, 2007). Interestingly, a large-scale study showed 26% of elderly people (>75 years) to have pre-existing cross-reactive antibodies to the 1957 H2N2 pandemic virus. Although this was not associated with any protective effect in this age population, it has been suggested to result from the 1890 (H2) pandemic (Kasowski, Garten & Bridges, 2011).

1.4.3.3. 1968 ‘Hong Kong’ pandemic (H3N2)

The H3N2 strain was isolated in Hong Kong in 1968. Like the previous pandemic, this strain was derived from a genetic reassortment between human and avian viruses (Webster, 1998). The pandemic Hong Kong IA virus obtained its HA (H3) and PB1 genes from an avian (duck) virus while NA (N2) and remaining genes came from the H2N2 circulating in the human population (Oxford, 2000). Although the virus spread globally and caused a significant

number of deaths, it was not as severe as Asian influenza pandemic (H2N2). This was presumably due to the presence of pre-existing N2 antibodies in the human population as a result of exposure to the previously circulating H2N2 (Kasowski, Garten & Bridges, 2011).

1.4.3.4 1977 ‘Russian’ pandemic (H1N1) – re-emergence of a H1N1 strain

The last IA pandemic of the 20th century was a ‘Russian’ influenza and was caused by a H1N1 strain. Mortality was exclusively limited to persons younger than 25 years-old born after 1957 with 50% of cases among children of school age (Goldrick & Goetz, 2007). This unusual age distribution was due to pre-existing immunity in older individuals from exposure to H1N1 circulating before 1957. The lack of any apparent genetic drift in the ‘Russian’ strain led to the conclusion that this virus was a previous H1N1 strain that had been reintroduced into the human population by an accidental release from a laboratory freezer (Neumann, Noda & Kawaoka, 2009). A characteristic of pandemic IA virus infection is that when a new pandemic strain emerges, it tends to replace the previously circulating subtype. The Russian pandemic H1N1 was an exception, which superimposed itself on the pre-existing H3N2, such that both virus subtypes have co-circulated in the human population causing predictable seasonal influenza outbreaks since 1977 (Kasowski, Garten & Bridges, 2011).

1.4.3.5 2009 pandemic (H1N1)

All influenza pandemics of the 20th century were associated with the emergence of influenza serotypes that differed from the IA virus already circulating in the human population at the time (Xu *et al.*, 2010). In 2009, the new IA pandemic was triggered by a distant variety of an already circulating HA subtype (H1N1) (van de Sandt, Kreijtz & Rimmelzwaan, 2012).

This novel strain originated from swine and was generated by reassortment between (i) North American H3N2 and H1N2 swine viruses with (ii) Eurasian avian-like viruses. The American H3N2 and H1N2 swine viruses themselves were already triple reassortments between avian, human, and swine IA viruses. Together, this means that the 2009 H1N1 pandemic strain was the result of a quadruple reassortment (Girard *et al.*, 2010; Neumann, Noda & Kawaoka, 2009; Taubenberger & Morens, 2010).

The 2009 pandemic H1N1 strain possesses PB2 and PA from North American virus origin, PB1 from human H3N2 virus origin, HA (H1), NP and NS proteins from classical swine virus and NA (N1) and M genes from Eurasian avian-like swine virus origin (Girard *et al.*, 2010; Neumann, Noda & Kawaoka, 2009; Smith *et al.*, 2009). Recent studies have demonstrated that both the 1918 and the 2009 H1N1 have a high level of antigenic similarity, especially in the hemagglutinin (HA) protein where amino acid sequence is near identical between the two viruses (Krause *et al.*, 2010). This high level of similarity is believed to be a result of the common pig origin of HA (H1) in both viruses, such that HA of the 2009 strain is a direct descendent of HA from the Spanish pandemic IA virus that has since been circulating in pigs. The remarkable antigenic stability of the HA is thought to be a result of the short life span of pigs. This provided an explanation for why older individuals had immunity to the H1N1 pandemic strain (see below) (Peiris, Tu & Yen, 2009). In addition, serological tests showed that individuals born prior to 1918, and who likely experienced the 1918 Spanish IA pandemic, had the highest titres of serum neutralizing antibodies against the 2009 H1N1 viruses (Krause *et al.*, 2010).

Young children, young adults and pregnant women were at highest risk from 2009 H1N1 infection and disease; whereas older adults were relatively protected due to pre-existing immunity from previously circulating H1N1 viruses (Kasowski, Garten & Bridges, 2011). Clinical symptoms ranged from being largely asymptomatic or causing a mild, self-limiting

upper respiratory infection to more rare cases of pneumonia, multi-organ failure and death, especially among younger people (Girard *et al.*, 2010; Peiris, Tu & Yen, 2009). Pulmonary symptoms in some patients were severe, which is believed to be associated with the ability of HA to bind both α 2,6- and α 2,3 -linked sialic acid receptors in the upper respiratory tract and deep in the lungs, respectively (Childs *et al.*, 2009; Girard *et al.*, 2010). The 2009 pandemic H1N1 strain continues to co-circulate with seasonal IA virus strains, and has been since incorporated into the seasonal vaccine (Leung & Nicoll, 2010).

IA virus is spread mainly by virus-laden droplets produced through sneezing or coughing. After inhalation, the viral particle primarily targets epithelial cells lining the respiratory tract, which are an important first line of defence against IA virus (Samji, 2009). The host mounts a robust antiviral response to limit viral replication. Within a week, both innate and adaptive immune systems participate in containment and clearance of IA virus infection (Tamura & Kurata, 2004).

1.4.4.1 Innate immune responses

The first barrier of defence against IA virus infection is the innate immune system, which is activated within a few hours of infection (van de Sandt, Kreijtz & Rimmelzwaan, 2012). The first line of innate immunity against infection is a physical barrier, including the intact epithelial cell layer itself, as well as secreted effector molecules. Mucin (primarily MUC5AC and MUC5AB) is secreted from goblet cells in the respiratory epithelium where it serves to trap virus, which can then be expelled by broncho-pulmonary ciliary action (Pittet *et al.*, 2010; Rubin, 2014). Virus that has compromised this barrier can be neutralized by soluble antimicrobial factors such as lysozymes, defensins and lactoferrin. In humans, replication of

IA virus has shown to be inhibited by alpha-defensins and neutrophils that produce cationic peptides (Salvatore *et al.*, 2007).

Pathogen-associated molecular patterns (PAMPs) of IA viruses such as viral RNA are recognized by pattern recognition receptors (PRRs), including: toll-like receptors (TLRs), retinoic acid inducible gene-1 (RIG-1) receptors, melanoma differentiation-associated gene 5 (MDA5) and NOD-like receptors (NLR). These specific receptors recognize virus-associated PAMPs, whilst NLR also has the ability to recognize the activity of the virus replication strategy (Pang & Iwasaki, 2011). Among the 11 known TLRs known, TLR-3 and TLR-7 play an essential role in recognition of ds- and ss-RNA, respectively. In addition, it has been shown that both RIG-1 and MDA5 bind to ds-RNA virus. This recognition leads to the secretion of inflammatory cytokines from infected host cells such as interferon (IFN), tumor necrosis factor (TNF) and macrophage inflammatory protein (MIP), which is released by natural killer cells (NK cells) (Alexopoulou *et al.*, 2001; Lund *et al.*, 2004; McGill, Heusel & Legge, 2009). These cytokines have strong antiviral activity, limiting viral replication and killing virus infected cells (Achdout *et al.*, 2003).

Virus infection also induces chemokines that recruit immune cells such as neutrophils, NK cells and monocytes to aid in viral clearance from the lung (Hashimoto *et al.*, 2007). Many studies have revealed the importance of NK cells for control of IA virus infection. NK cells have been shown to lyse IA virus-infected cells through recognition of the Fc portion of IA virus-specific antibodies bound to these cells through a process called antibody-dependent cell cytotoxicity (ADCC) (Ma *et al.*, 2013; Sun, 2003). NK cells can also target IA virus-infected cells for killing by binding of NK-expressed cytotoxic receptors NKp44 and NKp46 to HA on the surface of infected cells (Arnon *et al.*, 2001). The critical role of NK activity for IA virus control is shown in mice lacking the NKp46 receptor, where IA virus infection was associated with increased morbidity and mortality (Gazit *et al.*, 2006).

The importance of the innate immune response for IA virus control is also seen by the myriad mechanisms by which the virus subverts these pathways. For example, both PB1 and PB2 limit the production of IFN- β through the association with MAVS (mitochondrial antiviral signalling protein). NS1 can also block interferon production through inhibiting recognition of viral ss-RNA by the RIG-I receptor (van de Sandt, Kreijtz & Rimmelzwaan, 2012). Interestingly, a recent study has shown IA virus can also inhibit autophagy by interaction of M2 with the essential autophagy protein, microtubule-associated protein 1A/1B-light chain (LC3), which promotes re-localization of LC3 to the plasma membrane of virus infected cells (Beale *et al.*, 2014). Autophagy has been identified as an important aspect of both the innate and adaptive immune response (Ma *et al.*, 2013), and this recent study identifies a further means by which IA virus attempts to subvert host immunity.

1.4.4.2 Adaptive immune responses to IA virus infection

The adaptive immune response represents the second line of host defence against IA virus infection. Hallmarks of the adaptive immune response are antigen specificity and memory. IA virus infection induces both virus-specific humoral (represented by virus-specific antibodies produced by B lymphocytes), and cellular (represented by virus-specific T lymphocytes; CD4⁺ and CD8⁺) immunity (Cox, Brokstad & Ogra, 2004). Both of these arms of the adaptive immune response are important in host defence against IA virus infection (Stanecková & Vareckova, 2010).

Dendritic cells (DCs) are an important bridge between the innate and adaptive immune system. Following their activation at the site of IA virus infection, DCs migrate to lymph nodes draining the site of infection where they present viral antigens to activate naïve T lymphocytes (Tamura & Kurata, 2004; van de Sandt, Kreijtz & Rimmelzwaan, 2012). DCs

activate both CD4⁺ and CD8⁺ T cells, by supplying both antigen-specific signals through activation of T cells through the T cell receptor (TCR) together with the necessary co-stimulatory signals. For activation of CD8⁺ T cells, IA virus-derived peptides must be presented in the context of MHC-I. DCs can acquire viral peptides for MHC-I loading either through the canonical pathway with peptides derived from IA virus within the cytoplasm, or through cross-presentation of viral peptides acquired by endocytosis of extracellular viral antigens (discussed in more detail below). The MHC-I: peptide complexes are then transported to the cell membrane where they stimulate CD8⁺ cytotoxic T cells possessing the appropriate virus-specific TCR (Banchereau & Steinman, 1998; Joffre *et al.*, 2012). In the case of MHC-II molecules, extracellularly acquired viral proteins are degraded in endosomes in a fashion believed to be similar to cross-presentation, but peptides are then loaded onto MHC-II molecules. These MHC-II: peptide complexes are transported to the cell membrane to stimulate CD4⁺ T cells (Braciale, Sun & Kim, 2012).

1.4.4.2.1 Antibody-mediated protection against IA infection

Antibodies play an important role in resistance to IA infection and recovery from disease (Hampson & Mackenzie, 2006). Standard seasonal (epidemic) IA virus vaccines provide protection primarily by inducing antibodies against surface glycoproteins of homologous IA viruses circulating within the human population. Upon exposure to the IA virus, whether through vaccination or infection, specific antibodies are induced that have the ability to neutralize infection (Potter & Oxford, 1979). Neutralizing antibodies are primarily directed against the two surface proteins HA and NA, blocking the function of these molecules. This is the standard mechanism of action of current inactivated or subunit seasonal IA virus vaccines (Belshe *et al.*, 2004).

Studies using recombinant vaccinia virus encoding different IA virus proteins have shown the prime importance of antibodies against HA and NA for protection. Antibodies against HA bind to the trimeric globular head of HA and provide protection by inhibiting binding of the virus to cellular receptors (Virelizier, 1975). These antibodies can also neutralize the virus by facilitating phagocytosis and ADCC (Brown & Kelso, 2009; Kreijtz, Fouchier & Rimmelzwaan, 2011). Antibodies against NA have been shown to inhibit release of influenza virus from cells restricting the spread of the virus within the respiratory tract. This aggregation of the virus particles leads to a decrease in the effective number of infectious units (Kreijtz, Fouchier & Rimmelzwaan, 2011). Antibodies against NA are therefore not protective, but rather limit the spread of virus by inhibiting NA enzymatic activity (Hampson & Mackenzie, 2006; Webster & Laver, 1967).

Due to the high level of sequence variation between different serotypes of HA and NA, protection provided by antibodies is highly IA virus serotype-specific and limited to antigenically closely related viral strains and serotypes. As standard seasonal IA virus vaccines provide protection primarily by inducing antibodies against surface proteins of homologous IA viruses circulating within the human population, these vaccines do not create cross-protective (heterosubtypic) immunity (Boon *et al.*, 2004; Brown & Kelso, 2009). This is the reason that IA vaccines need to be updated annually and ‘matched’ against IA viruses currently circulating within the human population.

1.4.4.2.2 Cell-mediated protection against IA infection

IA virus infection also induces a cellular immune response involving CD4⁺, CD8⁺ and regulatory T cells. The cellular immune response to IA virus infection is thought important for clearance of virus-infected cells and for preventing IA-associated complications (Karzon,

1996; (Cox, Brokstad & Ogra, 2004; Karzon, 1996). In humans, virus specific T-cell responses are first detected within 3 to 6 days of infection and then return approaching baseline levels by day 21 to 28 (Dolin, Murphy & Caplan, 1978; Ennis *et al.*, 1981). Following primary infection, naïve T-cells expand and differentiated into cytotoxic effector T cells that are capable of eliminating virus infected cells. When the virus has been cleared from the body, a small residual component of cytotoxic effector CD8⁺ T cell population will develop into a virus-specific memory T cells pool. This memory CD8⁺ T cell are long lived and constantly circulate through the body primed to undergo rapid reactivation in the event of a secondary virus infection.

The main task of CD4⁺ T cells (also called T 'helper' (Th) cells) is to orchestrate development of an appropriate antibody and cytotoxic CD8⁺ T cell response against the IA virus. CD4⁺ Th cells are divided into several subgroups including Th1 cells and Th2 cells. CD4⁺ T cells are activated in response to their cognate recall peptide in the context of MHC-II. In humans, a broad range of peptides can be presented by MHC-II molecules encoded by three different MHC class II genes: HLA-DR, HLA-DQ and HLA-DP, with MHC-II molecules encoded by each of these genes binding to a distinct range of peptides. Activated CD4⁺ T cells perform their function, in large part, based on the cytokines that they express. For example, Th1 cells express IFN- γ that biases immunity towards enhancing CD8⁺ T cell cytotoxicity, whereas Th2 cells secrete IL-4 promoting B cell responses and production of IgG, IgA, and IgE antibodies.

CD4⁺ T cells capable of cytotoxicity function have also been described. These cells express effector cytokines such IFN- γ , but also have an ability to destroy IA virus infected cells by a perforin/granzyme-mediated pathway (Brown, 2010). Another recent study by Wilkinson *et al.* (2012) explored the importance of CD4⁺ T cells in protective immunity against IA virus infection in a unique human challenge study. Healthy volunteers were challenged with IA

virus, and IA virus-specific T cell and antibody responses were then monitored during the course of infection. The results showed a strong correlation between levels of pre-existing IA virus specific CD4⁺ T cells and reduced virus shedding and disease severity. Further characterization of these CD4⁺ T cells showed that they possessed cytotoxic function (Wilkinson *et al.*, 2012).

CD8⁺ T cell responses are crucial for clearance of virus from the host cells. These cells recognize virus peptides presented in the context of MHC-I on the surface of either professional APCs (during T cell priming; see above) or infected cells (prior to activation of effector killing mechanisms) through an antigen-specific interaction with the T cell TCR. During the canonical MHC-I presentation pathway, replication of viruses within cells leads to the degradation of virus proteins by the cellular proteasome. These virus peptides are then transported into the ER by transporter associated protein (TAP), where they are loaded onto MHC-I molecules. The MHC-I peptide binding groove contains two pockets that restrict the length of binding peptides to 8-12 amino acids. Following peptide binding, the MHC-I:peptide complexes are transported to the cell surface through the Golgi network where they are presented to the TCR of CD8⁺ T cells (Kim *et al.*, 2008).

Humans have three major classes of MHC-I molecules: HLA-A, HLA-B, and HLA-C. Within the human population the major MHC-I classes exist as >16,000 multiple alleles, each binding its own distinct family of peptides. During priming, professional APCs (primarily DCs) present the MHC-I: peptide complex (derived by either the canonical pathway or via cross-priming; see above) to naïve CD8⁺ T cells, which recognise the MHC-I presented peptide via their unique TCR. This antigen-specific selection of naïve T cells, together with additional co-stimulatory signals provided by the activated APC via CD80/86 and CD28, results in clonal selection of the naïve CD8⁺ T cell for proliferation and differentiation. The

activated virus-specific ‘effector’ CD8⁺ T cells then migrate to the site of infection and target the infected cells expressing the cognate MHC-I: peptide complex on their cell surface.

Virus-infected cells are killed by CTLs through two distinct pathways called the ‘intrinsic’ (granzyme (Gzm)/perforin-dependent) and ‘extrinsic’ (Fas: FasL-dependent) pathway; both pathways kill infected target cells by apoptosis. Intrinsic killing is mediated by permeabilization of the plasma membrane of infected cells through the action of perforin, which enables entry of GzmA/B to gain access to the cytoplasm inducing apoptosis (Andrade, 2010). GzmA also has non-cytotoxic inhibitory activity through its effect on viral protein synthesis and induction of pro-inflammatory cytokines. Extrinsic killing can occur in the absence of GzmA/B, and involves a receptor: ligand interaction between Fas and FasL that results in induction of apoptosis in the Fas-expressing infected target cell (Regner *et al.*, 2009; Topham, Tripp & Doherty, 1997; Waring & Müllbacher, 1999). CD8⁺ T cells also have the ability to enhance anti-viral activity through expression of different cytokines (La Gruta, Turner & Doherty, 2004).

Multiple studies have shown that CD8⁺ T cells play a critical role in protective immunity against IA virus. In humans, data from several sources have shown decreased morbidity and virus replication in the lungs being associated with CTL levels (Boon *et al.*, 2004; McElhaney *et al.*, 2006), while in mice CTLs have been shown to be involved in protective immunity against multiple IA serotypes (Bender *et al.*, 1992). The ability of T cell responses to target more conserved internal structural proteins appears important for cross-protective immunity (Braciale, Sun & Kim, 2012; Yewdell *et al.*, 1985). The presence of cross-reactive IA virus specific CD8⁺ T cells has been well-documented in humans (Boon *et al.*, 2004; Jameson *et al.*, 1999). Archival data from the Cleveland Family Study that captured data from the Asian influenza (H2N2) pandemic in 1957 as it swept through a monitored cohort of ~ 60 families has been recently re-analysed (Epstein, 2006). Despite the absence of

antibodies to the newly emerging H2N2 pandemic serotype, adults who reported symptomatic IA infection during 1950-1957 (H1N1) experienced a clinical attack rate with H2N2 IA three times lower than individuals with no documented prior H1N1 infection (Epstein, 2006). Since the H2N2 pandemic virus was a reassortant containing internal proteins from the previously circulating H1N1 strain, this strongly implicates immunity (presumably cell-mediated) against the common internal proteins of the viruses providing heterosubtypic control. A study by Sridhar *et al.* (2013) during emergence of the 2009 pandemic (H1N1) showed a similar effect. In this study, individuals with higher numbers of pre-existing CD8⁺ T cells against internal conserved CD8⁺ T cell epitopes developed less severe illness during infection with the emerging pandemic H1N1 virus (Sridhar *et al.*, 2013).

The importance of CTL responses for protection against different IA virus serotypes has also been shown in experimental human studies, where the presence of cross-reactive CD8⁺ CTLs was shown to correlate with the efficiency of recovery from IA infection in the absence of antibodies (McMichael *et al.*, 1983). Similarly, Kreijtz *et al.* (2008) showed that IA virus-specific CTLs that had developed in individuals in response to previous exposure to seasonal IA virus (H1N1 and H3N2) had significant cross-reactivity with H5N1 avian IA virus. Results from mouse studies corroborate these findings. Vaccination with a recombinant Ad5 expressing NP and M2 induced heterosubtypic immunity against H1N1, H3N2, and H5N1 IA viruses following intranasal administration, that corresponded to the IA-specific CTLs (Price *et al.*, 2010). Breadth of T cell immunity also appears to be important for broad heterosubtypic immunity (Gianfrani *et al.*, 2000). Vaccination of mice with recombinant a vaccinia virus-based IA vaccine expressing multiple internal proteins (NP, PA, M1, PB1, and PB2) increased the breadth of the IA-specific T cell response and as a consequence the level of heterosubtypic protection against both closely and distantly related IA virus strains (Kwon *et al.*, 2014). T cell responses in humans are most often directed to the epitopes of the internal

viral proteins NP, PA, and M1, which are conserved across IA subtypes (Chen *et al.*, 2014; Grant *et al.*, 2013; Liu *et al.*, 2013; Wang *et al.*, 2007). IA virus infections have been studied extensively in inbred strains of mice. CTLs are primarily targeted against internal virus proteins, and are conserved among different strains compared to surface glycoproteins (Townsend & Skehel, 1984). The primary T cells response to IA virus infection establishes an immunodominance hierarchy that becomes even more pronounced following secondary infection (Doherty *et al.*, 2006). The primary IA virus-specific T cell response (using either H1N1 or H3N2 laboratory strains) is dominated by equivalent levels of CD8⁺ T cells against NP and PA (Andreansky *et al.*, 2005; Belz *et al.*, 2000). During infection of C57/BL6 (H2b-restricted) mice, the immunodominant epitope of NP has been defined as NP₃₆₆₋₃₇₄, while in PA the equivalent epitope is PA₂₂₄₋₂₃₃ (Belz *et al.*, 2000). In contrast, CTL levels against these two epitopes differ substantially during the secondary response. Following re-exposure to the IA virus, responses against PA₂₂₄₋₂₃₃ are markedly diminished relative to those against NP₃₆₆₋₃₇₄, with NP₃₆₆₋₃₇₄-specific responses now accounting for ~80% to 90% of all IA-specific CD8⁺ T cells (Flynn *et al.*, 1999).

Together the studies above show the ability of vaccination and natural IA virus infection to induce virus-specific antibody and T cell responses (Boon *et al.*, 2004; McElhaney *et al.*, 2006). The relative importance of these responses for control of IA virus infection will depend on the level of antigenic similarity of the challenging virus, with T cells being more important for protection against antigenically more distinct viruses (McElhaney *et al.*, 2006). These studies also suggest that vaccination strategies focused on generating T cell responses directed towards the more conserved internal proteins of the IA virus may be an effective approach to generate an efficacious, broadly protective immune response against divergent IA virus subtypes. This strategy would be beneficial both for annual IA virus epidemics, but

even more importantly for pandemic IA, where the subtype and time of emergence are highly unpredictable but frequently devastating to human health at a global scale.

1.5 Objectives of the thesis

Objective 1: To test the hypothesis that targeting of essential CMV tegument proteins by using regulatable protein-destabilization is suitable for use as a conditional vaccine attenuation strategy. These studies detail construction and *in vitro* characterization of recombinant MCMVs targeting two distinct tegument proteins (pp28 and pp150) using this DD-based destabilization strategy.

Objective 2: To test the hypothesis that targeting of more conserved IA virus proteins with CD8⁺ T_{EM} cell-based immunity by using CMV-based vectors as a quintessential inducer of such ‘effector’ memory responses, will provide the desired heterotypic immunity capable of preventing spread of emergent pandemic IA virus strains. This initial study determined the capacity of a MCMV-based vaccine expressing the epitopes from conserved IA proteins nucleoprotein (NP), polymerase (PA) and non-structural protein 2 (NS2) to induce immunity in mice as a strategy to prevent pandemic IA emergence.

Chapter Two:
Materials And Methods

2. Materials and methods

2.1 Maintenance of eukaryotic cell lines

All *in vitro* cell culture work was carried out under sterile conditions in a Class II biological safety cabinet (Holten LaminAir, UK). Cell lines were cultured at 37°C using a Binder CO₂ incubator (Binder, Germany) under 95% humidity and 5% CO₂.

2.1.1 Murine embryonic fibroblast (MEF) cell line

MEFs containing an inactivated p53 (MEF p53^{-/-}) were used for these studies (kindly provided by Dr. Daniel Streblov, Oregon Health and Sciences University, OHSU, Portland, OR, USA). Throughout the thesis, these cells will be termed MEFs. MEF cultures were maintained at 37°C under 5% CO₂ in Dulbecco's modification of Eagle's medium (DMEM; Gibco, Paisley, UK) supplemented with 5% (v/v) fetal bovine serum (FBS; heat-inactivated for 30 min at 56°C), 1% (v/v) penicillin/streptomycin (100 unit/ml and 100 µg/ml) and glutamine (2 mM; Invitrogen, Paisley, UK).

2.1.1.1 Sub-culturing of MEF cells

MEFs were sub-cultured when monolayers reached 85-90% confluence. Prior to sub-culturing, all reagents were brought to 37°C. Culture medium was removed and the adherent monolayer was washed three times with 1× Dulbecco's phosphate buffered saline (DPBS). Trypsin/EDTA (0.25% Gibco, Paisley, UK) was added to the cells, and was returned to the incubator until cells had detached from the surface of the flask. Detached cells were re-suspended as a single cell suspension in fresh fully supplemented DMEM medium (Section 2.1.1.) to neutralize trypsin. Cells were harvested by centrifugation at 1000 rpm (1500 × g) for 10 min at room temperature (RT), and then re-suspended in 5 ml DMEM. Cells were then

either transferred to a new flask using an appropriate volume for a split ratio between 1:3 or 1:5 according to the experimental requirement or counted using a haemocytometer and seeded into dishes for use in experiments [Appendix 1].

2.1.1.2 Storage of MEF cells

For long-term preservation frozen cell stocks were stored at -80°C . Cells from one 175 cm^2 flask were grown to 80% confluence, washed and trypsinized as described above. The single cell suspension was centrifuged at 1000 rpm ($1500 \times g$) for 5 min at RT and the cell pellet was re-suspended to a density of $2 \times 10^5 - 5 \times 10^6$ cells/ml in freezing medium containing 80% FBS and 20% (v/v) dimethyl sulfoxide (DMSO; Sigma-Aldrich, Dorset, UK). The suspension was aliquoted into 1.5 ml cryovials which were placed in a freezing pod; Mr. Frosty (Fisher Scientific, Leicestershire, UK) and subsequently stored at -80°C or under LN_2 .

2.1.1.3 Reviving frozen cell stocks

DMSO is toxic to cells at temperatures above 4°C , and its rapid removal is critical to maintain high cell viability. Cells (in cryovials) were rapidly thawed at 37°C with gentle agitation. Cells were then transferred to pre-warmed fully supplemented DMEM followed by centrifuged at 1000 rpm ($1500 \times g$) for 10 min at RT. Pelleted cells were re-suspended in 10 ml fresh, pre-warmed DMEM by gentle pipetting and seeded into a 25 cm^2 tissue culture flask. Cells were then incubated at 37°C in a 5% CO_2 as described above.

2.1.2 Visual monitoring of cell monolayers

Microscopic observation and imaging of cell cultures were performed using an Olympus inverted microscope (MoTic AE2000, UK).

2.1.3 Cell quantitation

Cells were counted using a haemocytometer. The haemocytometer consists of nine 1 mm^2 squares, each square representing a volume of $1 \times 10^{-4} \text{ ml}$. Cells were counted in the four corner 1 mm^2 squares using an inverted microscope and the total number of cells recorded was divided by four to give the average number of cells per 1 mm^2 square. The concentration of the cells was calculated by applying the following formula:

$$C = \frac{V}{N}$$

C : Cell concentration in cells/ml

V : Volume counted = $1 \times 10^{-4} \text{ ml}$.

N : Average number of cells per mm^2 So: $C = N \times 10^{-4} \text{ cells/ml}$.

Cells were then diluted to the appropriate seeding density and plated at the required density for use in experiments [Appendix I].

2.2 Bacteriology methods

2.2.1 Bacteria and plasmids

BACs and plasmids were maintained in *Escherichia coli* (*E. coli*) strains. Bacteria and plasmids used in this study are shown in Table 2.1. EL250 and SW105 *E. coli* strains were kindly provided by Dr. Donald L. Court (Centre of Cancer Research, National Cancer Institute Frederick, MD, USA). The EL250 strain is based on DY380 (DH10B [λ cl857 (*cro-bioA*) < > *araC-P_{BAD} flpe*]). EL250 cells express E/T recombinases under the control of a temperature-sensitive repressor (λ cl857 repressor) providing the temperature regulatable expression. EL250s also contains a replication defective lambda prophage (Yu *et al.*, 2000) coding for an arabinose-inducible FLP recombinase gene (Lee *et al.*, 2001). The SW105 strain is comparable to EL250, but also carries a functional *gal* operon except for deletion of *galK* enabling positive/negative using the GalK system (Warming *et al.*, 2005).

Culturing of EL250/SW105s under the permissive temperature at 32°C maintains the λ cl857 repressor in an active state, resulting in repression of the E/T recombinase system. Shift to the permissive (de-repressive) temperature of 42°C for 15 min inactivates the λ cl857 repressor resulting in rapid induction of the E/T recombinase system, which then promotes efficient homologous recombination between linear ds-DNA recombination fragment introduced by transformation into the EL250/SW105s and the BAC DNA being targeted. The *Exo* gene encodes a 5' to 3' exonuclease that recognizes the end of the linear ds-DNA fragment containing the necessary region of homology to the region being targeted within the BAC thereby producing 3'-overhangs. The *Beta* gene encodes a ss-DNA binding protein that binds to this 3'-overhang and promotes homologous recombination, whilst the *Gam* gene prevents degradation of the linear DNA cassette by inhibiting the *E.coli* RecBCD exonuclease.

EL250/SW105s contained the MCMV (Smith strain) BAC pSMfr3 as the genetic background for recombineering of MCMV recombinant vectors (kindly provided by Dr. Ulrich H. Koszinkowski, Max von Pettenkofer-Institute, Ludwig-Maximilians-University, Germany; (Messerle *et al.*, 1997; Wagner *et al.*, 1999). For all of these studies, the natural killer (NK) cell activating m157 gene of MCMV has been inactivated by deletion (pSMfr3Δm157), which is referred to as wild-type (WT) MCMV BAC throughout.

All bacterial cultures were grown in Luria-Bertani (LB medium) or on plates containing LB and Bacto®-Agar (Fisher Scientific, Leicestershire, UK; Appendix I). All media was autoclaved at 121°C for 20 min, pressure 15 lbs/in² and mixed with appropriate antibiotics (Table 2.1). LB plates were incubated overnight at 30°C in a standard incubator. LB liquid cultures were incubated overnight at 30°C in an orbital incubator at 230 rpm (VWR, West Sussex, UK). All bacterial strains were cultured at 30°C, as growth at >32°C will result in instability of the BAC genome due to inadvertent induction of the E/T recombination system (Paredes & Yu, 2012).

2.2.2 Culture and long-term storage of bacteria

A single colony was transferred from an agar plates into LB broth supplemented with appropriate antibiotics (Table 2.1) and cultured as above. For long-term storage of bacteria, overnight bacterial cultures were mixed at a 1:1 ratio with 80% (w/v) sterile glycerol (Fisher Scientific, Leicestershire, UK) using 800 µl of overnight culture. Glycerol stocks were then stored at -80°C. Fresh cultures were revived from glycerol stocks on a regular basis by culturing of glycerol stock ‘scrapings’ in 5 to 50 ml LB with appropriate antibiotics as above.

2.2.3 Preparation of electrocompetent bacteria

A single colony was transferred into 5 ml LB medium supplemented with appropriate antibiotics and cultured as above. The overnight culture was then added at a 1:50 dilution into 50 ml of LB medium supplemented with antibiotics. Bacteria were then cultured at 30°C with shaking for approximately 4 hours until reaching an optical density of 0.6 at 600 nm (OD₆₀₀). Cells were harvested by centrifugation at 7,000 rpm for 10 min in a pre-cooled (4°C) centrifuge. Excess LB was discarded and the pellet was washed in 250 ml of 10% (w/v) glycerol, followed by centrifugation at 7,000 rpm for 10 min at -4°C. The supernatant was discarded and the washing step was repeated. Cells were pelleted and re-suspended in residual 10% glycerol and kept on ice until use. Electrocompetent bacteria were always prepared fresh immediately before use.

2.2.4 Transformation of electrocompetent bacteria

EL250/SW105 *E.coli* strains containing the WT MCMV BAC were used for construction of MCMV BAC recombinants. Electroporation of electrocompetent bacteria (see above) was performed using pre-cooled 0.2 cm cuvettes in a Bio-Rad Gene Pulser (BIO-RAD, Hertfordshire, UK). Electrocompetent bacteria and recombination fragments were mixed gently in the cuvette by shaking followed by electroporation using pre-programmed 'EC2' conditions for *E. coli* in 0.2 cm cuvettes. Immediately after electroporation, 800 µl of LB media (without antibiotics) was added to the cuvette and the entire mixture was transferred to a 5 ml centrifuge tube for recovery for 2 h at 30°C with shaking. Following recovery, bacteria were plated on agar plates (supplemented with appropriate antibiotics) and incubated for 24-48 h at 30°C. Single colonies were isolated. Each colony was used to inoculate 5 ml LB broth (supplemented with appropriate antibiotics) and cultured overnight at 30°C as above.

Table 2.1: Plasmids, BACs and bacterial strains

Plasmid/BAC	Antibiotic Selection	Growth Temp (°C)	Source or Reference
EL250	None	30	Dr. Donald L. Court Centre of Cancer Research, National Cancer Institute Frederick, USA
pSMfr3 MCMVBAC	17 µg/ml Cam ¹	30	Dr U. Koszinowski Ludwig-Maximilians-University, Germany (Messerle <i>et al.</i> , 1997)
pOri-WTFRT	25 µg/ml Kan ²	30	(Gustafsson <i>et al.</i> , 1994)
pOri-FRT5	25 µg/ml Kan ²	30	(Gustafsson <i>et al.</i> , 1994)
pYD-C255	25 µg/ml Kan ²	30	Dr. Donald L. Court Centre of Cancer Research, National Cancer Institute Frederick, USA (Warming <i>et al.</i> , 2005)
SW105	None	30	Dr. Donald L. Court Centre of Cancer Research, National Cancer Institute Frederick, USA (Warming <i>et al.</i> , 2005)
AcGFP-DHFR-E134G	50 µg/ml Carb ³	30	Prof. Thomas J. Wandless Stanford University, USA (Cho <i>et al.</i> , 2013)
YFP-DHFR-Y100I	50 µg/ml Carb ³	30	Prof. Thomas J. Wandless Stanford University, USA (Iwamoto <i>et al.</i> , 2010)
AcGFP-DHFR-F140P	50 µg/ml Carb ³	30	Prof. Thomas J. Wandless Stanford University, USA (Not Published)

2.3 Molecular Biology methods

2.3.1 Isolation and purification of nucleic acids

2.3.1.1 Isolation of plasmid DNA (Mini preps)

Bacteria containing plasmids of interest were grown in 5 ml LB broth supplemented with appropriate antibiotics as above. Overnight cultures were centrifuged (Denley BR401, Hampshire, UK) at 3,500 rpm ($2,000 \times g$) for 15 min at RT and plasmid DNA was extracted using a plasmid Miniprep kit (Sigma-Aldrich, Dorset, UK) in accordance with Manufacturer's instructions. Briefly, the pellet was re-suspended in 200 μ l suspension buffer containing 100 μ l/ml RNase. Bacteria were lysed by addition of 200 μ l lysis buffer (200 mM NaOH, 1% SDS) and then mixed by gentle inversion six times. Neutralization buffer (3 M potassium acetate, pH 4.8) was added to neutralize the alkaline lysis reaction and to precipitate chromosomal DNA together with cellular debris and denatured proteins. Lysates were pelleted by centrifugation at 10,000 rpm ($12,000 \times g$) for 10 min at RT and clarified supernatants were transferred to a DNA binding column followed by centrifugation at 10,000 rpm for 1 min at RT. The flow through was discarded followed by two additional wash steps. Columns were then centrifuged for an additional 1 min to dry the membrane prior to elution of DNA by addition of 100 μ l of Elution buffer (10 mM Tris-HCl, pH 8.5). After 1 min incubation at RT, plasmid DNA was eluted by centrifugation at 10,000 rpm ($12,000 \times g$) for 1 min at RT. The concentration of purified DNA was determined using a Nanodrop spectrophotometer (see below). Purified plasmid DNA was analysed by restriction enzyme digestion and agarose gel electrophoresis as described below.

2.3.1.2. Isolation of BAC DNA from bacteria (BAC preps) using Alkaline Lysis

BAC DNA was prepared from overnight bacterial cultures using the alkaline lysis method (Sambrook & Russell, 2001). Briefly, overnight bacterial cultures were pelleted at 3,500 rpm ($12000 \times g$) for 15 min at RT to pellet bacteria. Supernatant was discarded and bacteria were re-suspended in 300 μ l P1 buffer [50 mM Tris base, 10 mM EDTA, adjusted with HCL to pH 8.0; containing 100 μ g/ml RNAase Appendix III], followed by transfer to a 2 ml microcentrifuge tube (Greiner Bio-One Ltd, Stonehouse, UK). Three hundred microliters of P2 buffer [5 M NaOH, 10% SDS; Appendix III] was added and mixed by gentle inversion six times. Chromosomal DNA and protein were precipitated by addition of 300 μ l P3 buffer [3 M $\text{CH}_3\text{CO}_2\text{K}$ adjusted with glacial acetic acid to pH 5.5; Appendix III], and mixing as before by gentle inversion. One millilitre of phenol/chloroform (CHCl_3 , Fisher Scientific Leicestershire, UK) was added and mixed by gentle rocking on a rotator for 10 min. To separate aqueous from organic phases the mixture was centrifuged at 14,000 rpm ($12,000 \times g$) for 10 min at RT. Following centrifugation, the upper aqueous phase was transferred into a fresh 2 ml microcentrifuge tube. One hundred microliters of 3M sodium acetate [Appendix III] was added and mixed by inversion. One millilitre of isopropanol (Fisher Scientific, Leicestershire, UK) was then added followed by centrifugation at 14,000 rpm ($12,000 \times g$) for 10 min at RT to precipitate the DNA. DNA pellets were washed to remove excess salt with 500 μ l 75% ethanol (w/v in molecular grade water; both from Fisher Scientific, Leicestershire, UK), and centrifuged at 14,000 rpm ($12,000 \times g$) for 10 min at RT. Ethanol was removed and pellets were air-dried at RT. DNA was gently resuspended in 50 μ l of EB buffer (10 mM Tris-HCl, pH 8.5) to avoid shearing of BAC DNA.

2.3.1.3 Isolation of viral DNA from virus stocks

Isolation of viral DNA from virus infected tissue culture cells was performed using a QIAamp®MinElute ®Virus Spin Kit (Qiagen, Manchester, UK), in accordance with Manufacturer's instructions. Briefly, 40 µl of concentrated virus stock was brought up to a volume of 200 µl with DPBS. Twenty-five microliters of proteinase solution and 200 µl of buffer AL were added, vortexed to mix thoroughly and then incubated at 56°C for 15 min. Two hundred and fifty microliters of 100% ethanol (Fisher Scientific, Leicestershire, UK) was added, mixed thoroughly by vortexing and then incubated for 5 min at RT. The mixture was transferred to a QIAamp MinElute column and centrifuged at 8,000 rpm ($6,000 \times g$) for 1 min at RT. Flow through was discarded and columns were washed with 500 µl of buffer AW1 followed by 500 µl volumes of buffer AW2 and then 100% ethanol. Residual ethanol was removed by centrifugation at 14,000 rpm ($12,000 \times g$) for 3 min at RT, followed by incubation at 56°C for 3 min to evaporate residual ethanol. Fifty microliters of AVE elution buffer (RNase-free water with 0.04% Sodium azide) was added to the column. Following incubation for 1 min at RT, DNA was eluted by centrifugation at 14,000 rpm ($12,000 \times g$) for 1 min at RT. Viral DNA was stored at 4°C prior to further down-stream analysis.

2.3.2 Quantitation of DNA

Purified plasmid DNA or PCR product concentrations were determined using a NanoDrop ND-1000 Spectrophotometer (Labtech International Ltd, UK). Two microliters of DNA was required for determination of DNA concentration, which was based on OD₂₆₀ readings. Readings at 260_{nm}/280_{nm} and 260_{nm}/230_{nm} were also evaluated to determine the quality of DNA. A ratio of 260_{nm}/280_{nm} \geq 1.8 and 260_{nm}/230_{nm} ratios of between 1.8 and 2.2 indicate good quality DNA, free from contaminants such as salt or proteins.

2.3.3 Polymerase chain reaction (PCR)

2.3.3.1 PCR primer design and preparation

All primers were purchased from (Eurofins Genomics, Wolverhampton, UK). Primers were used for cloning, mutagenesis and sequencing. Primers used for amplification of recombinant DNA fragments for use in E/T recombination contained 60 bases homologous to the region flanking the site within the MCMV genome targeted for mutagenesis followed by 21 bases homologous to the template recombination plasmid. All primers other than those used for DNA sequencing were HPLC purified (Tables 2.2 to 2.6).

2.3.3.2 Standard PCR

PCR was performed towards a number of purposes. PCR was used to generate fragments for cloning and recombination. PCR in combination with DNA sequencing of recombinant MCMV BAC clones and reconstituted derivative viruses (see below) was also used to confirm the presence of desired mutations. Finally, PCR was used to confirm the absence of WT virus contamination in recombinant MCMV virus stocks. Reagents were kept on ice to minimize primer dimer formation and reactions were prepared as indicated [Appendix II]. Reagents were mixed thoroughly by pipetting and centrifuged briefly to collect the mixture at the bottom of the tubes. PCR controls using molecular grade water alone were always included. Specific thermo-cycling conditions are detailed in Appendix II. PCR products were separated and visualised on 1% agarose gel in 1 × TAE buffer (242 g Tris Base, 0.5 M EDTA, glacial acetic acid, ethidium bromide (EtBr) (0.5 µg/ml)) together with a 1 kb DNA molecular weight marker ladder. DNA bands were visualized and imaged under UV light using a gel documentation system (UVi Tech, UK).

Table 2.2: Primers for generating and sequencing MCMV influenza recombinants

Primer name	Sequence	T_m (°C)
IE2-NPF5-F	TTTCTCTTGACCAGAGACCTGGTGACCGTCAGGAAGAAGA TTCAGGGTGCCAGCAACGAGAACATGGAGACCATGTGA AGCTTAGTACGTAAA	>75
IE2-NPF5-R	CACTTAACGGCTGACATGGG	>75
IE2-PAF5-F	TTTCTCTTGACCAGAGACCTGGTGACCGTCAGGAAGAAGA TTCAGGTAGCAGCCTGGAGAACTTCAGGGCCTACGTGTGA AGCTTAGTACGTAAA	>75
IE2-PAF5-R	CACTTAACGGCTGACATGGG	>75
IE2-NS2F5-F	TTTCTCTTGACCAGAGACCTGGTGACCGTCAGGAAGA AGATTCAGGGTAGGA CCTTCAGCTTCCAGCTGATCTG AAGCTTAGTACGTAAA	>75
IE2-NS2F5-R	CACTTAACGGCTGACATGGG	>75
IE2-NPFWT-F	TTTCTCTTGACCAGAGACCTGGTGACCGTCAGGAAGAA GATTCAGGGTGCCAGCAACGAGAACATGGAGACCATG TGA ACTTAACGGCTGACATG	>75
IE2-NPFWT-R	CTGTCCGATGAATAAAACCTCTTTATTTATTGATTA AAAA CCATGACATACCTCGTGTCTAGCTTAGTACGTAAAC	>75
IE2-Flank-F	ACACCGAGTACGAGGAGACC	61.4
IE2-Flank-R	CTGTCCGATGAATAAAACC	52.4
BIE-Flank-F	AGTCCCGACTACGATCCGGA	61.4
BIE-Flank-R	CTGTCCGATGAATAAAACC	52.4

Table 2.3: Primers used for cloning and sequencing MCMV-ecDHFR recombinants using galK strategy

Primer name	Sequence	T _m (°C)
Pc255 galK-F	GACATCTGTTGATGATAAAAAATTATATTTTTTTTA GAGAGCCTGTTGACAATTAATCATCGGCA	71.3
Pc255 galK-R	CGGCGATCATGATCATGTTGCAACTGGGTGCGGC GGCTCCATTTAACCAATTCTGATTAGAA	>75
GalK-POS-F	GACATCTGTTGATGATAAAAAATTATATTTTTTTTAG AGAGCCTGTTGACAATTAATCATCGGCA	71.3
GalK-POS-R	CGGCGATCATGATCATGTTGCAACTGGGTGCGGCG GGCTCCATTTAACCAATTCTGATTAGAA	>75
GalK-E134G-F	GACATCTGTTGATGATAAAAAATTATATTTTTTTTAG AGAGACCATGATCAGTCTGATTGCGGCG	73.2
GalK-E134G-R	CGGCGATCATGATCATGTTGCAACTGGGTGCGGCG GGCTCCATCGTAGAATCGAGACCGAGGAGGGTT AGGATAGGCTTACCTCGCCGCTCCAGAATCTCAA	>75
GalK-IE3 Inter-F	CGGTTCTCATCCAAGTGACGG	61.8
GalK-IE3 Inter-R	TATATCAAATGAGTGCCTG	52.0

Table 2.4: Primers used for cloning and sequencing MCMV-ecDHFR recombinants

Primer name	Sequence	T _m (°C)
pOri E134G-F	GCGCCCCGGGGCCACCATGATCAGTCTGATTGCG	>75
pOri E134G-R	GCGCGAGCTCTTACGTAGAATCGAGACCGAGGAG AGGGTTAGGGATAGGCTTACCTCGCCGCTCCAGAA TCTCAA	>75
pOri Y100I-F	GCGCCCCGGGGCCACCATGATCAGTCTGATTGCG	>75
pOri Y100I-R	GCGCGAGCTCTTACGTAGAATCGAGACCGAGGAGAGG GTTAGGGATAGGCTTACCTCGCCGCTCCAGAATCTCAA	>75
pOri F140P-F	GCGCCCCGGGGCCACCATGATCAGTCTGATTGCG	>75
pOri F140P-R	GCGCGAGCTCTTACGTAGAATCGAGACCGAGGAGAGG GTTAGGGATAGGCTTACCTCGCCGCTCCAGAATCTCAA	>75

Table 2.5: Primers used for generating and sequencing MCMV-IE recombinants

Primer name	Sequence	T _m (°C)
IE1 E134G-F	GTTGACGGATGCCTGATCGGCGATCATGATCATGTTGCAACT GGGTGCGGCGGGCTCCATCGTAGAATCGAGACCGAGGAG	>75
IE1 E134G-R	GATATCTTCTGGTCTCTGTGGACATCTGTTGATGATAAAAAA TTATATTTTTTTAGAGAGACTTAACGGCTGACATGGGAA	>75
IE1 WT-F	GTTGACGGATGCCTGATCGGCGATCATGATCATGTTGCAACT GGGTGCGGCGGGCTCCATGGTGGCCCCGGGGATCTTGAA	>75
IE1 WT-R	GATATCTTCTGGTCTCTGTGGACATCTGTTGATGATAAAAAA ATTATATTTTTTTAGAGAGACTTAACGGCTGACATGGGAA	>75

Table 2.6: Primers used for generating and sequencing MCMV-pp150 recombinants

Primer name	Sequence	T _m (°C)
PP150 F140P-F	CCATTCGCCGGTTCTGATGGGGACGGTGGCGGCCTGGTA AAAAAATCGTCGTCGTCTCACATCAGTCTGATTGCGGCG	>75
PP150 F140P-R	CTGTGATGATAATAAAAAAATAATAAAAACCAACCAGGAGC GAGCGATCATCGATCTTGTACTTAACGGCTGACATGGGAATTA	>75
PP150 Short-F	CCACTGCCAAACCCTCAA	53.7
PP150 Short-R	GGTCTGGAGGGTATAGAT	51.4

Table 2.7: Primers used for generating and sequencing MCMV-pp28 recombinants

Primer name	Sequence	T _m (°C)
PP28 F140P-F	ACGTCGTCTTTGAAATCCGCCAAGAACGGCGCCGGCGTGA AGAAAAAAGTCAGGGCCTTGATCAGTCTGATTGCGGCG	>75
PP28 F140P-R	TAAATCTCCTCCACTCTTTCTCCCTTTCTCCCCCCTCACGGT CGATCGATAGATAGATAACTTAACGGCTGACATGGGAATTA	>75
PP28 Inter-F	TACGTTAGCCATGAGAGCTTA	55.9
PP28 Inter-R	CCTCTAAGTTTTTAAGTTTTA	50.1
PP28 Short-F	GACAAGAATAGCGCTATACCC	57.9
PP28 Short-R	GAGAACATGTTGTTGTCACCA	55.9

2.3.4 Restriction enzyme analysis of BAC DNA

Restriction enzyme analysis was used to confirm overall genomic integrity of MCMV BAC recombinants. BAC DNA was prepared as described above. Digestions were performed in a final volume of 50 μ l using 41 μ l of BAC DNA, 5 μ l of (10 \times) Cut Smart restriction buffer (50 mM potassium acetate, 20 mM Tris-acetate, 10 mM magnesium acetate, 100 μ g/ml BSA, pH 7.9) and 4 μ l of High-Fidelity (HF[®]) restriction enzyme (EcoRI, HindIII or BamHI) (New England Bio lab, UK). Reactions were mixed thoroughly by vortexing, pulsed down and then incubated at 37°C for 18 to 24 hours. Following digestion, samples were analysed by gel electrophoresis and resultant DNA bands were visualized under UV light as described above.

2.3.5 Agarose gel electrophoresis

PCR products and DNA digests (see above) were separated and visualised on 1% agarose (TAE) Tris acetate EDTA gels containing EtBr (0.5 μ g/ml). Gels were run in horizontal tanks containing 1 \times TAE running buffer [Appendix II]. DNA samples (5 to 40 μ l) were mixed with 6 \times loading dye (10 mM Tris-HCl, 0.03% bromophenol blue, 0.03% xylene cyanol FF, 60% glycerol, 6 mM EDTA) (to a final 1x concentration) before loading onto gels, and electrophoresis at 80 V for 50-60 min. 1kb DNA ladder [Invitrogen, UK; Appendix II] was included on every gel as a marker for DNA size. DNA was visualized under UV light using a gel documentation system (UVi Tech, Japan).

2.3.6. Agarose gel electrophoresis DNA purification

When necessary, PCR products and cloning fragments generated by restriction digestion were purified by electrophoresis followed by excision from the gel. Briefly, DNA bands of interest were visualized under low intensity UV light and excised from the gel using a clean, single-use, razor blade. A Quick Gel Extraction Kit (Invitrogen, Paisley, UK) was used to extract DNA from the agarose plug, in accordance with the Manufacturer's instruction. Briefly, three volumes of a chaotropic solubilisation buffer (5.5M guanidine thiocyanate, 20 mM Tris-HCl, pH 6.6) were added to 1 volume of gel segment (based on gel fragment weight). Samples were then incubated using a 50°C heat block until the gel slice had completely dissolved (approximately 10 min). After the gel slice was completely dissolved, the mixture was incubated for a further 5 min at 50°C.

One volume of isopropanol was then added and the mixture was transferred to a DNA binding column followed by centrifuged for 1 min at 8,000 rpm ($6,000 \times g$) at RT. The flow-through was discarded and the column was washed with 500 μ l of wash buffer (2 mM Tris.HCl pH 7.5, 20 ml NaCl in 80% EtOH). DNA was eluted from the column by addition of 50 μ l of elution buffer (10 mM Tris-HCl, pH 8.5), incubation for 1 min at RT and centrifugation followed by collection of the eluted DNA. An aliquot of the purified sample (5 μ l) was then electrophoresed on a 1% TAE agarose gel to confirm isolation of a fragment of the desired size. The concentration of purified DNA was determined by Nanodrop, and purified DNA was stored at 4°C for immediate use or at -20°C for long-term storage.

2.3.7 Spin-column DNA purification

PCR products and cloning fragment were also purified by using a QIA-Quick PCR Purification Kit (Invitrogen, Paisly, UK) in accordance with the Manufacturer's instructions. Briefly, one volume of PCR sample was mixed with 5 volumes of HC B3 binding buffer. The mixture was then loaded on to a QIA-quick spin-column and centrifuged at 10,000 rpm ($12,000 \times g$) for 30 s at RT. The flow-through was discarded and 650 μ l of wash buffer (W1) buffer was added and the column was centrifuged at 10,000 rpm ($12,000 \times g$) for 3 min at RT. The flow-through again was discarded, and the column was centrifuged for 1 minute. Fifty microliters of elution buffer (10 mM Tris-HCl, pH 8.5) was added to the column followed by incubation for 1 min at RT. Centrifugation at 14,000 rpm ($12,000 \times g$) for 2 min at RT was used to elute the DNA, which was stored at 4°C for immediate use or at -20°C for long-term storage.

2.3.8 Sequencing

Sequencing was performed by a commercial vendor (Eurofin Genomic, UK), using primers listed in Tables 2.2- 2.7. Sequencing reactions were prepared in 20 μ l reaction volumes, consisting of 10 pmol primer and 50-100 ng/ μ l of DNA. Sequence data obtained was analysed by using MacVector software (Version 15.1.5).

2.4 Cloning

2.4.1 Preparation of insert and vector

The ecDHFR domains used for destabilization of MCMV pp150 (M32) and MCMV pp28 (M99) were prepared by PCR amplification from the following pBMN DHFR plasmids: AcGFP-DHFR-E134G (E134G), YFP-DHFR-Y100I (Y100I) and AcGFP-DHFR-F140P (F140P) using primers listed in Table 2.4. pBMN is a moloney leukemia virus (MMLV)-based vector containing 5` and 3` LTR (retroviral long terminal repeats), which contains promoter, enhancer, and transcription elements. The plasmid also contains an internal ribosome entry site (IRES) and a fluorescent (YFP/AcGFP) gene as a fluorescent reporter for ecDHFR domains located immediately downstream of the IRES. This plasmid also contains a multiple cloning site (MCS) and a tandem-dimeric red fluorescent protein (HcRed-t) behind the IRES as well as antibiotic selection marker (ampicillin resistance) [Appendix III]. The N-terminal DHFR genes (E134G and Y100I) contain a Kozak translation initiation signal with a start codon while the C-terminal DHFR gene (F140P) contains a stop codon.

PCR was performed using high-fidelity polymerase as detailed above, and PCR products were quantified by Nanodrop. PCR fragments were cloned into the pOri-FRT(WT) plasmid. This plasmid contains a kanamycin resistance marker for selection, two *FRT* sites, an *R6K* (suicide) origin of replication and an MCS for insertion of the PCR fragment. These plasmids were then used as PCR templates to generate the necessary recombinant fragments for targeting destabilization domain for genetic fusion to either the pp28 (M99) or pp150 (M32) genes in the WT MCMV BAC by using homologous recombination.

2.4.2 Digestion of DNA with restriction enzymes

DNA (plasmid or PCR products) was digested with desired restriction enzymes at 37°C for 2 hr, as described above. Digests were generally performed in a final reaction volume of 50 µl using 40 µl of PCR product or plasmid, 4 µl of 10 × restriction buffer (50 mM Potassium acetate, 20 mM Tris-acetate, 10 mM Magnesium acetate, 100 µg/ml BSA, pH 7.9), 7 µl molecular distilled water and 4 µl of High-Fidelity (HF®) restriction enzyme (New England Biolab, UK). The contents were mixed thoroughly and incubated at 37°C for 2 h. If necessary the restriction enzymes were heat-inactivated according to Manufacturer's instructions. Digested samples were then visualised by agarose gel electrophoresis.

2.4.3 Ligation of DNA

Purified restriction enzyme digested PCR products and pOri-FRT(WT) plasmids were ligated by using DNA ligase enzyme. Ligation was performed by mixing 2 µl (10 ×) ligation buffer, 1 µl pOri- FRT(WT) plasmid (50 ng/µl), 1 µl of T4 DNA ligase (3 unit/µl; New England BioLab, UK) and 1µl of a PCR amplified DNA made to a final volume of 20 µl with distilled H₂O. Ligation reactions were incubated at RT for 30 min. Reactions with no DNA insert served as negative controls. Ligation reactions were inactivated by incubation at 75°C for 2 min prior to either their immediate use for transformation competent bacteria or storage at 20°C.

2.4.4 Transformation of *E. coli* with DNA plasmids

Commercially available Pir1 competent bacteria (Invitrogen, Paisley, UK) were used for transformation. Pir1 bacteria encode the replication protein π that is required to enable replication of plasmids containing the R6K γ (suicide) origin of replication present within the

pOriFRT(WT) plasmid. Four microliters of ligation reaction was added to pre-cooled 15 ml polypropylene tubes (Fisher Scientific, Leicestershire, UK). Non-digested pOriFRT(WT) plasmid was used as a positive transformation control to determine the efficiency of competent cells. Pir1 cells were thawed on ice and 50 µl were transferred into tubes containing the ligation mixture. The mixture was then gently mixed and incubated on ice for 30 min. Cells were heat shocked at 42°C for 40 s followed by 5 min recovery on ice. SOC medium [2.0 g Tryptane, 0.5 g yeast extract, 1M MgCl₂, 1M MgSO₄, 1M NaCl, 1M KCl, 20% Glucose; Appendix IV] was added up to 1ml and bacteria were incubated at 30°C with shaking for 2 h. Bacteria were then plated on LB agar containing 25 µg/ml Kan (Table 2.1.) and incubated at 30°C for 24 to 48 h. Colonies were screened by restriction enzyme analysis and agarose gel electrophoresis. Sequence integrity of the respective ecDHFR domains of selected clones were confirmed by using PCR and Sanger DNA sequencing. Glycerol stocks of selected recombinants were prepared and stored at -80°C.

2.5. Mutagenesis of MCMV BACs

2.5.1 Mutagenesis of MCMV BACs by using E/T homologous recombination

The large size of BACs makes standard cloning procedures unfeasible (Ruzsics & Koszinowski, 2008). Instead, homologous E/T (Red) recombination using small linear recombination fragments to target the BAC DNA for genetic manipulation are used. This technique, called Red E/T homologous recombination was established by Wagner and colleagues (Wagner & Koszinowski, 2004) and has been described in detail above (see Introduction). An overview of the process is shown in Figure 2.1. Recombinant PCR fragments being used to target the MCMV BAC genome contain short sequences of homology (approx. 60 bp) flanking the target site. Recombination fragments also contain an

antibiotic resistance marker to allow for selection of recombinants. The R6K γ suicide origin of replication prevents replication of 'carry-over' PCR plasmid template from the PCR reaction used to produce the recombination fragment due to the absence of the π replication protein. In this study the linear PCR fragments carried the DNA sequence to be inserted (ecDHFR domains or IA virus epitopes), flanked by DNA sequence homologous to the targeted gene of MCMV (either *M32* or *M99*) and a kanamycin resistance marker (Kan^R) flanked by *FRT* sites for subsequent removal of Kan^R (Cox, 1988).

2.5.1.1 Preparation of DNA recombinant fragment for recombineering

Recombination fragments were generated by PCR using primers listed in Tables 2.2-2.7. Each primer contained 60 nucleotides of sequence homology flanking the targeted site of insertion within the MCMV BAC genome with additional sequence complementary to the template plasmids required for PCR amplification. PCR products were spin-column purified and characterized as described in above (Sections 2.3.6 to 2.3.8) prior to use for E/T recombination.

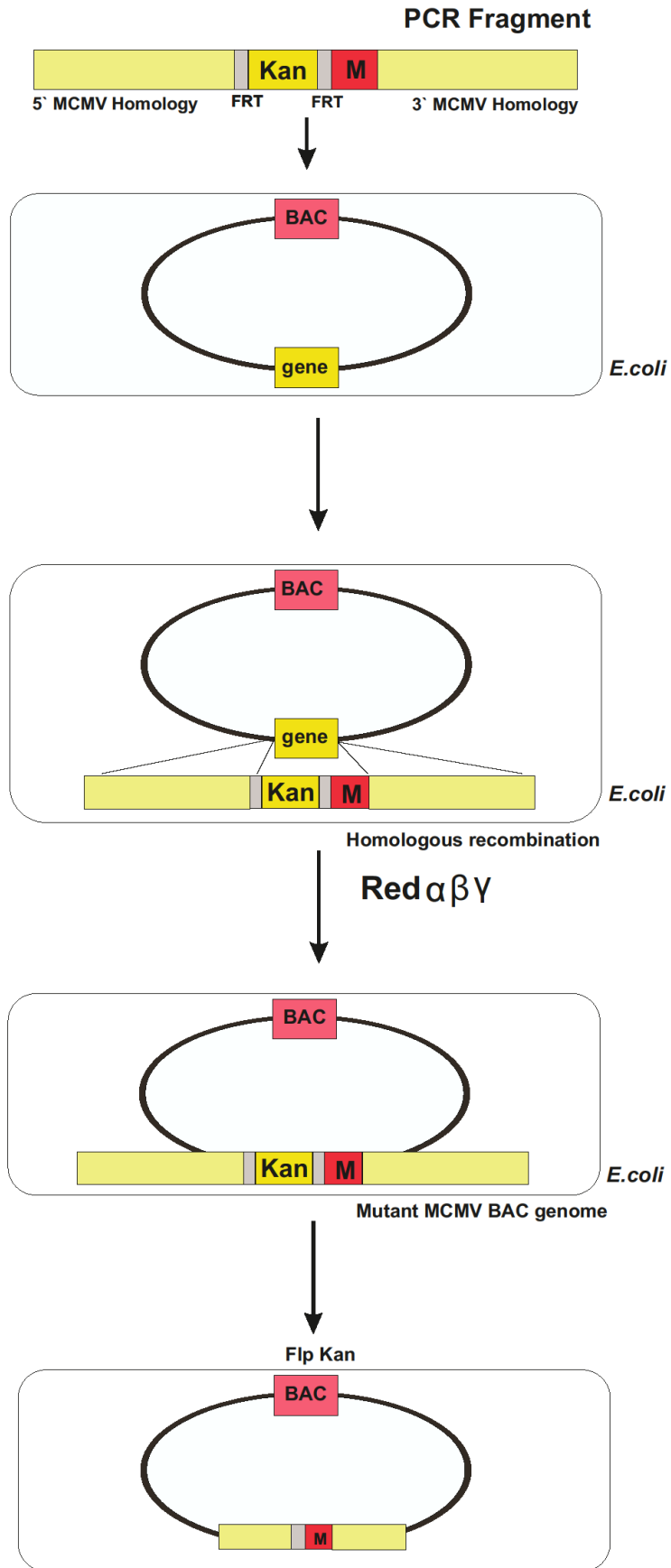


Figure 2.1 Schematic of E/T (Red) homologous recombination ('recombineering) strategy used for construction of recombinant MCMV vaccine vectors. Recombinant fragments carrying a selectable marker (Kan^R) flanked by *FRT* sites and desired mutation (M) (ecDHFR or IA virus epitope) are amplified by PCR. The recombination fragment also contains approx. 60 bp of sequence flanking the site targeted for insertion of the mutation within the MCMV BAC. Recombination fragments are electroporated into *E.coli* strains (either EL250 or SW105) expressing α , β , and γ proteins of bacteriophage gamma required for homologous recombination. Following selection of recombinant BACs on the basis of kanamycin resistance, the *FRT*-flanked selectable marker is removed by FLP mediated-excision. The desired mutation and a single *FRT* 'scar' remain in the mutant MCMV genome. BAC, bacterial artificial chromosome (pink box); *FRT*, FLP-recombinase recognition site from *Saccharomyces cerevisiae* (grey box); Kan^R; kanamycin resistance marker (yellow box); and M, desired mutation (red box).

2.5.1.2 Recombineering of the MCMV BAC Genome

Five millilitres LB cultures of EL250 bacteria containing the MCMV BAC were incubated overnight at 30°C under chloramphenicol (Cam) selection (Cam, 17 µg/ml), which is required for maintenance of the MCMV BAC. One millilitre of the overnight culture was transferred to 50 ml LB broth (Cam, 17 µg/ml) and incubated at 30°C for 4 h or until the OD₆₀₀ reached 0.6. After incubation, the recombination system was induced by incubating the culture at 42°C for 17 min in a shaking water bath. Following temperature induction of the E/T recombination system, bacteria were rapidly cooled and then incubated on ice for 15 min. Bacteria were then prepared made electrocompetent and electroporated with the respective recombination fragment as described above (see Section 2.2.4). Immediately after electroporation, bacteria were transferred into 800 µl LB medium (without any antibiotic) and incubated at 30°C with shaking for 2 h at 30°C to allow E/T recombination and recovery. Bacteria were then plated on LB agar plates with appropriate antibiotics (Table 2.1) and

incubated at 30°C for two days until colonies became visible. Colonies were picked and the recombinant BAC DNA was isolated for further diagnostic analysis by restriction digest and PCR as described above.

2.5.1.3 Removal of the FRT-flanked selection marker

Following confirmation of genomic integrity of recombinant MCMV BACs by restriction enzyme digestion (see Section 2.3.4), *FRT*-flanked Kan^R markers were removed by arabinose induction of the FLP-recombinase present within the EL250 strain. Induction of FLP-recombinase results in the removal of the entire Kan^R gene leaving a single *FRT* ‘scar’ (Wagner *et al.*, 1999). One hundred microliters from an overnight starter culture was added to 5 ml fresh LB broth (1:50 dilution) containing 17.5 µg/ml c and incubated for a 4 h or until the OD₆₀₀ reached 0.6. One milliliter of 10% (w/v) arabinose solution (Fisher Scientific, Leicestershire, UK) was then added, and the culture was incubated for an additional 1 h to induce FLP recombinase expression. Five hundred microliters of the arabinose-induced culture was transferred into 4.5 ml LB (17.5 µg/ml Cam) and incubated at 30°C shaking for 1 hr. After performing a 10-fold dilution series, 50 µl of the 1x10⁻⁴ dilution was plated onto LB plates (17.5 µg/ml Cam) and incubated at 30°C for two days until colonies became visible. Single colonies were picked and replica-plated overnight at 30°C on fresh LB plates containing either Cam alone or Cam and Kan, to identify Kan-sensitive colonies (indicative of *FRT*-flanked Kan^R excision). Overnight cultures of Cam-resistant, Kan-sensitive colonies were prepared and BAC DNA was isolated and characterized by restriction digest analysis, and PCR and DNA Sanger sequencing as described above.

2.5.2 Mutagenesis of MCMV BAC plasmid using Galk recombination

EL250-based E/T recombination leaves heterologous sequence as a residual *FRT* ‘scar’. To enable ‘seamless’ recombination that leaves no heterologous sequences, Warming and colleagues developed a two-step E/T-based strategy that uses a combination of positive (antibiotic-based) and negative (*galK*-based) markers for recombinant BAC selection (Warming *et al.*, 2005). An outline of this strategy is shown in Figure 2.2. The SW105 bacterial strain used is derived from EL250 and contains the same temperature induced E/T homologous recombination system. However, SW105s differ in the presence of a complete galactose operon with a precise deletion of the *galactokinase K* gene (*galK*), which is required for the *galK*-based negative selection.

In the first step, a *KanR/galK* cassette is inserted by homologous recombination into the MCMV BAC genome as described above. The *KanR/galK*-containing recombination cassette is generated by PCR using pYD-C255 plasmid as the PCR template. Bacteria that have recombined the *KanR/galK* gene into the MCMV BAC are then selected for growth in the presence of Kan/Cam and on minimal plates that contain galactose as the only carbon source. A further round of purification of *KanR/galK*⁺ colonies is then achieved by streaking of single colonies on MacConkey galactose indicator plates and selection of bright red colonies. This colour change enables identification of *KanR/galK*⁺ colonies as a result of galactose metabolization by the *galK*⁺ bacteria acidifying the media and changing an indicator dye on the MacConkey plate to bright red. Bright red colonies are picked for the second recombination step.

In the second recombination step, a PCR-derived recombination fragment containing the desired mutation flanked by the homologous targeting sequence is then used to replace the *Kan/galK* cassette. Bacteria are then grown on agar plates containing 2-deoxy-galactose (DOG) as the selection and glycerol as the carbon source. DOG is harmless in the absence of

galK. However, in the presence of *galK*, DOG serves as negative selection through its metabolization to a toxic intermediate (2-deoxy-galactose-1-phosphate) via phosphorylation by the product of the *galK* gene, galactokinase. Growth in the presence of DOG will therefore select for bacteria that have undergone recombination with the desired mutation fragment to replace the *Kan/galK* cassette.

2.5.2.1 Insertion of MCMV BAC into SW105 bacterial strain

The MCMV BAC was transformed into SW105 *E. coli* as described above (see Section 2.2.3 and 2.2.4). Bacterial cultures were selected on LB agar plates containing (12.5 µg/ml Cam) and incubated at 30°C for two days until colonies became visible. Colonies were picked and the recombinant BAC DNA was isolated for further diagnostic analysis by restriction digest as described in above. Glycerol stocks of MCMV transformed SW105 cells were then made for long-term permanent storage as described in Section 2.2.2.

2.5.2.2 Preparation of galK cassette

The *KanR/galK* cassettes were generated by PCR using 60 to 65 bp primers listed in Table 2.3. Each primer contained 40 nucleotides of sequence homology flanking the targeted site of insertion within the MCMV genome. PCR was performed on pgalK-kan (pYD-C255) plasmid (Warming *et al.*, 2005). PCR products were spin-column purified and characterised as above prior to use for recombination in SW105 bacteria containing the MCMV BAC genome.

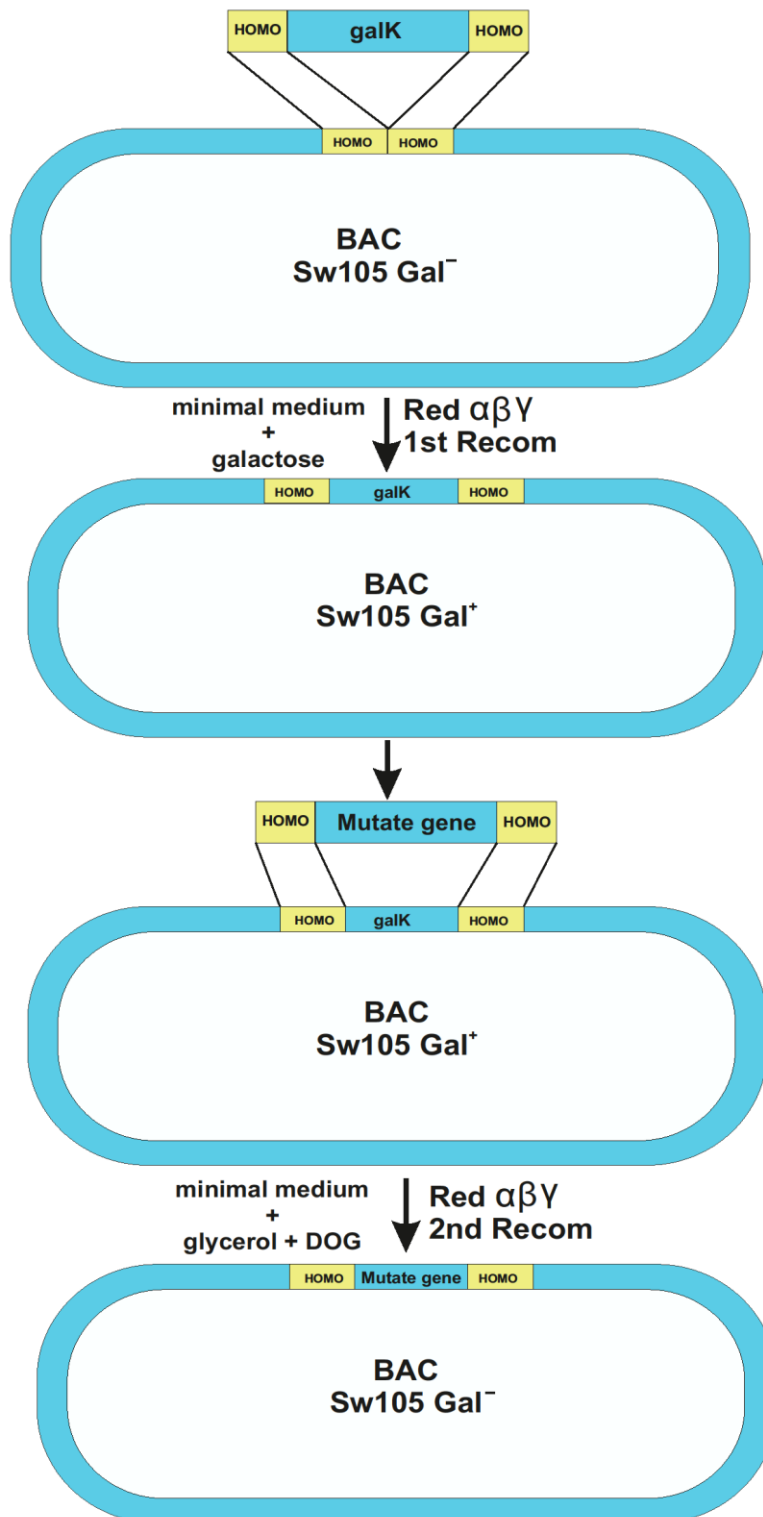


Figure 2.2 Schematic representation of the galK recombination strategy used for construction of recombinant MCMV vaccine vectors. Step 1: Recombinant fragments carrying the *Kan^R/galK* gene flanked by 60 bp homologous sequence are produced by PCR and electroporated into *E.coli* (SW105) host harbouring MCMV BAC. Homologous E/T recombination is used to insert the *Kan^R/galK* targeting cassette into the desired position targeted for mutagenesis within the MCMV BAC. Bacteria are then selected on M63 minimal medium containing Kan and Cam with galactose as the sole source of carbon. **Step 2:** After a round of purification on MacConkey agar plates, a second round of E/T recombination is used to replace the *Kan^R/galK* marker with the a PCR recombination fragment containing the desired mutation. Bacteria then undergo negative selection by growth on minimal medium containing 2-deoxy-galactose (DOG) with glycerol as a sole carbon source to select for galK⁻ bacteria that have replaced the *Kan^R/galK* marker with the desired mutation. BAC, bacterial artificial chromosome; HOMO, homology arms; Mutate gene: desired mutation. SW105 is an *E. coli* strain; derived from EL250 containing the complete galactose operon except for targeted deletion of the *galactokinase K* gene (*galK*).

2.5.2.3 Electroporation of the galK cassette into electro-competent SW105 bacteria and positive selection

Recombination PCR fragments were electroporated into SW105 bacteria harbouring MCMV BAC essentially as described for EL250s above. After recovery, bacterial cultures were transferred to an Eppendorf tube (Greiner Bio-One Ltd, Stonehouse, UK), pelleted at 14,000 rpm (12,000 × g) for 30 sec at RT. Pellets were washed three times in 1 ml 1× M9 salt solution [Appendix IV] to remove any carbohydrate. Bacterial pellets were re-suspended in 1 ml fresh M9 salt solution and then 10 µl, 50 µl and 100 µl were plated onto M63 minimal media plates [Appendix IV]. Plates were incubated at 30°C for 4-5 days until colonies became visible. Colonies were selected based on the Kan resistant gene. Single colonies were picked and struck onto MacConkey plates and incubated at 30°C overnight. Bright colonies were used for the second recombination step.

2.5.2.4 Electroporation of the DNA cassette into electrocompetent SW105 bacteria for reversion of galK followed by selection on DOG plates

The DNA cassette containing the *KanR/galK*⁺ marker was replaced in a second round of E/T recombination by using a DNA recombination fragment containing the desired mutation and homologous sequence flanks. Electrocompetent *KanR/galK*⁺ bacteria were prepared as described and 1 µg of the DNA cassette (with desired mutation) was introduced by electroporation as before. Following electroporation, bacteria were transferred into 10 ml LB broth (without any supplements) and incubated with shaking for 4.5 h at 30°C in a shaker for E/T recombination and recovery. Bacterial cultures were pelleted and washed as described in (Section 2.5.2.3) and then plated on DOG plates [Appendix IV]. DOG plates were incubated for three to five days at 30°C until colonies became visible.

2.6 Virology

2.6.1 Virology Methods

All eukaryotic tissue culture and virus work was carried out under sterile conditions in a biological safety cabinet Class II (Holten LaminAir, UK). Infected cells were incubated at 37°C using a Binder CO₂ incubator (Binder, Germany) supplemented with 95% humidity and 5% CO₂.

2.6.1.1 Reconstitution of viral progeny from recombinant MCMV BAC DNA in MEF cells

Recombinant and WT viruses were reconstituted by electroporation of BAC DNA into MEF cells. MCMV BAC DNA was isolated and purified as described in (Section 2.3.1.2). MEFs were prepared, washed and trypsinized as described in (Section 2.1.1.1). MEFs were grown in 175 cm² tissue culture flasks and were used for electroporation when monolayers were 85-

90% confluent. Cells were counted and re-suspended at a concentration of 1×10^7 cells/ml. Cells (250 μ l) were used for each electroporation reaction. Five microliters of BAC DNA was transferred into 0.4 cm² cuvettes (BIO-RAD Gene Pulser, UK) and 250 μ l of the cell suspension was added and gently mixed immediately prior to electroporation using a Bio-Rad Gene Pulser (BIO RAD, Hertfordshire, UK). Cells were pulsed at 0.25 KV, 950 μ FD. Immediately following electroporation, 1 ml of DMEM medium was added to the cuvette and cells were transferred to a 10 cm² dish containing 10 ml complete DMEM. Cells were incubated overnight at 37°C / 5% CO₂.

One day post-transfection media was removed and cell monolayers were washed once with 3 ml DPBS followed by being overlaid with a 1.2% seaplaque agar overlay (Lonza, Slough, UK) [Appendix I]. Prior to use, the 1.2% seaplaque agar was melted by microwaving and allowed to cool in a 37°C water bath. The 1.2% seaplaque agar was mixed at a final ratio of 1:1 with 2 \times DMEM (500 ml sterile H₂O, 13.38 g DMEM powder, 7.5% Sodium bicarbonate and 10% FBS; Life technology, Paisley, UK) and 10 ml was added to each plate. The plates were left at room temperature until the overlay agar solidified and were then returned to the 37°C incubator and monitored daily for plaque formation using an inverted microscope (Motic AE2000, UK). MCMV plaques were picked by gently stabbing a sterile 1000 μ l pipette tip (Dutscher, Essex, UK) through the agar until the area of the plaque was reached. A small agar plug was then removed and transferred to a 2 ml microcentrifuge tube containing 200 μ l fresh medium and stored at -80°C until required.

2.6.1.2 Reconstitution of viral progeny from recombinant MCMV BAC DNA in MEF cells in the presence of trimethoprim (TMP)

The ecDHFR-tagged viruses (attenuated viruses) were reconstituted as described above, with the exception that the synthetic chemical ligand trimethoprim (TMP; Cat. No T7883, Sigma-Aldrich, Dorset, UK) was added to the overlay to enable virus growth. After electroporation, cells were incubated overnight in 10 ml DMEM media supplemented with 50 or 100 μ M TMP. The following day, the desired concentration of TMP was added to the seaplaque overlay. Plates were then incubated at 37°C/5% CO₂ as previously described, but fresh seaplaque overlay was added every 24 h to maintain the TMP concentration at the desired level. Plaque formation was monitored for up to 7 days using an inverted microscope (Motic AE2000, UK) and plaques were picked as described above. Seed and concentrated stocks of these recombinant viruses were always prepared in the presence of 50 or 100 μ M TMP, which was replenished every 24 hours to maintain levels.

2.6.1.3 Removal of the BAC cassette from reconstituted MCMV

After reconstitution, viral progeny derived from recombinant MCMV BAC DNA still contain the BAC cassette. The presence of this BAC cassette has been shown to have a negative impact on virus replication *in vivo* (Wagner *et al.*, 1999); (Section 1.2.1.2.1). To excise the BAC cassette from the reconstituted virus genome, MCMV virus was passaged five times on MEFs. Infected MEFs were incubated at 37°C / 5% CO₂ for 3-4 days until 100% CPE was observed in the culture. Cells were then harvested by scraping, centrifuged at 3800 rpm (4600 \times g) for 20 min at RT and the clarified supernatant was aliquoted and labelled as passage one (P1). The process was repeated until 5 passages were harvested. The passage 5 virus was then used as a starter virus stock from which to prepare MCMV seed stocks.

2.6.1.4 Preparation of virus seed stocks

Seed stocks of MCMV were prepared in 175 cm² tissue culture flask, in 20 ml volumes of DMEM as described in Section 2.1.1.1. The cells were infected with 120 µl of passage 5 virus. Both cells and supernatant were harvested after 4 to 5 days when full CPE was observed. After centrifugation at 3,800 rpm (4,600 × g) for 20 min at RT to remove cellular debris, the clarified supernatant was stored at -80°C in 1 ml aliquots. These aliquots were then used to make the concentrated viral stocks.

2.6.1.5 Production of High Titre MCMV Virus Stocks

Twelve 175 cm² flasks of 80-90% confluent MEFs were infected at MOI of 0.01 in 20 ml of pre-warmed growth medium and incubated at 37°C / 5% CO₂ for 4 to 5 days until full CPE was observed. Cells and supernatant were harvested as described above and stored at -80°C. Supernatant was rapidly thawed followed by centrifugation at 3,800 rpm (4,600 × g) for 20 min at RT. The clarified supernatant (32 ml) was then added to Oakridge Nalgene-style tubes (Cat. No. 1053-8341, Fisher scientific, Leicestershire, UK), underlaid with a 4 ml 20% Sorbitol cushion [1mM MgCl₂; 5mM Tris-HCl; pH7.4; Appendix I] and centrifuged at 22,000 rpm (3,200 × g) for 80 min at RT to pellet the virus using a high speed centrifuge (Beckman Coulter, Fisher Scientific, UK). The supernatant was decanted and the viral pellet was re-suspended in 2 ml of 2% FCS in DPBS. Concentrated virus stocks were aliquoted and stored at - 80°C. One aliquot was thawed and used to determine the titre of the stock and confirm sequence.

2.6.1.6 Titration of virus by TCID₅₀ Limiting Dilution (median tissue culture infectious dose) assay

Concentrated viral stocks were tittered on MEF cells using a TCID₅₀ (defined as the dilution of virus required to infect 50% of the cells) assay. MEF cells were seeded at a density of 1×10^5 per well in 96 well plates in 100 μ l volumes the day before the assay. Ten-fold serial dilutions of virus stocks were prepared and 100 μ l of each dilution was added to replicate wells. The plate was incubated for four to five days at 37°C, and wells with CPE were counted using a light microscope. Titres were expressed as TCID₅₀/ml, and then plaque forming units per ml (PFU/cell) were calculated (Reed & Munech, 1938).

2.6.1.7 Virus titration using a plaque assay

MEF cells were seeded at a density of 1×10^5 cells per well of a 24 well plate in 500 μ l volumes and incubated overnight in a 37°C incubator. 10-fold serial dilutions of samples were prepared in triplicate from 10^{-1} to 10^{-8} . Media was removed and 500 μ l of each dilution was added to relevant wells. Plates were incubated overnight at 37°C and the following day, media was removed, monolayers were washed with $1 \times$ DPBS, and overlaid with 1 ml of semi-solid methylcellulose [MTC; Appendix I]. MTC was used in order to prevent the spread of virus from infected cells to uninfected cells. On day three post-infection the monolayers were stained with Neutral Red [Appendix I] and returned to the incubator. Plaque development took 4-5 days at 37°C/ 5% CO₂. Five days post-infection plaques were counted using a light microscope and viral titres were expressed as PFU/cell, calculated using the following equation:

$$\text{Viral titre (PFU/ml)} = \frac{\text{counted plaques} \times \text{dilution of counted well}}{\text{Volume of virus dilution}}$$

2.6.1.8 Virus growth curve kinetics

To analyse the growth properties of the MCMV recombinants generated during this study, multi-step growth curves were performed. MEF cells were seeded at a density of 2×10^5 cells per well of 6 well plate or 4×10^5 cells per T75 cm² tissue culture flask. Cells were infected at a multiplicity of infection (MOI) of 0.01 or 0.1 plaque forming units (PFU/cell). After 2 h of incubation at 37°C, the inoculum was removed, cells were washed twice with $1 \times$ DPBS and fresh media was added. At selected times post infection, monolayers were scraped into supernatant, centrifuged at 14,000 rpm ($12,000 \times g$) for 5 min at RT to pellet cells and clarified supernatants were stored at -80°C. Viral titres were determined by TCID₅₀ or plaque assay (Section 2.6.1.6 and 2.6.1.7, respectively).

2.7 Analysis of MCMV proteins

2.7.1 SDS-PAGE

Sodium dodecyl sulphate-polyacrylamide gel electrophoresis (SDS-PAGE) is a widely used analytical technique for fractionation of protein samples and for estimation of molecule protein weight. In this study SDS-PAGE was performed using Laemmli's discontinuous buffer system (Laemmli, 1970) and a BioRad mini gel apparatus (Bio-Rad, Leicestershire, UK). Glass plates (10 cm x 20 cm) were secured together using magnetic clips, the plate then transferred to the casting tray and secured in places with clamps. Glass plates were washed with distilled water, followed by 70% ethanol and then dried prior to use. A well-forming comb was inserted between the plates and the glass was marked 1 cm below the bottom of the comb, to mark the height of the resolving gel to be poured. The comb was removed and resolving gel prepared [Appendix V] and poured. To prevent atmospheric oxygen from interfering with gel polymerisation, 70% isopropanol was used to overlay the resolving gel.

The gel was left at RT for polymerisation. When polymerisation was complete, the isopropanol was removed and the gel interface was washed three times with distilled water. Filter paper (Whatman) was used to remove the excess water. A stacking gel [Appendix V] was then laid over the resolving gel followed by reinsertion of the comb was inserted. After polymerisation the magnetic clips were removed and the gel was transferred to the electrophoresis tank for electrophoresis. Running buffer (1×) [Appendix V] was added to the chamber unit. Wells were loaded with 25 µl of protein sample. Twenty-five microliters of 1× sample buffer [Appendix V] was added to empty wells. A protein molecular weight marker was always included to enable protein molecular weight determination. Electrophoresis was then performed at 90 V for 2 h.

2.7.2 Western blotting analysis

2.7.2.1 Transfer

Proteins resolved by SDS-PAGE electrophoresis were transferred to PVDF membranes for western blot analysis by using a Criterion™ Blotter system (Bio-Rad, UK); (Towbin, Staehelin & Gordon, 1979). Two pieces of filter paper and foam, and one piece of PDVF membrane (Bio-Rad, Hertfordshire, UK) were cut to the same size as the gel (approximately 7 cm × 8 cm). Two transfer pads were soaked in 1 × transfer buffer [Appendix V] for 10 min prior to use. Layers were then arranged within the transfer ‘sandwich’. The foam layer was placed on top of the filter paper followed by the gel. The PVDF membrane was placed directly on top of the gel using forceps, and then the remaining layers of filter paper were placed on top. Air bubbles were removed and the entire gel cassette sandwich was placed into the transfer gel tank containing TBST buffer [Appendix VII]. Transfer was performed at 100 V for 1 h at 4°C, with an ice pack to maintain temperature.

2.7.2.2 Immunodetection

Following transfer, PVDF membranes were blocked in 25 ml of 5% non-fat milk (blocking buffer [2.5 g skimmed milk powder in 50 ml of 1× PBS-T or 1× TBS; Appendix VII] on an orbital shaker at 150 rpm for 1 h at RT or overnight at 4°C. Membrane were then washed twice for 5 min with 1× TBST-T or 1× PBST-T [Appendix VII]. Membrane were then incubated with the primary antibody for 1 h, followed by washing three times with 1× TBST-T or 1× PBST-T at RT with gentle shaking. The appropriate dilution of secondary antibody was added to the membrane and incubated for 1 h at RT with gentle shaking at 150 rpm. Secondary antibody was removed and the membrane was washed three times for 5 min with 1× TBST-T or 1× PBST-T at RT before developing by chemiluminescence (Pierce, ECL, UK).

2.7.2.3 Membrane Stripping

PVDF membranes were stripped and re-probed up to three times. Thirty-five milliliters of stripping solution was added to the membrane and incubated on a shaker for 5 min. The membrane was then washed three times for 15 min with 1× TBST-T or 1× PBST-T at RT. The membrane was then ready to be probed again.

2.8 Animal models and vaccination

To characterize the CD8⁺ T cell responses induced by recombinant MCMV/IA (NP, PA and NS2) strains, immunogenicity studies were performed in H2^b-restricted mice. 6-8 week old C57BL/6 female mice were purchased from authorized vendors and allocated into four groups of 10 mice each (See Figure 2.3). All animal use complied with Guide for the Use and Care of Laboratory Animals, USDA Animal Welfare Regulations, PHS Policy on Humane Care and Use of Laboratory Animals and other relevant regulations. Studies were all performed only after obtaining necessary approval. Mice were inoculated intraperitoneally (i.p.). Group 1 was the negative control group and received a mock inoculum. Group 2 and group 3 were inoculated with 3×10^5 PFU/animal of wild type (MCMV-WT) and 1×10^5 PFU/animal of inactivated H5N1. Group 4 was inoculated with a single dose of 1×10^5 PFU of the three recombinant MCMV-IA (NP, PA, and NS2) vectors combined as a single bolus, giving a total of 3×10^5 PFU/ animal (1×10^5 PFU of each virus). At weeks 8 and 12 post-inoculation, mice from each group were humanely euthanized to harvest splenocytes and additional organs (i.e. lung) for analysis of T cell responses.

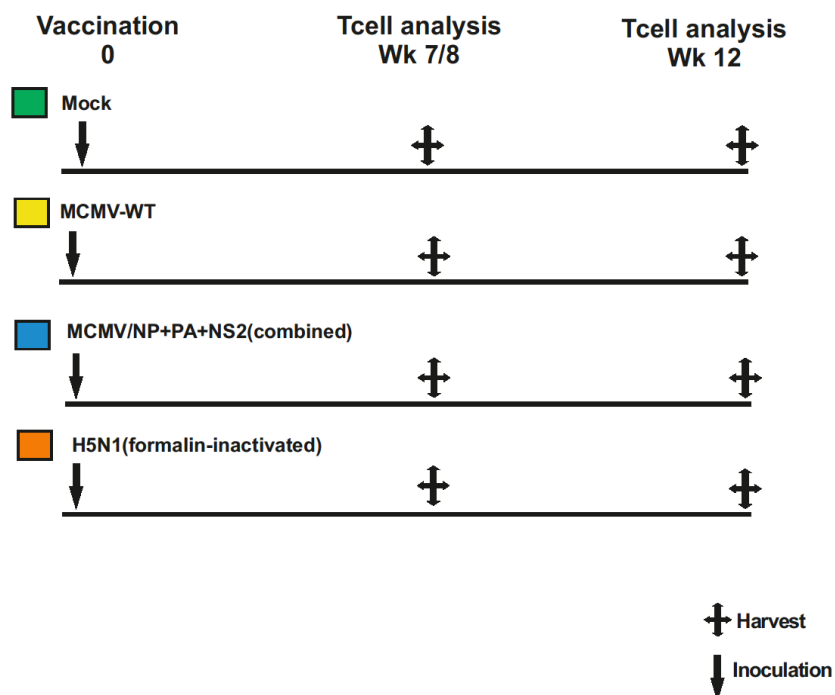


Figure 2.3 Schematic showing MCMV/IA vaccinated mouse groups. Schematic showing MCMV-IA vaccinated mouse groups. C57BL/6 (H2b-restricted, 6-8 weeks old) female mice were immunized using a single ip dose of 1×10^5 PFU of the indicated MCMV-IAV vector(s). Mice receiving the combination of the 3 MCMV IA vectors were inoculated with 1×10^5 PFU of each vector as a single ip bolus for a total of 3×10^5 PFU. Control groups received MCMV WT (3×10^5 PFU), diluent (Mock) or formalin-inactivated H5N1. At weeks 8 and 12, splenocytes as well as other organs were harvested for analysis of T cell responses.

2.8.1 T cell analysis by ICS

Spleens isolated at times indicated were analysed for $CD8^+$ T cells directed against the MCMV-IA (NP, PA, and NS2) or MCMV-encoded M38 and M45 CTL epitopes by intracellular cytokine staining (ICS). Spleens were harvested into 5 ml RP-10 media on ice and were then homogenized on 100 micron pore-size cell strainers. Cell strainers were washed with an additional 5 ml RP-10, and splenocytes were centrifuged at 18,000 rpm ($700 \times g$) for 5 min at RT. Supernatants were discarded and pellets were resuspended in 20 ml RP-

10 and re-centrifuged as above. Erythrocytes were removed from the samples by resuspension of the pellet in 2 ml $1 \times$ RBC lysis buffer [See Appendix I for the recipe] and incubating for 4 min at RT. Lysis buffer was removed by washing twice with RP-10 media (20 ml, then 5 ml). Pellets were resuspended in 5 ml RP-10 media and cells were counted as described in (Section 2.1.3).

Splenocytes at 1×10^6 cells/ml were seeded into 96 well-plates and then centrifuged at 18,000 rpm ($700 \times g$) for 3 min at RT. Supernatants were discarded and cells were detached from the plate bottom by briefly vortexing the plate. One hundred microliter of RP-10 media was added to the cells and mixed thoroughly by pipetting. Cells were stimulated in the presence of brefeldin A (BFA; $10 \mu\text{g/ml}$) with peptides ($1 \mu\text{g/ml}$); H2^b-restricted epitopes IA virus proteins: (NP, PA, and NS2), PB or MCMV M38 or M45 (Munks *et al.*, 2006). The H2^b-restricted PB peptide was used as an AI virus-derived peptide not contained within the MCMV IA vaccine antigen. The well-characterised H2^b- restricted epitopes (M38 and M45) from MCMV were used as an indicator of MCMV infection [Appendix X]. Cells were stimulated for 6 h at 37°C, washed twice with 200 μl DPBS and centrifuged at 18,000 rpm ($700 \times g$) for 3 min at 4°C. Cells were then stained for surface markers by incubating with monoclonal antibodies [CD8, CD4 and CD3; Appendix X] in a total volume of 100 μl DPBS buffer and incubated overnight at 4°C in the dark.

After surface staining cellular markers (CD3, CD4 and CD8) cells were washed twice with 200 μl of DPBS buffer and centrifuged at 18,000 rpm ($700 \times g$) for 3 min at 4°C. Cells were then resuspended by vortexing and fixed by adding 100 μl of fixation buffer (eBioscience, Ireland), and incubating for 5 min at 4°C. Cells were then permeabilized with 100 μl $1 \times$ permeabilization buffer (eBioscience, Ireland). Cells were incubated for 3 min at 4°C, followed by washing twice with 200 μl of $1 \times$ permeabilization buffer and centrifugation at

18,000 rpm ($700 \times g$) for 3 min at 4°C . The supernatant was decanted and cells were resuspended by vortexing. The appropriate monoclonal antibodies (IFN- γ and TNF- α ; Appendix IV) were added in $100 \mu\text{l}$ /sample volumes of $1 \times$ permeabilization buffer and then incubated for 1 hr at 4°C . The stained cells were washed in cold $1 \times$ permeabilization buffer twice, and then centrifuged at 18,000 rpm ($700 \times g$) for 3 min at 4°C and resuspended in $100 \mu\text{l}$ of DPBS buffer for analysis by flow cytometry on a LSR II (BD Biosciences), and data was analysed by using FlowJo software (version 10.0.7; Tree Star, Inc.). Samples were performed in triplicate. Response frequencies were determined by subtracting background and then averaging background subtracted responses.

2.9 Statistics

Data are presented as mean \pm standard deviation. GraphPad Prism software program (Version 7) was used to assess statistical significances as well as to plot the graphs. Specific statistical test indicated in each experiment. P-values ≤ 0.05 were considered significant and displayed by (*) in the figures, (** = P- values < 0.05 , *** = P-values < 0.005). In general, values corresponded to two experiments, each performed in triplicate.

Chapter Three:

*Development of a conditionally-attenuated cytomegalovirus
(CMV) vaccine vector platform*

3.1 Introduction

As discussed in detail above, CMV- and other herpesvirus-based vaccines represent a promising vaccine vector platform, not only for humans but also for animals such as pigs that are involved in transmission of infectious pathogens like IA virus to humans. In this regard, CMV vectors are unique in the high level of immunity that they induce against their heterologous encoded pathogen target antigens, the long duration (even after a single dose) and immediate effector function associated with this immunity (Hansen *et al.*, 2011; Hansen *et al.*, 2009; Marzi *et al.*, 2016; Redwood *et al.*, 2007; Tierney *et al.*, 2012; Tsuda *et al.*, 2011; Tsuda *et al.*, 2015). Presumably due to the long period of coevolution and adaptation to their specific animal host, herpesviruses are largely benign in the presence of a normal healthy immune system. However, these viruses can cause severe and frequently fatal disease in the immunocompromised host (McCormick & Mocarski, 2015; Nassetta, Kimberlin & Whitley, 2009). Environmental safety is an additional concern for any replicating genetically-modified organism (GMO), especially one so well adapted for spread. A considerable focus of our, as well as other, laboratories has therefore been the development of attenuation strategies for herpesvirus-based vectors.

A number of studies indicate that herpesvirus replication may not be required for priming and maintenance of immune responses against herpesviruses. In these studies, completely replication-defective CMV (Mohr *et al.*, 2010; Snyder *et al.*, 2011) and HSV (Brockman & Knipe, 2002; Dudek & Knipe, 2006) have been shown to maintain levels of immunogenicity to those approaching and in many cases comparable to WT virus. Consistent with their *inability* to replicate, these replication-deficient viruses are completely non-pathogenic *in vivo* even in immune-compromised animals (Mohr *et al.*, 2010). All of these studies have used permanent deletion of the gene encoding for an essential herpesvirus protein in order to achieve attenuation. This approach necessarily requires the production of replication-

defective viruses on cell lines expressing the essential virus protein in *trans* for complementation of the virus replication deficiency. However, such cell lines can be difficult or impossible to create due to toxicity and stability issues, which are further complicated by kinetic requirements of gene expression due to the complexities of the herpesvirus replication cycle (Borst *et al.*, 2008; Glaß *et al.*, 2009; Mocarski *et al.*, 1996).

Conditional replication defective CMV based on genetic fusion of essential genes to DDs that can be modulated by a small binding molecule has been identified as one means to overcome the need for *trans*-complementation in CMV (Glaß *et al.*, 2009) (see Section 1.3.2). In this earlier study the MCMV (IE1/3) or HCMV (UL51 and UL77) genes were targeted for regulation using the FKBP/shield DD system. In the present thesis two essential tegument proteins were selected based on a number of criteria. First, a recent study had suggested that T cell versus antibody bias of CMV-based vectors can be modulated by use of Early (E) versus Late (L) promoters to regulate the heterologous target antigen (Marzi *et al.*, 2016). Therefore, any replication defective vector must be able to transit the virus replication cycle to the point where L gene expression can occur. This requirement necessarily limits attenuation to targeting of L genes. Second, tegument proteins, and pp28 and pp150 in particular, were targeted as they may be less structurally constrained functionally than other L proteins such as glycoproteins.

Finally, selection of pp28 and pp150 was based on previous studies that had identified the ability of these proteins to maintain function and virus replication following their genetic fusion to heterologous domains. The ability of pp28 and pp150 to maintain function after fusion of heterologous protein domains to their carboxyl-terminus was consistent with this region being devoid of key functional information (AuCoin *et al.*, 2006; Baxter & Gibson, 2001; Seo & Britt, 2006; Silva *et al.*, 2003). To align with their potential application to low

and middle-income countries (LMICs), where such conditional-replication strategies are most suited, an ecDHFR-based DD system was utilized that uses the inexpensive TMP stabilizing ligand compared to the far more costly Shield-1 molecule associated with the FKBP-based system.

3.2 Results

As discussed in the Introduction (Section 3.1) a main hypothesis being examined in this thesis is whether targeting of essential tegument proteins is a suitable strategy for development of conditionally-replication defective MCMV vectors as a means for production of immunogenic, inexpensive attenuated vaccine vectors. Given the host species restriction of CMVs, MCMV infection in mice is an ideal small animal CMV model system in which this question can be explored. Although beyond the scope of this thesis (which is focused on *in vitro* studies to examine the practicality of this approach in a WT virus background before moving into defined pathogen challenge systems) the work performed in this present thesis has been used to support subsequent CMV-based vaccine studies in mouse pathogen systems such as Ebola virus.

3.2.1 Cloning of MCMV recombinants conditionally attenuated by genetic fusion of ecDHFR to genes encoding pp150 or pp28 tegument proteins

To construct the MCMV recombinants expressing destabilized essential tegument proteins, a number of factors need to be taken into account. DD domains differ in a number of important characteristics, including their dynamic range, basal expression level in the absence of the stabilizing TMP molecule and the requirement for their fusion to either the N or C-terminus of the protein being targeted for destabilization. It is also critical that fusion of the ecDHFR domain to the targeted protein does not affect the normal function of the essential virus protein when in the stabilized (TMP-bound) state. Although this can be predicted to a certain extent based on the effect of fusion of other domains to the proteins being targeted (when data is available), it can only be definitively determined by empirical analysis after construction of the respective recombinant viruses (Wang *et al.*, 2016).

We therefore selected three ecDHFR versions for analysis in our studies for fusion to the N- or C-terminal regions: E134G and Y100I ecDHFR for N-terminal positioned destabilization, and F140P ecDHFR for destabilization through fusion to the C-terminus. Additionally, two N-terminal ecDHFR domains (E134G and Y100I) that differed in basal expression level and dynamic range were included to assess the effect of these parameters on tegument stabilization and virus attenuation (Table 3.1).

Data from previous published studies clearly showed that the N-terminus of pp28 is absolutely essential for the virus replication. An acidic cluster (aa 44 to 57) in the N-terminus is required for the cytoplasmic localization of pp28 in virus infected cells and for replication of infectious virus (Jones & Lee, 2004; Seo & Britt, 2006). The N-terminus of pp28 was therefore not targeted destabilization, and ecDHFR was fused only to the C-terminus of pp28, which has been shown as non-essential for virus replication. A schematic of the entire cloning strategy is shown in Figure 3.2.

Table 3.1 Characteristics of ec-DHFR DDs

ec-DHFR Versions	Basal level of protein stability		Position
	-TMP	+TMP	
E134G	400	5399	N-terminus
Y100I	327	1871	N-terminus
F140P	247	4757	C-terminus

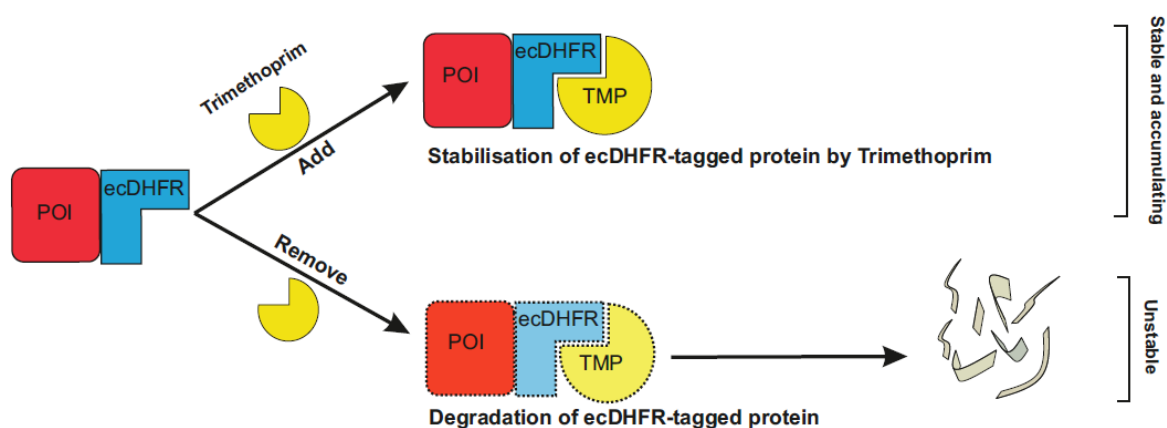


Figure 3.1 Schematic showing the DD strategy. A destabilizing version of the *E. coli* dihydrofolate reductase (ecDHFR) is genetically fused to a protein of interest (POI). This fusion results in degradation of the entire fusion protein. Addition of the small synthetic ligand: TMP stabilizes the entire fusion protein, preventing degradation. Adapted from (Banaszynski *et al.*, 2006; Iwamoto *et al.*, 2010).

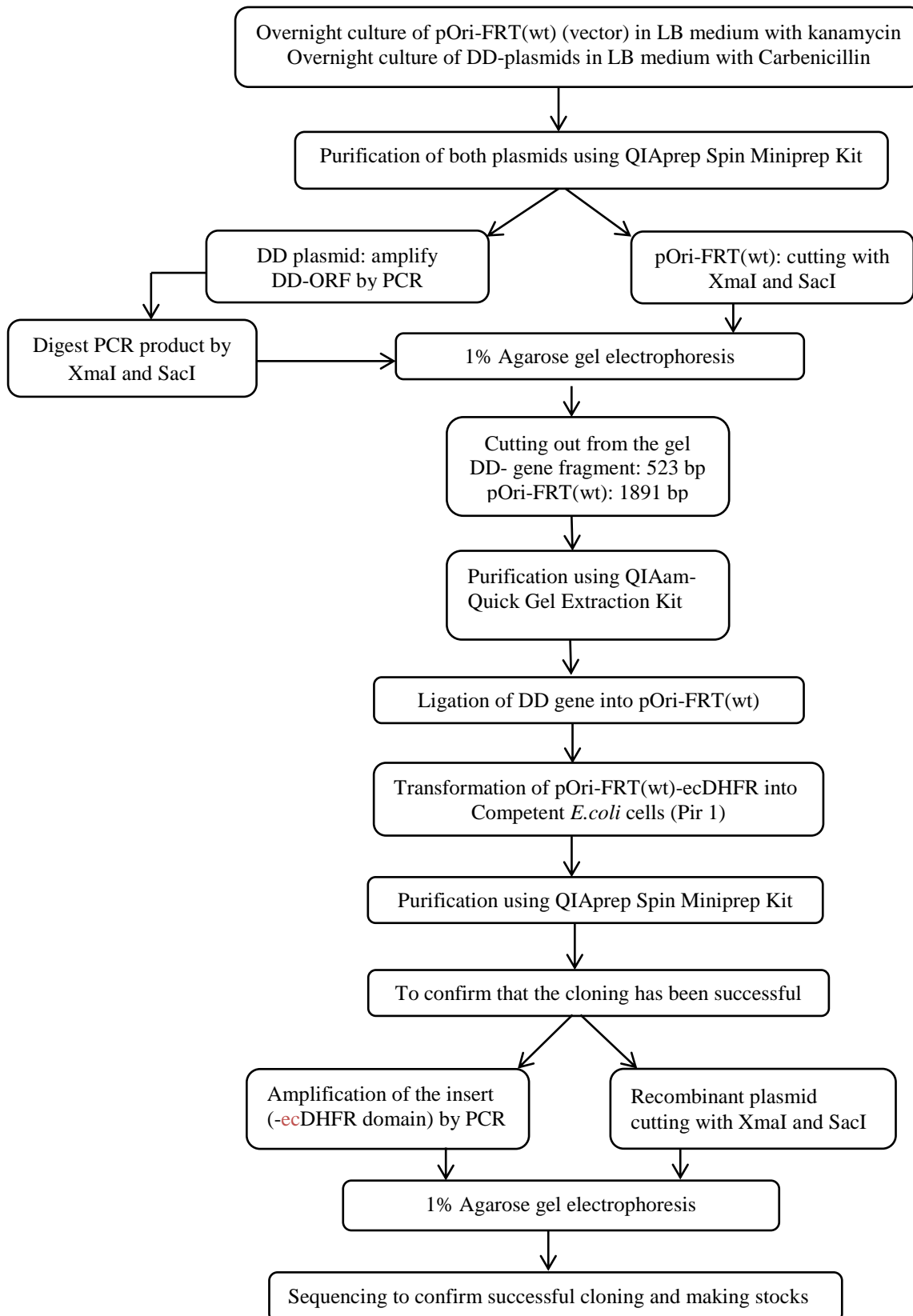


Figure 3.2 A flow-chart showing cloning ecDHFR into the pOriFRT(wt) vector.

3.2.1.1 Cloning of ‘suicide’ plasmid containing ecDHFR for use as PCR template in construction of MCMV recombinants

MCMV recombinant vectors were constructed using E/T linear homologous recombination, as described in (Sections 1.1.5.2.2). Figure 3.3 shows a flow-chart diagram of the construction process. The first step in E/T cloning is to generate the necessary recombination fragment encoding sequences of the destabilized protein together with the FRT flanked Kan^R marker, which requires cloning of the individual ecDHFR variants into a ‘suicide’ vector called pOriFRT(wt). The pOriFRT(wt) plasmid contains a ‘suicide’ R6K γ origin of replication, which prevents replication of the plasmid in bacteria other than those expressing the replication protein π . This prevents false-positive Kan-resistant clones due to template carry-over from the recombination fragment PCR, as the EL250 and SW105 cells lack the π protein. These ecDHFR containing plasmids are then used as templates to generate the necessary recombination fragments by PCR. Inclusion of homologous targeting sequences at the 5’ ends of the primers target the recombination cassette containing the ecDHFR for genetic fusion to the desired position of the pp150 or pp28 gene.

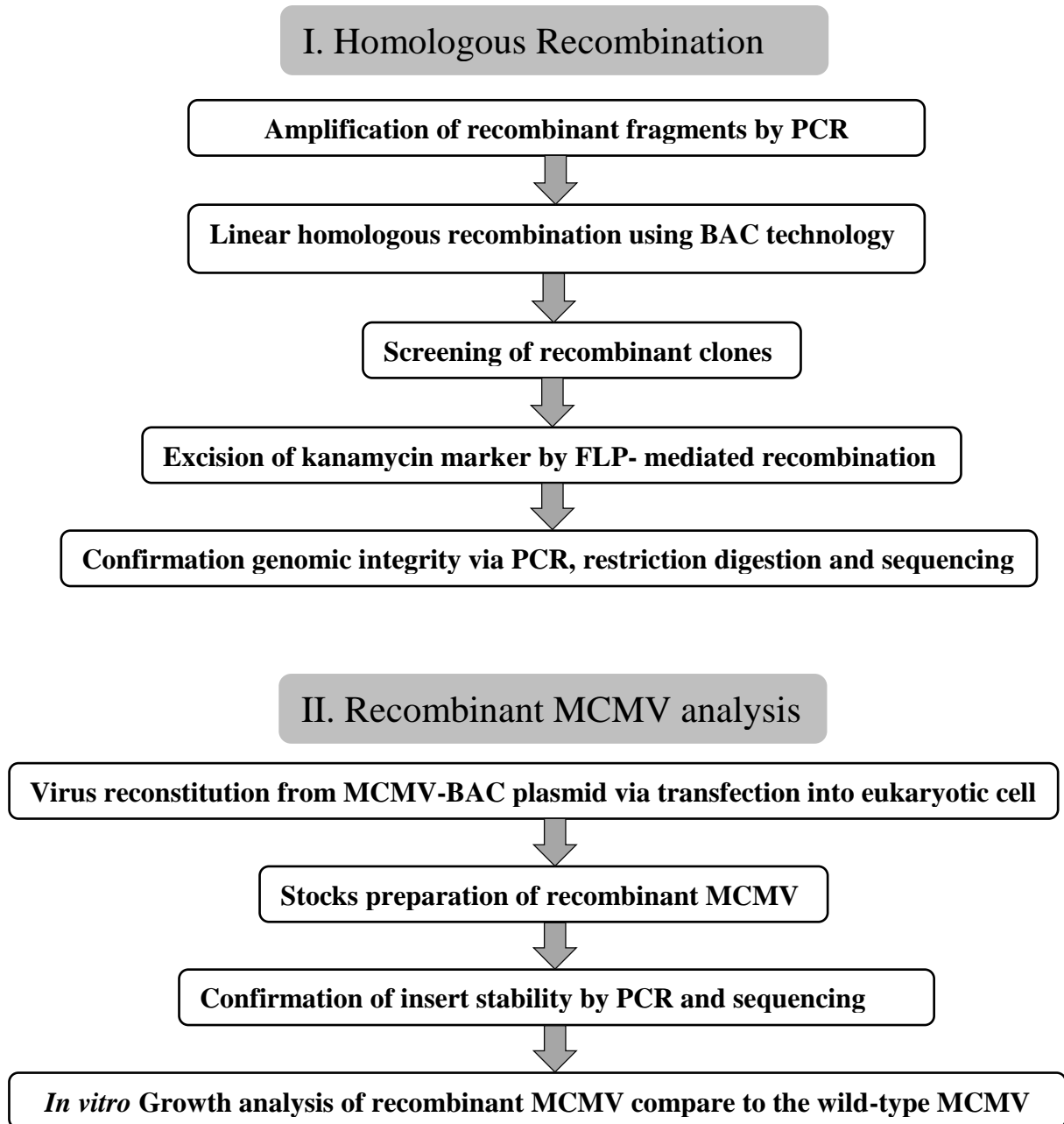


Figure 3.3 A flow-chart of construction of the recombinant MCMV vector vaccine.

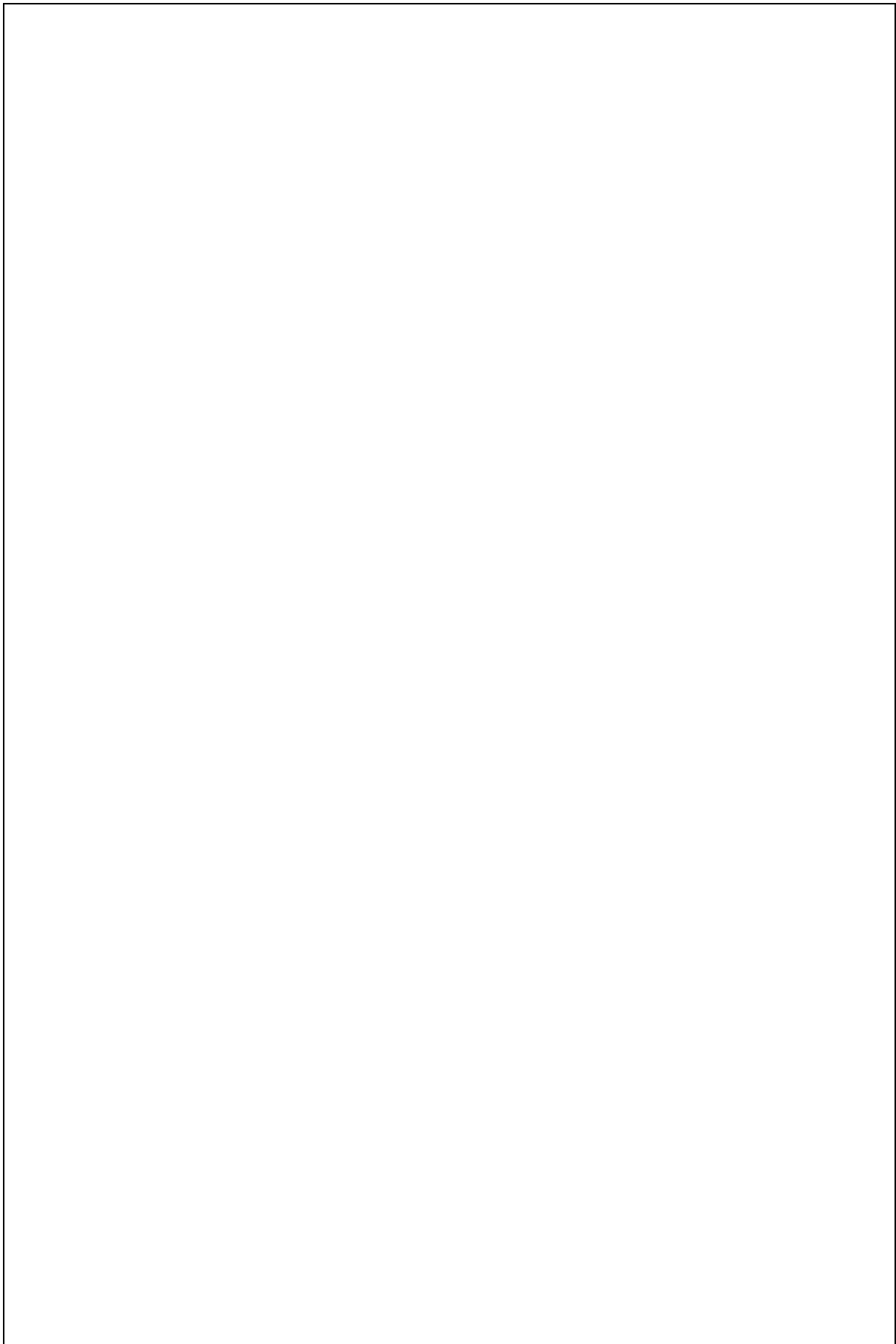


Figure 3.4 Schematic illustrating cloning of ecDHFR (E134G) domain to the pOriFRT(wt) vector. (A) The first step in the construction was amplification of ecDHFR-(E134G) domain from ACGFP-DHFR-E134G plasmid by PCR, using synthetic oligonucleotide that contained restriction enzyme sites (XmaI and SacI) and a V5 tag. (B) In the second step, PCR products and pOriFRT(wt) (suicide-based vector) containing a KanR gene flanked by FRT sites as well as XmaI and SacI (for insertion of the E134 domain) were digested with XmaI and SacI followed by ligation. (C) Schematic of resulting plasmid pOriFRT(wt)-E134G. (D) PCR was then used to amplify recombination fragment containing the necessary flanking homology to pp150 for E/T based recombination within the MCMV genome.

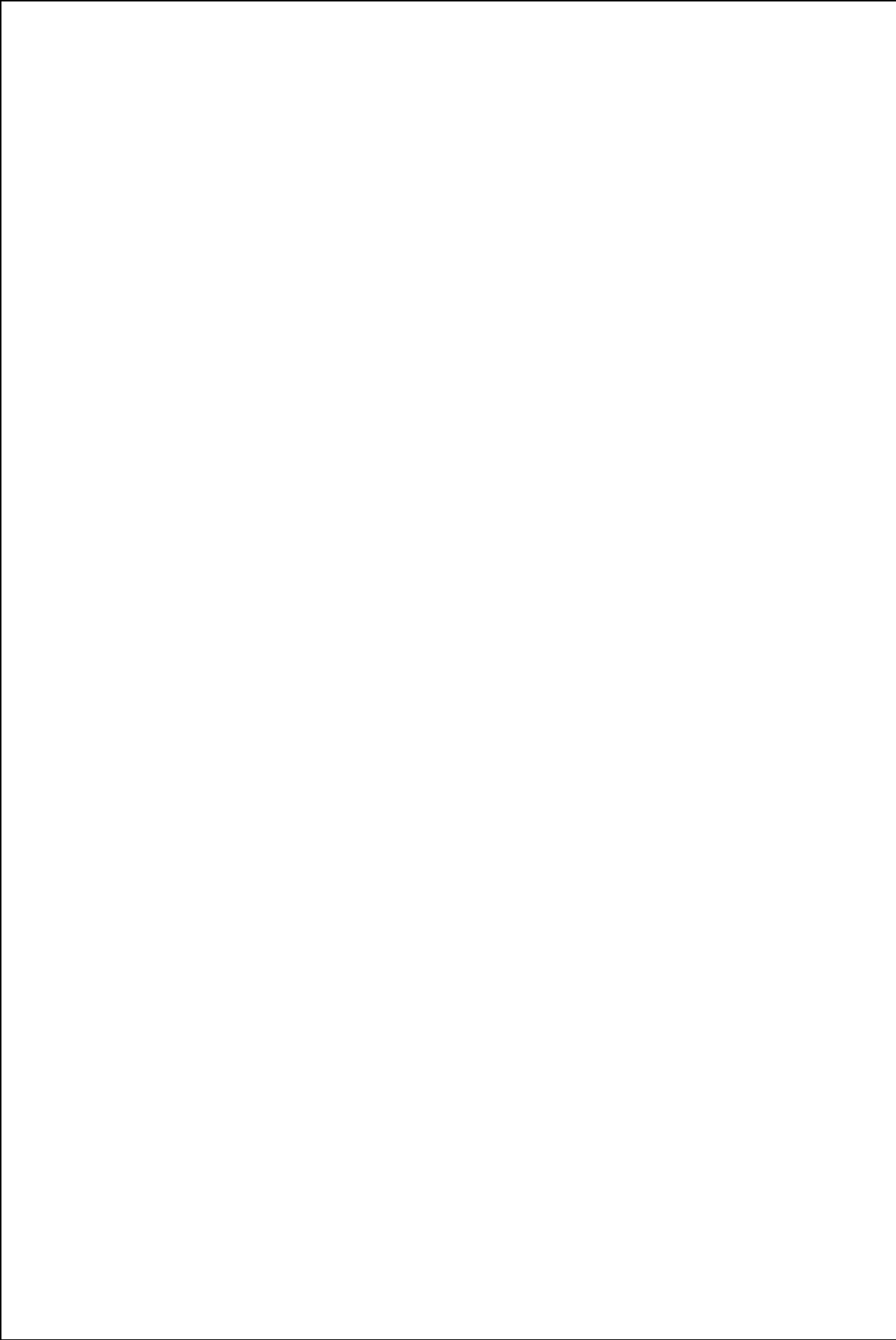


Figure 3.5 Schematic illustrating cloning of ecDHFR (Y100I) domain to the pOriFRT(wt) vector. (A) The first step in the construction was amplification of ecDHFR-(Y100I) domain from YFP-DHFR-Y100I plasmid by PCR, using synthetic oligonucleotide that contained restriction enzyme sites (XmaI and SacI) and a V5 tag. (B) In the second step, PCR products and pOriFRT(wt) (suicide-based vector) containing KanR gene flanked by FRT sites as well as XmaI and SacI (for insertion of the Y100I domain) were digested with XmaI and SacI followed by ligation. (C) Schematic of resulting plasmid pOriFRT(wt)-Y100I. (D) PCR was used to amplify recombination fragment containing the necessary flanking homology to pp150 for E/T based recombination within the MCMV genome.

3.2.1.1.1 Cloning of E134G and Y100I into pOriFRT(wt)--ecDHFR plasmid

The aim was to clone the 540 bp ecDHFR gene domain into the pOriFRT(wt) vector in order to genetically fuse these domains to the N-terminus of the targeted pp28 and pp150 proteins. E134G or Y100I domains were amplified by PCR from parental plasmids (AcGFP-DHFR-E134G and YFP-DHFR-Y100I (kindly provided by Dr. Thomas Wandless, University of Stanford, CA, USA) containing the ecDHFR (E134G) or ecDHFR (Y100I) domain fused in-frame to GFP or to the yellow fluorescent protein (YFP), respectively. PCR amplification was performed using synthetic pOri E134G or pOri Y100I primers (Table 2.4; Figures 3.4-3.5). After a GCGC anchor region, each primer contained restriction enzyme sites (SacI and XmaI) to enable insertion into the pOriFRT(wt) vector. PCR products were separated on a 1% agarose DNA gel for 1 h (Section 2.3.5) to confirm PCR amplification of the desired domain. The results shown in (Figure 3.6 A and B) indicate that the E134G and Y100I domain-fragments had been amplified, resulting in production of a single, well-defined DNA band at the expected molecular size (540 bp; Figure 3.6 A and B lanes 2-5).

The PCR products (Figure 3.6) were spin column purified (Section 2.3.7), digested with SacI and XmaI for 2 h at 37°C and were then separated on a 1% agarose DNA gel, which yielded

a band of 1880 bp (Figure 3.7). The pOriFRT(wt) vector was also digested with SacI and XmaI. Single restriction digests of pOriFRT(wt) with SacI and XmaI alone were used to confirm digestion of the PCR products as a size shift would not be observable for the PCR products (Figure 3.7). Digested PCR products and vector were then gel extracted and purified using Quick Gel Extraction Kit (Section 2.3.6), and re-analysed on an agarose gel to ensure gel extraction was successful (Figure 3.7). The 1800 bp linearized vector and 540 bp PCR products show the presence of the desired gel-purified DNA of the correct size. The purified PCR product was then cloned into SacI and XmaI sites of pOriFRT(wt) plasmid.

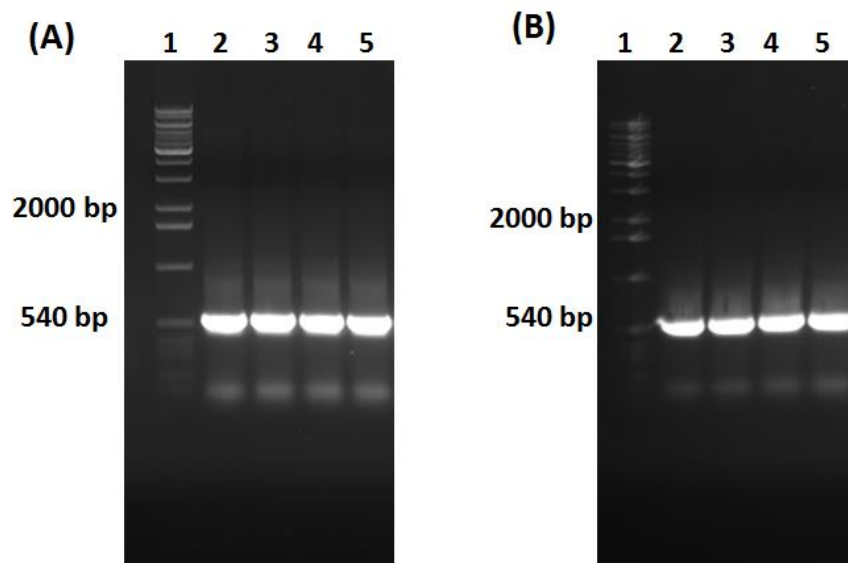


Figure 3.6 DNA gel showing PCR amplification of ecDHFR: (A) E134G domain from AcGFP-DHFR-E134G and (B) Y100I domain from YFP-DHFR-Y100I. PCR product were separated on a 1% agarose DNA gel and visualized by using EtBr (0.5 μ g/ml). The single DNA band at 540 bp shows amplification of the desired ecDHFR E134G and Y100I domain.

The purified E134G or Y100I *SacI*/*XmaI* digested fragments were then ligated into the linearized pOriFRT(wt) vector (Figures 3.4 and 3.5), generating pOriFRT(wt)-E134G and pOriFRT(wt)-Y100I plasmids containing DD ecDHFR genes (E134G and Y100I), respectively. The ligated DNA was transformed into competent Pir 1 *E.coli* cells that express the necessary π protein for ‘suicide’ R6K γ origin of replication complementation (as described in Section 2.4.4) and then plated onto agar with 25 μ g/ml Kan. The following day 20 single colonies were picked from the plates and grown overnight with 25 μ g/ml Kan (Table 2.1). Plasmid DNA was extracted and purified using a plasmid Miniprep kit (Section 2.3.1.1) and analysed by restriction enzyme digest and PCR to confirm presence the E134G or Y100I insert.

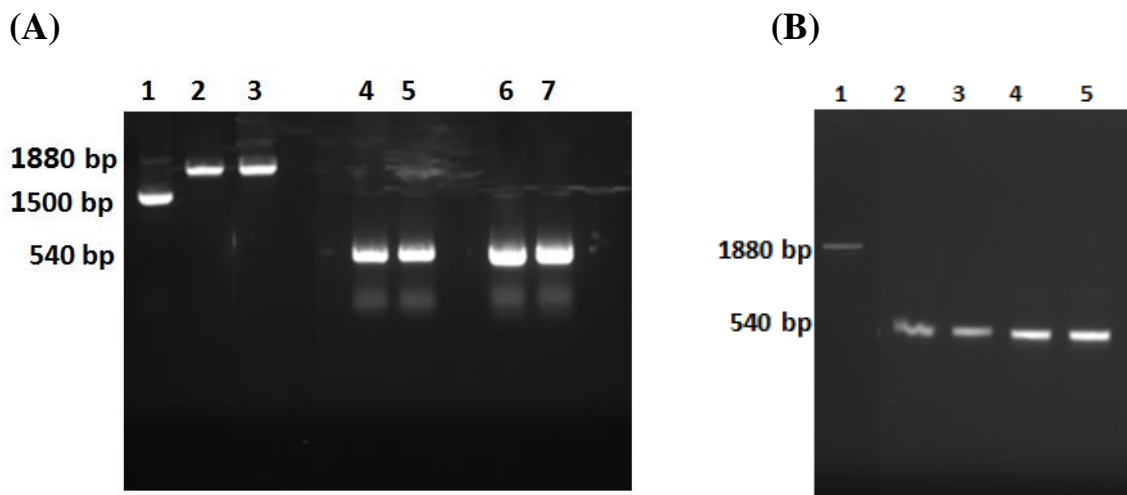


Figure 3.7 Gel electrophoresis showing *SacI* and *XmaI* digestion of PCR product and pOriFRT(wt) plasmid during cloning of pOriFRT(wt)-ecDHFR (E134G/Y100I). (A): the uncut vector (lane 1) was compared to single digested *SacI* (lane 2) and *XmaI* (lane 3) producing DNA fragment of approx. 1880 bp indicating digestion of the vector. Lanes 4, 5 and 6, 7 show the restriction digestion of PCR product (E134G and Y100I) amplified from AcGFP-DHFR-E134G and YFP-DHFR-Y100I plasmids using *SacI* and *XmaI* digestion of fragments of the correct size (540 bp). (B): confirming the size bands following gel extraction and purification of pOriFRT(wt) vector (lane 1) and PCR amplified products: E134G lanes 2, 3 and Y100I lanes 4, 5.

3.2.1.1.1.1 Restriction digestion analysis of recombinant plasmid pOriFRT(wt)-E134G/Y100I

To determine whether the E134G and Y100I domains had been inserted into the pOriFRT(wt) plasmid, plasmid DNA isolated from 25 individual Kan-resistant clones from each vector were analysed by SacI and XmaI restriction digestion. As shown in Figures 3.8 and 3.9, a subset of the clones yielded the expected 540 bp (insert) and 1880 bp (vector backbone) bands as expected for pOriFRT(wt)-ecDHFR(E134G) and pOriFRT(wt)-ecDHFR(Y100I). The results (Figures 3.8 and 3.9) show successful cloning and correct size insert in 5 colonies of E134G and 6 colonies of Y100I domain, respectively of total of 25 recombinant colonies subjected to screening. Other screened recombinant plasmids were parental pOriFRT(wt) and contained no inserts following restriction enzyme analysis; examples are shown in Figures 3.8 and 3.9 lanes 2. Recombinant pOriFRT(wt)-ecDHFR(E134G) and pOriFRT(wt)-ecDHFR(Y100I) clones are shown in lanes 3-7. In these lanes two bands were observed, the lower band indicated the inserted E134G/Y100I gene at the expected molecular size each (~540 bp). While the upper band indicated the vector of the pOriFRT(wt)-E134G/Y100I without insert (~1880 bp; Figures 3.8 and 3.9).

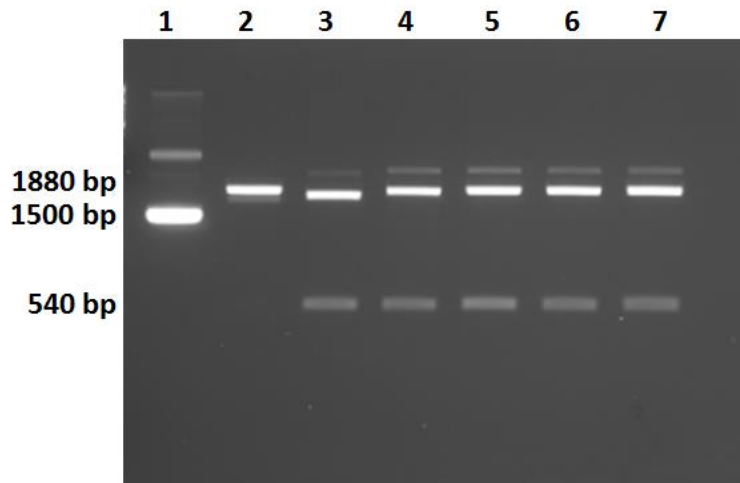


Figure 3.8 Restriction enzyme screening of pOriFRT(wt)-ecDHF(R(E134G)) clones. Lane 1 shows uncut pOriFRT(wt)-control. Lane 2 shows control pOriFRT(wt) parental plasmid without insert, digested with SacI and XmaI. Lanes 3-7 show confirmed pOriFRT(wt)-ecDHF(R(E134G)) clones following digestion with SacI and XmaI lanes (3-7). Two bands are observed; upper band of approximately 1880 bp indicated that the vectors are linearized and the lower bands indicated the insert (E134G) of approximately 540 bp.

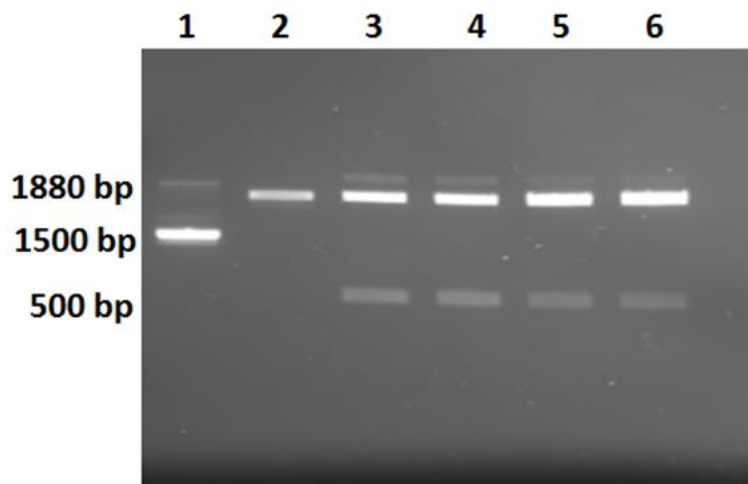


Figure 3.9 Restriction enzyme screening of pOriFRT(wt)-ecDHF(R(Y100I)) clones. Lane 1 shows uncut pOriFRT(wt)-control. Lane 2 shows second control pOriFRT(wt) parental plasmid without insert, digested with SacI and XmaI. Lanes 3-6 show confirmed pOriFRT(wt)-ecDHF(R(Y100I)) clones following digestion with SacI and XmaI lanes (3-6). Two bands are observed; upper band of approximately 1880 bp indicated that the vectors are linearized and the lower bands indicated the insert (Y100I) of approximately 540 bp.

3.2.1.1.1.2 Sequence analysis of pOriFRT(wt)-ecDHFR(E134G) and (Y100I) template plasmids

The colonies that screened positive for either the E134 or Y100I inserts by restriction digest (Figures 3.8-3.9) were analysed by PCR and Sanger sequencing to confirm the integrity of the ecDHFR domains. The E134G or Y100I domains were amplified using the same primers initially used to amplify the E134G/Y100I domains from the parental ecDHFR plasmids: AcGFP-DHFR-E134G and YFP-DHFR-Y100I. Consistent with the restriction digest analysis, PCR amplification produced a single band of the expected 540 bp size. Two clones (number 1 and 3) of pOriFRT(wt)-ecDHFR(E134G) and pOriFRT(wt)-ecDHFR (Y100I) were selected for Sanger sequencing. The insert sequence from both clones of each plasmid showed 100% identity with the E134G or Y100I domains, followed by the sequence encoding the V5 epitope tag that had been fused in-frame during the PCR process (Figures 3.10 and 3.11). Glycerol stocks of clones (1 and 3) of the pOriFRT(wt)-ecDHFR (E134G) and (Y100I) plasmids were prepared and stored at -80°C (Section 2.2.2). Following cloning of ecDHFR domain into the pOriFRT(wt) plasmid, the recombinant plasmids pOriFRT(wt)-ecDHFR(E134G) and pOriFRT(wt)- ecDHFR(Y100I) were used to generate two versions of conditional replication-defective MCMV vaccine vectors destabilized by fusion of the DD to the N-terminus of the targeted tegument proteins.

```

CTAGAATCGAGACCGAGGAGAGGGTTAGGGATAGGCTTACCGGGATAGGCTTACCTCGCCG
TCCAGAATCTCAAAGCAATAGCTGTGAGAGTTCTGCGCATCAGCATCGTGGAATTGCTGAA
TACCGATCCCCAGTCGTCCGGCTCGTAATCCGGGAAATGGGTGTCGCCTTCCACTTCTGGTC
GATATGCGTCAGATACAGTTTTTCGCGCTTTTGGCAAGAACTGTTTCATAAACGCGACCGCCG
AATCACCATGATTTCTGGTACGTCACCACACGCCGCGATGGCTTCATCCACCGACTTCACCCA
CGTTACGCGATCGTCCGTA CTGCTGACTGCTGAGGATAATATTTTTGCGTCCTGGCAACGG
ACGACCGATTGATTCCCAGGTATGGCGGCCATAATCACGGGTTTATTTAAGGTGTTGTGTT
TAAACCAGGCGAGATCGGCAGGCAGGTTCCACGGCATGGCGTTTTCCATGCCGATAACGTGA
TCTACCGCTAACGCCGAATCAGACTGATCATGGTGGCCCCGGGGATCTTGAAGTTCCTATTC
CGAAGTTCCTATTCTCTAGAAAGTATAGGAACTTCAGAGCGCTTTTGAAGCTGGGGTGGGCG
AAGAACTCCAGCATGAGATCCCCGCGCTGGAGGATCATCCAGCCGGCGTCCCGGAAAACGATT
CCGAAGCCCAACCTTTCATAGAAGGCGGCGGTGGAATCGAAATCTCGTGATGGCAGGTTGGG
CGTCGCTTGGTCGGTCATTTTGAACCCAGAGTCCCGCTCAGAAGA ACTCGTCAAGAAAGGCG
ATAGAAGGCGATGCGCTGCGAATCGGGAGCGGCGATACCGTAAAGCACGAGGAAGCGGTCAG

```

Figure 3.10 Confirmation of ecDHFR (E13G) cloned into the pOriFRT(wt) plasmid via Sanger sequencing. PCR was performed on the recombinant plasmid expressing E134G domain. Two independent PCR products (A) clone 1 and (B) clone 2 were sequenced. Green sequence represents the ecDHFR (E134G) domain and black represent sequence homology to the pOriFRT(wt) plasmid.

```

AATCGAGACCGAGGAGAGGGTTAGGGATAGGCTTACCGGGATAGGCTTACCTCGCCGCTCCA
GAATCTCAAAGCAATAGCTGTGAGAGTTCTGCGCATCAGCATCGTGGAATTCGCTGAATACC
GATTCCCAGTCATCCGGCTCGTAATCCGGGAAATGGGTGTCGCCTTCCACTTCTGCGTCGATA
TGCGTCAGATACAGTTTTTTCGCTTTTGGCAAGAAGTGTTCATAACGCGACCGCCGCAATC
ACCATGATTTCTGGTACGTCACCACACGCCGCGATGGCTTCATCCACCGACTTCACCCACGTT
ACGCGATCGTCCGTA CTGCTGACTGCTGAGGATAATATTTTTGCGTCCTGGCAACGGACG
ACCGATTGATTCCCAGGTATGGCGGCCATAATCACGGGTTTATTTAAGGTGTTGCGTTTAA
ACCAGGCGAGATCGGCAGGCAGGTTCCACGGCATGGCGTTTTCCATGCCGATAACGTAATCT
ACCGCTAACGCCGCAATCAGACTGATCATGGTGGCCCCGGGGATCTTGAAGTTCTATTCCGA
AGTTCCTATTCTCTAGAAAGTATAGGAACTTCAGAGCGCTTTTGAAGCTGGGGTGGGCGAAG
AACTCCAGCATGAGATCCCCGCGCTGGAGGATCATCCAGCCGGCGTCCCGGAAAACGATTCCG
AAGCCCAACCTTTCATAGAAGGCGGCGGTGGAATCGAAATCTCGTGATGGCAGGTTGGGCGT
CGCTTGGTCGGTCATTTTGAACCCAGAGTCCCGCTCAGAAGAAGTTCGTCAGAAGGCGATAG
AAGGCGATGCGCTGCGAATCGGGAGCGGCGATACCGTAAAGCACGAGGAAGCGGTCAGCCCA

```

Figure 3.11 Confirmation of ecDHFR (Y100I) cloned into the pOriFRT(wt) plasmid via Sanger sequencing. PCR was performed on the recombinant plasmid expressing E134G domain. Two independent PCR products (A) clone 1 and (B) clone 2 were sequenced. Green sequence represents the ecDHFR (Y100I) domain and black represent sequence homology to the pOriFRT(wt) plasmid.

3.2.1.1.2 Cloning of F140P into pOriFRT(wt)-ecDHFR plasmid

The F140P domain was cloned in a similar fashion to the N-terminal ecDHFR template constructs (Section 3.2.1.1). The ecDHFR (F140P) domain was amplified from AcGFP-DHFR-F140P plasmid containing the ecDHFR domain fused in-frame to the yellow fluorescent protein (YFP) (kindly provided by Dr Thomas Wandless, University of Stanford, CA, USA) containing ecDHFR (F140P) domain by PCR using specific primers pOriF140P-F/R (Table 2.4). As described in (Section 3.2.1.1), each primer contained restriction enzymes sites (SacI and XmaI see Figure 3.12) after a GCGC anchor region to enable insertion into the pOriFRT (wt) vector. PCR was performed and products were digested and separated on a agarose gel as described above (Section 3.2.1.1).

The results shown in Figure 3.13 indicate that the ecDHFR (F140P)-fragment had been amplified, resulting in production of a single, well-defined DNA band at the expected molecular size (540 bp; Figure 3.13 lanes 2 and 3). As detailed in (Section 3.2.1.1.1), the PCR product and pOriFRT(wt) plasmid were digested with SacI and XmaI and then separated on a 1% agarose DNA gel. Results shown in Figure 3.14 indicate that digestion of pOriFRT(wt) plasmid yielded the expected 1800 bp band (lanes 2 and 3). The PCR product (F140P domain of approximately 540 bp) digested with the same restriction enzymes was gel extracted and purified using Quick Gel Extraction Kit (Section 2.3.6), followed by cloning into the SacI and XmaI sites of pOriFRT(wt) plasmid as described above. Single Kan-resistant colonies were picked and characterized to confirm construction of the desired template plasmid (Figure 3.14) containing the ecDHFR (F140P) domain, which is designated as plasmid pOriFRT(wt)- ecDHFR (F140P).

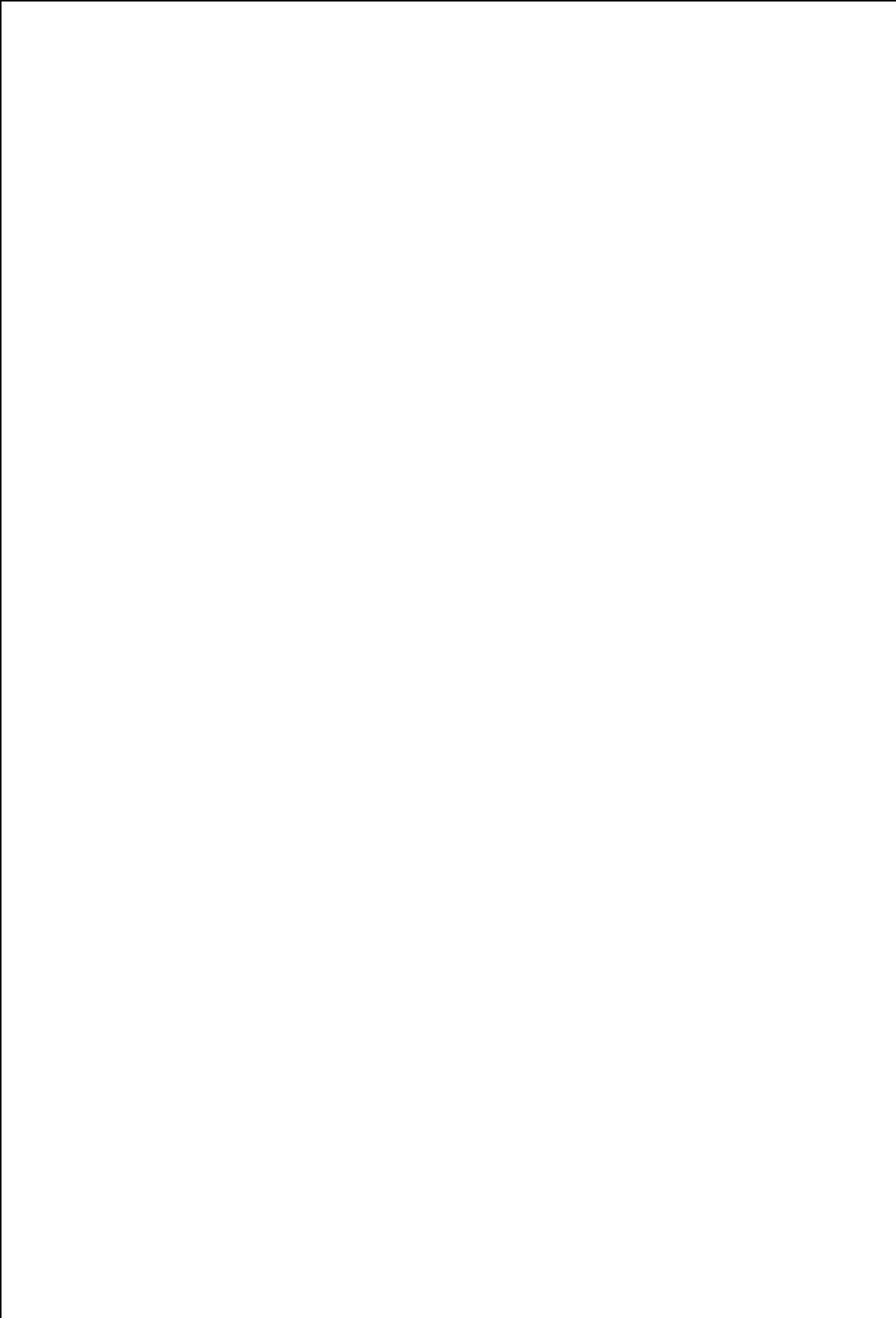


Figure 3.12 Schematic illustrating cloning of ecDHFR (F140P) domain to the pOriFRT(wt) vector. (A) The first step in the construction was amplification of ecDHFR-(Y100I) domain from ACGFP-DHFR-F140P plasmid by PCR, using synthetic oligonucleotide that contained restriction enzyme sites (XmaI and SacI) and V5 tag. (B) In the second step PCR products and pOriFRT(wt) (suicide-based vector) containing Kan^R gene flanked by FRT sites as well as XmaI and SacI (for insertion of the F140P domain) were digested with XmaI and SacI followed by ligation. (C) Schematic of resulting plasmid pOriFRT(wt)-F140P. (D) PCR was used to amplify recombination fragments containing the necessary flanking homology to pp150 or pp28 for E/T based recombination within the MCMV genome.

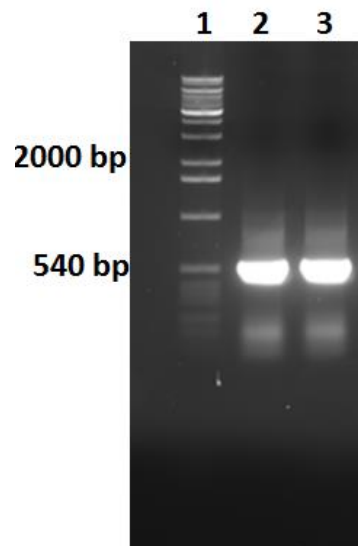


Figure 3.13 DNA gel showing PCR amplification of ecDHFR (F140P) domain from AcGFP-DHFR-F140P. PCR products were separated on a 1% agarose DNA gel and visualized by using EtBr (0.5 μ g/ml). The single DNA band at 540 bp shows amplification of the desired ecDHFR (F140P) domain.

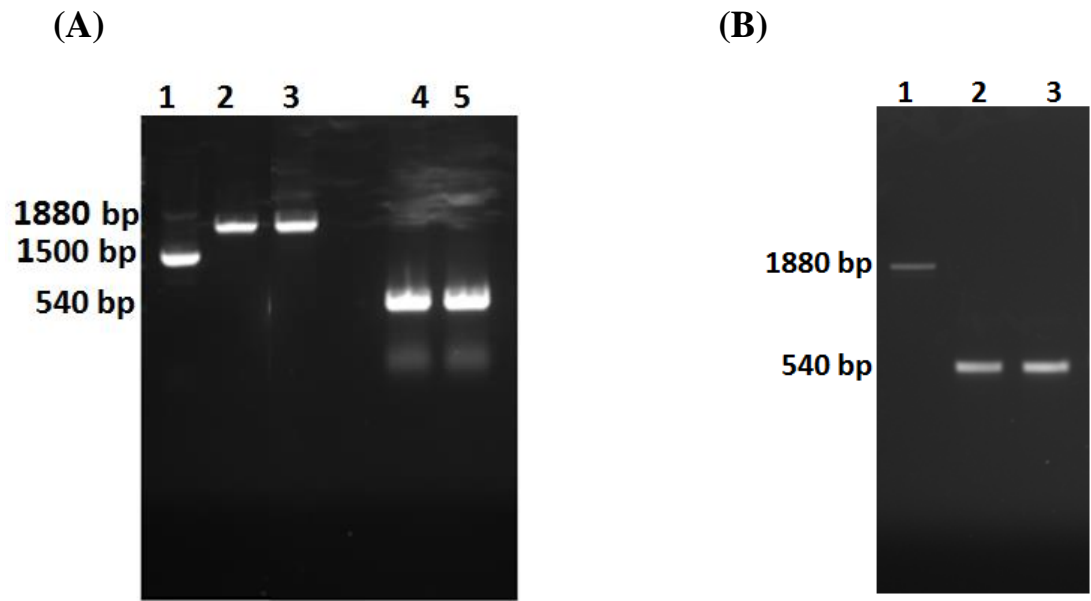


Figure 3.14 Gel electrophoresis showing **SacI** and **XmaI** digestion of PCR product and **pOriFRT(wt)** plasmid during cloning of **pOriFRT(wt)-ecDHFR (F140P)**. (A): uncut vector (lane 1) was compared to single digested **SacI** (lane 2) and **XmaI** (lane 3) producing DNA fragment about 1880 bp indicating digestion of the vector. Lanes 4 and 5 show the restriction digestion of PCR product amplified from **AcGFP-DHFR-F140P** plasmid using **SacI** and **XmaI** producing fragments of the correct size (540 bp). (B) confirming the size bands following gel extraction and purification of **pOriFRT (wt)** vector (lane 1) and PCR amplified product (lane 2).

3.2.1.1.2.1 Restriction digest analysis of recombinant **pOriFRT(wt)-ecDHFR(F140P)** plasmid

The next step was to determine whether the **ecDHFR-(F140P)** domain had been correctly inserted within the **pOriFRT(wt)** plasmid by selection of recombinant clones and analysis by restriction enzyme digestion. As shown in Figure 3.15, a subset of clones showed the expected 540 bp (insert) and 1880 bp (vector backbone) bands as expected for **pOriFRT(wt)-ecDHFR(F140P)**. The result shows correct sized inserts in 5 of total of 25 recombinant colonies that were screened (Figure 3.15). Non-recombinant clones appeared to be parental **pOriFRT(wt)**, which contained no inserts by restriction enzyme analysis; examples are shown

in Figure 3.15 lane 1. Recombinant pOriFRT(wt)-ecDHFR(F140P) clones are shown in lanes 3-7. Two bands were observed, the lower band indicated the F140P domain insert at the expected molecular size (~540 bp), while the upper band represented the pOriFRT(wt)-ecDHFR(F140P) vector following excision of the insert (~1880 bp) Figure 3.15.

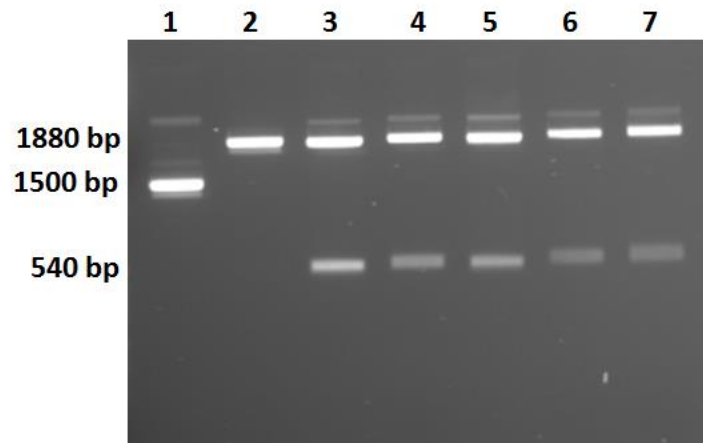


Figure 3.15 Restriction enzyme screening of pOriFRT(wt)-ecDHFR(F140P) clones. Lane 1 shows uncut pOriFRT(wt) control. Lane 2 shows pOriFRT(wt) parental plasmid without insert digested with SacI and XmaI. Lanes 3-7 show confirmed pOriFRT(wt)-ecDHFR(F140P) clones following digestion with SacI and XmaI. Two bands are observed: an upper band of approximately 1880 bp corresponds to linearized vector and the lower bands are the insert (F140P) of approximately 540 bp, lanes (3-7).

3.2.1.1.2.2 Sequencing analysis of pOriFRT(wt)-ecDHFR(F140P) template plasmid

The five plasmids that had screened positive for the 540 bp insert were PCR amplified to confirm presence of a insert representing the F140P domain by using the same primers used during initial amplification of the F140P domain from AcGFP-DHFR-F140P plasmid. Consistent with the restriction enzyme digestion results, PCR amplification produced a single band of the expected 540 bp size. Two clones (numbers 1 and 3) were selected for Sanger DNA sequencing. Sequence analysis showed sequence integrity of the 540 bp sequence F140P-V5 tag insert within the pOriFRT(wt)-ecDHFR(F140P) plasmids. The full length of

the insert sequence from both clone 1 and 3 showed 100% identity with the F140P from AcGFP-DHFR-F140P plasmid, followed by presence of sequence encoding the V5 epitope tag that had been fused in-frame during the PCR process (Figure 3.16). Following cloning of dDHFR-F140P domain into the pOriFRT (wt)-F140P plasmid, the recombinant pOriFRT(wt)-ecDHFR(F140P) plasmid was used to generate conditional replication-defective MCMV vaccine vectors destabilized by fusion of the DD to the C-terminus of the targeted tegument proteins (see below).

```

CATGCCGTGGAACCTGCCTGCCGATCTCGCCTGGTTTAAACGCAACACCTTAAATAAACCCGT
GATTATGGGCGCCATACCTGGGAATCAATCGGTCGTCCGTTGCCAGGACGCAAAAATATTA
TCCTCAGCAGTCAACCGAGTACGGACGATCGCGTAACGTGGGTGAAGTCGGTGGATGAAGCC
ATCGCTGCGTGTGGTGACGTACCAGAAATCATGGTGATTGGCGGCGGTCGCGTTTATGAACA
GTTCTTGCCAAAAGCGCAAAAAGTGTATCTGACGCATATCGACGCAGAAGTGAAGGCGACA
CCCATTTCCCGGATTACGAGCCGGATGACTGGAATCGGTATTCAGCGAACCCACGATGCTG
ATGCGCAGAAGTCTCACAGCTATTGCTTTGAGATTCTGGAGCGGCGAGGTAAGCCTATCCCTA
ACCCTCTCCTCGGTCTCGATTCTACGTAACCCGGGGATCTTGAAGTTCTATTCCGAAGTTCC
TATTCTCTAGAAAGTATAGGAACTTCAGAGCGCTTTTGAAGCTGGGGTGGGCGAAGAAGTCC
AGCATGAGATCCCCGCGCTGGAGGATCATCCAGCCGGCGTCCCGGAAAACGATTCCGAAGCCC
AACCTTTCATAGAAGGCGGCGGTGGAATCGAAATCTCGTGATGGCAGGTTGGGCGTCGCTTG
GTCGGTCATTTCGAACCCAGAGTCCCGCTCAGAAGAACTCGTCAAGAAGGCGATAGAAAGG
CGATGCGCTGCGAATCGGGAGCGGCGATACCGTAAAGCACGAGGAAGCGGTCAGCCCATTG
CCGCCAAGCTCTTCAGCAATATCACGGGTAGCCAACGCTATGTCCT

```

Figure 3.16 Confirmation of ecDHFR (F140P) cloned into the pOriFRT(wt) plasmid via Sanger sequencing. PCR was performed on the recombinant plasmid expressing E134G domain. Two independent PCR products (A) clone 1 and (B) clone 2 were sequenced. Green sequence represents the ecDHFR (F140P) domain and black represent sequence homology to the pOriFRT(wt) plasmid.

3.2.2 Construction of recombinant MCMV BAC clones carrying the ecDHFR-tagged to essential tegument protein M32 (pp150) or M99 (pp28)

In the next section, the N-terminal (pOriFRT(wt)-E134G and pOriFRT(wt)-Y100I and C-terminal pOriFRT(wt)-F140P ecDHFR template plasmids constructed above were used to derive the recombination PCR products required for construction of conditionally replication defective versions of the MCMV vector expressing either destabilized pp150 (M32) or pp28 (M99). We targeted these essential tegument proteins of MCMV as they have been reported to support fusion of heterologous domains (i.e. GFP) without impacting functions necessary for virus replication (Sampaio *et al.*, 2005). Based on these earlier studies as well as the observation that most of the critical information for function of these proteins appears to reside in the N-terminus (Baxter & Gibson, 2001; Chen *et al.*, 1999; Trus *et al.*, 1999; Jones & Lee, 2004 & Seo & Britt, 2006), we hypothesized that the C-terminus DD fusion would have the least impact on tegument function. As BAC-based cloning removes functional constraints on the virus since the virus genome is maintained as a bacterial chromosome, N- and C-fused DD versions at the level of the BAC would be expected to be viable in terms of ability to E/T clone the respective BAC constructs. The lethality of the N-terminal fusions would only be seen during the attempt to reconstitute the viruses by transfection into the MCMV permissive MEFs (performed in the presence of TMP).

We BAC cloned two N-terminal versions and one C-terminal version of both pp150 and pp28 MCMV by fusion of ecDHFR to these tegument proteins individually. As we indicated above we decided to avoid ecDHFR domain fusion to the N-terminus of the pp28 protein, focusing on only the C-terminus, as the N-terminus has been shown essential for virus replication (Britt *et al.*, 2004). Using E/T recombination, the two different versions of ecDHFR (E134G and Y100I) were fused in-frame to the N-terminus of pp150 (designated as MCMV-pp150-E134G and MCMV-pp150-Y100I), respectively. Similarly ecDHFR (F140P) was fused in-

frame to the carboxyl-terminus of pp150 and pp28 (designated MCMV-pp150-F140P and MCMV-pp28-F140P, respectively). We anticipated that fusion of ecDHFR domain to these essential tegument proteins would lead to rapid tegument protein degradation as a result of this genetic fusion. However, these tegument proteins should be stabilized in the presence of synthetic TMP ligand molecule and retain their function and activity (Figure 3.17). This strategy would result in replication of the MCMV vector being conditionally dependent on TMP, enabling production of vaccine stocks *in vitro*, but attenuation *in vivo*.

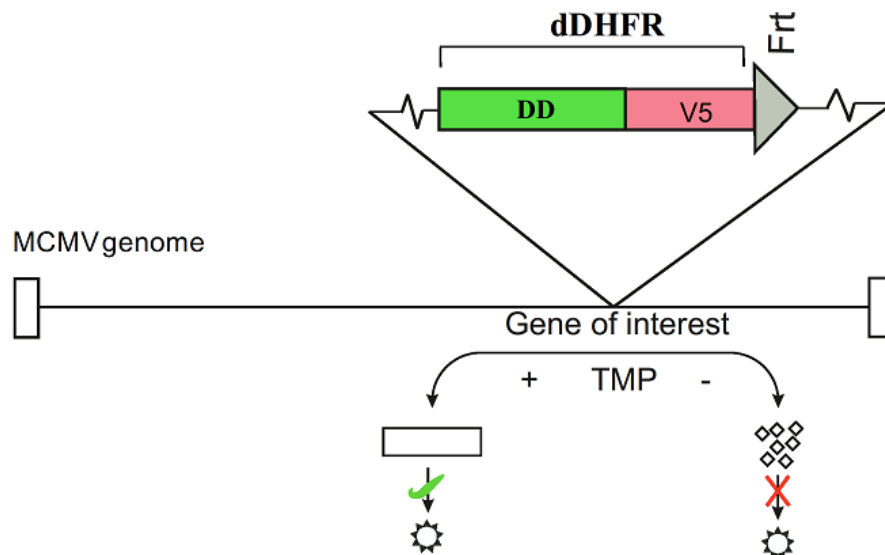


Figure 3.17 Schematic illustration of the conditionally replication-defective MCMV vaccine using DD strategy. The attenuated MCMV vector was made by fusion of the ecDHFR domain to the essential tegument protein of MCMV. In the absence of the TMP, the ecDHFR directs the entire fusion protein for rapid degradation, preventing virus replication due to the absence of the essential protein. In the presence of TMP, the TMP molecule binds ecDHFR thereby stabilizing the fusion protein and enabling virus replication. The ecDHFR domain was epitope (V5) tagged as shown for ease of detection.

3.2.2.1 Construction of conditionally replication-defective MCMV-pp150-E134G/Y100I vector by E/T homologous recombination

Two replication-defective vectors (MCMV-pp150) were constructed by fusion of E134G or Y100I in-frame to the N- terminus of pp150 (Figure 3.18). To construct the conditional recombinant MCMV-pp150-ecDHFR vaccines, linear DNA fragments encoding the sequence of the ecDHFR (E134G or Y100I) followed by the V5 tag and a Kan^R marker flanked on either end by sequence homologous to the targeted pp150 insertion site were generated by PCR, as described in (Section 2.3.3) using pOriFRT(wt)-ecDHFR(E134G/Y100I) templates (Figures 3.4 and 3.5). These recombinant PCR fragments were transformed by electroporation into electrocompetent recombinase-induced EL250 cells (see Section 2.2.4). Recombinant clones were then selected based on resistance to both Cam and Kan. The Kan^R marker was then removed from selected recombinants by arabinose induction of the FLP recombinase system (Section 2.5.1.3).

**MCMV/M32 (PP150)-dDHFR
N-Terminus**

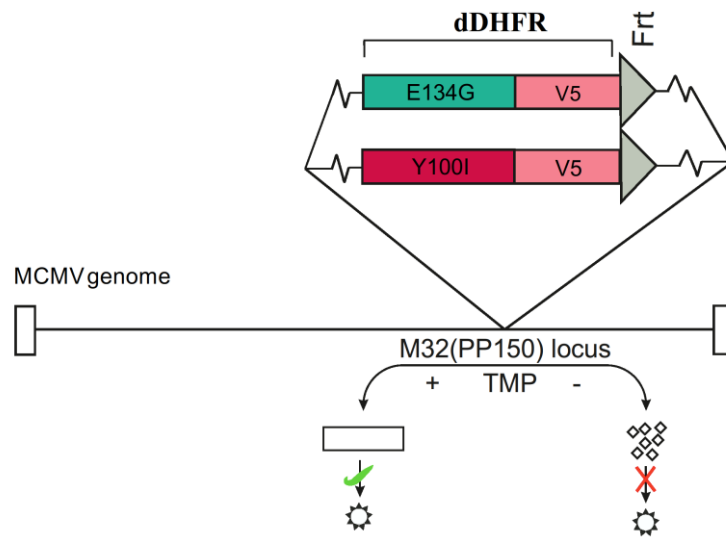


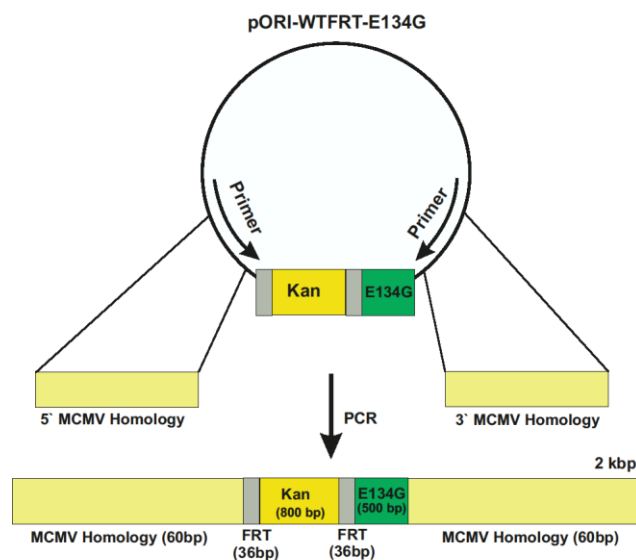
Figure 3.18 Schematic illustrations of the conditionally replication-defective MCMV-PP150-E134G/Y100I vectors using DD strategy. The attenuated MCMV vector was made by fusion of the ecDHFR domain to the N-terminus of pp150 protein. In the presence of TMP, the TMP molecule binds to ecDHFR thereby stabilizing the pp150 fusion protein and enabling virus replication. While in the absence of TMP, the ecDHFR directs the entire fusion protein for rapid degradation, preventing virus replication due to the absence of the essential pp150 protein. The ecDHFR domain was epitope tagged within the N-terminus of pp150 as shown for ease of detection.

3.2.2.1.1 Generation of PCR fragments with flanking viral homologies to pp150 (N-terminus)

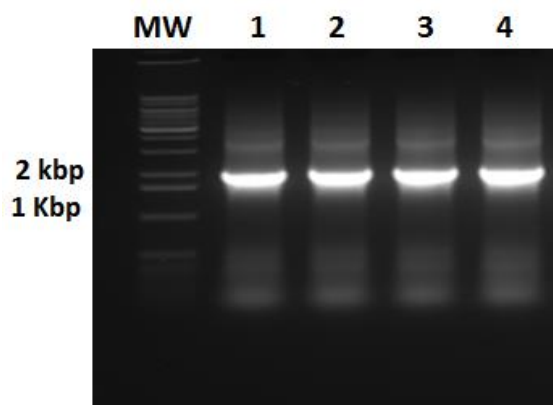
The initial step in construction of the MCMV-pp150 BAC vectors was generation of linear PCR recombination fragments. Linear DNA fragments were amplified from pOriFRT(wt)-ecDHFR(E134G) or pOriFRT(wt)-ecDHFR(Y100I) plasmids by PCR using 78 and 84nt synthetic oligonucleotides primers (pOri E134G-F/R and pOri Y100I-F/R primers; Table 2-4). The 5' end of each primer contained a 60 bp sequence with homology to the site of DD

fusion to pp150 followed by sequence required for annealing to the template plasmids (from which the Kan^R gene and ecDHFR were amplified; Section 2.3.3.1; Figures 3.19 and 3.20). The final recombination fragments therefore contain a Kan^R gene flanked by FRT sites with sequence of the 500 bp of ecDHFR (E134G or Y100I) domain and 60 nucleotides sequence homology flanking the site of insertion at the N-terminus of the pp150 gene locus of the MCMV BAC genome. Amplification of the PCR recombinant fragments was confirmed by electrophoresis on a 1% agarose DNA gels containing EtBr stain (Figures 3.19 and 3.20). Prior to gel extraction, purified fragments showed the expected 2 kb size (Figures 3.19 and 3.20 C).

(A)



(B)



(C)

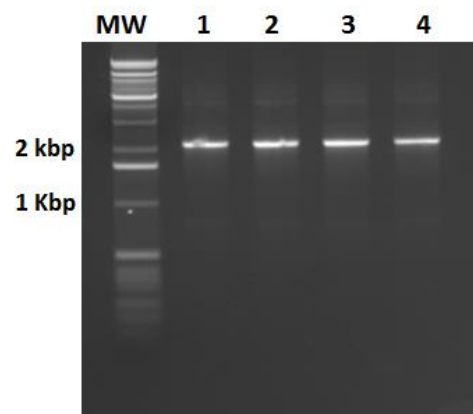
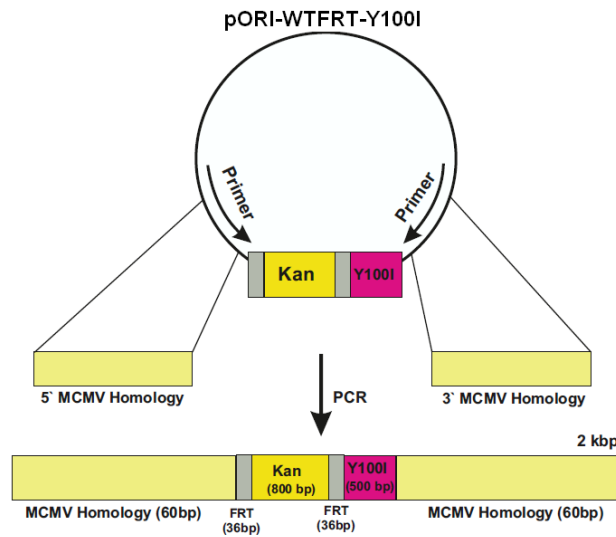
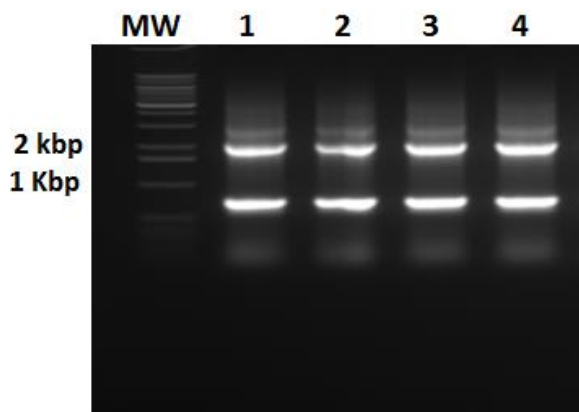


Figure 3.19 Recombinogenic PCR fragments used for construction of the recombinant MCMV-pp150-E134G vaccine vector. (A): Schematic showing recombinant PCR generated linear fragments used for construction of recombinant MCMV-pp150-E134G attenuated vaccine vector. Kan^R flanked by *FRT* sites and sequences carrying the ecDHFR (E314G) domain with 60 bp of homologous sequences flanking at either end which is homologous to upstream and downstream coding sequences of the tegument protein pp150 of the MCMV virus were constructed by PCR, using pOriFRT(wt)- ecDHFR(E314G) plasmid as a template. (B): DNA gel showing recombinant PCR generated fragments containing E134G domain. The single DNA band at 2 kb shows amplification of the desired recombinogenic sequence. Two independent PCR reactions were prepared for each clone. (C) Gel purified PCR products confirming the extraction procedure was successful and the correct sized bands were purified. MW = 1kb molecular weight marker.

(A)



(B)



(C)

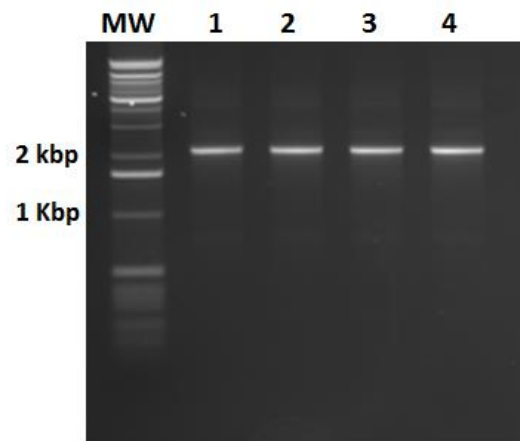


Figure 3.20 Recombinogenic PCR fragments used for construction of the recombinant MCMV-pp150-Y100I vaccine vector. (A): Schematic showing recombinant PCR generated linear fragments used for construction of recombinant MCMV-pp150-Y100I attenuated vaccine vector. Kan^R flanked by *FRT* sites and sequences carrying the ecDHFR (F140P) domain with 60 bp of homologous sequences flanking at either end which is homologous to upstream and downstream coding sequences of the tegument protein pp150 of the MCMV virus were constructed by PCR, using pOriFRT(wt)-ecDHFR(Y100I) plasmid as a template. (B): DNA gel showing recombinant PCR generated fragments containing Y100I domain. The single DNA band at 2 kb shows amplification of the desired recombinogenic sequence. Two independent PCR reactions were prepared for each clone. (C) Gel purification of PCR products confirming the extraction procedure was successful and the correct sized bands were purified. MW = 1kb molecular weight marker.

3.2.2.1.2 Construction of recombinant MCMV-pp150 based vector using E/T- based linear recombination strategy

The recombination PCR products generated above were used to fuse the respective ecDHFR DD domain to the N-terminus of the pp150 locus of the MCMV BAC genome using red mediated homologous recombination (E/T recombination; Figure 3.21; Section 2.5.1) to generate MCMV vaccine vector. These recombinant PCR fragments were transformed by electroporation into electrocompetent, recombinase-induced EL250 cells as described in Section 2.2.4. Following recombination, bacteria were plated out onto Kan/Cam plates to select clones containing recombinant BACs. Colonies were counted (Table 3.2), and 4 clones from each recombinant were selected for further characterization. Overnight cultures were set up and recombinant BACs were isolated by alkaline lysis (Sambrook & Russell, 2001) as described in (Section 2.3.1.2).

Table 3.2 Numbers of recombinant MCMV-pp150-(E134G or Y100I) BAC clones following E/T recombination

MCMV Construct	PCR fragment	Number of colonies
MCMV-pp150-E134G	1	100-200
	2	150-200
MCMV-pp150-Y100I	1	50-100
	2	100-200

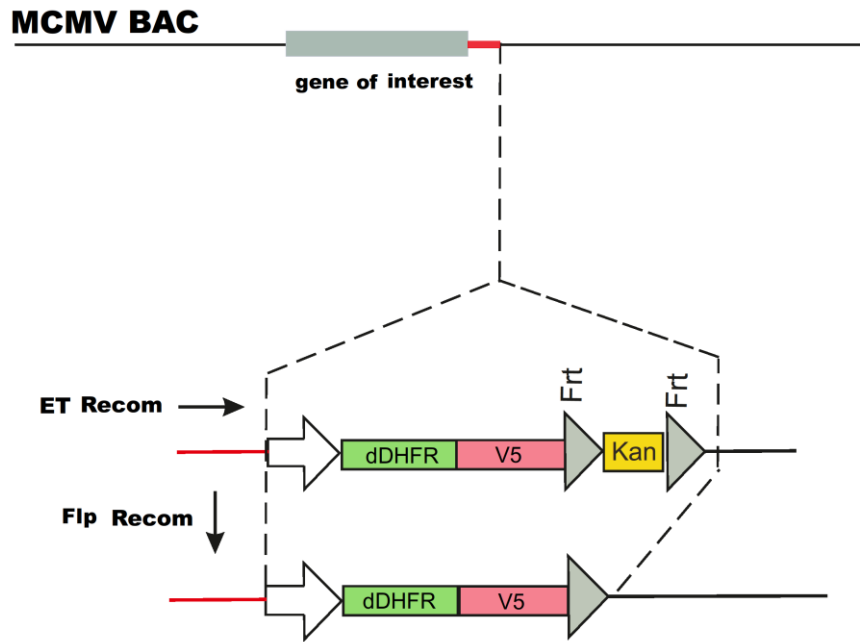


Figure 3.21 Schematic illustrating the construction of MCMV-pp150-ecDHFR (E134G/Y100I) vectors. The E/T- based linear recombination strategy used for construction of the two MCMV-pp150 vectors. Recombinant fragments carrying the Kan^R marker flanked by FRT sites and the sequence encoding the E134G/Y100I domain were amplified by PCR, and electroporated into *E. coli* expressing α , β and γ proteins of bacteriophage gamma recombinases. Following selection of recombinant BACs on the basis of the kan resistance, the Kan^R marker was removed using FLP mediated-recombination. The recombinant virus constructs were electroporated into MEFs to reconstitute recombinant MCMV-PP150-ecDHFR virus. Frt, FLP-recombinase recognition site from the yeast *Saccharomyces cerevisiae*; Kan^R, kan resistance gene; ecDHFR, destabilization domain protein (E134G or Y100I); V5 Tag was tagged to the ecDHFR proteins to facilitate detection of fused protein.

3.2.2.1.3 Restriction digestion of mutant BAC DNA to ensure intact genome

During E/T based recombination, it is possible that elements of the BAC genome may be deleted or undergoes rearrangement. Restriction digest analysis was performed to ensure that all selected clones have maintained genomic integrity. A wild-type control (MCMV-WT) and four different recombinant MCMV-pp150-E134G/Y100I BAC clones were selected and digested by using restriction enzyme (EcoRI). The resulting restriction DNA digest was then separated on a 1% agarose DNA gel (Section 2.3.5). Banding patterns (size and number) generated by recombinant pp150 BACs were compared with those of the MCMV-WT BAC control sample. As shown in Figure 3.22 there were no genomic rearrangement in recombinant MCMV-pp150-E134G (lanes 1-4) or Y100I (lanes 1-4) compared to the parental MCMV-WT BAC DNA.

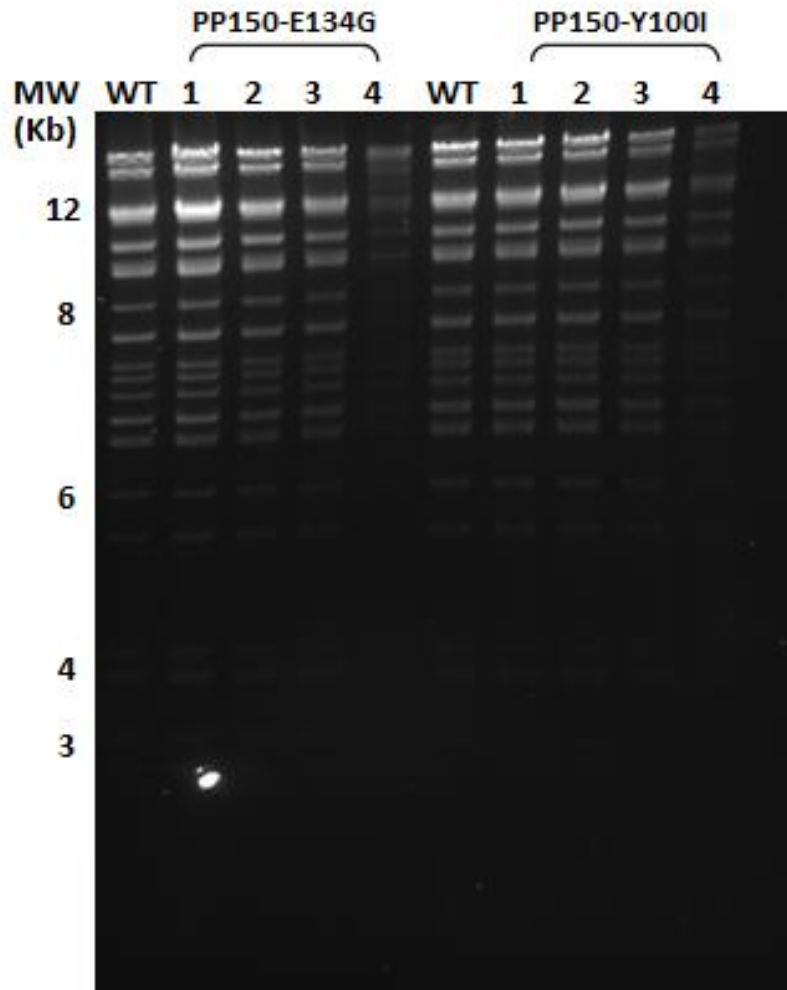


Figure 3.22 Characterization of the recombinant MCMV-pp150-E134G/Y100I BAC genome using EcoRI restriction enzyme digestion. MCMV-WT and four independent clones from MCMV- pp150-E134G and MCMV-pp150-Y100I BACs were digested with EcoRI restriction enzyme and the resulting fragments were separated on a 1% agarose gel by electrophoresis for 18-20 h at 45 V, and visualization with EtBr (0.5 $\mu\text{g/ml}$). Comparable restriction digestion pattern of MCMV-pp150-E134G and MCMV- pp150-E134G/Y100I clones with MCMV-WT BAC show the lack of any gross genomic rearrangements. Molecular size marker lane (MW) in kb is indicated. WT: wild type.

3.2.2.1.4 Kan^R cassette excision from recombinant MCMV-pp150-E134G/Y100I BACs

In the next step the FRT-flanked Kan^R selectable marker was removed by arabinose induction of FLP recombinase (Section 2.5.3). In addition to removal of antibiotic resistance marker from the final BAC, removal of the Kan^R marker also prevents potential size issues with packaging of the genome into the viral capsid during replication in eukaryotic cells, which could lead to attenuation of the recombinant viruses. To confirm that Kan^R was removed from recombinant MCMV-pp150-E134G/Y100I BACs, 25 arabinose-induced colonies from each recombinant MCMV-pp150 BAC were screened by replica-plating on Cam/Kan versus Cam only plates (Section 2.5.1.3). Excision of Kan^R results in colonies growing only on plates containing Cam, with no growth on plates containing both Kan and Cam. However, results showed growth of bacterial colonies on both agar plates, indicating that Kan^R marker was still present within the BAC genome. Twenty-five more colonies from each recombinant BAC were selected to test for the excision of Kan^R, but with the same result. A third attempt was made to remove the Kan^R by preparing new independently generated PCR fragments and repeating the entire homologous recombination to derive a second set of MCMV recombinants. However, again for both recombinant viruses, FLP recombinase induction using arabinose failed to remove the Kan^R marker (Table 3.3).

Table 3.3 Analysis of MCMV BAC clones following excision of Kan cassette

MCMV construct	Recombination	Clone	Selected colonies	Sensitive to Kan
MCMV- pp150-E134G	1	1	25	Non
	1	3	25	Non
	2	2	25	Non
	2	4	25	Non
MCMV- pp150-Y100I	1	1	25	Non
	1	3	25	Non
	2	2	25	Non
	2	4	25	Non

3.2.2.2 Construction of conditionally replication-defective MCMV-pp150/pp28-F140P vectors by Red E/T homologous recombination

In the next section, a carboxyl targeted DD ecDHFR domain (F140P) was fused in-frame to the C terminus of pp150 and pp28 designated as MCMV-pp150-F140P and MCMV-pp28-F140P, respectively (Figures 3.23 and 3.24) essentially as described above (Section 3.2.2.1).

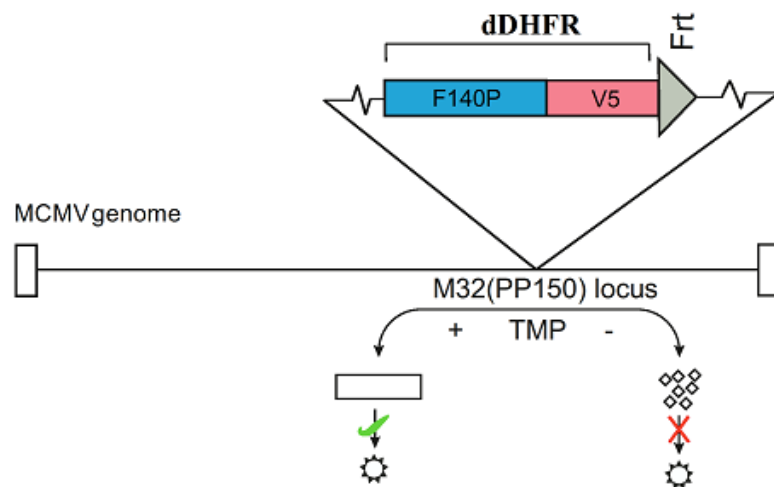


Figure 3.23 Schematic illustration of the conditionally replication-defective MCMV-PP150-F140P vector using DD strategy. The attenuated MCMV vector was made by fusion of the ecDHFR domain to the C- terminus of pp150 protein. In the presence of TMP, the TMP molecule binds to ecDHFR thereby stabilizing the pp150 fusion protein and enabling virus replication. While in the absence of TMP, the ecDHFR directs the entire fusion protein for rapid degradation, preventing virus replication due to the absence of the essential pp150 protein. The ecDHFR domain was epitope tagged within the C-terminus of pp150 as shown for ease of detection.

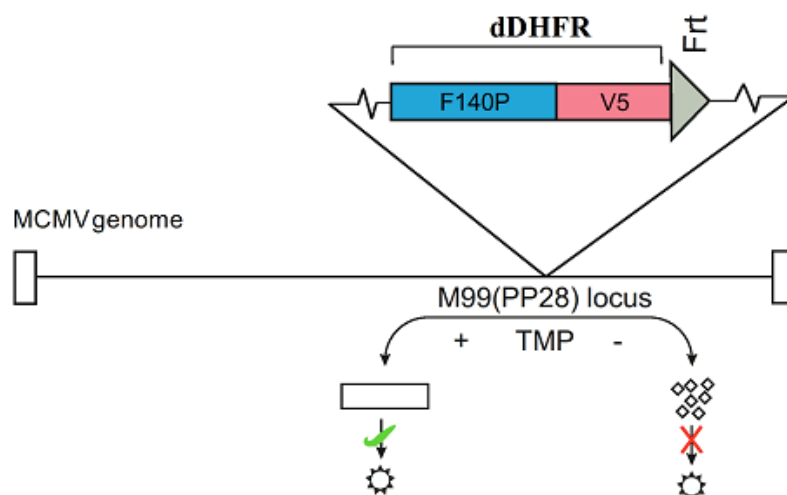


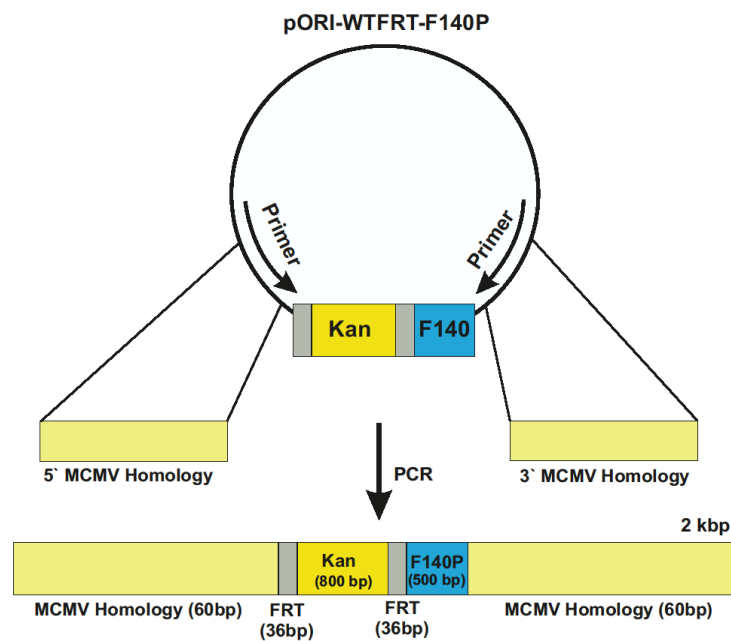
Figure 3.24 Schematic illustration of the conditionally replication-defective MCMV-PP28-F140P vector using DD strategy. The attenuated MCMV vector was made by fusion of the ecDHFR domain to the C-terminus of pp28 protein. In the presence of TMP, the TMP molecule binds to ecDHFR thereby stabilizing the pp28 fusion protein and enabling virus replication. While in the absence of TMP, the ecDHFR directs the entire fusion protein for rapid degradation, preventing virus replication due to the absence of the essential pp28 protein. The ecDHFR domain was epitope tagged within the N-terminus of pp28 as shown for ease of detection.

3.2.2.2.1 Generation of PCR fragments with flanking viral homologies to pp150/pp28 (C-terminus)

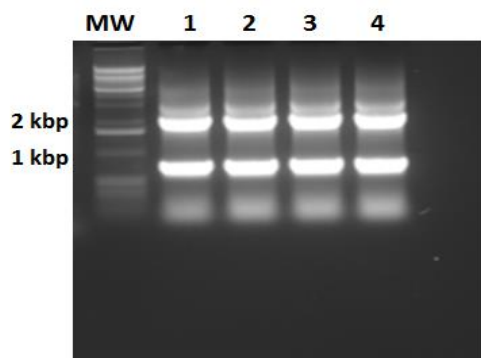
Generation of linear recombinant fragments by PCR was the first step in the construction of recombinant MCMV-pp150-F140P and MCMV-pp28-F140P vectors. Linear DNA fragments were amplified by PCR using the pOriFRT(wt)-ecDHFR(F140P) plasmid template that was constructed above (Section 3.2.1.1.2) using synthetic oligonucleotides primers (pp150F140P F/R and pp28F140P F/R (Tables 2.6 and 2.7). The 5' end of each primer contained a 60 bp sequence with homology to the site of DD fusion to pp150 or pp28 followed by sequence required for annealing to the template plasmids (from which Kan^R gene and ecDHFR (F140P) was amplified; Section 2.3.3.1; Figures 3.25 and 3.26). The final recombination fragments

therefore contain a Kan^R gene flanked by FRT sites with sequence of the 500 bp of ecDHFR (F140P) domain and 60 nucleotides of homology to each end of the site of cassette insertion at the 3' end of the pp150 or pp28 gene locus within the MCMV BAC genome. Electrophoresis of PCR products on a 1% agarose DNA gel (Figures 3.25 and 3.26 B) showed amplification of the desired 2 kb PCR product, which was the correct size for the anticipated PCR recombination fragment. An approximately 1.2 kb band was also present following amplification of the pp150 template. The 2 kb PCR recombination fragment was therefore purified by gel electrophoresis (Section 2.3.6) and gel extraction (Section 2.3.7). Electrophoresis confirmed isolation of only the expected 2 kb sized fragments (Figures 3.25 and 3.26 C).

(A)



(B)



(C)

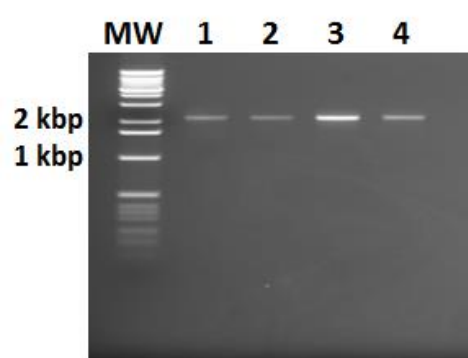
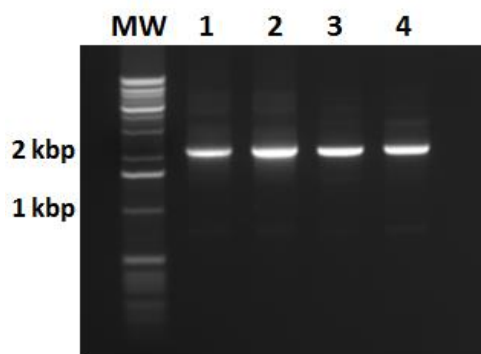


Figure 3.25 PCR recombination fragments used for construction of the recombinant MCMV-pp150-F140P vaccine vector. (A): Schematic showing PCR recombination fragments used for construction of recombinant MCMV-pp150-F140P attenuated vaccine vector. PCR using pOriFRT(wt)-ecDHFR(F140P) plasmid as a template was used to construct recombination fragments comprised of Kan^R flanked by *FRT* sites and sequences carrying the ecDHFR (F140P) domain with 60 bp of homologous sequences flanking at either end homologous to upstream and downstream coding sequences of the carboxyl terminus of pp150 (B): DNA gel showing recombinant PCR generated fragments containing F140P domain. The DNA band at 2 kb shows amplification of the desired recombinogenic sequence fragments. Two independent PCR reactions were prepared for each clone. (C) Gel purification of PCR products confirming purification of the correct sized bands. MW = 1kb molecular weight marker.

(A)



(B)



(C)

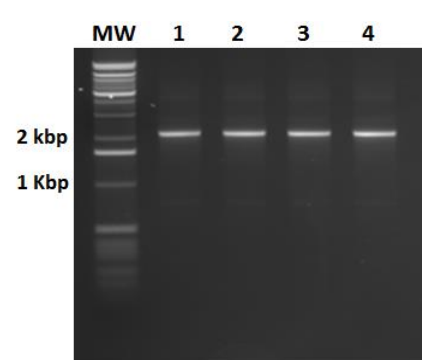


Figure 3.26 PCR recombination fragments used for construction of the recombinant MCMV-pp28-F140 vaccine vector. (A): Schematic showing PCR recombination fragments used for construction of recombinant MCMV-pp28-F140P attenuated vaccine vector. PCR using pOriFRT(wt)-ecDHFR(F140P) plasmid as a template was used to construct recombination fragments comprised of Kan^R flanked by *FRT* sites and sequences carrying the ecDHFR (F140P) domain and 60 bp of homologous sequences flanking at either end homologous to the upstream and downstream site of insertion at the carboxyl terminus of pp28 (B): DNA gel showing recombinant PCR generated fragments containing F140P domain. The DNA band at 2 kb shows amplification of the desired recombinant fragments. Two independent PCR reactions were prepared for each clone. (C) Gel purification of PCR products confirming purification of the correct sized bands. MW = 1kb molecular weight marker.

3.2.2.2.2 Construction of recombinant MCMV-pp150/pp28 based vectors using E/T based linear recombination strategy

The recombination PCR products generated above were used to fuse the ecDHFR(F140P) domain to the C-terminus of the pp150/pp28 locus within the MCMV BAC genome using E/T recombination (Figure 2.1; Section 2.5.1). Following recombination, bacteria were plated on Kan/Cam plates to select clones containing recombinant BACs. Bacterial colony number was quantified (Table 3.2), and 4 clones from each recombinant were selected for further characterization. Overnight cultures were set up and the recombinant BACs were isolated by alkaline lysis (Sambrook & Russell, 2001) as described in (Section 2.3.1.2).

3.2.2.2.3 Restriction digestion of mutant BAC DNA to ensure intact genome

To assess genome structure following recombination, restriction enzyme digest analysis of recombinant BACs was performed and compared to MCMV-WT. Eight independent recombinant MCMV-pp150-F140P and MCMV-pp28-F140P BAC clones were selected for analysis. The resulting DNA bands were then separated on a 1% agarose DNA gel (Section 2.3.5). As shown in Figures 3.28 and 3.29, the banding patterns generated by digestion of recombinant pp150 and pp28 BACs were comparable with those of the digested MCMV-WT BAC control sample indicating absence of gross genomic rearrangement within recombinant MCMV-pp150 or pp28/F140P BACs.

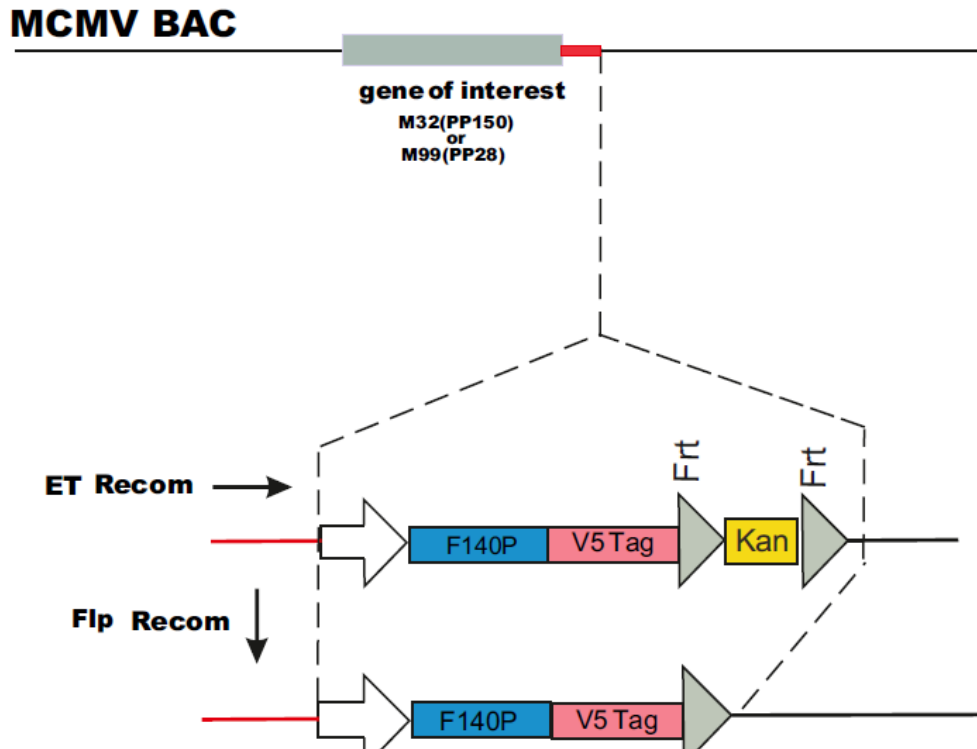


Figure 3.27 Schematic illustrating the construction of MCMV-pp150/pp28-ecDHFR (F140P) vectors. The E/T- based linear recombination strategy used for construction of the two MCMV-pp150/pp28 vectors. Recombinant fragments carrying the Kan^R marker flanked by FRT sites and the sequence encoding the F140P domain was amplified by PCR, and electroporated into *E. coli* expressing α , β and γ proteins of bacteriophage gamma recombinases. Following selection of recombinant BACs on the basis of the kan resistance, the Kan^R marker was removed using FLP mediated-recombination. The recombinant virus constructs were electroporated into MEFs to reconstitute recombinant MCMV-PP150/pp28-F140P virus. Frt, FLP-recombinase recognition site from the yeast *Saccharomyces cerevisiae*; Kan^R, kan resistance gene; ecDHFR, destabilization domain protein (F140P); V5 Tag was tagged to the ecDHFR proteins to facilitate detection of fused protein.

Table 3.4 Number of recombinant MCMV-pp150/pp28-F140P BAC clones following E/T recombination.

MCMV Constructs	PCR fragment	Number of colonies
MCMV-pp150-F140P	PCR1	100 -150
	PCR2	150-200
MCMV-pp28-F140P	PCR1	50-100
	PCR2	100 -150

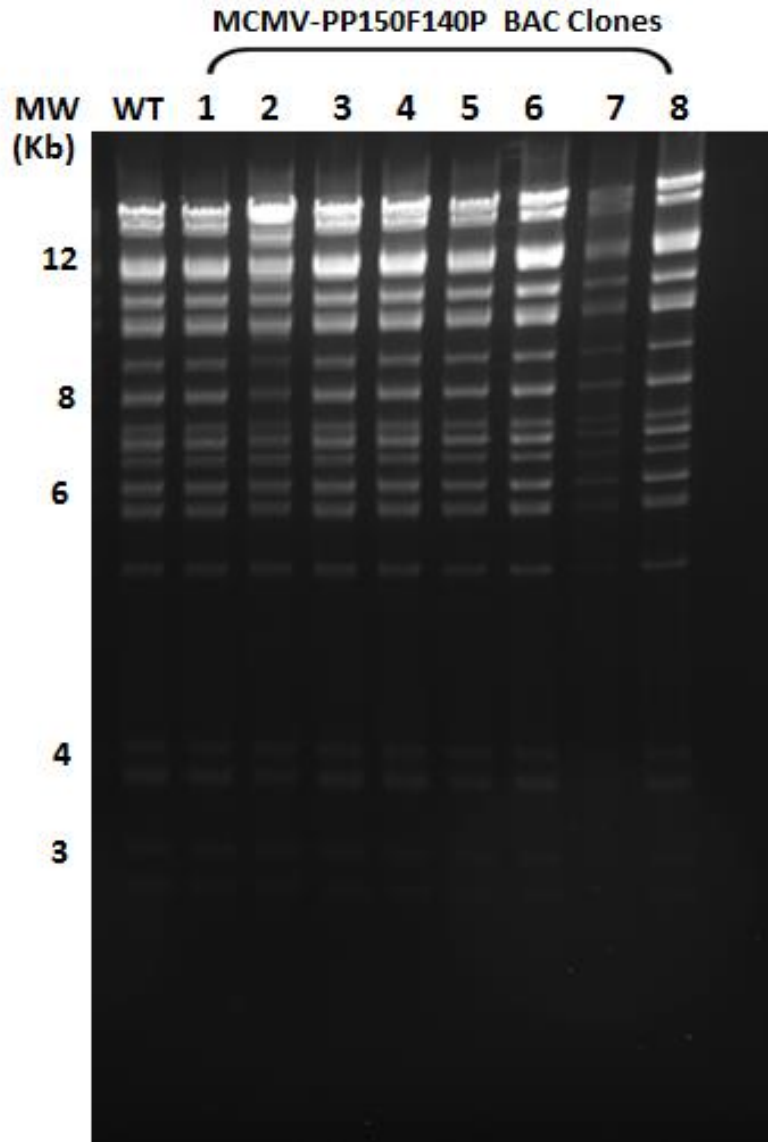


Figure 3.28 Characterization of recombinant MCMV-pp150-F140P BACs by using EcoRI restriction enzyme digestion. MCMV-WT and eight independent clones from MCMV-pp150-F140P BACs were digested with EcoRI restriction enzyme and the resulting fragments were separated on a 1% agarose gel by electrophoresis for 18-20 h at 45 V, followed by visualization with EtBr (0.5 $\mu\text{g/ml}$). Comparable restriction digestion pattern between MCMV-pp150-F140P recombinants and MCMV-WT BAC showed the absence of any gross genomic rearrangements. Molecular size marker lane (MW) in kb is indicated.

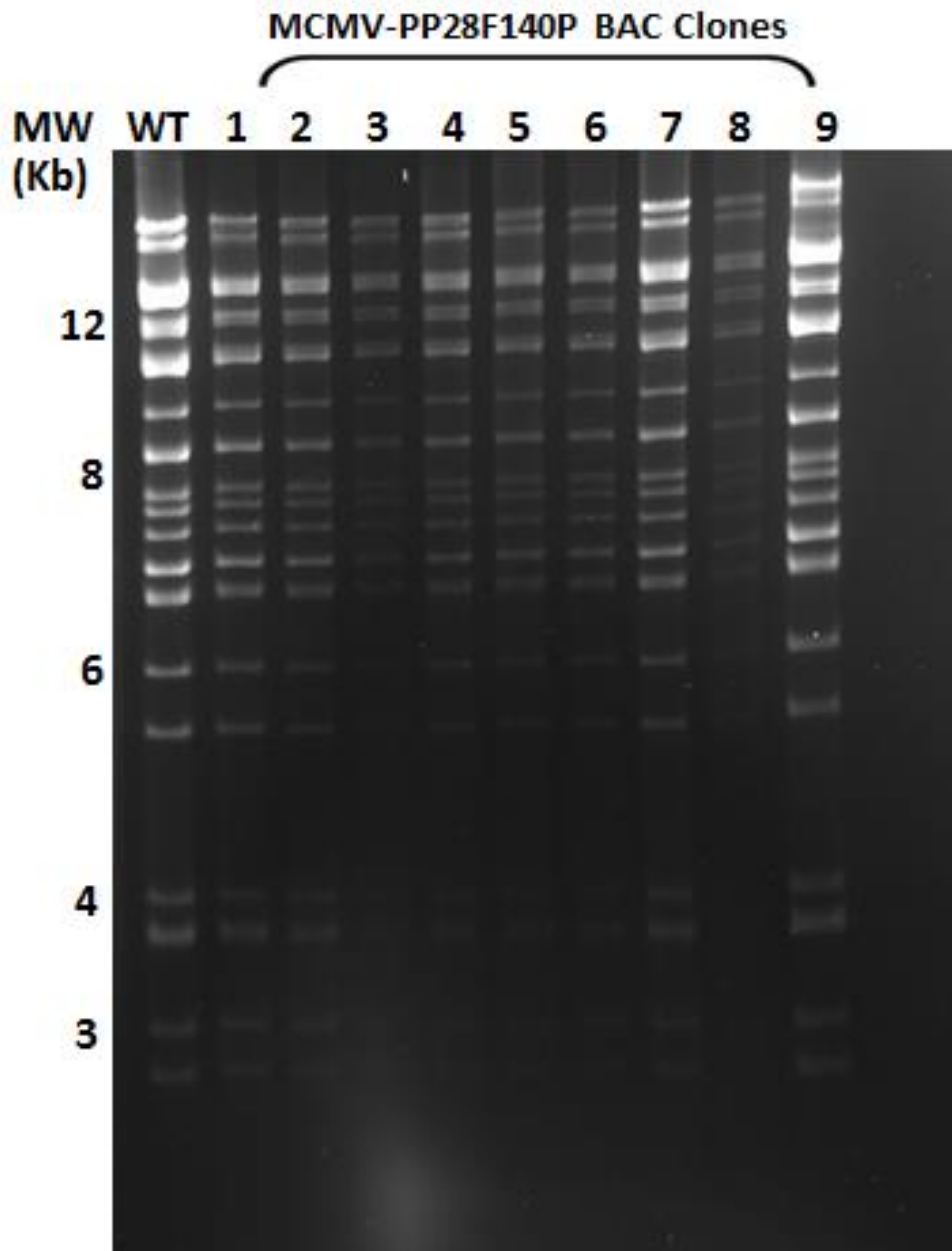


Figure 3.29 Characterization of recombinant MCMV-pp28-F140P BACs, by using EcoRI restriction enzyme digestion. MCMV-WT and eight independent clones from MCMV-pp28-F140P BACs were digested with EcoRI restriction enzyme and the resulting fragments were separated on a 1% agarose gel by electrophoresis for 18-20 h at 45 V, followed by visualization with EtBr (0.5 $\mu\text{g/ml}$). Comparable restriction digestion pattern between MCMV-pp28-F140P recombinant and MCMV-WT BAC showed the absence of any gross genomic rearrangements. Molecular size marker lane (MW) in kb is indicated.

3.2.2.2.4 Kan^R cassette excision from recombinant MCMV-pp150/pp28-F140P BACs

In the next step, the FRT-flanked Kan^R selectable marker was removed from selected recombinant MCMV-pp150-F140P and MCMV-pp28-F140P BACs by arabinose induction of FLP recombinase as described previously (Section 3.2.2.1.4). Twenty-five arabinose-induced colonies from each recombinant BAC were screened by replica-plate on Cam and Kan versus Cam only plates. Results show the FLPed clones were no longer able to grow in the presence of Kan, but retained the ability to grow in the presence of Cam indicating that the Kan^R gene had indeed been removed as the bacterial colonies become sensitive to Kan. In contrast to the repeated inability to remove the Kan^R marker from the MCMV-pp150-E134G/Y100I BACs (see above), these results confirmed excision of the Kan^R cassette from both recombinant MCMV-pp150-F140P and MCMV-pp28-F140P BACs (Table 3.5).

To confirm the excision of the Kan^R cassette from BAC genomes, PCR analyses were performed using a pair of pp150 and pp28-specific primers (Tables 2.6 and 2.7). These primers were designed to flank the site of ecDHFR insertion within the respective recombinant MCMV genome. Primers were located at an adequate distance from the site of ecDHFR insertion to enable high quality DNA sequence reads over the ecDHFR insertion site. This was generally about 150 to 200 bps from the site of ecDHFR insertion (Tables 2.6 and 2.7). PCR was performed on recombinant BAC DNA (pre- and post- FLP) (Figures 3.30 and 3.31). The size of the amplified PCR products indicated excision of the Kan^R cassette, with pre-FLP BAC clones yielding PCR products of approximately 2 kb followed by a reduction in size by 1 kb after FLP-mediated removal of the Kan^R cassette (Figures 3.30 and 3.31).

Table 3.5 Analysis of recombinant MCMV BAC clones following excision of Kan^R

MCMV Construct	Recombination	Clone	Selected colonies	Sensitivity to Kan
MCMV-pp150-F140P	1	3	25	All
	2	6	25	All
MCMV-pp28-F140P	1	1	25	All
	2	5	25	All

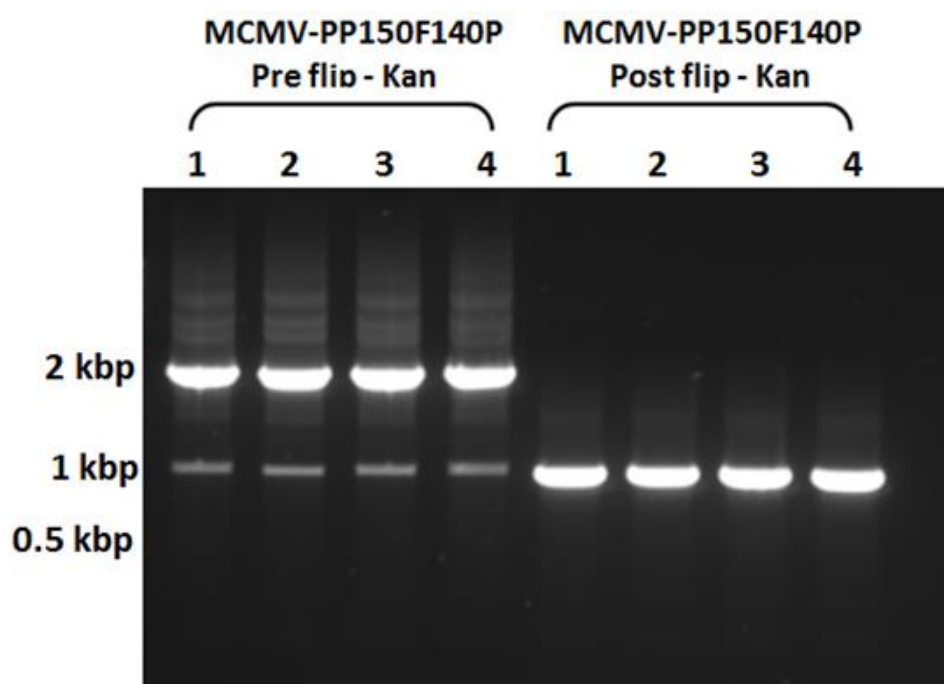


Figure 3.30 Confirmation of Kan^R marker removal from MCMV-pp150-F140P BAC genome by PCR. DNA from 4 clones of recombinant MCMV-pp150-F140P BACs (pre and post FLP) were screened by PCR using primers flanking the site of recombination. PCR products were separated on a 1% agarose gel for 60-90 min at 75 V, and visualized by staining with EtBr (0.5 µg/ml). PCR of pre- and post-FLP MCMV-pp150-F140P yielded PCR products of approximately 2 and 1 kb, respectively. Molecular size marker (MW) in kb is indicated.

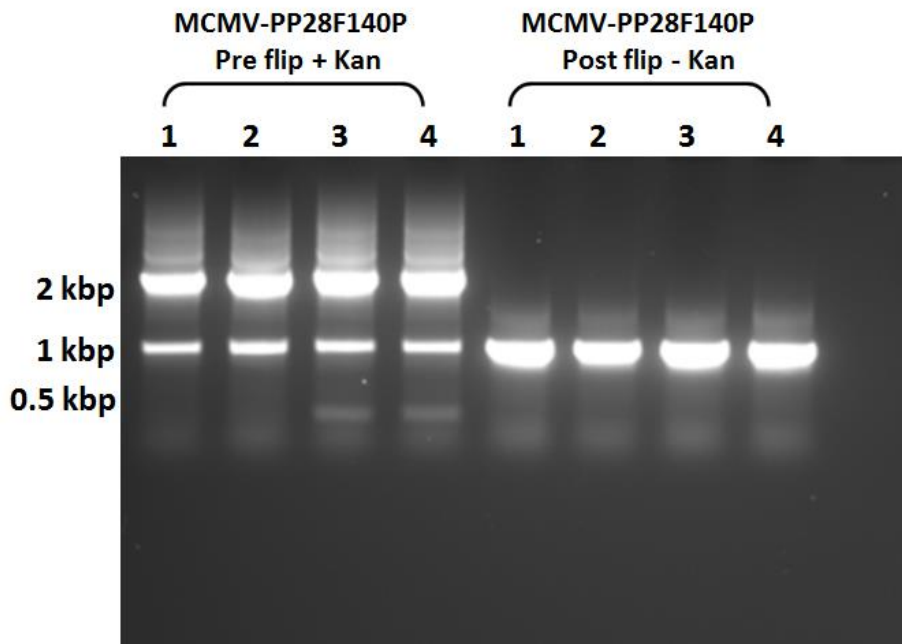


Figure 3.31 Confirmation of Kan^R marker removal from MCMV-pp28-F140P BAC genome by PCR. DNA from 4 clones of recombinant MCMV-pp28-F140P BACs (pre and post FLP) were screened by PCR using primers flanking the site of recombination. PCR products were separated on a 1% agarose gel for 60-90 min at 75 V, and visualized by staining with EtBr (0.5 µg/ml). PCR of pre- and post-FLP MCMV-pp28-F140P yielded PCR products of approximately 2 and 1 kb, respectively. Molecular size marker (MW) in kb is indicated.

To confirm the absence of genomic rearrangements in recombinant BACs following Kan^R excision, BAC DNA was again analysed by restriction digests with EcoRI followed by electrophoresis on a 1% agarose gel (Figures 3.32 and 3.33) and sequencing (Figures 3.34 and 3.35). MCMV-WT BAC DNA and MCMV-pp150/pp28-F140P recombinant BAC DNA (pre- and post-FLP) were compared side by side on the gel to confirm genomic integrity of the post-FLP recombinant clones. The banding patterns generated by restriction enzyme digestion of the recombinant MCMV-pp150/pp28 BACs were consistent with those of the MCMV-WT BAC control. Banding patterns were also comparable between the pre- and post-FLP samples, indicating the absence of genome rearrangement in the recombinant BAC DNA

following FLP recombinase mediated removal of the Kan^R marker. As a final level of characterization, the F140P domains from the recombinant MCMV BACs were amplified by PCR and sequenced by Sanger DNA sequencing (Section 2.3.8). Two recombinant BAC clones from each recombinant MCMV-PP150/PP28-F140P were selected for sequence characterization. The sequence data indicated that full-length sequence of the F140P domain was present in the recombinants with the absence of any mutations (Figure 3.34 and 3.35). Together, these results demonstrate excision of Kan^R cassette from recombinant MCMV-pp150-F140P and MCMV-pp28-F140P BAC clones prior to virus reconstitution in MCMV permissive eukaryotic MEF cells.

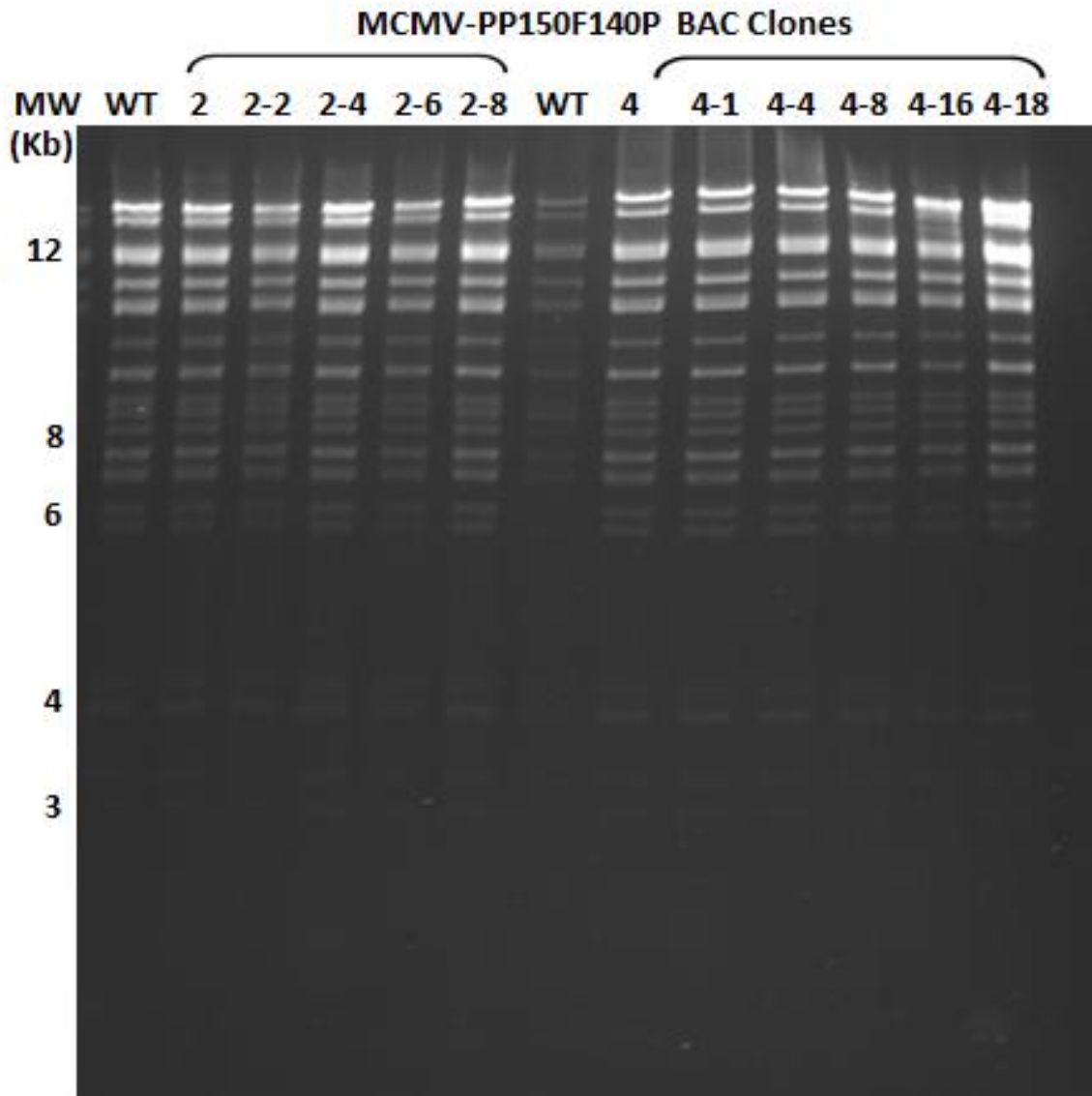


Figure 3.32 Characterization of the recombinant (post-FLP) MCMV-pp150-F140P BAC genome using EcoRI restriction enzyme digestion. MCMV-WT and recombinant MCMV-pp150-F140P pre-FLP (clones 2 and 4) and post-FLP (2-2, 2-4, 2-6, 2-8, 4-1, 4-4, 4-8, 4-16, and 4-18) BACs were digested with EcoRI restriction enzyme and the resulting fragments were separated on a 1% agarose gel for 18-20 hours at 45 V followed by visualization with EtBr (0.5 $\mu\text{g/ml}$). Comparable restriction digestion pattern between the MCMV-pp150-F140P clones pre- and post-FLP recombinase mediated removal of Kan^R demonstrates lack of any gross genomic rearrangements. Molecular size marker lane (MW) in kb is indicated.

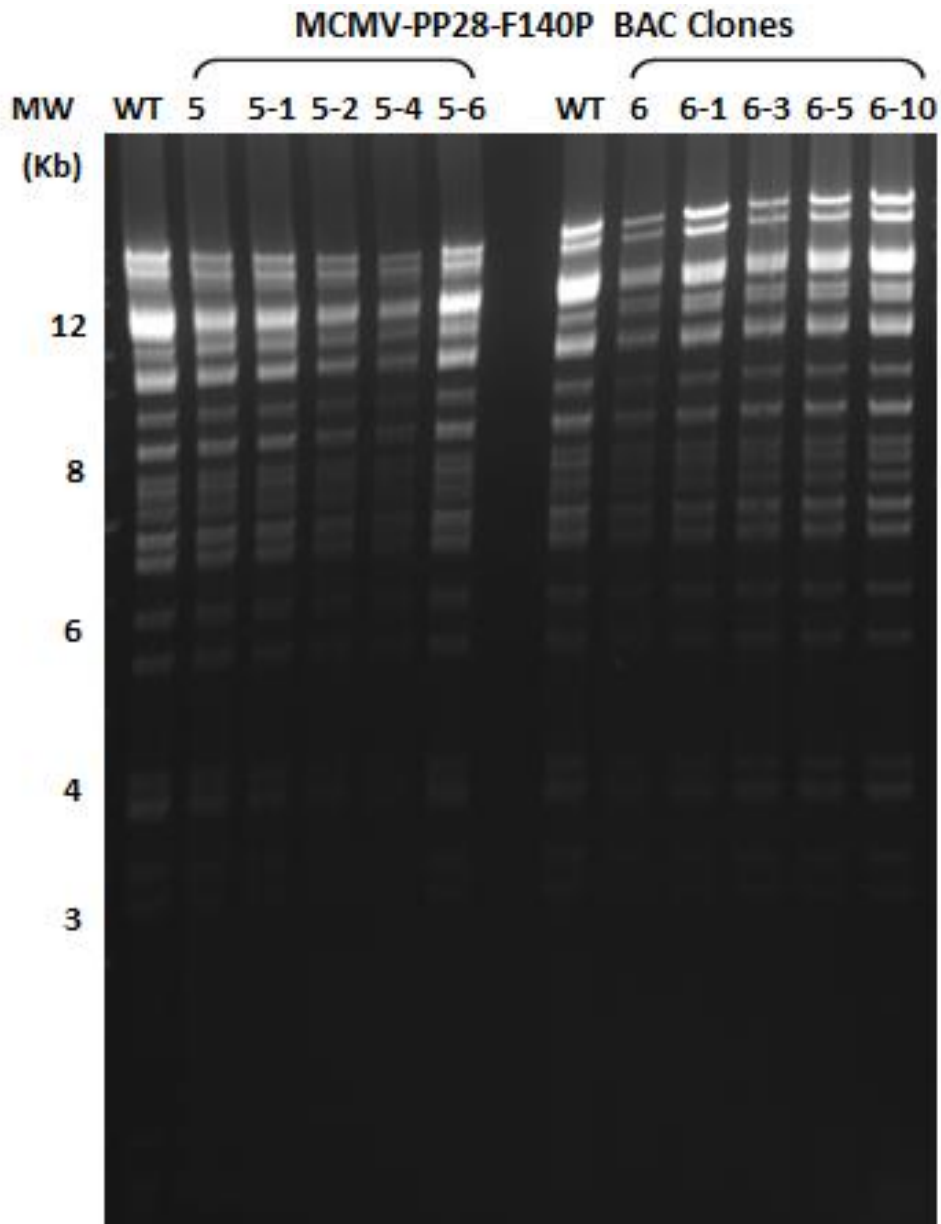


Figure 3.33 Characterization of the recombinant (post-FLP) MCMV-pp28-F140P BAC genome using EcoRI restriction enzyme digestion. MCMV-WT and recombinant MCMV-pp28-F140P pre-FLP (clones 5 and 6) and post-FLP (5-1, 5-2, 5-4, 5-6, 6-1, 6-3, 6-5, and 6-10) BACs were digested with EcoRI restriction enzyme and the resulting fragments were separated on a 1% agarose gel for 18-20 hours at 45 V followed by visualization with EtBr (0.5 $\mu\text{g/ml}$). Comparable restriction digestion pattern between the MCMV-pp28-F140P clones pre- and post-FLP recombinase mediated removal of Kan^R demonstrates lack of any gross genomic rearrangements. Molecular size marker lane (MW) in kb is indicated.

(A)

```
GCCACACTCTCCACAGTTCGCCGGCTCCCCATTCGCCGGTCTGATGGGGACGGTGGCGGCCT
GGTAAAAAATCGTCGTCGTCTCACATCAGTCTGATTGCGGGCTTAGCGGTAGATCACGTTA
TCGGCATGGAAAACGCCATGCCGTGGAACCTGCCTGCCGATCTCGCCTGGTTTAAACGCAACA
CCTTAAATAAACCCGTGATTATGGGGCCGACATACCTGGGAATCAATCGGTCTCCGTTGCCAG
GACGCAAAAATATTATCCTCAGCAGTCAACCGAGTACGGACGATCGCGTAACGTGGGTGAAG
TCGGTGGATGAAGCCATCGCTGCGTGTGGTGACGTACCAGAAATCATGGTGATTGGCGGGCG
TCGCGTTTATGAACAGTTCTTGCCAAAAGCGCAAAAAGTGTATCTGACGCATATCGACGCAG
AAGTGAAGGGCGACACCCATTTCCCGGATTACGAGCCGGATGACTGGGAATCGGTATTCAGC
GAACCCACGATGCTGATGCGCAGAACTCTCACAGCTATTGCTTTGAGATTCTGGAGCGGCGA
GGTAAGCCTATCCCTAACCTCTCCTCGGTCTCGATTCTACGTAACCCGGGGATCTTGAAGTT
CCTATTCCGAAGTTCCTATTCTCTAGAAAGTATAGGAACTTCAGAGCGCTTTTGAAGCTGCG
GATATCGCTAATTCCTATGTCAGCCGTTAAGTACAAGATCGATGATCGCTCGCTCCTGGTTGG
TTTTTATTATTTTTTTTATTATCATCACAGTAAAAAGAAAGACACTGTTACACACTCTCTCG
```

(B)

```
CCCACTCTCCACAGTTCGCCGGCTCCCCATTCGCCGGTCTGATGGGGACGGTGGCGGCCTG
GTAAAAAATCGTCGTCGTCTCACATCAGTCTGATTGCGGGCTTAGCGGTAGATCACGTTAT
CGGCATGGAAAACGCCATGCCGTGGAACCTGCCTGCCGATCTCGCCTGGTTTAAACGCAACAC
CTTAAATAAACCCGTGATTATGGGGCCGACATACCTGGGAATCAATCGGTCTCCGTTGCCAGG
ACGCAAAAATATTATCCTCAGCAGTCAACCGAGTACGGACGATCGCGTAACGTGGGTGAAGT
CGGTGGATGAAGCCATCGCTGCGTGTGGTGACGTACCAGAAATCATGGTGATTGGCGGGCGGT
CGCGTTTATGAACAGTTCTTGCCAAAAGCGCAAAAAGTGTATCTGACGCATATCGACGCAGA
AGTGAAGGGCGACACCCATTTCCCGGATTACGAGCCGGATGACTGGGAATCGGTATTCAGCG
AACCCACGATGCTGATGCGCAGAACTCTCACAGCTATTGCTTTGAGATTCTGGAGCGGCGAG
GTAAGCCTATCCCTAACCTCTCCTCGGTCTCGATTCTACGTAACCCGGGGATCTTGAAGTTC
CTATTCCGAAGTTCCTATTCTCTAGAAAGTATAGGAACTTCAGAGCGCTTTTGAAGCTGCGG
ATATCGCTAATTCCTATGTCAGCCGTTAAGTACAAGATCGATGATCGCTCGCTCCTGGTTGGT
TTTTTATTATTTTTTTTATTATCATCACAGTAAAAAGAAAGACACTGTTACACACTCTCTCGT
```

Figure 3.34 Confirmation of MCMV-pp150-F140P BAC genome via Sanger DNA sequencing. PCR was performed on selected post-FLP MCMV-pp150-F140P BAC clones: (A) clone (2-6) and (B) clone (4-16) followed by DNA sequencing. Black sequence represents the pp150 protein and green represents sequence homology to the F140P domain.

(A)

```
TCGGGGCGACAGGGAGGCGGAAAGCGGACGTCGTCTTTGAAATCCGCCAAGAACGGCGCCGG
CGTGAAGAAAAAAGTCAGGGCCTTGATCAGTCTGATTGCGGCGTTAGCGGTAGATCACGTTA
TCGGCATGGAAAACGCCATGCCGTGGAACCTGCCTGCCGATCTCGCCTGGTTTAAACGCAACA
CCTTAAATAAACCCGTGATTATGGGCCGCCATACCTGGGAATCAATCGGTCGTCCGTTGCCAG
GACGCAAAAATATTATCCTCAGCAGTCAACCGAGTACGGACGATCGCGTAACGTGGGTGAAG
TCGGTGGATGAAGCCATCGCTGCGTGTGGTGACGTACCAGAAATCATGGTGATTGGCGGCGG
TCGCGTTTATGAACAGTTCTTGCCAAAAGCGCAAAAAGTGTATCTGACGCATATCGACGCAG
AAGTGAAGGCGACACCCATTTCCCGGATTACGAGCCGGATGACTGGGAATCGGTATTCAGC
GAACCCACGATGCTGATGCGCAGAACTCTCACAGCTATTGCTTTGAGATTCTGGAGCGGCGA
GGTAAGCCTATCCCTAACCTCTCCTCGGTCTCGATTCTACGTAACCCGGGGATCTTGAAGTT
CCTATTCCGAAGTTCCTATTCTCTAGAAAGTATAGGAACTTCAGAGCGCTTTTGAAGCTGCG
GATATCGCTAATCCCATGTCAGCCGTTAAGTTATCTATCTATCGATCGACCGTGAGGGGGG
GAGAAAGGGAGAAAGAGTGGAGGAGATTTATTAATAAAAACGACATGGTGACAACACCAT
```

(B)

```
GCTCGGGGCGACAGGGAGGCGGAAAGCGGACGTCGTCTTTGAAATCCGCCAAGAACGGCGCC
GGCGTGAAGAAAAAAGTCAGGGCCTTGATCAGTCTGATTGCGGCGTTAGCGGTAGATCACGT
TATCGGCATGGAAAACGCCATGCCGTGGAACCTGCCTGCCGATCTCGCCTGGTTTAAACGCAA
CACCTTAAATAAACCCGTGATTATGGGCCGCCATACCTGGGAATCAATCGGTCGTCCGTTGCC
AGGACGCAAAAATATTATCCTCAGCAGTCAACCGAGTACGGACGATCGCGTAACGTGGGTGA
AGTCGGTGGATGAAGCCATCGCTGCGTGTGGTGACGTACCAGAAATCATGGTGATTGGCGGC
GGTCGCGTTTATGAACAGTTCTTGCCAAAAGCGCAAAAAGTGTATCTGACGCATATCGACGC
AGAAGTGAAGGCGACACCCATTTCCCGGATTACGAGCCGGATGACTGGGAATCGGTATTCAG
GCGAACCCACGATGCTGATGCGCAGAACTCTCACAGCTATTGCTTTGAGATTCTGGAGCGGC
GAGGTAAGCCTATCCCTAACCTCTCCTCGGTCTCGATTCTACGTAACCCGGGGATCTTGAAG
TTCCTATTCCGAAGTTCCTATTCTCTAGAAAGTATAGGAACTTCAGAGCGCTTTTGAAGCTG
CGGATATC
```

Figure 3.35 Confirmation of MCMV-pp28-F140P BAC genome via Sanger DNA sequencing. PCR was performed on selected post-FLP MCMV-pp28-F140P BAC clones: (A) clone (5-1) and (B) clone (6-10) followed by DNA sequencing. Black sequence represents the pp28 protein and green represents sequence homology to the F140P domain.

3.2.3 Reconstitution of MCMV-pp150/pp28-F140P recombinant viruses

CMV genomes are comprised of a single dsDNA molecule. As such production of infectious virus requires only introduction of the CMV DNA genome into CMV permissive cells for reconstitution of derivative CMV virus (Roizman & Pellett, 2001). Although labour-intensive, the impact of DD fusion to essential virus proteins on virus replication can only be ascertained empirically by construction and analysis of the respective recombinant viruses. To determine whether we were able to reconstitute recombinant CMVs expressing the pp150 or pp28 ORFs fused to the ecDHFR destabilizing domain (F140P), BAC DNA was introduced into MEFs by electroporation. The use of MEFs is essential for MCMV reconstitution due to the high species-specificity of CMVs. MEF cells were electroporated with the recombinant MCMV-pp150-F140P or MCMV-pp28-F140P BACs. WT-MCMV BAC DNA was used as a positive control (Section 2.6.2.2). Two independent clones from each vector were selected for reconstitution (Table 3.6) to mitigate effects of any potential second site mutations.

If the ecDHFR was destabilizing the targeted CMV tegument protein, then reconstitution of recombinant MCMVs was expected to require the presence of the stabilizing TMP molecule. To gain an initial insight into the conditionality of replication of the MCMV recombinants, the selected recombinant clones were grown in either the presence or absence of TMP. A TMP concentration of 50 μ M was used, which was based on the amount previously shown to be able to afford stabilization in a study by (Glaß *et al.*, 2009). Cell monolayers were monitored daily under the inverted microscope for signs of virus induced CPE (swelling, rounding, aggregation, cell death and plaque development); (Kim & Carp, 1971). In the presence of TMP viral plaques from both pp28 and pp150 MCMV recombinants were detected 3-7 days post-transfection, which then spread through the entire monolayer by day 10 at which point virus was harvested (Section 2.6.2.2).

In the absence of TMP, reconstitution was far less efficient with only 2 (clone 2-6) and 3 (clone 4-16) plaques resulting following reconstitution of the pp150 MCMV constructs, which were delayed until day 8 post-transfection. In the absence of TMP, neither of the pp28 MCMV constructs resulted in any detectable plaques at least until day 14 post-transfection. These initial results suggest that fusion of the ecDHFR (F140P) domain to pp150 and pp28 has resulted in TMP-dependent replication of the recombinant viruses that may be more stringent for the pp28 recombinant. Numbers of plaques were recorded in Table 3.6. MCMV-pp150-F140P and pp28-F140P plaques were picked up and isolated as described in (Section 2.6.2.1).

Table 3.6. Reconstitution of recombinant MCMV-pp150/pp28-F140P BAC clones in the presence or absence of the TMP

MCMV BAC construct	Clone	Plaque numbers	
		(+TMP)	(-TMP)
MCMV-pp150-F140P	(6-1)	12	4
	(3-9)	10	3
MCMV-pp28-F140P	(1-2)	1	0
	(5-1)	4	0

3.2.3.1 Preparation of seed stock from recombinant MCMV-pp150/pp28-F140P viruses in the presence of TMP

To enable further characterization of the different recombinant viruses following reconstitution of the MCMV BAC clones, seed stocks of MCMV-pp150-F140P and MCMV-pp28-F140P were prepared using individual reconstituted plaque-derived viruses (clones (3-9) and (1-2), respectively; Section 2.6.2.4). A parental MCMV-WT seed stock was also prepared. Monolayers infected with MCMV-pp150-F140P or MCMV-pp28-F140P recombinant viruses were incubated for 5 or 7 days, in the presence of 100 μ M TMP, until approximately 95% of cells demonstrated substantial CPE. The desired concentration of TMP was added to the media every 24 hr to maintain the TMP concentration at the desired level. Cells and supernatant were harvested, freeze thawed at -80°C , clarified at 3800 rpm ($4600 \times g$) for 20 min at RT, aliquoted and stored at -80°C .

3.2.3.2 Preparation of concentrated virus stocks in the presence of TMP

High titre stocks of recombinant MCMV-pp150-F140P and MCMV-pp28-F140P viruses were prepared from the seed stocks generated above in the presence of TMP, as described in (Section 2.6.1.5). Stocks of parental MCMV-WT were also prepared. Next, we assessed titre of recombinant and parental viruses by TCID₅₀ assay in the presence or absence of TMP (Section 2.6.1.6). We hypothesized that if the recombinant viruses were conditionally attenuated as suggested by differences in virus reconstitution levels, then this would be observed as a decrease in replication in the absence of the stabilizing TMP molecule. As shown in (Figure 3.36), the relative titre of MCMV-WT was unaffected by the presence or absence of TMP as expected. Using two-tailed t-test, there was no significant difference ($P=0.9333$) relative to the appropriate control (without TMP) on day 4 post-infection. In contrast, the titre of the MCMV-pp150-F140P stock was 10-fold higher in the presence of TMP than

in the absence of TMP. At this further level of characterization, this difference suggested an intermediate level of TMP-dependency of replication of MCMV-pp150-F140P. Statistical analysis using two-tailed t-test indicated that although there was a trend towards lower replication, this 10-fold difference was not statistically significant ($P= 0.5532$). In comparison to only a trend towards TMP-dependent replication for MCMV-pp150-F140P, MCMV-pp28-FF140P replication was clearly dependent on the presence of TMP for replication. As shown in (Figure 3.37) statistical analysis using a two-tailed t-test indicated a statistically significant reduction in the level of the recombinant virus in the absence versus the presence of TMP ($P<0.0001$). This result, suggests a level of destabilization of the pp28 resulting from fusion to the F140P DD that results in a complete attenuated replication phenotype of the virus in the absence of the stabilizing TMP molecule.

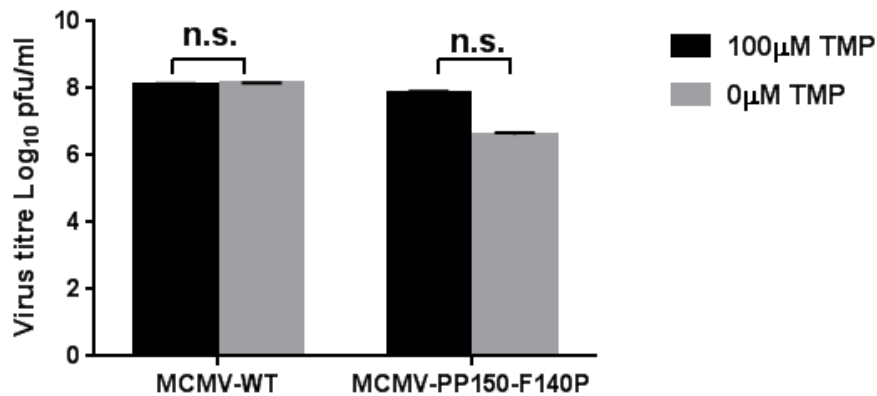


Figure 3.36 Titration of Concentrated stocks in the present or absence of TMP by TCID50 assay. MEFs were infected with MCMV-WT or MCMV-pp150-F140P virus at a MOI of 0.01 PFU/cell and cultivated with (100 μM) or without (0 μM) TMP at 37°C. Four days post infection the virus titres (log 10 PFU/cell) were determined in the cell monolayer. Error bars show the SE; N= 3 independent experiments. n.s.(not significant) $P>0.05$ indicates there was not statistically significant differences relative to the infected cells in the absence of TMP, using two-tailed t-test.

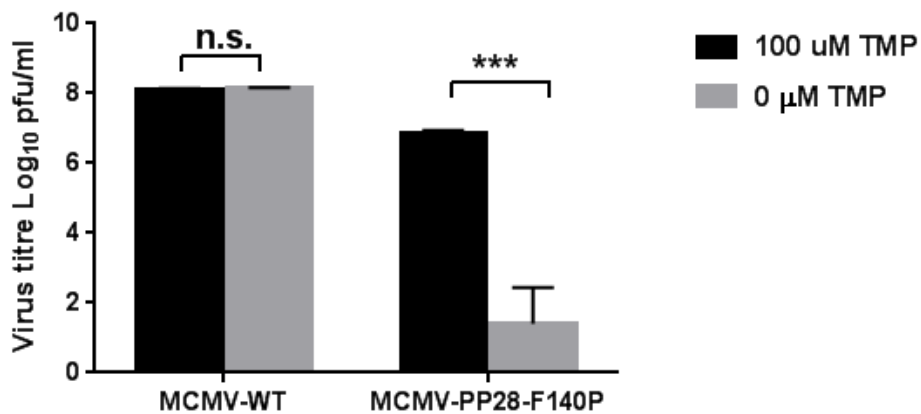


Figure 3.37 Titration of Concentrated stocks in the present or absence of TMP by TCID50 assay. MEFs were infected with MCMV-WT or MCMV-pp28-F140P virus at a MOI of 0.01 PFU/cell and cultivated with (100 μM) or without (0 μM) TMP at 37°C. Four days post infection the virus titres (log 10 PFU/cell) were determined in the cell monolayer. Error bars show the SE; N= 3 independent experiments. n.s.(not significant) $P>0.05$ ***, $P<0.05$ indicates significant differences relative to the infected cells in the absence of TMP, using two-tailed t-test.

3.2.3.3 Confirmation of the absence of MCMV-WT from recombinant MCMV-pp150/pp28-F140P

Full characterization of recombinant virus stocks was critical prior to their use in subsequent experiments. Virus stocks were experimentally verified to ensure the F140P domain sequence was intact in all clones, and that we had not inadvertently selected virus clones that had acquired mutations during the reconstitution process. It was also necessary to exclude contamination with the wild-type MCMV.

PCR amplification was performed using viral DNA extracted from concentrated stocks (Section 2.3.1.3). This was followed by direct DNA sequencing of the PCR products. Two independent PCR amplification reactions for each sample of viral DNA was performed using the same primer pair as was used previously to confirm excision of Kan^R from recombinant MCMV BAC (pp150Short-F/R and pp28Inter-F/R), (Section 2.3.3). Results showed that the bands of the expected sizes of 500 or 100 bp and 1000 bp were observed in the MCMV-WT lanes (1 & 2), and recombinant MCMV-pp150/pp28-F140P (lanes 3-6), respectively (Figures 3.38-3.39). These results confirm the presence of the F140P domain, and demonstrate that there is no MCMV-WT contamination within the recombinant stocks.

Two clones (number 1 and 4 of Figures 3.38 and 3.39) of each recombinant MCMV-pp150/pp28-F140P virus were selected for Sanger sequencing using the primers pp150Short F/R and pp28Inter F/R (Tables 2.6 - 2.7). Sequence data demonstrated that the full length of the F140P domain was present, in the correct position, and did not have any deletions or mutations that might impact the protein function (Figures 3.40 and 3.41).

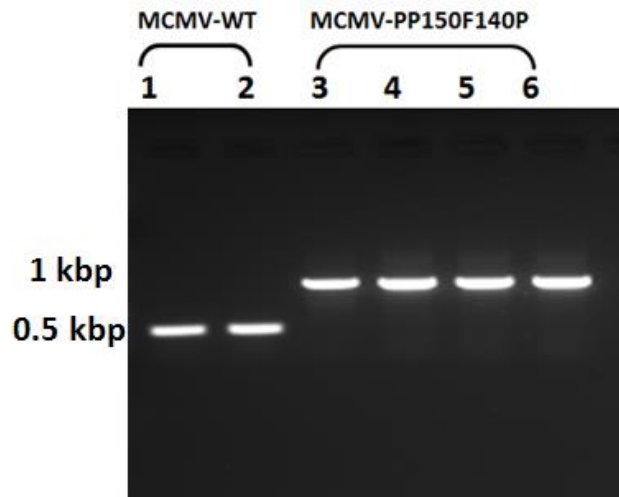


Figure 3.38 Confirming presence of F140P domain in MCMV-pp150-F140P virus by PCR. DNA was isolated from MCMV-pp150-F140P concentrated stocks using a QIAamp kit and PCR was carried out using pp150Short F/R primers. PCR products were separated on a 1% agarose gel. The presence of a 1000 bp band in recombinant virus lanes (3-6) confirmed that the F140P domain was present, and the absence of the MCMV-WT sized band (500 bp) in the MCMV-pp150-F140P virus lanes confirmed the absence of WT contamination of recombinant.

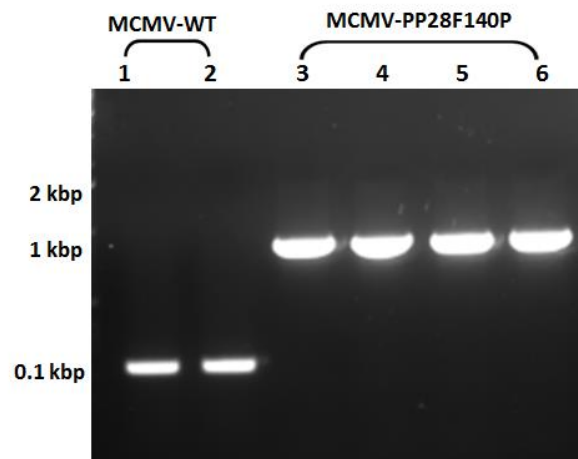


Figure 3.39 Confirming presence of F140P domain in MCMV-pp28-F140P virus by PCR. DNA was isolated from MCMV-pp28-F140P concentrated stocks using a QIAamp kit and PCR was carried out using pp28Inter-F/R primers. PCR products were separated on a 1% agarose gel. The presence of a 1000 bp band in recombinant virus lanes (3-6) confirmed that the F140P domain was present, and the absence of the MCMV-WT sized band (100 bp) in the MCMV-pp28-F140P virus lanes confirmed the absence of WT contamination of recombinant.

(A)

```
CCACACTCTCCACAGTTCGCCGGCTCCCATTGCGCGGTTCTGATGGGGACGGTGGCGGCCTG
GTAAAAAATCGTCGTCTCACATCAGTCTGATTGCGGGCTTAGCGGTAGATCACGTTAT
CGGCATGGAAAACGCCATGCCGTGGAACCTGCCTGCCGATCTCGCCTGGTTTAAACGCAACAC
CTTAAATAAACCCGTGATTATGGGCCGCCATACCTGGGAATCAATCGGTCGTCCGTTGCCAGG
ACGCAAAAATATTATCCTCAGCAGTCAACCGAGTACGGACGATCGCGTAACGTGGGTGAAGT
CGGTGGATGAAGCCATCGCTGCGTGTGGTGACGTACCAGAAATCATGGTGATTGGCGGCGGT
CGCGTTTATGAACAGTTCTTGCCAAAAGCGCAAAAACGTATCTGACGCATATCGACGCAGA
AGTGGAAGGCGACACCCATTTCCCGGATTACGAGCCGGATGACTGGGAATCGGTATTCAGCG
AACCCACGATGCTGATGCGCAGAACTCTCACAGCTATTGCTTTGAGATTCTGGAGCGGCGAG
GTAAGCCTATCCCTAACCTCTCCTCGGTCTCGATTCTACGTAACCCGGGGATCTTGAAGTTC
CTATTCCGAAGTTCCTATTCTCTAGAAAGTATAGGAACTTCAGAGCGCTTTTGAAGCTGCGG
ATATCGCTAATTCCCATGTCAGCCGTTAAGTACAAGATCGATGATCGCTCGCTCCTGGTTGG
```

(B)

```
CAGTTCGCCGGCTCCCATTGCGCGGTTCTGATGGGGACGGTGGCGGCCTGGTAAAAAATCG
TCGTCTCACATCAGTCTGATTGCGGGCTTAGCGGTAGATCACGTTATCGGCATGGAAA
CGCCATGCCGTGGAACCTGCCTGCCGATCTCGCCTGGTTTAAACGCAACACCTTAAATAAAC
CGTGATTATGGGCCGCCATACCTGGGAATCAATCGGTCGTCCGTTGCCAGGACGCAAAAATA
TTATCCTCAGCAGTCAACCGAGTACGGACGATCGCGTAACGTGGGTGAAGTCGGTGGATGAA
GCCATCGCTGCGTGTGGTGACGTACCAGAAATCATGGTGATTGGCGGCGGTGCGGTTTATGA
ACAGTTCTTGCCAAAAGCGCAAAAACGTATCTGACGCATATCGACGCAGAAAGTGAAGGCG
ACACCCATTTCCCGGATTACGAGCCGGATGACTGGGAATCGGTATTCAGCGAACCCACGATG
CTGATGCGCAGAACTCTCACAGCTATTGCTTTGAGATTCTGGAGCGGCGAGGTAAGCCTATCC
CTAACCTCTCCTCGGTCTCGATTCTACGTAACCCGGGGATCTTGAAGTTCCTATTCCGAAGT
TCCTATTCTCTAGAAAGTATAGGAACTTCAGAGCGCTTTTGAAGCTGCGGATATCGCTAATT
CCCATGTCAGCCGTTAAGTACAAGATCGATGATCGCTCGCTCCTGGTTGGTTTTTATTATTT
```

Figure 3.40 Conformation of ecDHFR (F140P) within MCMV-pp150-F140P virus genome via Sanger sequencing. PCR was performed on the DNA extracted from concentrated virus stocks clone (5-1). Two independent PCR products (A and B) were sequenced. Black text represent pp28 genome sequence, green sequences represented homology to the F140P domain, orange sequences represented V5 tag and blue text represented downstream of MCMV genome sequence.

(A)

```
CGATCAGCTCGGGGCGACAGGGAGGCGGAAGCGGACGTCGTCTTTGAAATCCGCCAAGAACG
GCGCCGGCGTGAAGAAAAAAGTCAGGGCCTTGATCAGTCTGATTGCGGCGTTAGCGGTAGAT
CACGTTATCGGCATGGAAAACGCCATGCCGTGGAACCTGCCTGCCGATCTCGCCTGGTTTAAA
CGCAACACCTTAAATAAACCCGTGATTATGGGCCGCCATACCTGGGAATCAATCGGTCGTCCG
TTGCCAGGACGCAAAATATTATCCTCAGCAGTCAACCGAGTACGGACGATCGCGTAACGTGG
GTGAAGTCGGTGGATGAAGCCATCGCTGCGTGTGGTGACGTACCAGAAATCATGGTGATTGG
CGGCGGTGCGGTTTATGAACAGTTCTTGCCAAAAGCGCAAAAAGTGTATCTGACGCACATCG
ACGCACAAGTGAACCGGACACCCATTTCCCGGATTACGAGCCGGATGACTGGGGAATCGGT
ATTCAGCGAACCCACGATGCTGATGCGCAGAAGTCTCACAGCTATAGCTTTGAGATTCTGGA
GCGGCGAGGTAAGCCTATCCCTAACCTCTCCTCGGTCTCGATTCTACGTAACCCGGGATCT
TGAAGTTCCTATTCGAAGTTCCTATTCTCTAGAATGTATAGGAACTTCAGAGCGCTTTTGA
```

(B)

```
AGGCGGAAGCGGACGTCGTCTTTGAATCCGCCAAGAACGGCGCCGGCGTGAAGAAAAAAGTC
AGGGCCTTGATCAGTCTGATTGCGGCGTTAGCGGTAGATCACGTTATCGGCATGGAAAACGC
CATGCCGTGGAACCTGCCTGCCGATCTCGCCCGGTTTAAACGCAACACCTTAAATAAACCCGT
GATTATGGGCCGCCATACCTGGGAATCAATCGGTCGTCCGTTGCCAGGACGCAAAATATTA
TCCTCAGCAGTCAACCGAGTACGGACGATCGCGTAACGTGGGTGAAGTCGGTGGATGAAGCC
ATCGCTGCGTGTGGTGACGTACCAGAAATCATGGTGATTGGCGGCGGTGCGGTTTATGAACA
GTTCTTGCCAAAAGCGCAAAAAGTGTATCTGACGCATATCGACGCACAATTGGAACGCGACA
CCCATTTCCCGGATTACGAGCCGGATGACTGGGAATCGGTATTCAGCGAACCCACGATGCTG
ATGCGCAGAAGTCTCACAGCTATTGCTTTGAGATTCTGGAGCGGCGAGGTAAGCCTATCCCTA
ACCCTCTCCTCGGTCTCGATTCTACGTAACCCGGGATCTTGAAGTTCCTATTCCGAAGTCC
TATTCTCTAGAATGTATAGGAACTTCAGAGCGCTTTTGAAGCTGCGGATATCGTTATCTCCC
```

Figure 3.41 Conformation of ecDHFR (F140P) within MCMV-pp28-F140P virus genome via Sanger sequencing. PCR was performed on the DNA extracted from concentrated virus stocks clone (5-1). Two independent PCR products (A and B) were sequenced. Black text represent pp28 genome sequence, green sequences represented homology to the F140P domain, orange sequences represented V5 tag and blue text represented downstream of MCMV genome sequence.

3.2.4 Characterisation of recombinant MCMV-pp150/pp28-F140P virus in vitro

3.2.4.1. Replication of MCMV-pp150/pp28-F140P at differing concentration of TMP

The reduced titre of virus stocks produced in the absence compared to the presence of TMP (Figures 3.36 and 3.37) indicates that virus replication is to a certain extent being influenced by TMP stabilization. It is possible that visualization of CPE was not sensitive enough to identify more subtle differences in TMP-dependent growth. To obtain a more quantitative assessment and to confirm that viral growth was dependent on the presence of TMP, we examined the viral growth by titration of progeny virus at the different concentrations of TMP. For these studies the range of (0, 1, 5, 10, 50 and 100) μM of TMP were selected, which was based on earlier published study (Glaß *et al.*, 2009). MEF cells were infected with recombinant MCMV-pp150-F140P or MCMV-pp28-F140P virus at MOI (0.01 PFU/cell) and then cultured under various concentrations of TMP. To maintain the concentration of the TMP in the culture as desired, we added TMP every 24 hr during the course of infection. Progression of infection was also visualized by CPE. Results presented in Figure 3.42 show the level of CPE at various TMP concentrations at day 4 post-infection (pi). The number of plaques at this time was also enumerated (Table 3.7). Consistent with the ability of the MCMV-pp150-F140P to be reconstituted in the absence of TMP, the virus grew in regardless presence or absence of TMP in the culture media. Results demonstrated that plaque numbers were increased with the increasing of TMP concentration, however at 100 μM of TMP e observed decrease of plaque number (Table 3.7). These result indicated that the presence of different concentration of TMP had little effect on the plaque numbers that formed by recombinant virus.

In contrast, for cells infected with the MCMV-pp28-F140P virus (clone 1-2) and cultured with different concentration of TMP, the number of plaques increased and the size become larger with increasing of TMP concentration (Table 3.7; Figure 3.43). Subsequent

characterization of the viruses showed that the MCMV-pp28-F140P mutant virus was clearly attenuated in the absence of TMP. Upon cultivation without TMP only a few minifoci became detectable, which did not develop into plaques. When the virus was cultured at 100 μ M TMP the plaque number of the virus was indistinguishable from that of wild-type virus.

Taken together, these results showed that fusion of the ecDHFR DD to essential tegument proteins of MCMV results in a conditional, TMP-dependent attenuated phenotype. However, the specific tegument protein targeted affects the level of attenuation ranging from intermediate to complete. The amount of TMP needed for optimal stabilization of the viruses also differed for each fusion protein and can only be established empirically.

Table 3.7 Number of MCMV-pp150/pp28-F140P plaques in representative sample from 6.2 mm² field of view

Recombinant MCMV vector	Plaque number in different concentration of TMP (μ M)					
	0	1	5	10	50	100
MCMV-pp150-F140P	13	15	18	20	25	18
MCMV-pp28-F140P	1	3	6	6	10	12

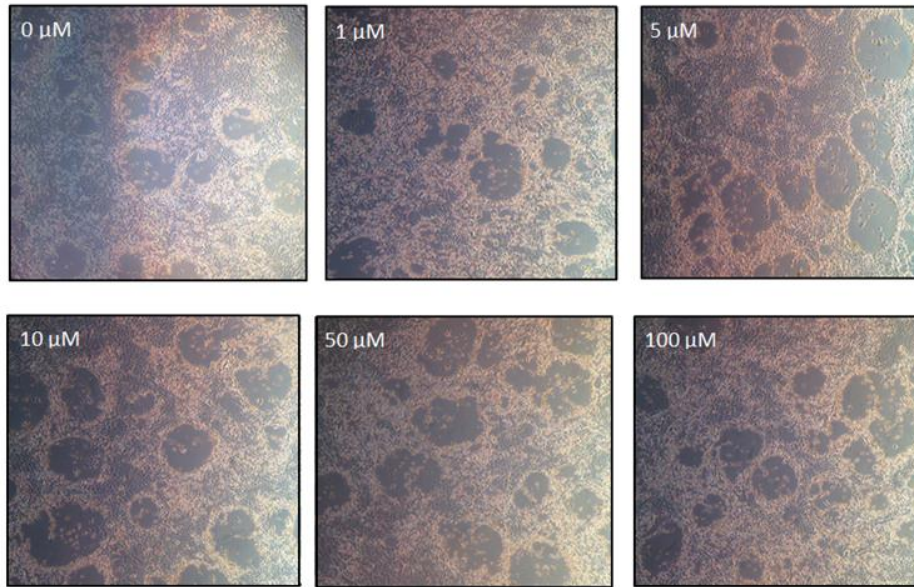


Figure 3.42 Image of Dose-dependent regulation of the recombinant MCMV-pp150-F140P replication and tunability of plaque formation by TMP. MEF cells were infected with the MCMV-pp150-F140P virus at a MOI of 0.01 PFU/cell and cultivated in the presence of various concentration of TMP as indicated. At day four post infection, images of infected cells were taken, depicting plaque formation by mutant MCMV under different concentration of TMP.

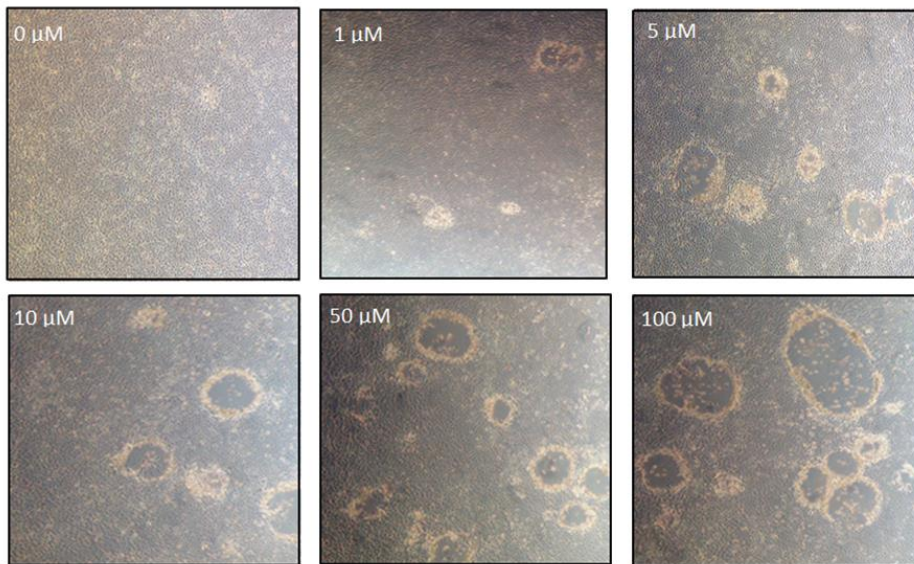


Figure 3.43 Image of Dose-dependent regulation of the recombinant MCMV-pp28-F140P replication and tunability of plaque formation by TMP. MEF cells were infected with the MCMV-pp28-F140P virus at a MOI of 0.01 PFU/cell and cultivated in the presence of various concentration of TMP as indicated. At day four post infection, images of infected cells were taken, depicting plaque formation by mutant MCMV under different concentration of TMP.

It is possible that visualization of CPE and counting plaque numbers were not sensitive enough to identify more subtle differences in TMP-dependent growth. Different concentrations of TMP were selected to obtain a more quantitative assessment and to provide additional evidence supporting the model of TMP, regulating MCMV-pp150/pp28-F140P virus replication by controlling the stability of the ecDHFR(F140P)-tagged pp150 or pp28 protein. We determined the titre of cell-free virus by TCID₅₀ assay in the presence of desired concentration of TMP (50µM or 100 µM TMP for culture of recombinant MCMV-pp150 or MCMV-pp28, respectively; Figures 3.44 & 3.45).

Results demonstrated that the stabilization of MCMV-pp150- F140P required higher amount of the ligand, which required as high as 50 µM TMP (Figure 3.44). Although the titre of the MCMV-pp150F140P virus were increased by increasing the TMP concentration, however statistical analysis using Tukey`s multiple comparison test revealed that there was no significant difference in the virus titre that grew at 0 µM compare to 1 or 5 µM TMP ($P=0.99$ and 0.19 , respectively). The virus titre at (10, 50 or 100 µM) was significantly different from virus titre that cultured in the absence of TMP ($P=0.0131$, 0.0003 or 0.0014 , respectively). Virus titres increased approximately 2 fold when using 50 µM TMP compare to the titres of the virus that cultured in the absence of TMP (Figure 3. 44 and Table 3.8).

Consistent with the more marked attenuated phenotype of pp28 from earlier characterization, the rescue of MCMV-pp28-F140P replication by TMP was dose dependent. While MCMV-pp28-F140P failed to produce detectable virion progeny without TMP, its replication and titre increased with increasing concentration of TMP. Statistical analysis revealed that there were significant differences between the titres of the virus cultured in the absence and presence of (1, 5, 10, 50 or 100 µM) TMP ($P=0.004$, 0.02 , 0.03 , 0.0001 or 0.0001 , respectively; Figure 3.45; Table 3.9).

This observation is in agreement with the low plaque numbers of virus at decreased concentration of TMP (Table 3.7). These data showed that there was significant difference between the virus titre that cultured in the different concentration of TMP it shows dose dependent regulation of attenuation which is not observed for pp150.

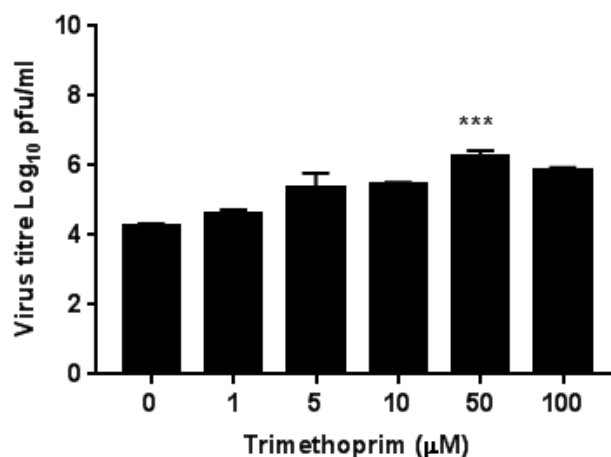


Figure 3.44 Dose-dependent regulation of the recombinant MCMV-pp150-F140P replication by ligand-TMP. MEF cells were infected with the MCMV-pp150-F140P virus at an MOI of 0.01 PFU/cell and cultivated in the presence of various concentration of TMP as indicated. At day four post infection the virus titres (log 10 PFU/cell) were determined in cell culture supernatants by TCID₅₀. The TCID₅₀ assay was performed on MEF cells maintained with 100 µM TMP. Virus titres were determined in triplicate. Statistical significance determined using a one way of variance (ANOVA) and Tukey's multiple comparison test, *** $P < 0.0003$.

Table 3.8 TMP concentration (0, 1, 5, 10, 50, 100 µM) and P values of Tukey's multiple comparison test of recombinant MCMV-pp150-F140P virus

Concentration of TMP (µM)	P value	Summary	Fold changes
0 VS. 1	>0.999	N.S.	0.5 fold
0 VS. 5	0.199	N.S.	1 fold
0 VS. 10	0.0003	*	1 fold
0 VS. 50	0.0131	***	2 fold
0 VS. 100	0.0014	**	1 fold

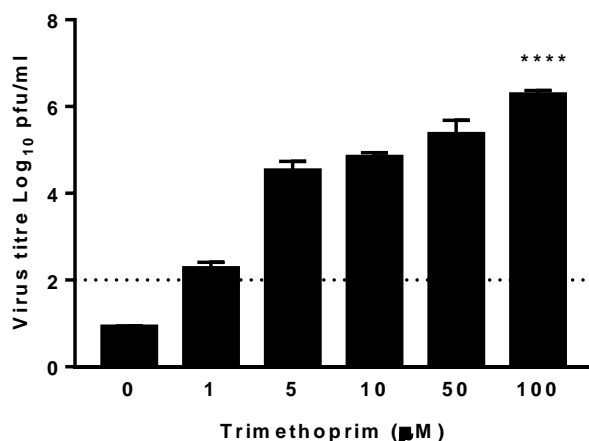


Figure 3.45 Dose-dependent regulation of the recombinant MCMV-pp28-F140P replication by ligand- TMP. MEF cells were infected with the MCMV-pp28-F140P virus at an MOI of 0.01 PFU/cell and cultivated in the presence of various concentration of TMP as indicated. At day four post infection the virus titres (log 10 PFU/cell) were determined in cell culture supernatants by TCID₅₀. The TCID₅₀ assay was performed on MEF cells maintained with 100 µM TMP. Virus titres were determined in triplicate. Statistical significance determined using a one way of variance (ANOVA) and Tukey`s multiple comparison test, **** $P < 0.00001$. Data values indicated below the threshold of detection arise from calculation of the average of values that vary across the threshold.

Table 3.9 TMP concentration (0, 1, 5, 10, 50, 100 µM) and P values of Tukey`s multiple comparison test of recombinant MCMV-pp28-F140P virus

Concentration of TMP (µM)	P value	Summary	Fold changes
0 VS. 1	0.0041	**	1.5 fold
0 VS. 5	0.02	*	3 fold
0 VS. 10	0.03	*	3.5 fold
0 VS. 50	0.0001	****	4 fold
0 VS. 100	< 0.0001	****	4.5 fold

3.2.4.1.1 Confirmation that F140P fused to MCMV-pp150/pp28 at the different concentration of TMP

3.2.4.1.1.1 PCR analysis of recombinant MCMV-pp150/pp28-F140P vectors

In order to test these viruses that released from the cells that cultured without TMP, were reverted into the wild type as a result of the insertion of ecDHFR mutant to the virus, we analysed those viruses by PCR and Sanger sequencing. Following infection of MEFs with the recombinant MCMV-pp150-F140P or MCMV-pp28-F140P and cultivation at the different concentrations of TMP, on day 4 post infection, infected cells were harvested and the DNA were extracted (Section 2.3.1.3). Purified DNA was then screened and analysed by PCR (Figures 3.46 and 3.47) to amplify the ecDHFR(F140P) from recombinant viruses at a different concentrations of TMP and also to confirm the absence of wild type sequence from recombinant viruses. PCR analyses were performed using the same primer pair used to confirm absence of wild type sequence from recombinant MCMV virus stocks (pp150Short-F and pp150Short-R as well as pp28Short-F and pp28Short-R) for recombinant MCMV-pp150 and MCMV-pp28, respectively (Tables 2.6 and 2.7). Two independent PCR were performed from each recombinant virus that was cultured in a desired concentration of TMP (Section 3.2.4.1). As shown in (Figures 3.46 and 3.47), the data revealed a band of the correct size to include the sequence for the F140P domain. The resulting PCR products gave one band about 500 bp (lanes 1 and 2) while 1000 bp (lanes 3 to 14), the sizes of the PCR products indicated the presence of the F140P gene (~ 1000 bp) compare to the band that we observed from MCMV-WT genome (~ 500 bp) fragment which indicated the absence of F140P gene from the MCMV-WT. These data confirmed similar band fragment size that were previously amplified and observed from concentrated virus stock (Figures 3.38 and 3.39. 29). The data also indicated that we did not observe any reversion to the wild-type virus. In addition to this analysis, the sequencing of these amplified fragments will provide a more detailed genomic sequence examination to confirm any genetic rearrangements or mutations.

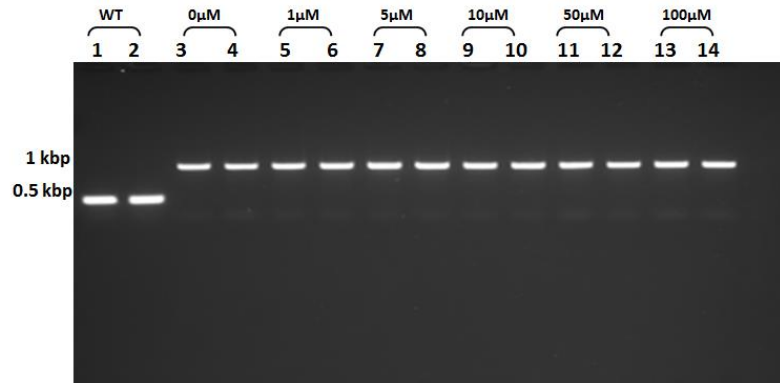


Figure 3.46 PCR screening of recombinant MCMV-pp150-F140P mutant virus maintained at different concentration of TMP. MEF cells were infected with the parental wild-type virus (1,2) or mutant MCMV-pp150-F140P virus at an MOI of 0.01 PFU/cell and cultivated in the presence of various concentrations of TMP; 0µM (3,4), 1µM (5,6), 5µM (7,8), 10µM (9,10), 50µM (11,12), 100µM (13,14) respectively. At day four post infection, supernatants were collected and the virus DNA were extracted and purified. PCR were performed using primers just outside the ecDHFR (F140P). PCR segment containing the F140P gives PCR products that are about 1 kbp (lanes 3 to 14) larger than the PCR products from the MCMV-WT genome which gave 500 bp (lanes 1 and 2) product . Molecular size marker (MW) in kbp is indicated.

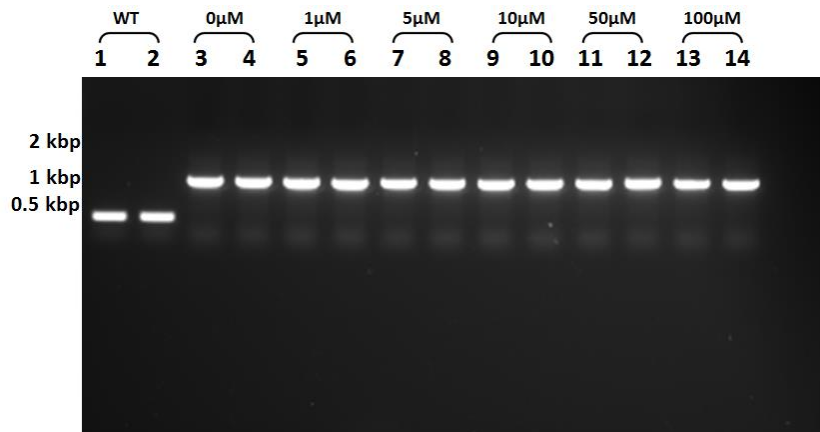


Figure 3.47 PCR screening of recombinant MCMV-pp28-F140P mutant virus maintained at different concentration of TMP. MEF cells were infected with the parental wild-type virus (1,2) or mutant MCMV-pp28-F140P virus at an MOI of 0.01 PFU/cell and cultivated in the presence of various concentrations of TMP; 0 µM (3,4), 1 µM (5,6), 5 µM (7,8), 10 µM (9,10), 50 µM (11,12), 100 µM (13,14) respectively. At day four post infection, supernatants were collected and the virus DNA were extracted and purified. PCR were performed using primers just outside the ecDHFR (F140P). PCR segment containing the F140P gives PCR products that are about 1 kbp (lanes 3 to 14) larger than the PCR products from the MCMV-WT genome which gave 500 bp (lanes 1 and 2) product. Molecular size marker (MW) in kbp is indicated.

3.2.4.1.1.2 Sequence confirmation of recombinant MCMV-pp150/pp28-F140P at a different concentration of TMP

To provide additional proof that the culturing of recombinant virus at different concentrations of TMP did not cause any gross changes in the ecDHFR(F140P) domain, sequence analyses were performed. The PCR products prepared above (Section 3.2.4.2.1) were used for Sanger sequencing. Two clones of each recombinant MCMV-pp150/pp28-F140P virus cultured at (0, 50 or 100) μM TMP were selected for screening by Sanger sequencing, using the pp150Short-F or pp28Short-F primer (Tables 2.6 and 2.7). As shown in Figures 3.38 and 3.39, the sequence data indicated that the full length sequence of the ecDHFR(F140P) domain was present and fused to the pp150/pp28 protein in recombinant virus cultured without TMP (A and B), with 50 μM (C and D) or with 100 μM of TMP (E and F), in the correct position and did not have any deletions or mutations which may impede the protein expression. Taken together these results confirmed that the MCMV-pp150-F140P and MCMV-pp28-F140P viruses which were cultivated at the different concentrations of TMP had a destabilization domain protein fused to the pp150 or pp28 protein and there was no alteration or mutation in the F140P domain sequences.

(A)

GCCACACTCTCCACAGTTCGCCGGCTCCCCATTGCGCGGTTCTGATGGGGACGGTGGCGGCCT
GGTAAAAAATCGTCGTCTCACATCAGTCTGATTGCGGCGTTAGCGGTAGATCACGTTA
TCGGCATGGAAAACGCCATGCCGTGGAACCTGCCTGCCGATCTCGCCTGGTTTAAACGCAACA
CCTTAAATAAACCCGTGATTATGGGCCGCCATACCTGGGAATCAATCGGTCGTCCGTTGCCAG
GACGCAAAAATATTATCCTCAGCAGTCAACCGAGTACGGACGATCGCGTAACGTGGGTGAAG
TCGGTGGATGAAGCCATCGCTGCGTGTGGTGACGTACCAGAAATCATGGTGATTGGCGGCGG
TCGCGTTTATGAACAGTTCTTGCCAAAAGCGCAAAAAGTGTATCTGACGCATATCGACGCAG
AAGTGAAGGCGACACCCATTTCCCGGATTACGAGCCGGATGACTGGGAATCGGTATTCAGC
GAACCCACGATGCTGATGCGCAGAACTCTCACAGCTATTGCTTTGAGATTCTGGAGCGGCGA
GGTAAGCCTATCCCTAACCTCTCCTCGGTCTCGATTCTACGTAACCCGGGGATCTTGAAGTT
CCTATTCCGAAGTTCCTATTCTCTAGAAAGTATAGGAACTTCAGAGCGCTTTTGAAGCTGCG
GATATCGCTAATCCCATGTCAGCCGTTAAGTACAAGATCGATGATCGCTCGCTCCTGGTTGG
TTTTTATTATTTTTTTTATTATCATCACAGTAAAAAGAAAGACACTGTTACACACTCTCTCG

(B)

TCTCCACAGTTCGCCGGCTCCCCATTGCGCGGTTCTGATGGGGACGGTGGCGGCCTGGTAAAA
AAATCGTCGTCTCACATCAGTCTGATTGCGGCGTTAGCGGTAGATCACGTTATCGGCATG
GAAAACGCCATGCCGTGGAACCTGCCTGCCGATCTCGCCTGGTTTAAACGCAACACCTTAAAT
AAACCCGTGATTATGGGCCGCCATACCTGGGAATCAATCGGTCGTCCGTTGCCAGGACGCAAA
AATATTATCCTCAGCAGTCAACCGAGTACGGACGATCGCGTAACGTGGGTGAAGTCGGTGGA
TGAAGCCATCGCTGCGTGTGGTGACGTACCAGAAATCATGGTGATTGGCGGCGGTCGCGTTT
ATGAACAGTTCTTGCCAAAAGCGCAAAAAGTGTATCTGACGCATATCGACGCAGAAGTGAA
GGCGACACCCATTTCCCGGATTACGAGCCGGATGACTGGGAATCGGTATTCAGCGAACCCAC
GATGCTGATGCGCAGAACTCTCACAGCTATTGCTTTGAGATTCTGGAGCGGCGAGGTAAGCC
TATCCCTAACCTCTCCTCGGTCTCGATTCTACGTAACCCGGGGATCTTGAAGTTCCTATTCC
GAAGTTCCTATTCTCTAGAAAGTATAGGAACTTCAGAGCGCTTTTGAAGCTGCGGATATCGC
TAATTCCCATGTCAGCCGTTAAGTACAAGATCGATGATCGCTCGCTCCTGGTTGGTTTTTATT
ATTTTTTTTATTATCATCACAGTAAAAAGAAAGACACTGTTACACACTCTCTCG

(C)

```
GCCACACTCTCCACAGTTCGCCGGCTCCCCATTGCGCGGTTCTGATGGGGACGGTGGCGGCCT
GGTAAAAAATCGTCGTCTCACATCAGTCTGATTGCGGGCTTAGCGGTAGATCACGTTA
TCGGCATGGAAAACGCCATGCCGTGGAACCTGCCTGCCGATCTCGCCTGGTTTAAACGCAACA
CCTTAAATAAACCCGTGATTATGGGGCCGACCTGGGAATCAATCGGTGTCGGTTGCCAG
GACGCAAAAATATTATCCTCAGCAGTCAACCGAGTACGGACGATCGCGTAACGTGGGTGAAG
TCGGTGGATGAAGCCATCGCTGCGTGTGGTGACGTACCAGAAATCATGGTGATTGGCGGGG
TCGCGTTTATGAACAGTTCTTGCCAAAAGCGCAAAAAGTGTATCTGACGCATATCGACGCAG
AAGTGAAGGCGACACCCATTTCCCGGATTACGAGCCGGATGACTGGGAATCGGTATTCAGC
GAACCCACGATGCTGATGCGCAGAACTCTCACAGCTATTGCTTTGAGATTCTGGAGCGGCGA
GGTAAGCCTATCCCTAACCTCTCCTCGGTCTCGATTCTACGTAACCCGGGGATCTTGAAGTT
CCTATTCCGAAGTTCCTATTCTCTAGAAAGTATAGGAACTTCAGAGCGCTTTTGAAGCTGCG
GATATCGCTAATTCCTATGTCAGCCGTTAAGTACAAGATCGATGATCGCTCGCTCCTGGTTGG
TTTTTATTATTTTTTTTATTATCATCACAGTAAAAAGAAAGACACTGTTACACACTCTC
```

Figure 3.48 Sequence conformation of recombinant MCMV-pp150-F140P vector cultured with the different concentration of TMP. (A) In the absence of TMP, (B) at 50 μ M or (C) 100 μ M. PCR were performed on the recombinant viruses and two PCR reactions from each virus were sequenced. Black sequences: represent sequence homology to the pp150 protein; Green sequences: represent sequence homology to the ecDHFR (F140P); Orange sequences: homology to V5 tag; Blue sequences: represent sequence homology to the pOriFRT(wt)-ecDHFR(F140P) plasmid.

(A)

AGGGAGGCGGAAGCGGACGTCGTCTTTGAAATCCGCCAAGAACGGCGCCGGCGTGAAGAAAA
AAGTCAGGGCCTTGATCAGTCTGATTGCGGCGTTAGCGGTAGATCACGTTATCGGCATGGAA
AACGCCATGCCGTGGAACCTGCCTGCCGATCTCGCCTGGTTTAAACGCAACACCTTAAATAAA
CCCGTGATTATGGGCCGCCATACCTGGGAATCAATCGGTTCGTCCGTTGCCAGGACGCAAAAAT
ATTATCCTCAGCAGTCAACCGAGTACGGACGATCGCGTAACTGGGTGAAGTCGGTGGATGA
AGCCATCGCTGCGTGTGGTGACGTACCAGAAATCATGGTGATTGGCGGCGGTTCGCGTTTATG
AACAGTTCTTGCCAAAAGCGCAAAAAGTGTATCTGACGCATATCGACGCACAAGTGAAGGC
GACACCCATTTCCCGGATTACGAGCCGGATGACTGGGAATCGGTATTCAGCGAACCCACGAT
GCTGATGCGCAGAACTCTCACAGCTATTGCTTTGAGATTCTGGAGCGGCGAGGTAAGCCTAT
CCCTAACCTCTCCTCGGTCTCGATTCTACGTAACCCGGGGATCTTGAAGTTCCTATTCCGAA
GTTCTATTCTCTAGAAAGTATAGGAACTTCAGAGCGCTTTTGAAGCTGCGGATATCTCTAA
TTCCCATGTCAGCCGTTAAGTTATCTATCTATCGATCGACC

(B)

GGACGTCGTCTTTGAATCCGCCAAGAACGGCGCCGGCGTGAAGAAAAAAGTCAGGGCCTTGA
TCAGTCTGATTGCGGCGTTAGCGGTAGATCACGTTATCGGCATGGAAAACGCCATGCCGTGG
AACCTGCCTGCCGATCTCGCCTGGTTTAAACGCAACACCTTAAATAAACCCGTGATTATGGGC
CGCCATACCTGGGAATCAATCGGTTCGTCCGTTGCCAGGACGCAAAAATATTATCCTCAGCAGT
CAACCGAGTACGGACGATCGCGTAACTGGGTGAAGTCGGTGGATGAAGCCATCGCTGCGTG
TGGTGACGTACCAGAAATCATGGTGATTGGCGGCGGTTCGCGTTTATGAACAGTTCTTGCCAA
AAGCGCAAAAAGTGTATCTGACGCATATCGACGCAGAAGTGAAGGCGACACCCATTTCCCG
GATTACGAGCCGGATGACTGGGAATCGGTATTCAGCGAACCCACGATGCTGATGCGCAGAA
CTCTCACAGCTATTGCTTTGAGATTCTGGAGCGGCGAGGTAAGCCTATCCCTAACCTCTCCT
CGGTCTCGATTCTACGTAACCCGGGGATCTTGAAGTTCCTATTCCGAAGTTCCTATTCTCTAG
AAAGTATAGGAACTTCAGAGCGCTTTTGAAGCTGCGGATATCGCTATTCCCATGTCAGCCGT
TAAGTTATCTATCTATCGATCGACCGTGAGGGTGGGAGAAAGGTAGAAAGAGTGGAGGAGAT
TGATTAACAAACGACATGGTGTACGATTTGTTTCTTCTCCACGGGTAAGTTTTTTTAAAA
GGCTCTCTCGACTCTTTCTCGCTTTCTCCCCCTCACGTCGGATCG

(C)

```
ACGTCGTCTTTGAATCCGCCAAGAACGGCGCCGGCGTGAAGAAAAAGTCAGGGCCTTGATC
AGTCTGATTGCGGCGTTAGCGGTAGATCACGTTATCGGCATGGAAAACGCCATGCCGTGGAA
CCTGCCTGCCGATCTCGCCTGGTTTAAACGCAACACCTTAAATAAACCCGTGATTATGGGCCG
CCATACCTGGGAATCAATCGGTCGTCCGTTGCCAGGACGCAAAAATATTATCCTCAGCAGTCA
ACCGAGTACGGACGATCGCGTAACGTGGGTGAAGTCGGTGGATGAAGCCATCGCTGCGTGTG
GTGACGTACCAGAAATCATGGTGATTGGCGGCGGTCGCGTTTATGAACAGTTCTTGCCAAAA
GCGCAAAAACGTGATCTGACGCATATCGACGCAGAAGTGGAAGGCGACACCCATTTCCCGGA
TTACGAGCCGGATGACTGGGAATCGGTATTCAGCGAACCCACGATGCTGATGCGCAGAACT
CTCACAGCTATTGCTTTGAGATTCTGGAGCGGCGAGGTAAGCCTATCCCTAACCCCTCCTCG
GTCTCGATTCTACGTAACCCGGGGATCTTGAAGTTCCTATTCCGAAGTTCCTATTCTCTAGAA
AGTATAGGAACTTCAGAGCGCTTTTGAAGCTGCGGATATCGCTATTCCCATGTCAGCCGTTA
AGTTATCTATCTATCGATCGACCGTGAGGGTGGGAGAAAAGGTAGAAAAGAGTGGAGGAGATTG
ATTAACAAACGACATGGTGTACGTATTTGTTTCTTCTCCACGGGTAAGTTTTTTTAAAAGG
CTCTCTCGACTCTTTCTCGCTTTCT
```

Figure 3.49 Sequence conformation of recombinant MCMV-pp28-F140P vector cultured with the different concentration of TMP. (A) In the absence of TMP, (B) at 50 μ M or (C) 100 μ M. PCR were performed on the recombinant viruses and two PCR reactions from each virus were sequenced. Black sequences: represent sequence homology to the pp28 protein; Green sequences: represent sequence homology to the ecDHFR (F140P); Orange sequences: homology to V5 tag; Blue sequences: represent sequence homology to the pOriFRT(wt)-ecDHFR(F140P) plasmid.

3.2.4.2 Dynamics of pp150 or pp28 stability impacting on virus replication were analysed during infection

As we detailed above (Section 1.1.6.3), one advantage of using DD strategy is the ability of a ligand to stabilize the DD protein restoring their biological function in a rapid, reversible and dose dependent manner (Banaszynski *et al.*, 2006; Iwamoto *et al.*, 2010). It has been shown that DHFR systems are reversible (Glaß *et al.*, 2009), to determine whether ecDHFR similarly has this characteristic, we tested reversibility of ecDHFR(F140P)-pp150/pp28 in response to TMP. We tested whether fused tegument proteins with ecDHFR could be reversed through withdrawal or adding of TMP. Although not the focus of this thesis, this would provide a tool for loss as well as gain of function experiments for pp150 and pp28 in future studies beyond the scope of this thesis.

A schematic of the experiment is shown in Figures 3.50-3.51. Briefly, MEFs were infected with recombinant MCMV-pp150-F140P, MCMV-pp28-F140P or MCMV-WT each in four separate cultures: two were maintained in the presence of 50 or 100 μ M TMP for MCMV-pp150-F140P and MCMV-pp28-F140P, respectively; and the other two were maintained in the absence of TMP. All cells were then cultured for four days at 37°C. On day four post-infection the cells that were cultivated in the presence of TMP were then either maintained with TMP (by adding fresh TMP), or withdrew from TMP (by removal of TMP-containing media, washing monolayers with DPBS and then adding fresh DMEM media without TMP). All cells were then cultured for 6 hr at 37°C (Figure 3.50). While the infected MEF cells cultivated in the absence of TMP were then either maintained in the absence of TMP by adding fresh media (as a positive control) or cultured in the presence of TMP (50 μ M) for 6 hr at 37°C (Figure 3.51).

To obtain a more quantitative assessment we examined the viral growth by titration of progeny virus before (harvesting supernatant only) and after adding of TMP for 6 hr (supernatant and cell associated virus were harvested). Infectious culture supernatants were collected at day 4 post infection and the titres of cell-free viruses were determined by TCID₅₀ assay in the presence of 50 µM or 100 µM TMP (for culture of recombinant MCMV-pp150 or MCMV-pp28, respectively). As expected, the titres of the MCMV-WT virus were the same regardless to add/withdrawal of TMP for 6 h. No significant difference was seen ($P>0.05$), (Figures 3.52 and 3.53A).

When TMP was withdrawn from the cells infected with MCMV-pp150-F140P initially cultured with TMP for 4 days, the virus titre decreased compared to the virus that was continuously kept with TMP. Statistical analysis using Tukey`s multiple comparison test revealed a significant difference ($P<0.00308$) between the titres (Figure 3.52 B). However, when the TMP was added to the cells kept initially without TMP, virus replication was increased compared to the viruses grown in the continuous absence of TMP. Statistical analysis revealed significant difference between them ($P<0.00417$); (Figure 3.53 B).

In contrast, when cells infected with MCMV-pp28-F140P for 4 days in the presence of TMP were studied, withdrawal of TMP from MCMV-pp28-F140P infected cells made the virus titre significantly decrease ($P<0.001$) compared to the virus grown in the continuous presence of TMP (Figure 3.52 C) indicating rapid degradation of pp28. However, when we added TMP to infected cells kept initially without TMP, the virus titre increased significantly ($P<0.0018$) compared to the virus grown in the continuous absence of TMP (Figure 3.53 C), indicating rapid stabilization of pp28 protein by TMP.

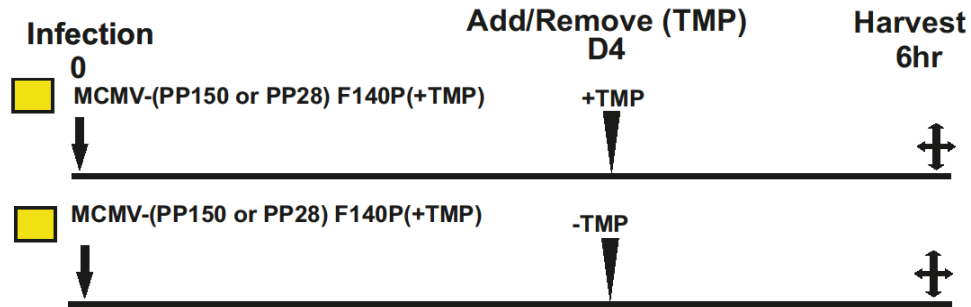


Figure 3.50 Schematic illustration of the pp150 or pp28 stability during infection in the presence of TMP. MEF cells were infected with MCMV-pp150-F140P or MCMV-pp28-F140P viruses at MOI of 0.01 PFU/cell and cultivated in the presence of TMP. At day four post infection the supernatants were collected (0 hr) and infected cells cultured for 6 hours in the presence or absence of TMP (6 hr +/- TMP).

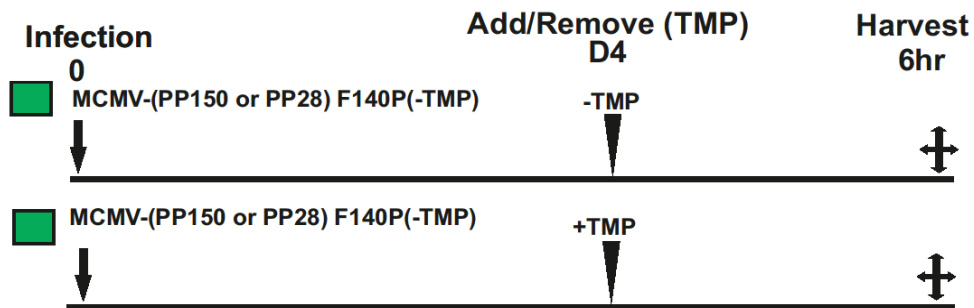
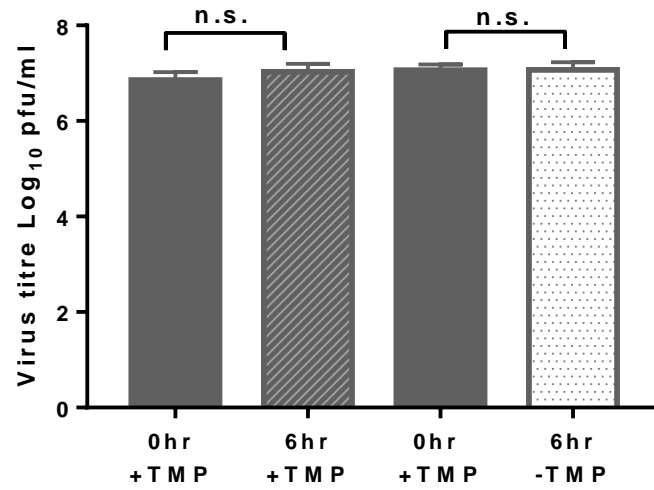
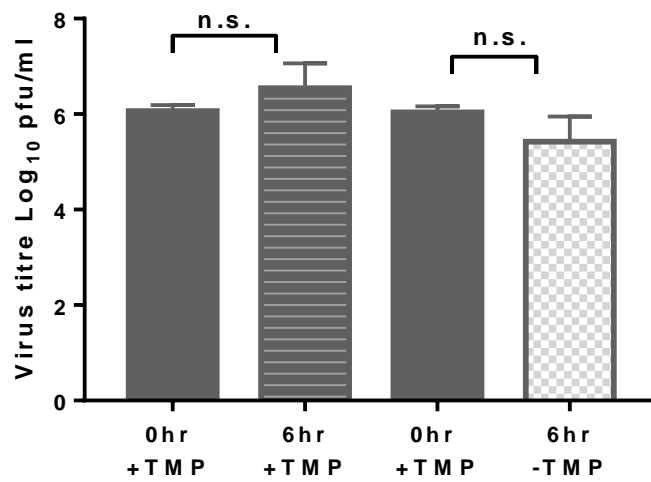


Figure 3.51 Schematic illustration of the pp150 or pp28 stability during infection in the absence of TMP. MEF cells were infected with MCMV-pp150-F140P or MCMV-pp28-F140P virus at MOI of 0.01 PFU/cell and cultivated in the absence of TMP. At day four post infection the supernatants were collected (0 hr) and infected cells cultured for 6 hours in the presence or absence of TMP (6 hr +/- TMP).

(A) MCMV-WT



(B) MCMV-pp150-F140P



(C)MCMV-pp28-F140P

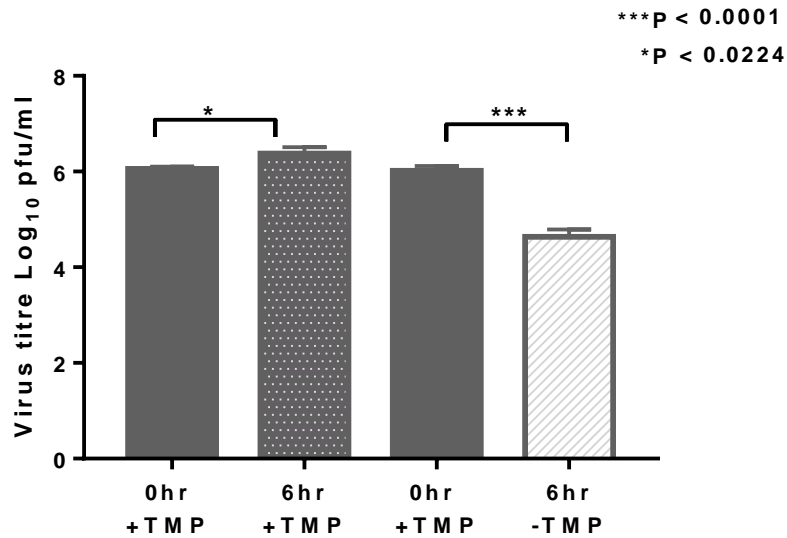
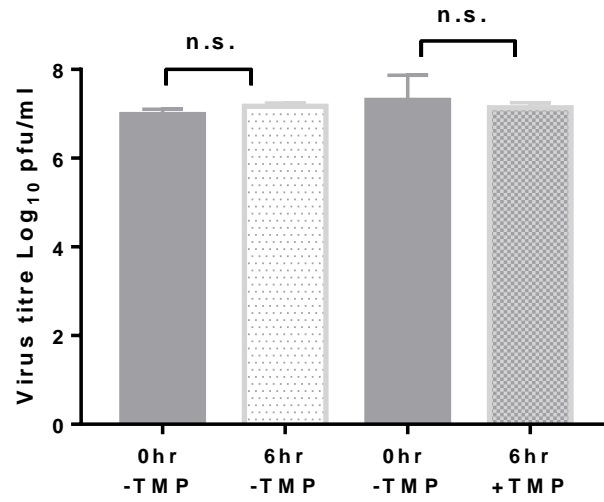
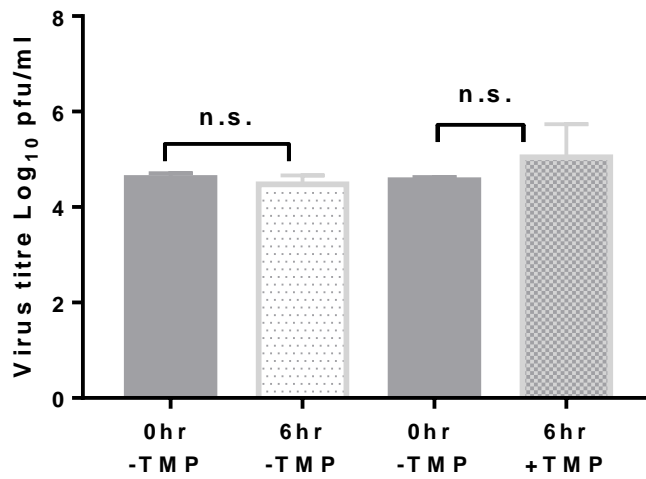


Figure 3.52 Dynamics of pp150 or pp28 stability were analysed during infection in the presence of TMP. MEF cells were infected with the (A) MCMV-WT, (B) MCMV-pp150-F140P or (C) MCMV-pp28-F140P at MOI of 0.01 PFU/cell and cultivated in the presence of TMP for four days. At day four post infection the supernatants were collected (0 hr) and infected cells cultured for 6 hours in the presence or absence of TMP. Supernatants and cell associated virus were collected (6 hr +/-) and analysed for the presence of virus by TCID₅₀ assay on MEF cells kept with TMP. Virus titres were determined in triplicate. Statistical significance determined using a one way of variance (ANOVA) and Tukey's multiple comparison test.

(A) MCMV-WT



(B) MCMV-pp150-F140P



(C) MCMV-pp28-F140P

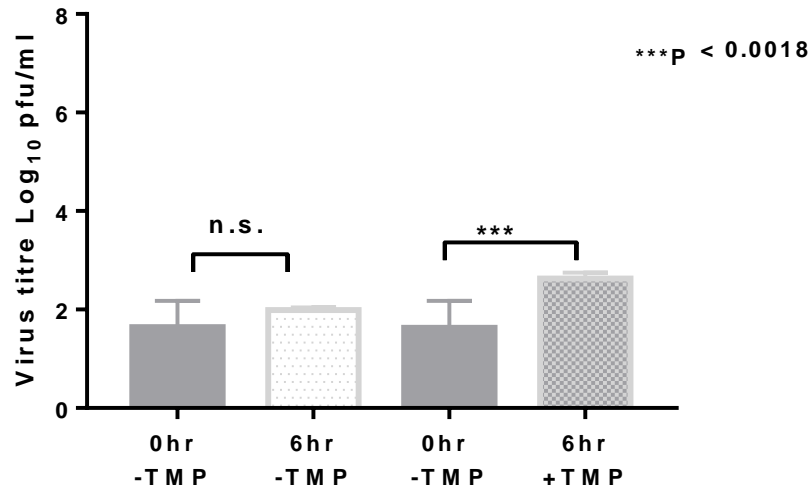


Figure 3.53 Dynamics of pp150 or pp28 stability were analysed during infection in the absence of TMP. MEF cells were infected with the (A) MCMV-WT (B) MCMV-pp150-F140P or (C) MCMV-pp28-F140P at MOI of 0.01 PFU/cell and cultivated in the absence of TMP for four days. At day four post infection the supernatants were collected (0hr) and infected cells cultured for 6 hours in the presence or absence of TMP. Supernatants and cell associated virus (6 hr +/- TMP) were collected and analysed for the presence of virus by TCID₅₀ assay on MEF cells kept with TMP. Virus titres were determined in triplicate. Statistical significance determined using a one way of variance (ANOVA) and Tukey's multiple comparison test.

3.2.4.3 Characterisation of the recombinant MCMV-pp150/pp28-F140P viruses phenotypes

The data shown in (Figures 3.44 and 3.45), revealed difference growth profiles between the viruses when cultured in relative to the concentration of TMP. These difference was most apparent at a concentration of 50 μ M TMP for recombinant MCMV-pp150-F140P; Figure 3.44) or at a concentration of 100 μ M TMP for MCMV-pp28-F140P virus Figure 3.45). As virus progeny production was measured at only a single time point (day 4 pi), it is possible that this difference reflected only a kinetic delay in replication of the virus under restrictive (-TMP) conditions. To determine whether destabilization of pp150 or pp28 influences virus growth, we compared the growth of two recombinant viruses (MCMV-pp150-F140P and MCMV-pp28-F140P) viruses with their parental wild-type (MCMV-WT). Time courses of production of extracellular infectious virions were examined in the presence or absence of TMP at low MOI (0.01PFU/cell; multi step growth curve). At low MOI, multiple rounds of replication of virus can take place, since not all cells are infected at the same time of inoculation. When cells are not exposed to large numbers of viral particles, this enables examination of virus dissemination in terms of features, such as plaque size or production of secondary plaques in an individual cell monolayer that gets infected. Using multi step growth curve amplifies effects of attenuation enabling more subtle effects to be seen the virus is moving through multiple replication cycles instead of just one.

The growth rates of the constructed viruses as well as the wild-type virus were studied on MEF cells (Section 2.6.2.8). Monolayers of MEF cells were infected with the recombinant viruses or parental virus at MOI (0.01 PFU/cell) in triplicate in the presence or absence of TMP. In order to maintain the concentration of the TMP at a desired concentration in the infected monolayer, TMP was added every 24 hr (by adding TMP to the media). Following incubation of the MEFs with respective viral progeny for two hours, the supernatant was

harvested and fresh medium with the TMP was added. The supernatant that had been harvested after 2 hours of infection, represent day 0. The titres of the virus were determined on day (0, 1, 2, 3, 4, and day 5) post infection. Virus progeny in cell culture supernatants was quantified by the TCID₅₀ assay on MEF cells (Section 2.6.2.6) in the presence of desired concentration of TMP. The growth rates of all viruses were performed and assayed in triplicate.

3.2.4.3.1 Mutant MCMV-pp150F140P has wild-type properties in MEF fibroblast cells in the presence of TMP, but shows intermediate attenuated growth in the absence of TMP

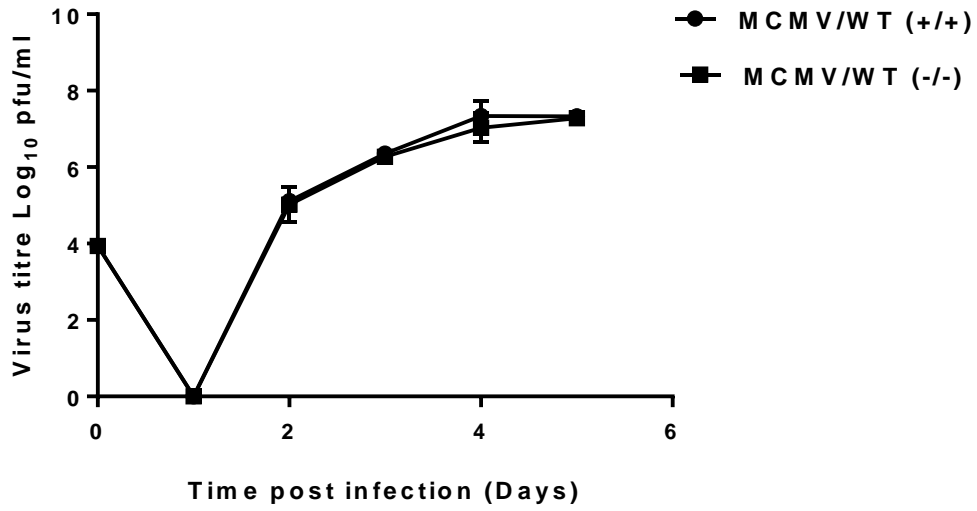
Wild-type MCMV was first tested with respect to growth on MEF cells in the presence of (50 μ M) or absence of TMP. As we expected (Figures 3.54-3.55 A) and consistent with previous data (Figures 3.52-3.53), the results demonstrate that the growth of MCMV-WT was similar regardless of whether TMP was present or absent. Replication kinetics of MCMV-WT were similar, virus (cultured with or without TMP) was first detected in cell culture supernatant on day 2 post infection and then reaching the maximum yield of $\sim 10^7$ PFU/cell on day 5 post infection. Statistical analysis using t-test showed that there were no significant differences between yield of the wild type virus that cultured in the presence or absence of TMP at any time point ($P= 0.9928$). No significant differences between the MCMV-WT yields in the presence or absence of TMP were identified from 2 to 5 days post infection ($P>0.05$).

Next, we compared the growth kinetics of recombinant MCMV-pp150-F140P to the MCMV-WT in the presence of TMP (Figure 3.54 B). Virus yields were first detected on day 2 post infection (approximately 10^3 PFU/cell), they then increased rapidly reaching the maximum level of ($\sim 10^6$ PFU/cell) on day 5 post infection. Data demonstrated that the growth rate of mutant MCMV virus in the presence of TMP was similar to that of the parental MCMV-WT

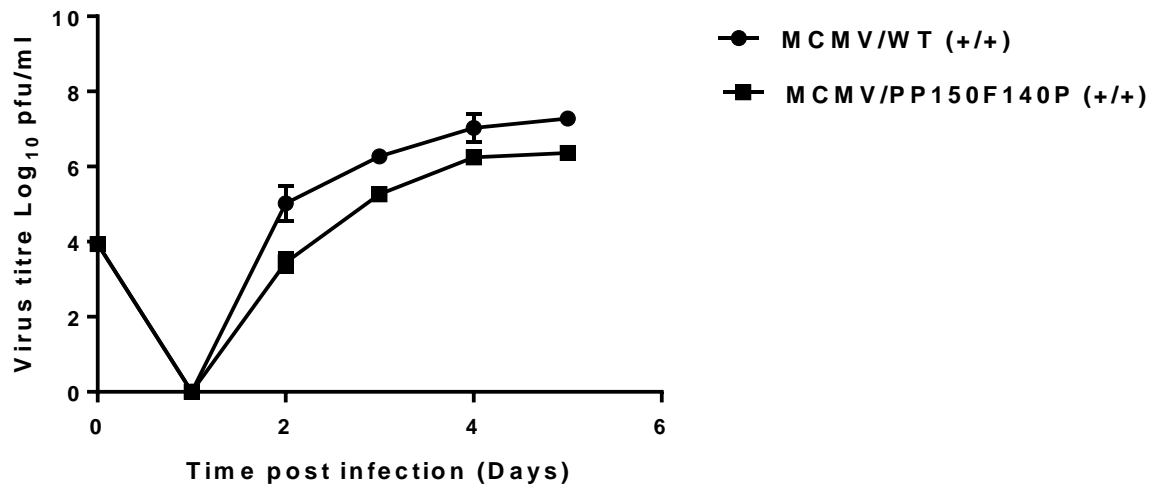
viruses at most time points, only a difference in the range of one log unit compared to parental WT was detected. Although statistical analysis showed no significant difference between yields of these two viruses from day 2 to 5 post infection ($P=0.8442$), the virus titre trended towards a decreased level. Thus the growth rate of recombinant virus on MEF cells in the presence of TMP was comparable to parental MCMV-WT confirming TMP-treatment restored the growth of mutant virus to wild-type level (Figure 3.54 B).

Next we compared the growth kinetics of recombinant MCMV-pp150-F140P in the presence or absence of TMP. Replication of mutant virus that grew in MEF cells without TMP was similar to that of the virus that grew in the presence of TMP (Figure 3.54 C). Initially, the yield of the virus (kept without TMP) on day 2 was only slightly lower than that kept with TMP, yields reached maximum of $\sim 10^4$ PFU/cell on day 5 without TMP compared to the virus titre of $\sim 10^6$ PFU/cell on day 5 for the virus kept with TMP (Figure 3.54 C). A difference in the range of two log units between the presence and absence of TMP was detected. In the absence of TMP, virus replication was diminished compared to the virus that grew in the presence of TMP. Statistical analysis using t-test revealed that there were no significant difference between them ($P=0.7804$). As a complement to the studies described above, although the F140P domain enables regulated stability of pp150 ORF, the F140P domain tag inhibits some aspect of replication of mutant MCMV we saw a little effect of TMP, suggesting a level of destabilization of the pp150 in an intermediate attenuated replication phenotype of the virus. Taken together, these results showed that in the presence of ligand TMP, the growth of recombinant MCMV-pp150-F140P was comparable to the parental MCMV-WT; the mutant shows wild-type properties in MEF fibroblast cells. While in the absence of TMP, we saw some aspect of intermediate attenuation phenotype of the MCMV-pp150-F140P compare to the parental MCMV-WT virus.

(A)



(B)



(C)

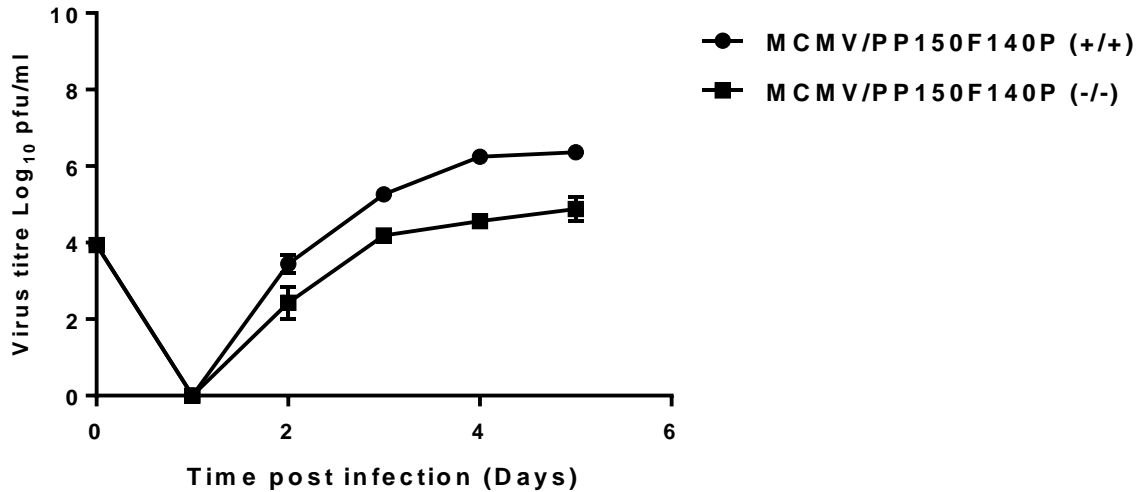


Figure 3.54 Replication of recombinant MCMV-pp150-F140P viruses in the presence or absence of TMP. Compare the (A) MCMV-WT in the presence or absence of TMP, (B) MCMV-pp150-F140P to the MCMV-WT in the presence of TMP and (C) MCMV-pp150-F140P in the presence and absence of TMP. MEF cells were infected with the MCMV-pp150F140P mutant virus at an MOI of 0.01 PFU/cell and cultivated with 100 μ M TMP or without TMP, at the time points indicated. Supernatants and cell associated virus were collected and analysed for the presence of virus by TCID₅₀ assay on MEF cells kept with 100 μ l TMP. (+), cells infected in the presence of TMP; (-), cells infected in the absence of TMP. Results are the mean \pm standard deviation (SD) of two experiments three replicates in each. Error bars representing the SD. Some of the SD are so small that the error bars are hidden behind the symbols representing the data points.

3.2.4.3.2 Recombinant MCMV-pp28-F140P growth properties in MEF fibroblast cells in the presence or absence of TMP

As explained above (Section 3.2.5), multiple growth curves were performed to compare the growth kinetics of recombinant MCMV-pp28-F140P to the MCMV-WT in the presence (100 μ M) or absence of the TMP using TCID₅₀ for the virus titration. As shown in (Figure 3.55 B) the data demonstrated that in the presence of TMP, the replication kinetics of recombinant MCMV-pp28-F140P was 2-logs down compare to that of MCMV-WT. Recombinant virus was first detected in cell culture supernatant on day 2 post infection and reached maximum levels on day 5 post infection. Maximum yields of the MCMV-pp28-F140P were $\sim 10^6$ PFU/cell compare to $\sim 10^7$ PFU/cell for MCMV-WT. Although the growth rate of the mutant was down 2 log compared to the parental virus, statistical analysis revealed that no significant difference was identified between yields of the two virus from day 2 to day 5 post infection ($P > 0.05$). Thus the growth rate of recombinant virus on MEF cells in the presence of TMP was comparable to parental MCMV-WT; there were no significant difference between them, confirming TMP-treatment restored the growth of mutant virus to wild-type level (Figure 3.55 B).

Next, we examined the multi-step growth kinetics of MCMV-pp28-F140P in the absence of TMP compared to the titre of the virus that grew in the presence of TMP. It was noticed that at day 3 and later post infection, in the absence of TMP, MCMV-pp28-F140P started to produce a low level of virus in the absence of TMP. It appeared these viruses may not establish a second round of infection because their titre did not increased over time (Figure 3.55 B). The titre of the virus reached maximum levels on day 5 post infection (less than 10^2 PFU/cell), while MCMV-pp-28-F140P in the presence of TMP reached maximum titres $\sim 10^5$ PFU/cell on day 5 post infection. Statistical analysis revealed that there were significant differences between the virus titre achieved in the presence or absence of TMP ($P < 0.0001$).

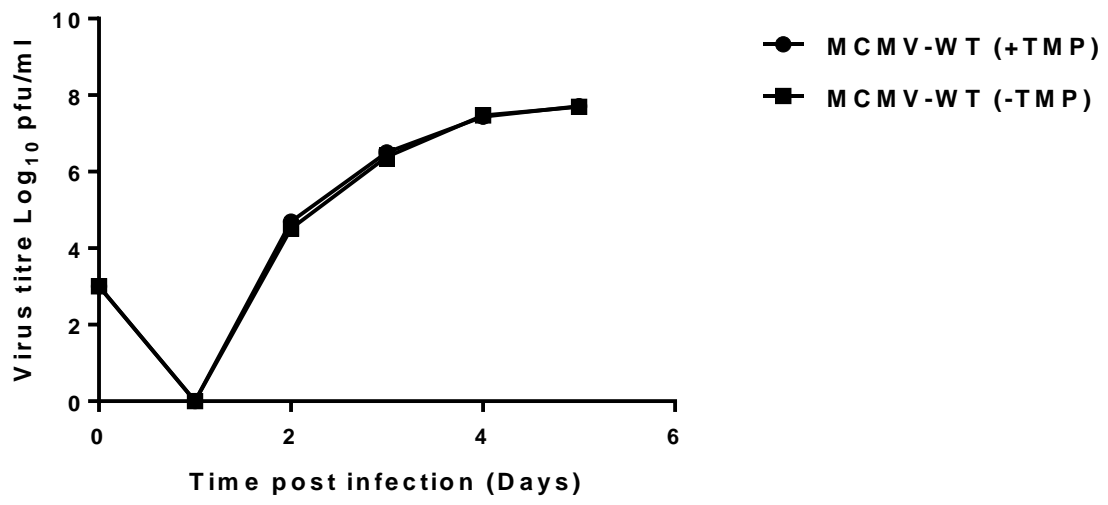
In addition to the TCID₅₀, another way to quantify viral titre is by performing plaque assay. Both of these assays depend on the ability to detect visible CPE on the infected cells *in vitro*. However, plaque assay is one of the most accurate and sensitive methods for the direct quantification of a virus via counting of the number of plaques in cell culture (Baer & Kehn-Hall, 2014; Dulbecco, 1952). In order to quantify the number of MCMV-pp28-F140P virus particles that grew in the absence of TMP in growth kinetics assay, plaques counts were determined by plaque assay to increase accuracy of the assay (see Section 2.6.2.7).

As explained above (Section 3.2.5), multiple growth curves were performed to compare the growth kinetics of recombinant viruses to the MCMV-WT in the presence (100 µM) or absence of TMP using plaque assay for the virus titration. As shown in (Figure 3.55 A) and consistent with previous data (Figure 3.54 A), there is no significant difference between MCMV-WT cultured in the presence or absence of TMP (P= 0.99; Figure 3.56 A). When recombinant MCMV-pp28-F140P virus compared to MCMV-WT in the presence of TMP, again the replication kinetics of recombinant MCMV-pp28-F140P were such that 2-logs down compared to MCMV-WT. Recombinant virus was first detected in cell culture supernatant on day 2 post infections and reached maximum levels on day 5 post infections. Maximum yields of the MCMV-pp28-F140P were $\sim 10^6$ PFU/cell compare to the MCMV-WT which was $\sim 10^7$ PFU/cell. Although the growth rate of mutant were down 1 log compared to the parental virus, however statistical analysis revealed that no significant difference were identified between yields of the two virus from day 2 to day 5 post infection (P=0.393). Thus the growth rate of recombinant virus on MEF cells in the presence of TMP was comparable to parental MCMV-WT; there were no significant difference between them, confirming TMP-treatment restored the growth of mutant virus to wild-type level (Figure 3. 55 B).

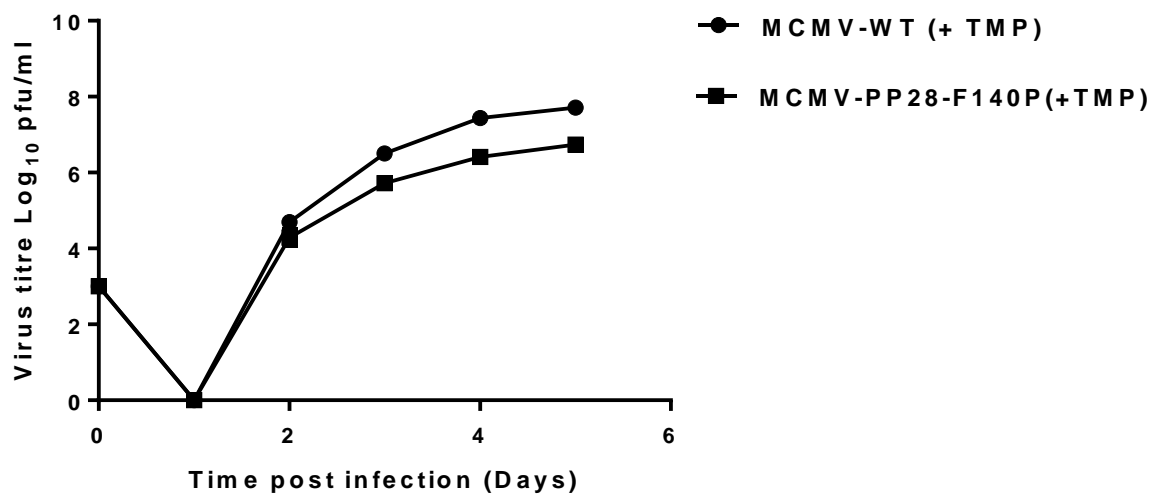
Next, we compared the multi-step growth kinetics of MCMV-pp28-F140P in the absence of TMP compared to the titre of the virus that grew in the presence of TMP. It was noticed that at day 3 and later post infection, MCMV-pp28-F140P started to produce a low level of virus even in the absence of TMP (approximately 88.2×10^{-1} PFU/cell). These viruses appeared not to establish a second round of infection because their titre did not increase over time (Figure 3.55 C). The titre of the virus reached maximum levels on day 5 post infection ($8.96 \times 10^{+1}$ PFU/cell), while MCMV-pp-28-F140P in the presence of TMP reached maximum titres $\sim 10^6$ PFU/cell on day 5 post infection. Statistical analysis revealed that there were significant differences between the virus titre achieved in the presence or absence of TMP ($P < 0.0001$). The level of the virus that was detected by plaque assay was consistent with the results from the TCID₅₀ assay (Figure 3.56).

Taken together, these results revealed that the growth rate of MCMV-pp28-F140P virus in the absence of TMP was slower than of the recombinant virus that grew in the presence of TMP at most time points. Using TCID₅₀ and plaque assay to assess virus titres, data indicated that there was a significant difference between the viruses when cultured in the presence or absence of TMP with respect to growth in MEF cells (Figures 3.55-3.56). As a complement to the studies described above, the F140P domain regulated stability of pp28 ORF, the F140P domain tag inhibits replication of recombinant MCMV-pp28, suggesting a complete destabilization of the PP28 and a complete attenuated replication phenotype of the virus.

(A)



(B)



(C)

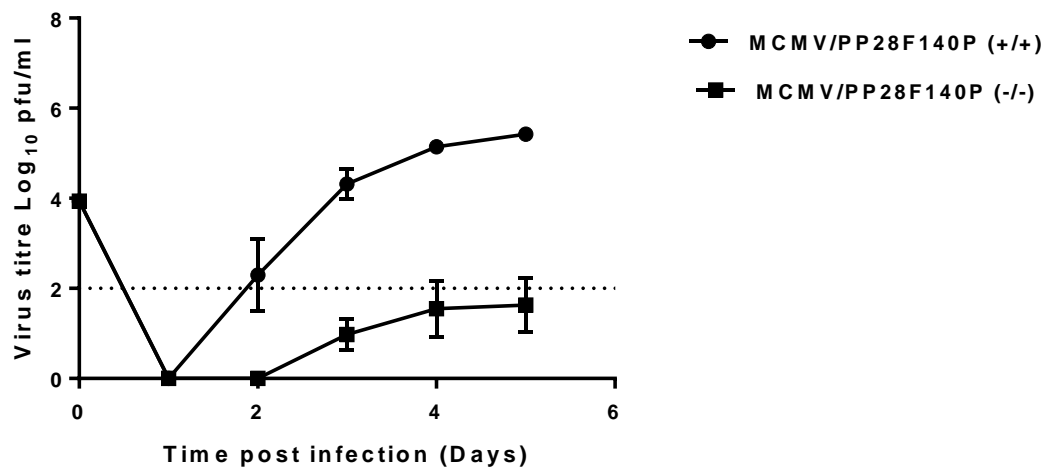
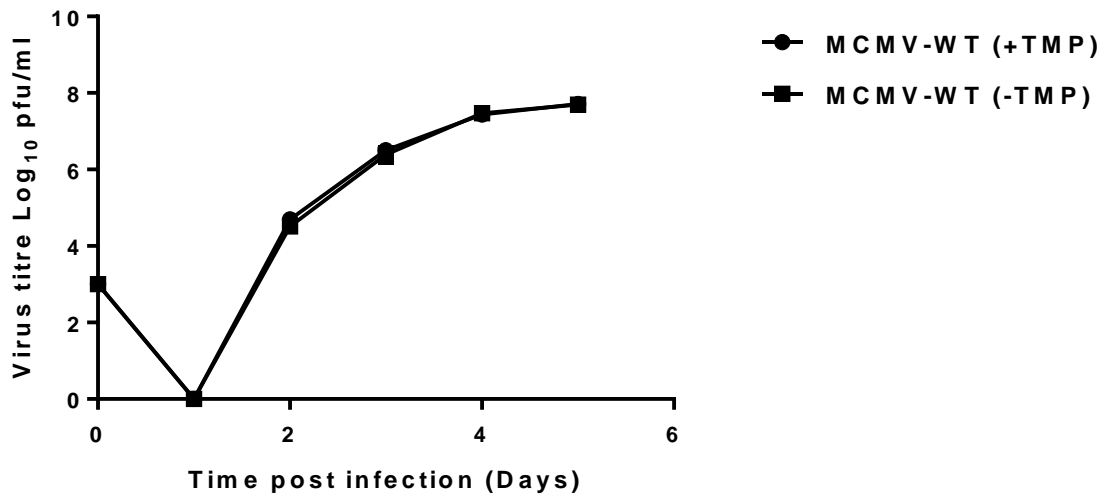
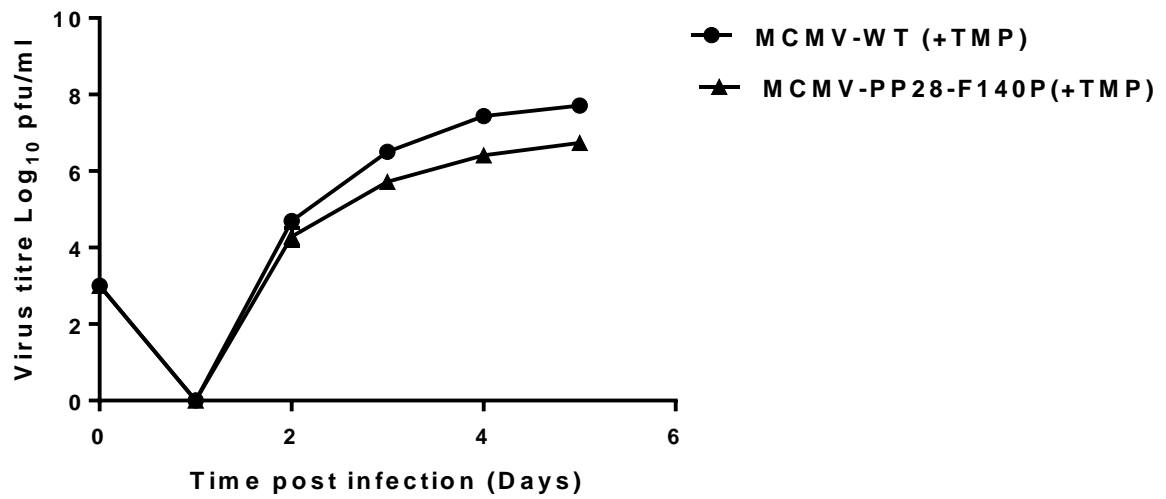


Figure 3.55 Replication of recombinant MCMV-pp28-F140P virus compared to its parental MCMV-WT virus in the presence or absence of TMP. MEF cells were infected with the MCMV-pp28F140P mutant or parental virus at an MOI of 0.01 PFU/cell and cultivated with 100 μ M TMP (A) or without TMP (B), at the time points indicated. Supernatants were collected and analysed for the presence of virus by TCID₅₀ assay on MEF cells kept with 100 μ l TMP. (+), cells infected in the presence of TMP; (-), cells infected in the absence of TMP. Results are the mean \pm standard deviation (SD) of two experiments three replicates in each. Error bars representing the SD. Some of the SDs are so small that the error bars are hidden behind the symbols representing the data points. Dashed lines mark the detection limit of the assay.

(A)



(B)



(C)

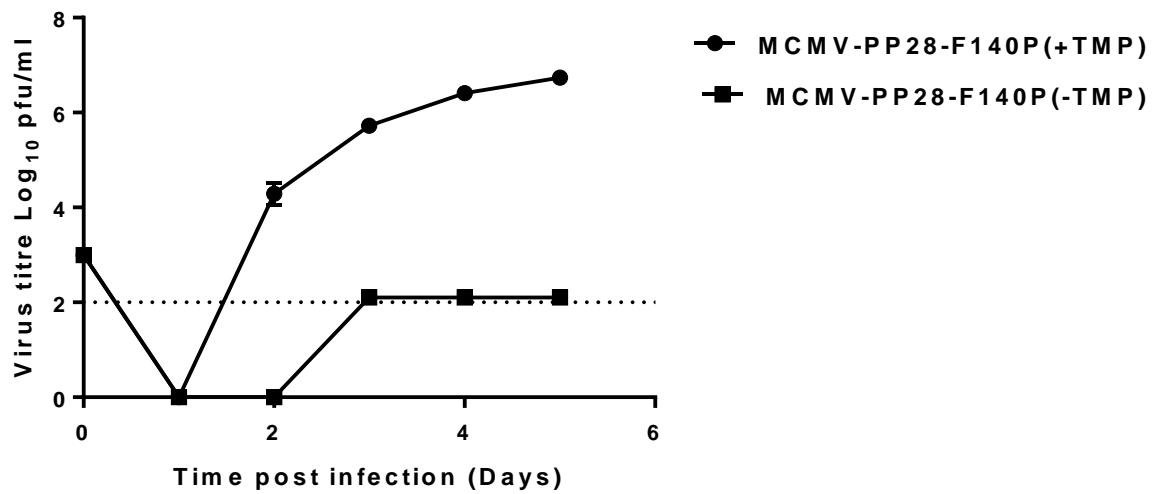


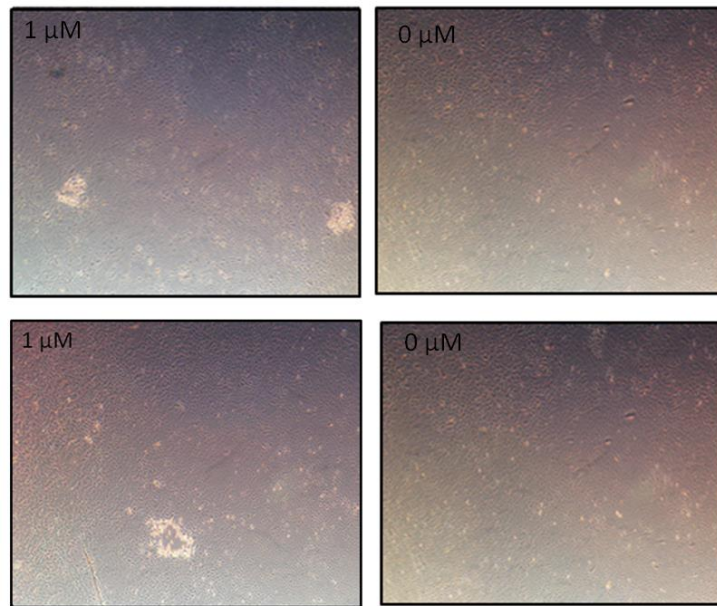
Figure 3.56 Replication of recombinant MCMV-pp28-F140P virus compared to its parental MCMV-WT virus in the presence or absence of TMP using standard plaque assay. MEF cells were infected with the MCMV-pp28-F140P mutant or parental virus at an MOI of 0.01 PFU/cell and cultivated with 100 μ M TMP or without TMP, at the time points indicated. Supernatants were collected and analysed for the presence of virus by standard plaque assay on MEF cells kept with 100 μ M TMP. (+), cells infected in the presence of TMP; (-), cells infected in the absence of TMP. Results are the mean \pm standard deviation (SD) of two experiments three replicates in each. Error bars representing the SD. Some of the SD is so small that the error bars are hidden behind the symbols representing the data points. Dashed lines mark the detection limit of the assay.

3.2.4.4 Recombinant MCMV-pp28-F140P that grew in the MEF cells in the absence of TMP could not cause secondary infection

After cultivation of the infected MEFs with recombinant MCMV-pp28-F140P virus without TMP a few minifoci became detectable, which did not develop into plaques as described in (Section 3.2.4.1; Figure 3.43). In the absence of TMP the recombinant MCMV-pp28-F140P virus produced almost no virus (approximately 10^1 PFU/cell) by day four post infection and a very low level of progeny while in the presence of TMP the recombinant virus reached peak titre of (1.96×10^6 PFU/cell) and restored the growth of the virus to wild-type level (Figure 3.45) only (2-logs below). The next step was to examine the secondary infection of a few viruses that were detectable in the absence of TMP. To determine whether growth of virus was due to the leakiness of the TMP degradation or represented escape mutants (i.e. whether the virus had the ability to cause secondary infection in MEF cells or not). When infected MEFs were cultured with minimum amount of ligand (1 μ M), we observed plaque formation at lowered levels by mutant MCMV-pp28 virus, consistent with stabilization of the MCMV-Protein requiring 1 μ M TMP (Figure 3.45).

In contrast, when the mutant viruses were cultured in the absence of TMP for 5 days, almost no viral progeny were produced. Following the third passage of infection we were unable to detect any viral progeny even in the presence of minimal amount of TMP (Table 3.10). Taken together, these data indicate that those few viruses that grew in the absence of TMP, are unable to produce secondary infection and they grew only with TMP. These data suggested that these viruses were not escape mutants and TMP regulation allows for tight control of the pp28 function during the virus replication cycle.

Day 4 post infection



Day five post infection

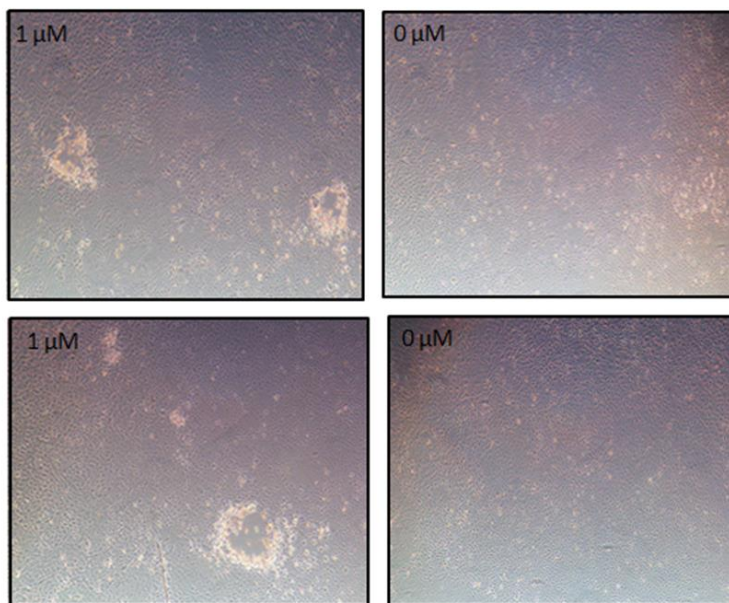


Figure 3.50 Secondary infection of the recombinant MCMV-pp28-F140P in the absence of TMP. MEF cells were infected with the MCMV-pp28-F140P mutant virus at an MOI of 0.01 PFU/cell and cultivated in the absence of TMP. At day four post infection the supernatants were collected and new MEFs were infected with 1 ml supernatant in the presence (1 μ M) or in the absence of TMP (0 μ M). Images of infected cells were taken at day four and five post infection, depicting plaque formation by mutant MCMV under different concentration of TMP.

Table 3.10 Mean plaque counts of mutant MCMV-pp28-F140P virus in the presence or absence of TMP. Summarizing total counts from two independent experiments

MCMV-pp28-F140P virus	Plaque numbers	
	(1 μ M TMP)	(0 μ M TMP)
Passage one	23	0
Passage two	15	0
Passage three	0	0

3.3 Discussion

Vaccination is perhaps one of the most important innovations in medical science and public health in history, since it has the ability to substantially reduce morbidity and mortality caused by infectious diseases. All current vaccines rely on the ability to elicit a host immune response that protects against microbial disease. As we described previously (Section 1.1.6), vectored vaccines are comprised of a carrier virus which has been modified to carry gene from the microbe being targeted. When the vector is given to the recipient, the antigen will be expressed and protective immune responses will be generated. CMV-based vectors are a promising addition to our arsenal of existing vaccines against infectious diseases. They are unique in the associated high level of immunity they induce against their heterologous encoded pathogen target antigen, as well as the duration of the immunity and its immediate effector T cell function. Although still in their early developmental phase, CMV-based vaccines are starting to become an attractive vaccine vector against different microbial pathogens via inducing protective immunity against encoded antigens (Hansen *et al.*, 2011; Jarvis *et al.*, 2013; Karrer *et al.*, 2004; Klyushnenkova *et al.*, 2012; Marzi *et al.*, 2016; Redwood *et al.*, 2005; Tierney *et al.*, 2012; Tsuda *et al.*, 2011; Tsuda *et al.*, 2015).

A fundamental problem associated with the clinical application of CMV vaccine vectors is their replication-competent nature (Skenderi & Jonjić, 2012). CMV is generally benign and asymptomatic in immunocompetent individuals, but can cause severe disease in individuals whose immune systems are immature or weakened, including: neonates, patients with human immunodeficiency virus infection/Acquired Immunodeficiency Syndrome (HIV/AIDS), individuals receiving immunosuppressive therapy or chemotherapeutic agents, organ transplant and bone marrow transplant recipients and pregnant women (Corona-Nakamura *et al.*, 2013).

Interestingly, previous studies have indicated that CMV replication is not required for induction of the characteristic immune response associated with CMV infection (Snyder *et al.*, 2011). Furthermore, replication-defective versions of CMV have been shown to maintain their immunogenicity at least in mouse studies (Mohr *et al.*, 2010). Replication-defective CMV vectors may therefore provide a means to enhance the safety profile of the CMV platform without affecting immunogenicity.

Replication-defective mutant viruses are specifically defective for one or more viral functions that are essential for viral genome replication or synthesis and assembly of progeny viral particles. The main advantages of the use of replication-defective viruses as vaccines are their high level of safety and ability to express viral antigens inside the infected cells. These antigens can be presented efficiently by MHC molecules with concomitant induction of immune responses, especially cell-mediated immunity (Nguyen *et al.*, 1992; (Morrison & Knipe, 1996; Nguyen, Knipe & Finberg, 1992). Although CMV is associated with disease, disease is very context specific with the virus only being harmful in individuals with an immature immune system; otherwise the virus is generally asymptomatic in the general population. However, given the potential for CMV to spread from vaccines to non-vaccinated individuals, efforts for attenuation of the CMV-based vaccine platform will be critical in an attempt to prevent or reduce any vaccine-associated morbidity in any population prone to CMV disease.

Although the high level of safety associated with replication-defective vaccines due to permanent deletion of essential genes is a main advantage of this method of attenuation, the requirement for cell lines expressing the missing viral gene product(s) to complement virus replication can prove problematic and, if not prohibitive, increases production costs. Cellular toxicity from expression of the *trans*-complementing viral gene can occur when expressed in isolation at levels necessary to fully complement virus replication. The production of stable

cell lines for viruses that require primary cells for growth and the requirement for expression at particular stages of the virus replication cycle may also be problematic for conventional complementation systems (Pan *et al.*, 2016). Cell lines to complement replication-defective herpesviruses are particularly difficult to obtain especially for β - and γ - subfamilies, since only a few complementing cell lines have been established, mainly because many of these viruses can be propagated only on primary cells (Borst *et al.*, 2008; Mocarski *et al.*, 1996; Silva *et al.*, 2003).

The main aim of the work detailed in this thesis was to develop the protein-destabilization strategy towards production of a conditional replication-defective version of a MCMV vaccine vector by targeting essential tegument proteins (pp150 and pp28). The tegument proteins of CMV are known to be essential and play important roles in all stages of the viral life cycle including viral entry, gene expression, immune evasion, assembly and egress (Kalejta, 2008). Many reports have demonstrated a crucial role for both pp150 and pp28 tegument proteins in virion assembly and morphogenesis. Pp150 plays an essential role in stabilizing nucleocapsid during virus maturation and directing their movement (AuCoin *et al.*, 2006; Tandon & Mocarski, 2008). Deletion of the pp150 leads to a complete loss of productive virus replication (Tandon & Mocarski, 2008). Pp28 is essential for virus replication due to its role in the secondary envelopment of virion in the cytoplasm (Britt *et al.*, 2004; Silva *et al.*, 2003). In the absence of pp28 tegument proteins, non-enveloped capsids accumulate in the cytoplasm of infected cells, late in infection (Silva *et al.*, 2003).

Since expression of the targeted antigen by CMV at L times appears to bias towards antibody responses, these two tegument proteins were also selected based on their L time of expression, as this would enable expression of any target antigen regulated with L kinetics. Use of a DD based on ecDHFR (Figure 3.1; (Banaszynski *et al.*, 2006; Iwamoto *et al.*, 2010) as opposed to FKBP made such a system suitable for development for use in LMICs due to the relative cost

of the TMP compared to Shield-1 stabilizing molecules. Importantly, the DD strategy was used for development of this complementation system for MCMV as it does not require the generation of complementing cell lines. In addition to L kinetics of expression, both pp150 and pp28 belong to the group of tegument proteins not glycoproteins, the latter of which consists of major targets for the neutralizing antibody response of HCMV. Finally, M32 encoding pp150 and M99 encoding pp28 of MCMV are the homologues of UL32 and UL99 of HCMV, which allows for potential translation into the human CMV platform. The pp150 and pp28 of MCMV were targeted and fused with DD separately in distinct MCMV vectors in parallel allowing for a direct parallel comparison.

CMV is highly species-specific, thus, the generation of vaccine strategies are dependent on animal model system to provide significant insight of host-pathogen interactions like immunity, infection routes and immune modulation *in vivo*. The use of MCMV in mice shares many similarities with HCMV infection in human and therefore serves an important biological model for vaccine development experiments (Armas *et al.*, 1996; Morello, Ye & Spector, 2002; Ye, Morello & Spector, 2002). Although analysis of immunogenicity induced by these conditionally attenuated MCMV vectors was not possible within this thesis, studies are ongoing in the Ebola virus mouse model using an identical strategy to the one developed in the current thesis. The aim of the *in vivo* studies will be to compare T cell immunity and efficacy induced by the conditionally attenuated MCMV Ebola vectors against those induced by the fully replicating version. Earlier studies have shown replication-defective MCMV based on permanent deletion of essential genes induce immune responses against endogenous MCMV proteins comparable to wild type virus, but these future studies will be the first to test immunity against a heterologous target antigen induced by such a replication-defective MCMV platform.

This study has been facilitated by the advances in mutagenesis of CMV that cloned and maintained the virus genome as a bacterial artificial chromosome (BACs) in *E. coli* (Dunn *et al.*, 2003; Messerle *et al.*, 1997; Wagner, Ruzsics & Koszinowski, 2002). This propagation of CMV as infectious BACs has made the genetics of the virus accessible to the tools of bacterial genetics (Messerle *et al.*, 1997). Other cloning strategies have been developed to genetically manipulate large herpesvirus genomes, including: yeast artificial chromosomes (YACs; (Burke, Carle & Olson, 1987), mammalian artificial chromosomes (MACs; (Harrington *et al.*, 1997), P1-derived artificial chromosomes (PACs; (Amemiya *et al.*, 1994), and cosmids (Collins & Hohn, 1978; Ish-Horowicz & Burke, 1981). However, these methods all present with limitations for cloning the large DNA genome of herpesviruses. YACs are amenable to cloning large DNA fragments even up to 1000 kb, but since they are propagated in yeast they are more prone to genetic rearrangement and generation of chimeric clones (Burke, Carle & Olson, 1987; Green *et al.*, 1991; Monaco & Larin, 1994). PACs and cosmids both have advantages of being bacterial based cloning vectors like BACs, but their ability for cloning large DNA genomes such as herpesviruses is limited with a carrying capacity of 100-300 and 35-45 kb, respectively (Amemiya *et al.*, 1994; Ish-Horowicz & Burke, 1981). Due to the unstable nature of repetitive sequence in herpesvirus genomes, BAC technology represented the best method of cloning. BACs are also able to maintain up to 300 kb of DNA stably in the bacterial host. In addition BACs encode an F-factor gene that maintain a single plasmid copy per bacterial cell so during propagation, limiting unprompted viral DNA recombination (Shizuya *et al.*, 1992).

Prior to the use of BAC-based technology, mutagenesis via homologous recombination of large CMV genomes within eukaryotic cells was a time-consuming task due to the slow replication of the virus in cell culture (Mocarski *et al.*, 1996). The advent of BAC technology allowed for easier mutation of the viral genome and the subsequent development of various

mutants that have helped shed light on viral gene functions in the context of infection. In addition to maintaining the viral genome as a BAC, simple and straightforward methods to generate CMV mutants are vital to characterise the viral functions of CMV leading to therapeutic and vaccine developments. In the current study, mutagenesis (insertion of ecDHFR domain) was performed in the MCMV BAC using E/T homologous recombination in *E. coli*, which is derived from bacteriophage λ . This system utilizes dsDNA ends as a substrate for the recombination reaction. The E/T system is comprised of three components: (i) Gam protein that protects dsDNA ends from degradation in bacteria (Sakaki *et al.*, 1973), (ii) Alpha protein, which is the 5'-3' exonuclease that generates 3' ssDNA overhangs (Kovall & Matthews, 1997), and (iii) Beta protein, which is the ssDNA binding protein that can bind and protect ssDNA from degradation (Wu *et al.*, 2006). These components of the E/T recombination system can be provided via use of *E. coli* bacteria (DY380 and its FLP-recombinase expressing derivative, EL250) containing a chromosomally encoded λ prophage. In this system, these three proteins are induced in a temperature-dependent manner (Lee *et al.*, 2001).

In order to insert the ecDHFR domain into the pp150 and pp28 of MCMV via homologous recombination, these domains must be cloned into a suitable plasmid (Figures 3.4, 3.5 & 3.12). To generate the recombinant viruses we constructed a plasmid vector where DD was cloned to the pOriFRT(wt) plasmid and placed next to Kan^R marker flanked by FRT-sites, to be able to select for transfer. The most widely used technique in molecular cloning is the use of restriction endonuclease enzymes. Cloning is a straightforward technique, whenever suitable restriction enzyme sites are available in sequence of both insert and vector DNA. PCR cloning has been widely used in biological engineering (Mead *et al.*, 1991; Mitchell, Ruggli & Tratschin, 1992). The first part of the cloning process consisted of a PCR amplification step. The primers used for amplification of these fragments contained a V5

epitope tag and recognition sites for single cutter restriction enzymes (single cutters target one restriction site only within the DNA sequence), which at a later stage would allow cloning each of the fragments to the desired vector. Furthermore, we identified the same unique restriction sites within the pOriFRT(wt) vector. According to this strategy, following PCR amplification the resultant PCR product could be digested with the respective enzymes and then cloned into the vectors which were similarly prepared by using the same restriction enzymes. This method worked well for amplifying the (E134G, Y100I and F140P) domain. There are a number of reasons for using the pOriFRT(wt) vector for these studies. First, this vector is known to be a vector amenable to genetic manipulation. Second, the pOriFRT(wt) vector contained the Kan^R gene flanked by FRT sites enabling removal of the marker by arabinose induction of the FLP-recombinase in the EL250 bacteria. Finally this plasmid contains a R6K γ origin of replication which only allows replication of plasmids that express the replication protein π , thereby avoiding false positive Kan^R BAC clones resulting from carry-over of the parental template used for generation of the recombination fragment by PCR.

Large oligonucleotides with a priming region homologous to a desired template plasmid that contained ecDHFR, the kan^R marker flanked by FRT sites and viral homologies to the targeted MCMV gene were used to amplify the recombination PCR fragments (Figures 3.19-3.21). Following amplification, the PCR fragment was then inserted by the flanking 60 bp viral homologies. This short homologous sequence required for the recombination is the major advantage of the R/T recombination system as it enables the homology targeting regions to be contained within a single DNA primer. In contrast, the other recombination system like the RecABCD require 2 kbp homologies on both sides for efficient homologous recombination, which requires preparatory cloning to assemble the necessary long homology domains within a single plasmid prior to use in recombination.

The Kan^R cassette was inserted to select for the relatively rare occurrence of double cross-over between the recombination fragment and the corresponding homologous viral sequences. The Kan^R gene was flanked by short 34 bp FRT-sites, which then enables removal by induction of FLP recombinase in the EL250 cells to remove the resistance marker (Cherepanov & Wackernagel, 1995; Figures 3.30-3.33). In this study, primers with a length of 75 to 80 nt were used for targeting of the E/T recombination system. Primers larger than 80 nt are costly and difficult to synthesise and also PCR amplification with long primers is difficult. Importantly, the primers used were HPLC purified as point mutations within the primer themselves resulting from inefficiency of the primer synthesis technology are a frequent source of inadvertent mutations during E/T recombination. Using this approach, the ecDHFR domain was fused into the viral genome, leaving a single FRT site along with flanking vector sequence for a total of 80 bp remaining after Kan^R marker excision. Previously, a similar strategy was used for fusion of the FKBP to other essential proteins of HCMV and MCMV (Glaß *et al.*, 2009). This strategy allowed the successful fusion of ecDHFR domain to the C- terminus of both pp150 and pp28 viral proteins in our study.

In order to confirm overall integrity of the mutated genome and the correct insertion of the ecDHFR domain sequence, The BAC DNA were analysed by restriction enzyme digestion (Figures 3.32-3.33) and Sanger sequencing (Figures 3.34-3.35). To analyse genomic integrity, the genomic pattern of the mutant BAC DNA was compared to the genomic pattern of the parental MCMV-WT. The most commonly used restriction digestion enzymes is EcoRI as upon agarose gel electrophoresis it produces evenly spaced fragments which are useful to detect any gross alteration of the viral genome (Paredes & Yu, 2012). The restriction enzyme method for confirmation of genomic integrity of the MCMV BAC DNA has been used widely by many studies. It is accepted as a definitive and reliable method for analysis of genomic integrity. Although comparison of the genomic integrity between the recombinant

virus and the parental MCMV BAC did not identify any gross genetic rearrangement, it is possible that more subtle genetic mutations could have occurred. As virus was able to be reconstituted from all BACs, any spontaneous small mutation is clearly in a region not critical for viral fitness. In this regard, NGS sequencing of the entire MCMV BAC genomes will need to be performed to determine whether any gene re-arrangements or deletions have occurred.

The E/T homologous recombination has been shown to be very effective and we were able to produce all the mutant virus constructs. However, some difficulties were experienced during this project. Although removal of the Kan^R cassette from MCMV-PP150/PP28-F140 was a straightforward process, removal from MCMV-PP150-E134G/Y100I that fused to the N-terminus, presented many challenges (Table 3.3). It is not clear why it was not possible to remove the selective marker from these MCMV BAC genomes, as many times many bacterial colonies presented the expected phenotype (Kan resistant) on the LB agar plate, but were negative when screened on LB plates and by PCR analysis. MCMV BAC recombination and the excision of the antibiotic resistance cassette are vastly used in the literature. The insertion of the ecDHFR domain to the MCMV BAC genome was quite simple and uncomplicated (Figure 3.22). Several independent attempts were tried to overcome this problem, but they all proved unsuccessful. Whether it was an unknown mutation or a reagent problem, we did not identify the source of the block preventing the excision of the Kan^R marker.

Reconstitution of viruses with genetically inactivated essential genes is a powerful method of studying viral gene function, but requires a complementation system for the growth of recombinant viruses. However, such complementing cell line are frequently difficult to derive for a number of reasons: 1) The exogenous promoter used to regulate the viral gene may not enable appropriate timing and expression levels of the mutated gene; 2) The viral gene may

be toxic to the cell when expressed in isolation; 3) primary cells required for growth of CMV are not amenable for production of stable cell lines. Following recombination, recombinant MCMV BAC DNA must be transfected into eukaryotic cells to determine whether derivative viruses can be reconstituted into infectious virus in tissue culture. MCMV BAC DNA was delivered into murine embryonic fibroblasts by electroporation in the presence of TMP.

Destabilization domain strategy is based on genetic fusion of essential genes to DD that can be stabilized by a small molecule known as ligand; in this project we used Trimethoprim (TMP; (Iwamoto *et al.*, 2010). TMP is an inexpensive small molecule with excellent pharmacological characteristics, as it is widely used at lower concentrations than for DD stabilization to treat urinary tract infection (Schnell, Dyson & Wright, 2004). All the experiments performed with replication defective versions of MCMV-pp150/pp28-F140P in this study were grown and titered on MEF cells in the presence or absence of TMP. Transfection of recombinant viruses into MEFs in the presence or absence of TMP demonstrated the drastic difference in the ability of recombinant to grow in the presence versus absence of TMP (Figures 3.36-3.37). Although this system has been used to assess gene function, our work represents one of the few studies that take advantage of this powerful approach towards development of a conditionally-attenuated vaccine platform (Table 1.4). Strict specificity has prevented the study of HCMV in animals, and MCMV has been widely used as a model for studying CMV in an animal system (Krpmotic *et al.*, 2003).

Characteristics of the pp150 and pp28 MCMV recombinants were distinct. Compared to the pp150 destabilized virus, the pp28 virus showed a severely delayed reconstitution (between 8 and 10 days) in the absence of TMP, which was associated with fewer plaques, smaller plaque size and lack of spread. This suggested that release of infectious particles after the virus reconstitution takes place with extremely low efficiency, similar to the pattern observed after deletion of the pp28 (Britt *et al.*, 2004; Silva *et al.*, 2003 & Seo & Britt, 2006).

In contrast, the mutant MCMVpp150-F140P has not shown delay in reconstitution (between day 4 and 5) in the absence of TMP, indicating that stabilization of the fusion protein was partial, and the degradation of pp150 protein in the absence of TMP ligand was not fully achieved. However in the presence of TMP both viruses grew almost the same as their parental MCMV-WT (Figures 3.36- 3.37).

A live attenuated CMV-based vaccine vector should possess the following features. First, the virus vector should grow to high titres in cell culture for easy production. Second, the vector should be severely attenuated *in vivo* in both immunocompetent and immunocompromised individuals. Third, the vector should induce a strong immune response sufficient to protect against a challenge to the same level as or even better than that of natural infection with the wild-type CMV. Evaluation of the conditional system using DD protein revealed that the CMV mutants grew to titres that were comparable to those of the parental virus when the optimal concentration of ligand was added. For efficient complementation of the CMV mutants, different concentration of ligand were required and used. Thus, the amount of ligand needed for stabilization of the target protein differed for each fusion protein indicating that the optimal ligand concentration has to be determined empirically (Glaß *et al.*, 2009). To indicate the tenability of plaque formation and determine optimal concentration of TMP, we grew infected MEF cells with different amount of TMP (Figures 3.42-3.45). We observed effective plaque formation by MCMV-PP150-F140P at 50 µM TMP. Similarly, higher amounts (100 µM) of TMP were needed for stabilization of PP28-F140P. This observation is in agreement with previous studies that proved that the concentration of ligand that stabilizing to each fusion protein should be determined individually (Banaszynski *et al.*, 2006; Iwamoto *et al.*, 2010).

Moreover, conditional expression of genes using ecDHFR strategy is a promising tool in order to study function (s) of essential genes to develop antiviral compounds and vaccine vectors. TMP-dependent rapid degradation/stabilization of ecDHFR-tagged proteins (Banaszynski *et al.*, 2006; Iwamoto *et al.*, 2010) provides a means to control essential genes, taking advantage of the possibility to study the “off” and “on” situations with the same virus stock preparation. Treating MCMV-pp150/pp28-F140P infected cells with TMP for four days and then withdrawal of TMP for 6 hr decreased the titre of the viruses significantly compared to virus maintained with TMP continuously ($P < 0.0308$ and $P < 0.0001$, respectively). Withdrawal of TMP for short times, even 6 hr, partially degraded their growth (Figure 3.53 B & C). Whereas treating MCMV-pp150/pp28-F140P infected cells without TMP for four days and then culture for 6 hr with TMP, partially restored their growth via increasing the titre of the virus compared to virus maintained without TMP continuously ($P < 0.0417$ and $P < 0.0018$, respectively). Indicating partially restored growth (Figure 3.54 B & C).

Based on the expression kinetics, both pp150 and pp28 are true L genes. Although there were significant differences between MEF cells infected with MCMV-pp150/pp28-F140P the titre of the virus regardless to add/withdrawal of TMP when cultured for 6 hr, probably if culture be followed for longer periods statistically significant difference may increase between them. Our results are consistent with previous studies that both pp150 and pp28 tegument protein are essential for late stages of CMV virion assembly and aggress.

To examine the growth kinetics of recombinant viruses (MCMV-pp150-F140P or MCMV-pp28-F140P), we compared the virus growth in the presence or absence of ligand TMP in the different time points. Compared to the MCMV-WT parental virus and in the presence of TMP, the virus grew to titres comparable to those of the wild-type virus (Figure 3.55 B). However in the absence of TMP the MCMV-pp150-F140P virus showed almost similar growth kinetics to the virus kept with TMP (Figure 3.55 C). Consistent with the previous

results, that indicated the virus grew regardless of the presence or absence of TMP (Figure 3.36). As a complement to the studies described above, although the F140P domain enables regulated stability of pp150 ORF, the F140P domain tag inhibits some aspect of replication of mutant MCMV we saw a little effect of TMP, suggesting a level of destabilization of the pp150 in an intermediate attenuated replication phenotype of the virus.

In the presence of TMP, the MCMV- pp28-F140P grew to titres comparable to the parental MCMV-WT (only 2 log lower; Figure 3.56 B). Infected cells kept without TMP produced a few viruses in day 3 post infection and later however the titres of these viruses did not increase over time (Figure 3.56 C). The TMP restored the function of recombinant MCMV-pp28-F140P virus through restoring the function of ecDHFR fused pp28. While in the absence of TMP only a few foci had developed and the titre did not increase over time (Figure 3.56). This provides evidence that the defective growth phenotype of the virus was due to degradation of the pp28 tegument protein.

In conclusion, the results described in this chapter highlight the potential of the generation and characterisation of the replication defective version of recombinant MCMV vector with fusion of ecDHFR to tegument proteins of late kinetic class which can be used as a valuable tool for design and development of an effective and inexpensive vaccine for potential use in all individuals regardless of immune status. This new strategy will provide the necessary groundwork for future studies evaluating the utility of MCMV model in which to study HCMV vaccine development and also to develop a vaccine platform that is suitable for development to target emerging viruses in low income countries. Future studies will now be able to exploit the MCMV infection model in mice to explore the efficacy of these conditionally attenuated vaccines against a variety of significant infectious and non-infectious diseases taking advantage of existing mouse models. These include various mouse cancer models, as well as infectious disease models of Ebola and IA viruses and tetanus.

Chapter Four:

CD8⁺ T cell targeting of conserved IA virus structural proteins using CMV-based vectors to elicits homo and heterosubtypic immunity

4.1 Introduction

IA virus is one of the most common causes of respiratory tract infection in humans, being responsible for annual outbreaks of influenza disease within the human population as seasonal or epidemic flu. The virus can also periodically and unpredictably lead to pandemic influenza that results from introduction of a completely new IA virus into an immunologically naïve population to devastating effect on human health worldwide. Current seasonal vaccination induces protective antibodies against the HA and NA of the IA virus. These vaccines are aimed only at induction of antibodies against the surface HA and NA glycoproteins and are poor inducers of T cell responses. These vaccines are relatively effective against the current IA viruses circulating in the human population. However, seasonal vaccines are completely ineffective against pandemic IA viruses possessing new HA and NA genes for which the human population has no immunological memory.

A universal vaccine that induces broad protection by targeting more conserved regions of the virus could be more effective, thereby inducing cross-protection against multiple IA virus subtypes (Altenburg, Rimmelzwaan & de Vries, 2015; Strutt *et al.*, 2013). The internal proteins are highly conserved among different virus subtypes and are not exposed to the humoral immune system. Therefore these proteins do not change as frequently as HA and NA (Lee *et al.*, 2014), and thereby may be able to induce a heterosubtypic immune response associated with CTL responses (Suda *et al.*, 2011). In our study we explored the use of fully replicating WT MCMV expressing conserved internal proteins of the IA virus (NP, PA and NS2) as a vaccine vector to induce heterosubtypic IA virus-specific CD8⁺ T cell immunity.

4.2 Results

4.2.1 Cloning of MCMV-IA-based vectors

As detailed in the introduction (Sections 1.7 and 4.1), the overall aim of this study was to establish at a proof-of-concept level in the mouse model that targeting T cell immune responses against more highly conserved regions of the IA virus for the development of a universal flu vaccine would yield a vaccine effective against all serotypes of IA virus. Not only would this protect against pandemic IA viruses, but it would also remove the need for vaccines to be reformulated annually. Given the accepted ability of CMV-based vaccines to induce high levels of T cell immunity, we explored a CMV-based approach using MCMV as a vaccine vector against IA virus expressing epitopes of conserved IA virus proteins. Three MCMV-based influenza vaccines (MCMV-IAV) were designed, each expressing a single H2^b-restricted CD8⁺ T cell epitope of a conserved IA structural protein: NP represented by NP₃₆₆₋₃₇₄ (ASNENMETM) (Andreansky *et al.*, 2005), PA by PA₂₂₄₋₂₃₃ (SSLENFRAYV) (Belz *et al.*, 2000) and NS2 by NS2₁₁₄₋₁₂₁ (RTFSFQLI) (Belz *et al.*, 2000). These epitopes were fused in-frame to the carboxyl terminus of IE2, a non-essential protein of MCMV (Figure 4.1). MCMV-IA (NP, PA, and NS2) vectors were constructed by E/T linear recombination using the pSMfr BAC containing the MCMV (Smith strain) genome (Messerle *et al.*, 1997), as described in Section 2.5.1. The m157 gene of MCMV was deleted from this BAC for these studies due to the NK activating effect of the m157 gene product on NK activity in the C57BL/6 mouse background, as discussed above. The E/T linear recombination strategy is outlined in the Chapter 3 (Figure 3.3.).

MCMV/Flu-CTL

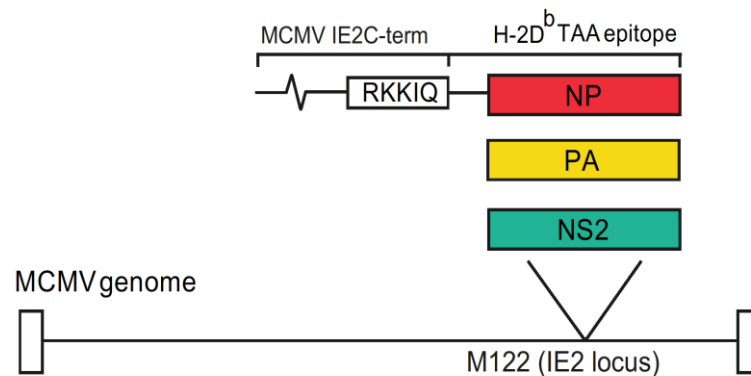


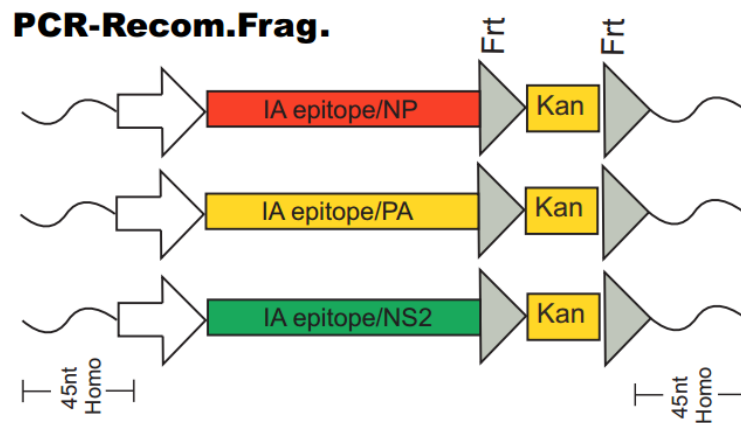
Figure 4.1 Schematic illustration of MCMV-IAV constructs expressing a single H2b-restricted cytotoxic T cell (CTL) epitope. H2^b-restricted T cell epitopes from IA conserved structural proteins NP (NP₃₆₆₋₃₇₄; ASNENMETM), PA (PA₂₂₄₋₂₃₃; SSLENFRAYV) or NS2 (NS2₁₁₄₋₁₂₁; RTFSFQLI) were fused in-frame to the carboxyl terminus of MCMV IE2 generating the recombinant MCMV/IA-NP, MCMV/IA-PA and MCMV/IA-NS2 vaccine vectors.

To construct the recombinant MCMV-IA vaccines, linear DNA fragments encoding the sequences of the IA epitopes and a Kan^R marker, flanked on either end by sequence homologous to the targeted IE2 insertion site were generated by PCR, as described in Section 2.3.3. These recombinant PCR fragments were transformed by electroporation into electrocompetent, E/T recombinase-induced EL250 cells as described in Section 2.2.4. Recombinant clones were selected based on resistance to both Cam and Kan. Following genomic characterization, the Kan^R marker was removed by arabinose induction of the FLP recombinase system (Section 2.5.1.3). Recombinant viruses were reconstituted by transfection using electroporation of BAC DNA into MEFs as described in Section 2.6.2.1. Following virus reconstitution, virus was passaged to remove the BAC cassette (Section 2.6.2.3) and seed and concentrated virus stocks of all three viruses were prepared (see Figure 2.1 for schematic of construction process).

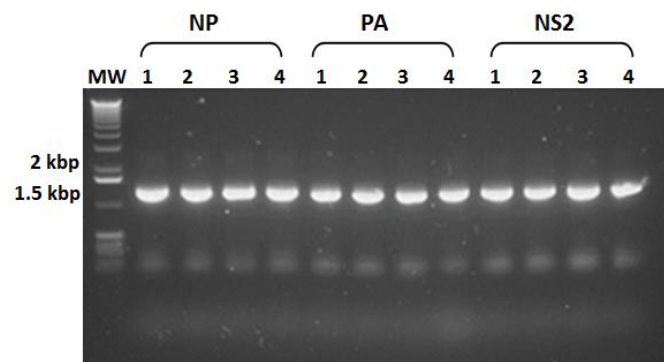
4.2.1.1 PCR fragments with flanking viral homologies to IE2 were generated

Recombination fragments were amplified by PCR using the forward primer IE2-NP-F5-F, IE2-PA-F5-F or IE2-NS2-F5-F together with a common reverse primer, IE2-NP/PA/NS2-F5-R (Table 2.2). The pOriFRT(F5) plasmid was used as a template for all reactions. This template plasmid contains the F5 mutant version of the FRT, which is necessary to prevent inadvertent recombination between the FRT (WT) 'scar' remaining from the m157 deletion. The 5' end of each primer contained 45 bp sequence with homology to the epitope insertion site at the immediate carboxyl terminus of the MCMV IE2 ORF with removal of the IE2 stop codon. This homology sequence was followed by sequence encoding the NP, PA or NS2 epitopes and a 16 bp sequence necessary for primer binding to the pOriFRT(F5) template plasmid. Each recombination fragment was prepared in duplicate using 2 independent PCR reactions, which were then used in parallel for cloning of independent versions of each MCMV-IA recombinant, to avoid concerns with spurious PCR-associated mutations during production of recombination fragments. Gel electrophoresis confirmed amplification of PCR recombination fragments of the expected 1.5 kb size (Figure 4.2 A and B). Recombination PCR fragments were extracted from the gel (Section 2.3.6) and purified using a gel extraction kit (Section 2.3.7). Gel purified recombination fragments were confirmed to be of the correct size by electrophoresis (Figure 4.2 C).

(A)



(B)



(C)

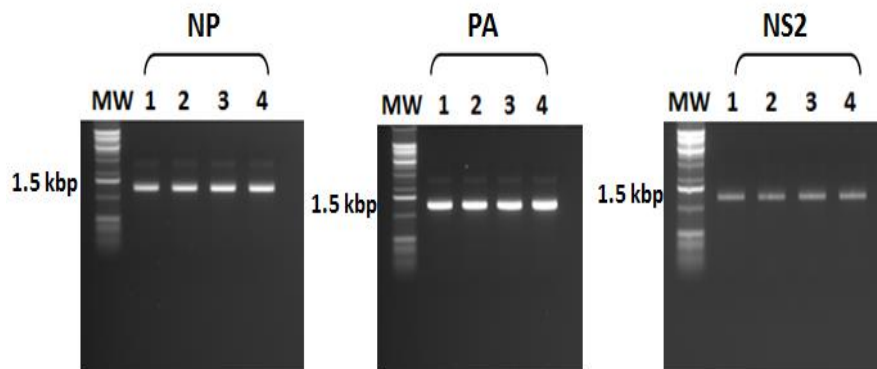


Figure 4.2 Recombination PCR fragments used for construction of three MCMV-IA vaccine vectors. (A) Schematic showing PCR generated E/T recombination fragments used for construction of the three MCMV-IA vaccine vectors. (B) DNA gel showing recombinant PCR generated fragments containing NP, PA, and NS2 H2^b - restricted CD8⁺ T cell epitopes. The single DNA band at 1.5 kb shows amplification of the desired recombination fragments. Two independent PCR reactions were prepared for each clone. (C) Gel purified PCR products confirming the extraction procedure was successful and the correct sized bands purified.

4.2.1.2 Construction of recombinant MCMV-IA (NP, PA and NS2) based vector using E/T-based linear recombination

PCR-derived recombination products prepared above were inserted at the extreme carboxyl terminus of the IE2 locus within the MCMV BAC genome using E/T recombination (Section 2.5.1.2) to generate the respective MCMV-IA BAC recombinants. Following recombination, bacteria were plated on Kan/Cam plates to select for clones containing recombinant BACs. Bacterial colonies were counted (Table 4.1) and two clones from each recombination were selected for further characterization. For each MCMV/IA virus, recombination was performed twice, each using a different independently generated recombination fragments. This was a precautionary necessity as DNA sequences of recombinant viruses are analysed only at the recombinant BAC stage. Overnight cultures were prepared and recombinant BACs were purified by alkaline lysis (Sambrook *et al.*, 2001) as described in Section 2.3.1.2.

MCMV BAC

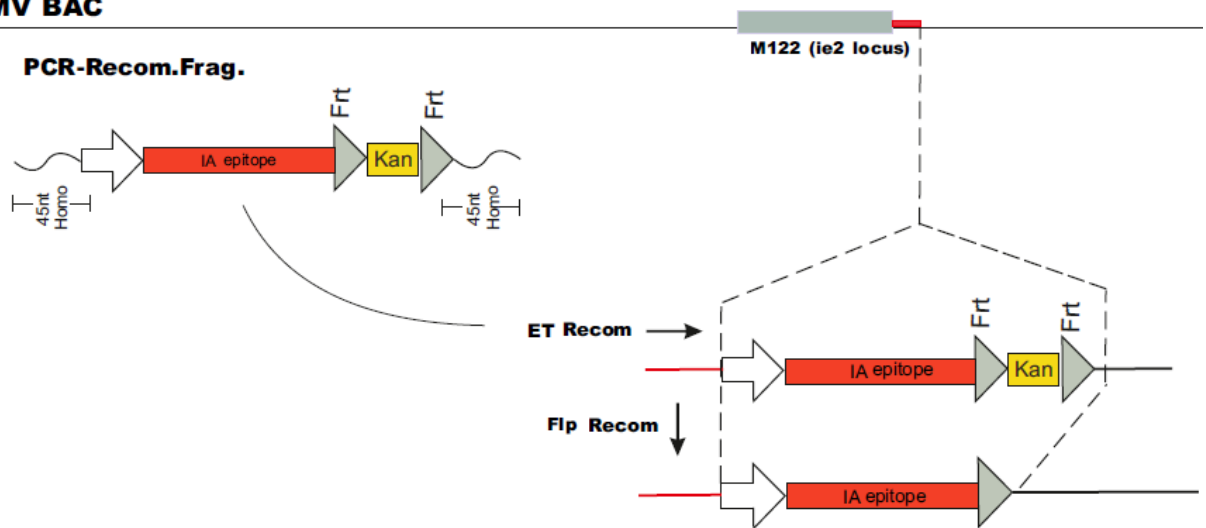


Figure 4.3 Schematic illustrating the construction of MCMV-IAV vectors. The E/T-based linear recombination strategy used for construction of the three MCMV-IAV vectors. Recombinant fragments carrying the Kan^R marker flanked by FRT sites and the sequence encoding the H2^b restricted epitopes from conserved IA structural proteins (NP, NS2 or PA) were amplified by PCR, and electroporated into EL250 bacteria containing the MCMV BAC. Following selection of recombinant BACs on the basis of Kan^R resistance, the Kan^R marker was removed using FLP mediated-recombination. Recombinant MCMV-IA BACs were electroporated into MEFs to reconstitute recombinant MCMV/IA virus. Frt, FRT FLP-recombinase recognition site from the yeast *Saccharomyces cerevisiae*; Kan^R, Kan resistance gene; IA epitope, conserved protein epitope (NP, NS2 or PA) of IA virus.

Table 4.1 Number of recombinant MCMV-IA (NP, PA or NS2) BAC clones following E/T recombination

MCMV Construct	PCR fragment	Number of colonies
MCMV-IA-NP	1	200-250
	2	200-250
MCMV-IA-NS2	1	200-250
	2	250-300
MCMV-IA-PA	1	100-150
	2	150-200

4.2.1.3 Restriction digestion analysis of recombinant BAC DNA

Rearrangement of the BAC genome can occur during E/T based recombination. To ensure selected Kan-resistant clones had retained genomic integrity, restriction digest analysis was performed. A MCMV-WT BAC and three clones of each of the recombinant MCMV-IA (NP, PA, and NS2) BACs were digested using EcoRI and the resulting banding pattern was analysed by gel electrophoresis on a 1% gel (see Section 2.3.5). The results are shown in Figure 4.4. The banding patterns generated by the digested recombinant MCMV-IA BACs were consistent with the banding pattern of the digested MCMV-WT BAC control sample, indicating that there were no gross genomic rearrangements in the recombinant MCMV-IA (NP, PA and NS2) BAC DNAs following the recombination process (Figure 4.4).

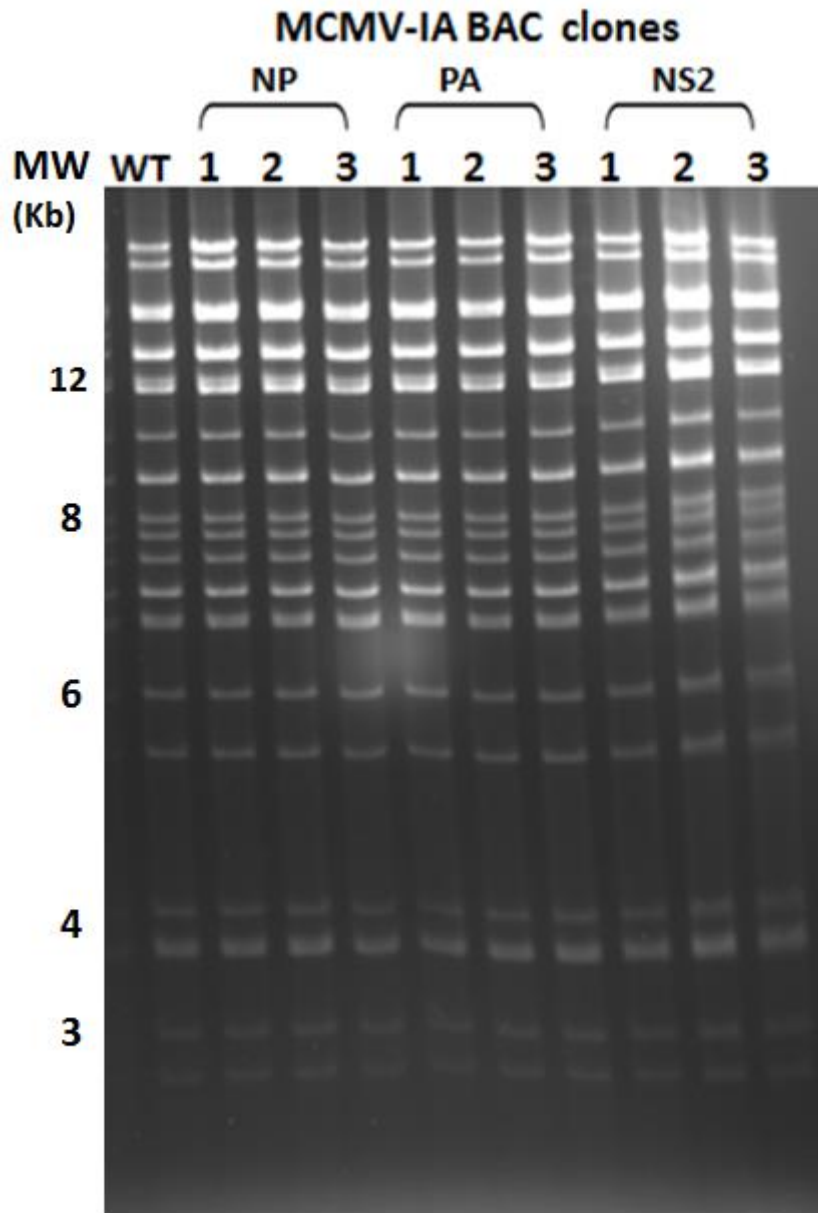


Figure 4.4 Characterization of the recombinant MCMV-IA BAC genome using *EcoRI* restriction enzyme digestion. MCMV-WT BAC and three independent clones of each MCMV-IAV vector (NP, PA and NS2) BACs were digested with *EcoRI* and the resulting fragments were separated on a 1% agarose gel for 18-20 h at 45 V, followed by visualization with 0.5 $\mu\text{g/ml}$ EtBr. Comparable restriction digestion pattern between the MCMV-IA clones and MCMV-WT(FRT F5) BAC shows the absence of any gross genomic rearrangements. Molecular size marker lane (MW) in kb is indicated.

4.2.1.4 Excision of the Kan^R cassette from recombinant MCMV-IA (NP, PA and NS2) BAC DNA

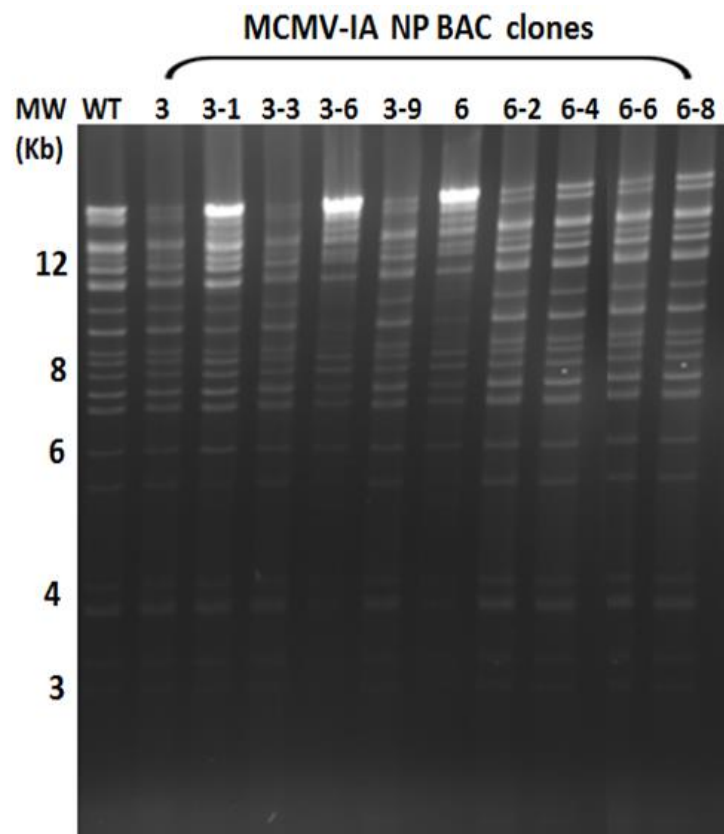
Following confirmation that recombinant BAC genomes were genetically intact, the next step was to remove the FRT-flanked Kan^R marker by arabinose induction of the EL250 FLP recombinase (see Section 2.5.3). To confirm that Kan^R was removed from recombinant MCMV-IA (NP, PA and NS2) BACs, 25 colonies from each ‘FLPed’ recombinant MCMV-IA BAC were replica-plated on Cam/Kan and Cam only plates (Section 2.5.3). Clones in which the FRT-flanked Kan^R marker had been excised were no longer able to grow in the presence of Kan, but retained the ability to grow in the presence of Cam (Table 4.2).

To confirm that the absence of genetic rearrangements during Kan^R excision, DNA from ‘FLPed’ BAC recombinants was again analysed by restriction digest with EcoRI (Figure 4.5), followed by electrophoresis on a 1% agarose gel. MCMV WT BAC DNA and MCMV-IA recombinant BAC DNA (pre-and post-FLP) were compared to confirm genomic integrity of the post FLP recombinant clones. The banding patterns generated by the EcoRI digested recombinant MCMV-IA BACs showed the absence of genomic rearrangements in the recombinant MCMV-IA (NP, PA and NS2) BACs following FLP recombinase-mediated removal of the Kan^R gene.

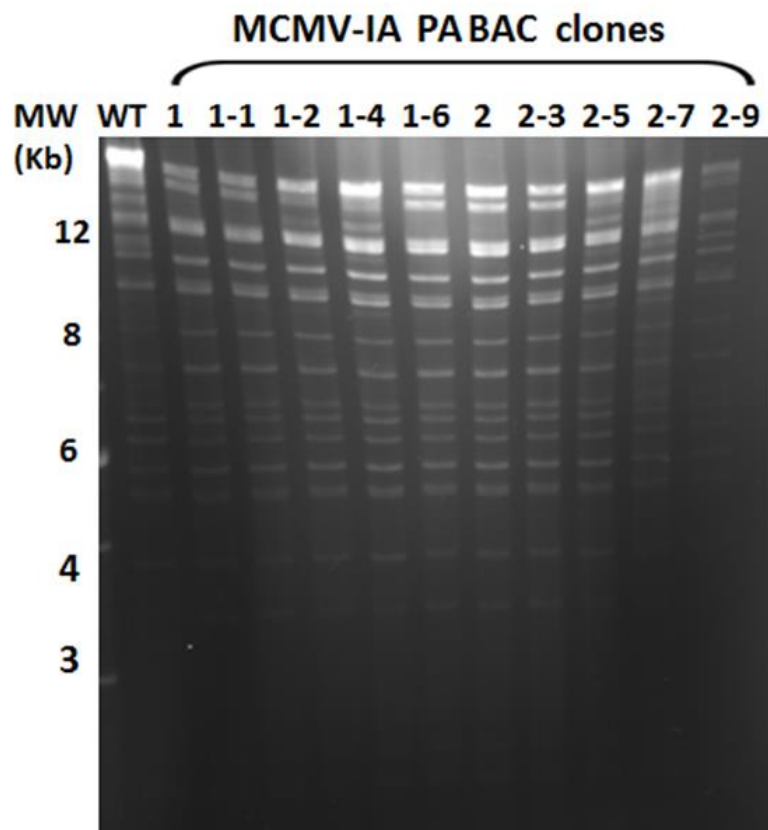
Table 4.2 Analysis of recombinant MCMV BAC clones following excision of Kan^R

MCMV Construct	Recombination	Clone	Selected colonies	Sensitive to Kan
MCMV-IA-NP	1	3	25	All
	2	5	25	All
MCMV-IA-PA	1	1	25	All
	2	1	25	All
MCMV-IA-NS2	1	4	25	All
	2	4	25	All

(A)



(B)



(C)

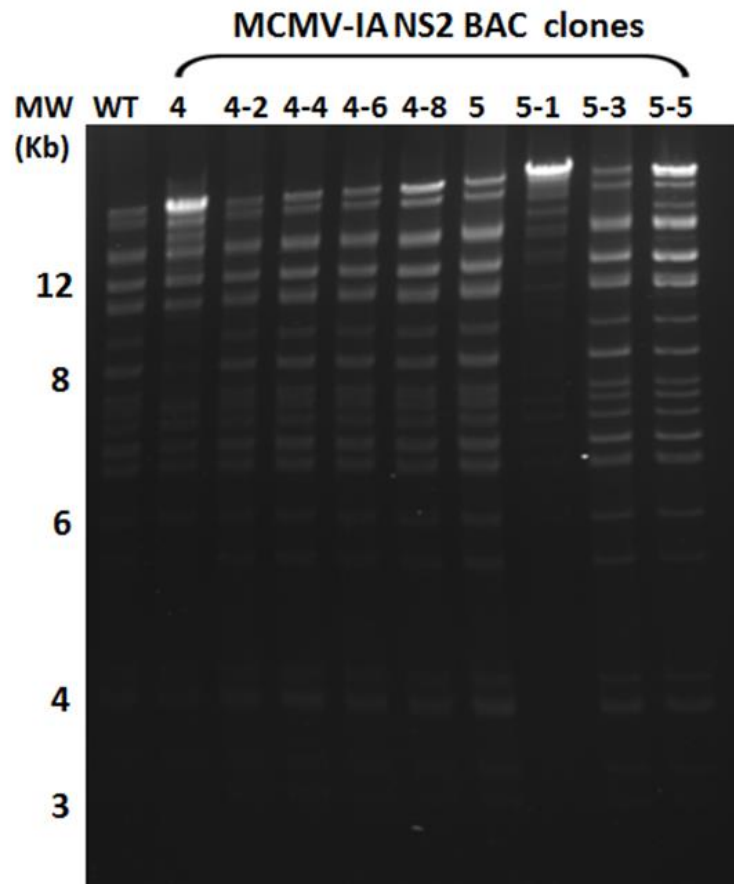
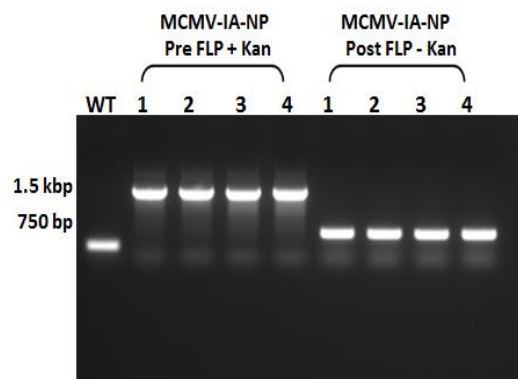


Figure 4.5 Characterization of recombinant post-FLP MCMV-IA BAC genomes using *EcoRI* restriction enzyme digestion. MCMV-WT and recombinant MCMV-IA pre-FLP and derivative post-FLP BACs were digested with *EcoRI* and the resulting fragments were separated on a 1% agarose gel for 18-20 h at 45 V and visualized by staining with 0.5 $\mu\text{g/ml}$ EtBr. (A) MCMV-WT and recombinant MCMV-IA-NP pre-FLP (clones 3 and 6) and derivative post-FLP (clones 3-1, 3-3, 3-6, 3-9, 6-2, 6-4, 6-6 and 6-8) BACs. (B) MCMV-WT and recombinant MCMV-IA-PA pre-FLP (clones 1 and 2) and derivative post-FLP (clones 1-1, 1-2, 1-4, 1-6, 2-3, 2-5, 2-7 and 2-9) BACs. (C) MCMV-WT and recombinant MCMV-IA-NS pre-FLP (clones 4 and 5) and derivative post-FLP (clones 4-2, 4-4, 4-6, 4-8, 5-1, 5-3 and 5-5) BACs. Comparable restriction banding patterns between the MCMV-IA-NP clones (both pre and post FLP- recombinase) and MCMV-WT demonstrate absence of any gross genomic rearrangements. Molecular size marker lane (MW) in kb is indicated.

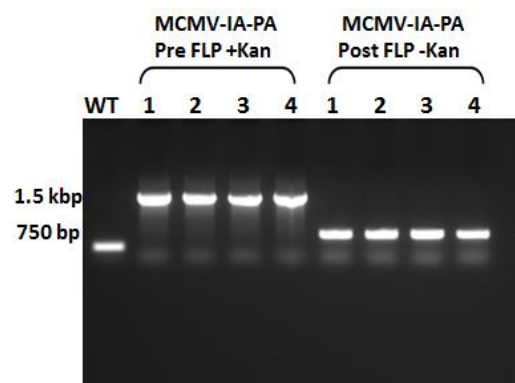
To confirm excision of the Kan^R marker from the recombinant BAC genomes, PCR was performed using IE2-Flank primers that flank the IA insertion site within the IE2 locus (Table 2.2). PCR was performed on recombinant BAC DNA (pre-and post-FLP), and on WT MCMV BAC DNA (included as a control; Figure 4.6). PCR of the WT MCMV BAC yielded a band of approximately 700 bp. In contrast, PCR of the pre-FLP BAC clones yielded bands of approximately 1.5 kbp, which was consistent with presence of the Kan^R gene (and presumably the respective IA epitope sequence) at the desired location within the MCMV BAC genome. The post-FLP clones yielded bands of approximately 750 bp reflecting the loss of the Kan^R gene.

To confirm sequence integrity of the IA epitopes, PCR using IE2-Flank-F and IE2-Flank-R primers was used to amplify the 3' end of the IE2 ORF from each of the MCMV-IA recombinants using BAC DNA as the template. Two independent clones of each recombinant MCMV-IA (NP, PA and NS2) BAC were then sequenced. The sequence data indicated that the full-length sequences of the IA virus CTL epitopes were present, without any deletions or mutations (Figure 4.7).

(A)



(B)



(C)

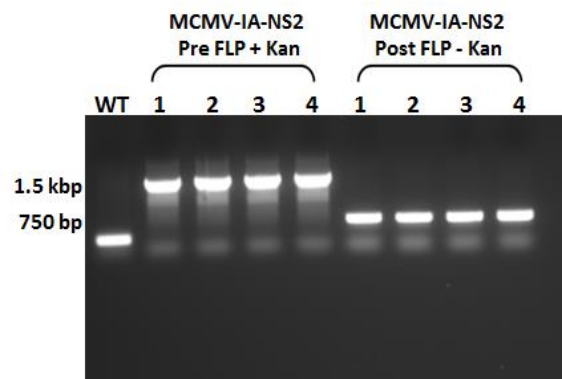


Figure 4.6 Confirmation of excision of the Kan^R marker from (A) MCMV-IA-NP, (B) MCMV-IA-PA, and (C) MCMV-IA-NS2 BACs genome by PCR. BAC DNA from MCMV-WT and four clones of each recombinant MCMV-IA (NP, PA and NS2) BAC (both pre and post-FLP) were screened by using PCR using primers flanking the IE2 site targeted by recombination. PCR products were separated on a 1% agarose gel for 60-90 min at 75 V, and visualized by staining with 0.5 μ g/ml EtBr. PCR pre-FLP MCMV-IA (NP, PA, and NS2) and post-FLP MCMV-IA (NP, PA, and NS2) yielded PCR products of 1.5 kb and 750 bp, respectively. Molecular size marker (MW) in bp is indicated.

(A)

MCMV-IA-NP Clone (1-3)

```
GTCCTGCAGTCCTTCGGTAGGGAAGGACTCTGCAGGTGCGACAACGTCTACACCGAGGACGGC
GGCGCTCCGTACGCTACTCCCGAGGACCCCGTGCTCAAGAACATCGTGTTACGCCCCATCTC
GGCGGGAAGGCGCTCCACCAGCACTGTAAGATCAAGGGACACACCTGGTACCTGAACGGTTG
CCCCGGCATGCTGAAGGACAGGGTGTTTCGTCGCCACGCCGGACATCCCCCCTTCGTCCGCCA
CGTGAACCTGGAACCTTTTGGACATAGGTTTCTACCCATCGGTAGGGTGACCGTTCCCCGAG
GATCCCGAGTGTGAGATGTTTATCATGGTGGACGCCGGGGGGCCATCTACGGGCACATGTT
AGATAGCGGGAAGGTGAGGAGGCTAGCTGATAACTTTGACCAGTTCATGCGGATGGGCACCC
GGAGGGCTTATTTAATTTCCAGATGGTTAAGGGAGATAGTCTCAACACCGAGTACGAGGAGA
CCTCGTTTGGGACCAAGAACCACGGGTTCTTTCTCTTGACCAGAGACCTGGTGACCGTCAGGA
AGAAGATTCAGGGTGCCAGCAACGAGAACATGGAGACCATGTGAAGCTTAGTACGTTAAACA
TGAGAGCTTAGTACGTGAAACATGAGAGCTTAGTACGTACTATCAACAGGTTGAACTGTTAC
TAGTTGCCACCTGCAGATCTGAAGTTCCTATACCTTTTGAAGAATAGGAACTTCTGAATTCCC
```

MCMV-IA-NP Clone (3-3)

```
GGGAGGACTCTGCAGGTGCGACAACGTCTACACCGAGGACGGCGGCGCTCCGTACGCTACTCC
CGAGGACCCCGTGCTCAAGAACATCGTGTTACGCCCCATCTCGGCGGGAAGGCGCTCCACCA
GCAGATCTGTAAGATCAAGGGACACACCTGGTACCTGAACGGTTGCCCGGCATGCTGAAGG
ACAGGGTGTTTCGTCGCCACGCCGGACATCCCCCCTTCGTCCGCCACGTGAACCTGGAACCTCT
TTGGACATAGGTTTCTACCCATCGGTAGGGTGACCCGTTCCCCGAGGATCCCGAGTGTGAGA
TGTTTATCATGGTGGACGCCGGGGGGCCATCTACGGGCACATGTTAGATAGCGGGAAGGTG
AGGAGGCTAGCTGATAACTTTGACCAGTTCATGCGGATGGGCACCCGGAGGGCTTATTTCAA
TTTCCAGATGGTTAAGGGAGATAGTCTCAACACCGAGTACGAGGAGACCTCGTTTGGGACCA
AGAACCACGGGTTCTTTCTCTTGACCAGAGACCTGGTGACCGTCAGGAAGAAGATTCAGGGT
GCCAGCAACGAGAACATGGAGACCATGTGAAGCTTAGTACGTTAAACATGAGAGCTTAGTAC
GTGAAACATGAGAGCTTAGTACGTACTATCAACAGGTTGAACTGCTACTAGTTGCCACCTGC
AGATCTGAAGTTCCTATACCTTTTGAAGAATAGGAACTTCTGAATTCCCATGTCAGCCGTT
```

(B)

MCMV-IA-PA Clone (2-1)

```
TACTCCCGAGGACCCCGTGCTCAAGAACATCGTGTTACGCCCCATCTCGGCGGGAAGGCGCT
CCACCAGCAGATCTGTAAGATCAAGGGACACACCTGGTACCTGAACGGTTGCCCCGGCATGCT
GAAGGACAGGGTGTTCGTGCGCCACGCCGGACATCCCCCCTTCGTCCGCCACGTGAACCTGGA
ACTCTTTGGACATAGGTTTCTACCCATCGGTAGGGTGACCCGTTCCCCGAGGATCCCGAGTG
TGAGATGTTTATCATGGTGGACGCCGGGGGGCCATCTACGGGCACATGTTAGATAGCGGGA
AGGTGAGGAGGCTAGCTGATAACTTTGACCAGTTCATGCGGATGGGCACCCGGAGGGCTTAT
TTCAATTTCCAGATGGTTAAGGGAGATAGTCTCAACACCGAGTACGAGGAGACCTCGTTTGG
GACCAAGAACCACGGGTTCTTTCTCTTGACCAGAGACCTGGTGACCGTCAGGAAGAAGATTC
AGGGTAGCAGCCTGGAGAACTTCAGGGCCTACGTGTGAAGCTTAGTACGTAAACATGAGAG
CTTAGTACGTGAAACATGAGAGCTTAGTACGTACTATCAACAGGTTGAACTGCTACTAGTTG
CCACCTGCAGATCTGAAGTTCCTATACCTTTTGAAGAATAGGAACTTCTGAATTTCCCATGTCA
GCCGTTAAGTGAGGACACGAGGTATGTCATGGGTTTTTAATCAATAAATAAAGAGGTTTTAT
```

MCMV-IA-PA Clone (2-2)

```
GTAGGGAAGGACTCTGCAGGTGCGACAACGTCTACACCGAGGACGGCGGGCGCTCCGTACGCT
ACTCCCGAGGACCCCGTGCTCAAGAACATCGTGTTACGCCCCATCTCGGCGGGAAGGCGCTC
CACCAGCAGATCTGTAAGATCAAGGGACACACCTGGTACCTGAACGGTTGCCCCGGCATGCTG
AAGGACAGGGTGTTCGTGCGCCACGCCGGACATCCCCCCTTCGTCCGCCACGTGAACCTGGAA
CTCTTTGGACATAGGTTTCTACCCATCGGTAGGGTGACCCGTTCCCCGAGGATCCCGAGTGT
GAGATGTTTATCATGGTGGACGCCGGGGGGCCATCTACGGGCACATGTTAGATAGCGGGAA
GGTGAGGAGGCTAGCTGATAACTTTGACCAGTTCATGCGGATGGGCACCCGGAGGGCTTATT
TCAATTTCCAGATGGTTAAGGGAGATAGTCTCAACACCGAGTACGAGGAGACCTCGTTTGGG
ACCAAGAACCACGGGTTCTTTCTCTTGACCAGAGACCTGGTGACCGTCAGGAAGAAGATTCA
GGGTAGCAGCCTGGAGAACTTCAGGGCCTACGTGTGAAGCTTAGTACGTAAACATGAGAGC
TTAGTACGTGAAACATGAGAGCTTAGTACGTACTATCAACAGGTTGAACTGCTACTAGTTGC
CACCTGCAGATCTGAAGTTCCTATACCTTTTGAAGAATAGGAACTTCTGAATTTCCCATGTCA
```

(C)

MCMV-IA-NS2 Clone (4-2)

```
TAGGGAAGGACTCTGCAGGTGCGACAACGTCTACACCGAGGACGGCGGCGCTCCGTACGCTAC
TCCCGAGGACCCCGTGCTCAAGAACATCGTGTTACGCCCCATCTCGGCGGGAAGGCGCTCCA
CCAGCAGATCTGTAAGATCAAGGGACACACCTGGTACCTGAACGGTTGCCCCGGCATGCTGA
AGGACAGGGTGTTCGTCGCCACGCCGGACATCCCCCCTTCGTCCGCCACGTGAACCTGGAAC
TCTTTGGACATAGGTTTCTACCCATCGGTAGGGTGACCCGTTCCCCGAGGATCCCGAGTGTG
AGATGTTTATCATGGTGGACGCCGGGGGGCCATCTACGGGCACATGTTAGATAGCGGGAAG
GTGAGGAGGCTAGCTGATAACTTTGACCAGTTCATGCGGATGGGCACCCGGAGGGCTTATTT
CAATTTCCAGATGGTTAAGGGAGATAGTCTCAACACCGAGTACGAGGAGACCTCGTTTGGGA
CCAAGAACCACGGGTTCTTTCTCTTGACCAGAGACCTGGTGACCGTCAGGAAGAAGATTGAG
GGTAGGACCTTCAGCTTCAGCTGATCTGAAGCTTAGTACGTTAAACATGAGAGCTTAGTAC
GTGAAACATGAGAGCTTAGTACGTACTATCAACAGGTTGAACTGCTACTAGTTGCCACCTGC
AGATCTGAAGTTCCTATACCTTTTGAAGAATAGGAACTTCTGAATTCATGTCAGCCGTTA
```

MCMV-IA-NS2 Clone (4-4)

```
ACGGCGGCGCTCCGTACGCTACTCCCGAGGACCCCGTGCTCAAGAACATCGTGTTACGCCCC
ATCTCGGCGGGAAGGCGCTCCACCAGCAGATCTGTAAGATCAAGGGACACACCTGGTACCTG
AACGGTTGCCCCGGCATGCTGAAGGACAGGGTGTTCGTCGCCACGCCGGACATCCCCCCTTC
GTCCGCCACGTGAACCTGGAACCTTTGGACATAGGTTTCTACCCATCGGTAGGGTGACCCGT
TCCCCGAGGATCCCGAGTGTGAGATGTTTATCATGGTGGACGCCGGGGGGCCATCTACGGG
CACATGTTAGATAGCGGGAAGGTGAGGAGGCTAGCTGATAACTTTGACCAGTTCATGCGGAT
GGGCACCCGGAGGGCTTATTTCAATTTCCAGATGGTTAAGGGAGATAGTCTCAACACCGAGT
ACGAGGAGACCTCGTTTGGGACCAAGAACCACGGGTTCTTTCTCTTGACCAGAGACCTGGTG
ACCGTCAGGAAGAAGATTGAGGGTAGGACCTTCAGCTTCAGCTGATCTGAAGCTTAGTACG
TTAAACATGAGAGCTTAGTACGTGAAACATGAGAGCTTAGTACGTACTATCAACAGGTTGAA
CTGCTACTAGTTGCCACCTGCAGATCTGAAGTTCCTATACCTTTTGAAGAATAGGAACTTCTG
AATTCATGTCAGCCGTTAAGTGAGGACACGAGGTATGTCATGGTTTTTAATCAATAAATA
```

Figure 4.7 Confirmation of IA epitope within MCMV-IA BACs via Sanger sequencing. PCR were performed on post-FLP BAC clones: (A) MCMV-AI-NP clones (3-1) and (3-3). (B) MCMV-AI-PA clones (2-1) and (2-2). (C) MCMV-AI-NS2 clones (4-2) and (4-4). Black text represents IE2 genome sequence, green represents represented IA epitope tag sequence and black text represents downstream MCMV genome sequence.

4.2.1.5 Reconstitution of recombinant MCMV-IA (NP, PA, and NS2) virus

Herpesvirus genomic DNA is infectious. This means that the DNA genome of the virus in itself (in this case contained within the BAC) is sufficient to reconstitute *de novo* progeny virus when introduced into permissive eukaryotic cells. To reconstitute the recombinant MCMV-IA (NP, PA, and NS2) viruses, each BAC DNA was introduced into MEFs by electroporation; MEFs were also electroporated with WT-MCMV BAC DNA as a positive control (see Section 2.6.2.1). Two independent clones from each vector were selected for reconstitution (Table 4.3) to mitigate effects of any potential second site mutations. Cell monolayers were monitored daily for signs of virus-induced CPE such as swelling, rounding, aggregation, cell death and plaque development (Kim & Carp, 1971). All recombinant MCMV-IA viruses were successfully reconstituted. Virus plaques were visible in MEF monolayers beginning at 3 to 7 days post-infection. Numbers of plaques are shown in Table 4.3. MCMV-IA (NP, PA, and NS2) plaques were picked as described in Section 2.6.2.1 and passaged as described in Section 2.6.2.3.

Table 4.3 Plaque numbers of recombinant MCMV-IA (NP, PA, and NS2) following reconstitution in MEFs

MCMV-IA BAC vector plaques	Clones	Plaque numbers
MCMV-WT	2443	12
MCMV-IA-NP	3-1 3-6	7 8
MCMV-IA-PA	1-4 1-14	6 5
MCMV-IA-NS2	4-6 4-8	13 7

4.2.1.6 Removal of BAC cassette from recombinant MCMV-IA viruses

Freshly reconstituted (passage 1) recombinant MCMV-IA viruses still contain the BAC cassette within their genome. The BAC cassette serves no function within the viral genome. However, the increased genome size, resulting from presence of the BAC cassette can interfere with packaging of the viral genome into the confined space of CMV capsid, which ultimately leads to *in vivo* attenuation of the recombinant viruses (Wagner *et al.*, 1999). To resolve this issue, the pSMfr BAC cassette has been flanked by homologous directly repeated genomic sequence regions of 527 bp (Wagner *et al.*, 1999). The presence of these homologous regions within the 'oversized genome' leads to targeted excision of the BAC cassette following serial passage *in vitro* (Wagner *et al.*, 1999). MCMV-IA viruses were serially passaged 5 times in MEFs to remove the BAC cassette followed by preparation of virus seed stocks.

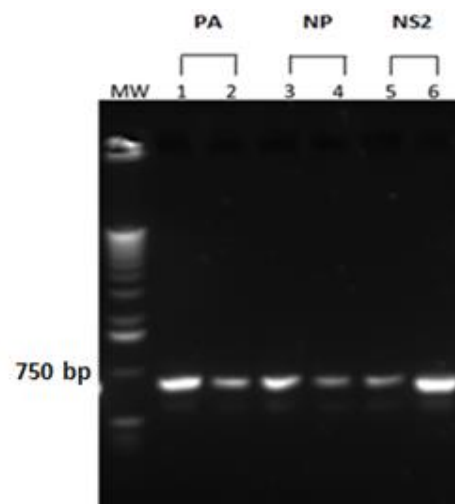


Figure 4.8 Confirming excision of BAC cassette from reconstituted MCMV-IA-(NP, PA or NS2) genome by PCR. DNA was isolated from cells infected with reconstituted MCMV-IA (NP, PA or NS2) virus after five passages using a QIAamp kit and PCR was carried out. PCR products were separated on a 1% agarose gel. The presence of a 750 bp band in recombinant MCMV-IA-PA (lanes 1 and 2), -NP (lanes 3 and 4) and -NS2 (lanes 5 and 6), respectively confirmed the excision of BAC cassette from the virus genome.

4.2.1.7 Preparation of recombinant MCMV-IA virus seed stocks

Seed stocks of MCMV-IA-NP, MCMV-IA-PA and MCMV-IA-NS2 were prepared using supernatants from passage 5 virus stocks (P5; Section 2.6.2.4). A parental MCMV-WT seed stock was also prepared. Infected cell monolayers were incubated for four days, by which time approximately 95% of cells demonstrated substantial CPE. Cells and supernatant were harvested, freeze thawed at -80°C, clarified at 3,800 rpm (4,600 × g) for 20 min at RT, aliquoted and stored at -80°C. Following preparation of the virus seed stocks, the infectivity titre in PFU/cell of the frozen stocks was determined using TCID₅₀, as described in Section 2.6.2.6.

4.2.1.8 Preparation of concentrated virus stocks from seed stock

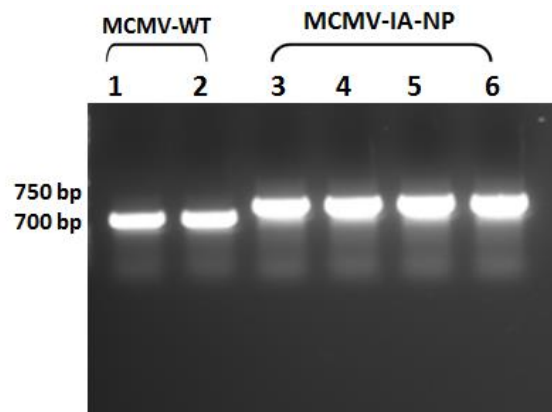
High titre virus stocks for use in *in vitro* characterization and in animal studies were prepared from seed stocks generated above, as described in Section 2.6.2.5. These stocks were fully characterized prior to use in animal experiments. It was particularly important to confirm that the sequence of the IA epitopes had remained intact in all of the MCMV-IA clones. Two clones of each recombinant MCMV-IA (NP, PA or NS2) virus were selected for characterization. Two independent PCR amplifications of viral DNA from each of these clones was then performed using IE2-Flank primers (Table 2.2) (see Section 2.3.3). Bands of the expected sizes of 700 bp and 750 bp were observed in the MCMV-WT lanes (1 & 2), and recombinant MCMV-IAV lanes (3-6), respectively (Figure 4.9). Sanger DNA sequencing of the PCR products showed that the respective full-length IA virus epitopes were located in the correct position at the carboxyl-terminus of the IE2 ORF and did not have any deletions or mutations which would possibly confound CTL recognition (Figure 4.10). These results confirm the presence of the IA epitopes, and also demonstrate the absence of MCMV-WT

contamination within recombinant MCMV-IA virus stocks. The presence of MCMV-WT contamination is due to the maintenance of BACs as low copy rather than single copy within bacteria. This is always a concern, but one which we have largely overcome by agarose overlay and plaque purification at the virus reconstitution stage.

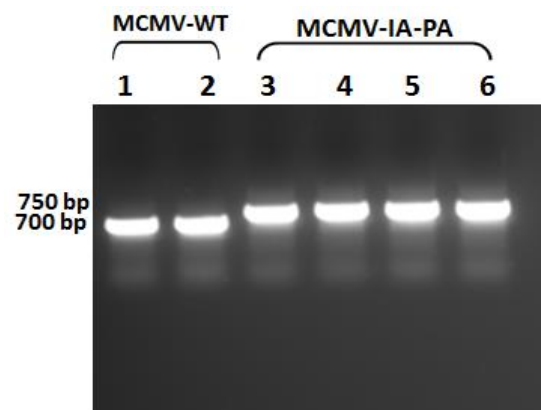
Table 4.4 Titres of MCMV-WT and the recombinant MCMV-IA virus vectors stocks.

Virus (MCMV)	Titre by TCID₅₀ (PFU/cell)
MCMV-WT(F5)	8.71×10^7
MCMV-IA-NP	8.48×10^7
MCMV-IA-PA	2.50×10^7
MCMV-IA-NS2	6.70×10^7

(A)



(B)



(C)

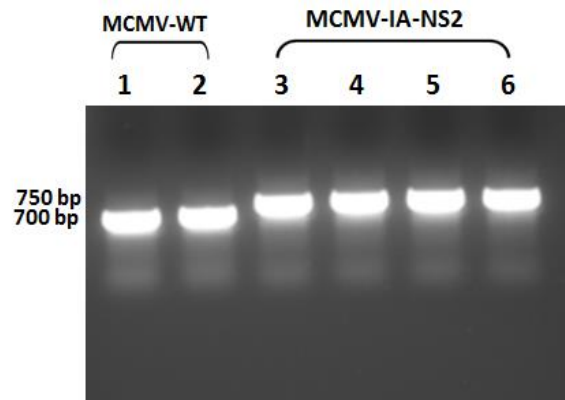


Figure 4.9 Confirming presence of IA epitopes in MCMV-IA viruses genome by PCR.

DNA was isolated from MCMV-IA (NP, PA, and NS2) concentrated stocks using a QIAmp kit and PCR was performed using IE2-Flank primers. PCR products were separated on a 1% agarose gel. The presence of a 750 bp band in recombinant (A) MCMV-IA-NP, (B) MCMV-IA-PA and (C) MCMV-IA-NS2 virus lanes (3-6) was consistent with presence of the desired epitope, which was then confirmed by DNA sequencing. Absence of the MCMV-WT sized band (700 bp) in the MCMV-IA (NP, PA and NS2) viruses lanes (1-2) confirmed the absence of WT contamination of recombinant stocks.

(A)

MCMV-IA-NP PCR 1

```
GGCGCTCCGTACGCTACTCCCGAGGACCCCGTGCTCAAGAACATCGTGTTACGCCCCATCTC
GGCGGGAAGGCGCTCCACCAGCACTGTAAGATCAAGGGACACACCTGGTACCTGAACGGTTG
CCCCGGCATGCTGAAGGACAGGGTGTTCGTCGCCACGCCGGACATCCCCCCTTCGTCCGCCA
CGTGAACCTGGAACCTTTGGACATAGGTTTCTACCCATCGGTAGGGTGACCGTTCCCCCGAG
GATCCCGAGTGTGAGATGTTTATCATGGTGGACGCCGGGGGGCCATCTACGGGCACATGTT
AGATAGCGGGAAGGTGAGGAGGCTAGCTGATAACTTTGACCAGTTCATGCGGATGGGCACCC
GGAGGGCTTATTTAATTTCCAGATGGTTAAGGGAGATAGTCTCAACACCGAGTACGAGGAGA
CCTCGTTTGGGACCAAGAACCACGGGTTCTTTCTCTTGACCAGAGACCTGGTGACCGTCAGGA
AGAAGATTCAGGGTGCCAGCAACGAGAACATGGAGACCATGTGAAGCTTAGTACGTAAACA
TGAGAGCTTAGTACGTGAAACATGAGAGCTTAGTACGTACTATCAACAGGTTGAACTGTTAC
TAGTTGCCACCTGCAGATCTGAAGTTCCTATACCTTTTGAAGAATAGGAACTTCTGAATTCCC
ATGTCAGCCGTAAAGTGAGGACACGAGGTATGTCATGGTTTTTAATCAATAAATAAAGAGGT
```

MCMV-IA-NP PCR 2

```
ACCGAGGACGGCGGCGCTCCGTACGCTACTCCCGAGGACCCCGTGCTCAAGAACATCGTGTTC
ACGCCCCATCTCGGCGGGAAGGCGCTCCACCAGCAGATCTGTAAGATCAAGGGACACACCTGG
TACCTGAACGGTTGCCCGGCATGCTGAAGGACAGGGTGTTCGTCGCCACGCCGGACATCCCC
CCCTTCGTCCGCCACGTGAACCTGGAACCTTTGGACATAGGTTTCTACCCATCGGTAGGGTG
ACCCGTTCCCCGAGGATCCCGAGTGTGAGATGTTTATCATGGTGGACGCCGGGGGGCCATC
TACGGGCACATGTTAGATAGCGGGAAGGTGAGGAGGCTAGCTGATAACTTTGACCAGTTCAT
GCGGATGGGCACCCGGAGGGCTTATTTCAATTTCCAGATGGTTAAGGGAGATAGTCTCAACA
CCGAGTACGAGGAGACCTCGTTTGGGACCAAGAACCACGGGTTCTTTCTCTTGACCAGAGACC
TGGTGACCGTCAGGAAGAAGATTCAGGGTGCCAGCAACGAGAACATGGAGACCATGTGAAGC
TTAGTACGTAAACATGAGAGCTTAGTACGTGAAACATGAGAGCTTAGTACGTACTATCAAC
AGGTTGAACTGCTACTAGTTGCCACCTGCAGATCTGAAGTTCCTATACCTTTTGAAGAATAG
GAACTTCTGAATTCATGTCAGCCGTAAAGTGAGGACACGACGTATGTCATGGTTTTTAAT
```

(B)

MCMV-IA-PA PCR 1

```
GGCGGCGCTCCGTACGCTACTCCCGAGGACCCCGTGCTCAAGAACATCGTGTTACGCCCCAT
CTCGGCGGGAAGGCGCTCCACCAGCAGATCTGTAAGATCAAGGGACACACCTGGTACCTGAA
CGGTTGCCCCGGCATGCTGAAGGACAGGGTGTTCGTGCGCCACGCCGGACATCCCCCCTTCGT
CCGCCACGTGAACCTGGAACCTTTGGACATAGGTTTCTACCCATCGGTAGGGTGACCCGTTT
CCCCGAGGATCCCGAGTGTGAGATGTTTATCATGGTGGACGCCGGGGGGGCCATCTACGGGC
ACATGTTAGATAGCGGGAAGGTGAGGAGGCTAGCTGATAACTTTGACCAGTTCATGCGGATG
GGCACCCGGAGGGCTTATTTCAATTTCCAGATGGTTAAGGGAGATAGTCTCAACACCGAGTA
CGAGGAGACCTCGTTTGGGACCAAGAACCACGGGTTCTTTCTCTTGACCAGAGACCTGGTGAC
CGTCAGGAAGAAGATTCAGGGTAGCAGCCTGGAGAACTTCAGGGCCTACGTGTGAAGCTTAG
TAGTTAAACATGAGAGCTTAGTACGTGAAACATGAGAGCTTAGTACGTACTATCAACAGGT
TGAAGTACTAGTTGCCACCTGCAGATCTGAAGTTCCTATACCTTTTGAAGAATAGGAAC
TTCTGAATTCCCATGTCAGCCGTTAAGTGAGGACACGAGGTATGTCATGGGTTTTTAATCAA
```

MCMV-IA-PA PCR 2

```
GCGCTCCGTACGCTACTCCCGAGGACCCCGTGCTCAAGAACATCGTGTTACGCCCCATCTCG
GCGGGAAGGCGCTCCACCAGCAGATCTGTAAGATCAAGGGACACACCTGGTACCTGAACGGT
TGCCCCGGCATGCTGAAGGACAGGGTGTTCGTGCGCCACGCCGGACATCCCCCCTTCGTCCGC
CACGTGAACCTGGAACCTTTGGACATAGGTTTCTACCCATCGGTAGGGTGACCCGTTCCCCC
GAGGATCCCGAGTGTGAGATGTTTATCATGGTGGACGCCGGGGGGGCCATCTACGGGCACAT
GTTAGATAGCGGGAAGGTGAGGAGGCTAGCTGATAACTTTGACCAGTTCATGCGGATGGGCA
CCCGGAGGGCTTATTTCAATTTCCAGATGGTTAAGGGAGATAGTCTCAACACCGAGTACGAG
GAGACCTCGTTTGGGACCAAGAACCACGGGTTCTTTCTCTTGACCAGAGACCTGGTGACCGTC
AGGAAGAAGATTCAGGGTAGCAGCCTGGAGAACTTCAGGGCCTACGTGTGAAGCTTAGTACG
TTAAACATGAGAGCTTAGTACGTGAAACATGAGAGCTTAGTACGTACTATCAACAGGTTGAA
CTGCTACTAGTTGCCACCTGCAGATCTGAAGTTCCTATACCTTTTGAAGAATAGGAACTTCTG
AATTCATGTCAGCCGTTAAGTGAGGACACGAGGTATGTCATGGGTTTTTAATCAATAAATA
```

(C)

MCMV-IA-NS2 PCR

```
GCGCTCCGTACGCTACTCCCAGGACCCCGTGCTCAAGAACATCGTGTTCACGCCCCATCTCG
GCGGGAAGGCGCTCCACCAGCAGATCTGTAAGATCAAGGGACACACCTGGTACCTGAACGGT
TGCCCCGGCATGCTGAAGGACAGGGTGTTCGTCGCCACGCCGGACATCCCCCCTTCGTCCGC
CACGTGAACCTGGAACCTTTTGGACATAGGTTTCTACCCATCGGTAGGGTGACCCGTTCCCC
GAGGATCCCAGTGTGAGATGTTTATCATGGTGGACGCCGGGGGGCCATCTACGGGCACAT
GTTAGATAGCGGGAAGGTGAGGAGGCTAGCTGATAACTTTGACCAGTTCATGCGGATGGGCA
CCCGGAGGGCTTATTTCAATTTCCAGATGGTTAAGGGAGATAGTCTCAACACCGAGTACGAG
GAGACCTCGTTTGGGACCAAGAACCACGGGTCTTTCTCTTGACCAGAGACCTGGTGACCGTC
AGGAAGAAGATTCAGGGTAGGACCTTCAGCTTCAGCTGATCTGAAGCTTAGTACGTAAAC
ATGAGAGCTTAGTACGTGAAACATGAGAGCTTAGTACGTACTATCAACAGGTTGAACTGCTA
CTAGTTGCCACCTGCAGATCTGAAGTTCCTATACCTTTTGAAGAATAGGAACTTCTGAATTCC
CATGTCAGCCGTTAAAGTGAGGACACGAGGTATGTCATGGTTTTTAATCAATAAATAAAGAG
```

MCMV-IA-NS2 PCR 2

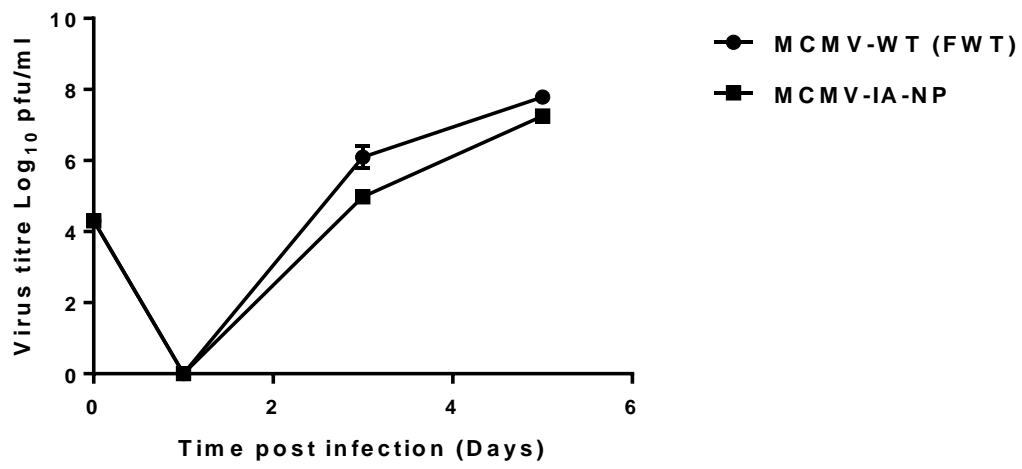
```
ACGGCGGCGCTCCGTACGCTACTCCCAGGACCCCGTGCTCAAGAACATCGTGTTCACGCCCC
ATCTCGGCGGGAAGGCGCTCCACCAGCAGATCTGTAAGATCAAGGGACACACCTGGTACCTG
AACGGTTGCCCCGGCATGCTGAAGGACAGGGTGTTCGTCGCCACGCCGGACATCCCCCCTTC
GTCCGCCACGTGAACCTGGAACCTTTTGGACATAGGTTTCTACCCATCGGTAGGGTGACCCGT
TCCCCGAGGATCCCAGTGTGAGATGTTTATCATGGTGGACGCCGGGGGGCCATCTACGGG
CACATGTTAGATAGCGGGAAGGTGAGGAGGCTAGCTGATAACTTTGACCAGTTCATGCGGAT
GGGCACCCGGAGGGCTTATTTCAATTTCCAGATGGTTAAGGGAGATAGTCTCAACACCGAGT
ACGAGGAGACCTCGTTTGGGACCAAGAACCACGGGTCTTTCTCTTGACCAGAGACCTGGTG
ACCGTCAGGAAGAAGATTCAGGGTAGGACCTTCAGCTTCAGCTGATCTGAAGCTTAGTACG
TTAAACATGAGAGCTTAGTACGTGAAACATGAGAGCTTAGTACGTACTATCAACAGGTTGAA
CTGCTACTAGTTGCCACCTGCAGATCTGAAGTTCCTATACCTTTTGAAGAATAGGAACTTCTG
AATTCCCATGTCAGCCGTTAAGTGAGGACACGAGGTATGTCATGGTTTTTAATCAATAAATA
```

Figure 4.10 Confirmation of IA epitope within MCMV-IA virus genome by Sanger DNA sequencing. PCR was performed on viral DNA isolated from concentrated viral stocks (show in Figure 4.9). The two independent PCR products were sequenced: (A) MCMV-IA-NP PCR 1 and PCR 2. (B) MCMV-IA-PA PCR 1 and PCR 2. (C) MCMV-IA-NS2 PCR 1 and PCR 2. IE2 genome sequence (blue), IA epitope tag sequence (green), downstream MCMV genome sequence (black). The stop codon is shown in red.

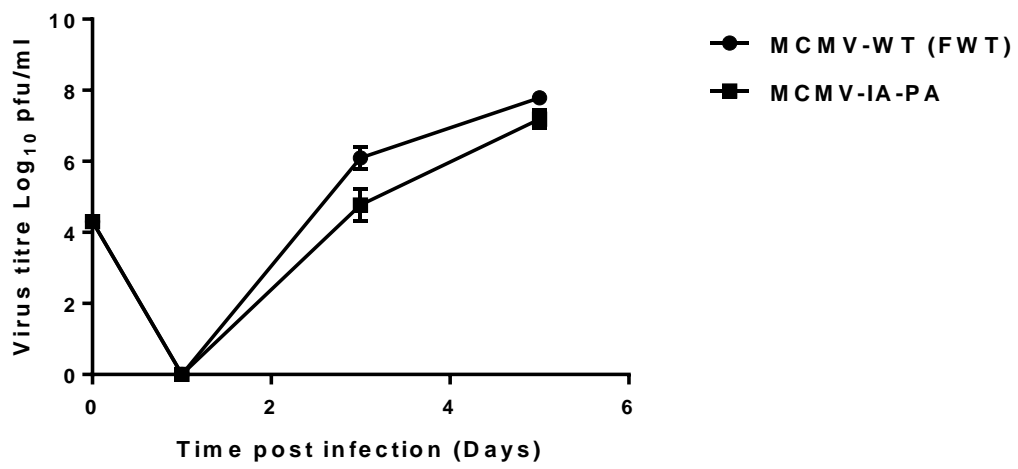
4.2.1.9 Recombinant MCMV-IA viruses show comparable replication to MCMV-WT virus

Virus stock titres were quantified by TCID₅₀ assay as described in Section 2.6.1.6. Results showing comparable yields of virus in the MCMV-IAV and MCMV-WT stocks suggested that the recombinant viruses were WT in characteristic as regards *in vitro* replication (Table 4.4). Multi-step growth curves were performed to confirm that the MCMV-IA viruses had *in vitro* replication kinetics comparable to MCMV-WT. MEFs were infected in triplicate at a multiplicity of infection (0.1 PFU/cell) with either MCMV-WT or the different MCMV-IA recombinant viruses. Supernatants were harvested at selected time-points (0, 1, 3, and day 5 post-infection) and viral titres were quantified by TCID₅₀ assay (see Section 2.6.1.6). As shown in Figure 4.11, levels of progeny virus production and kinetics of replication of the MCMV-IA recombinant viruses were comparable to MCMV-WT. Although all recombinant MCMV-IA viruses trended towards a slightly lower replication rate, this difference was not statistically significant (NP: $P= 0.5052$, PA: $P= 0.3728$ and NS2: $P= 0.4224$). These results indicated that insertion of influenza epitopes into the IE2 ORF does not negatively affect MCMV replication *in vitro*, which is consistent with other published studies (Karrer *et al.*, 2004; Tsuda *et al.*, 2011).

(A)



(B)



(C)

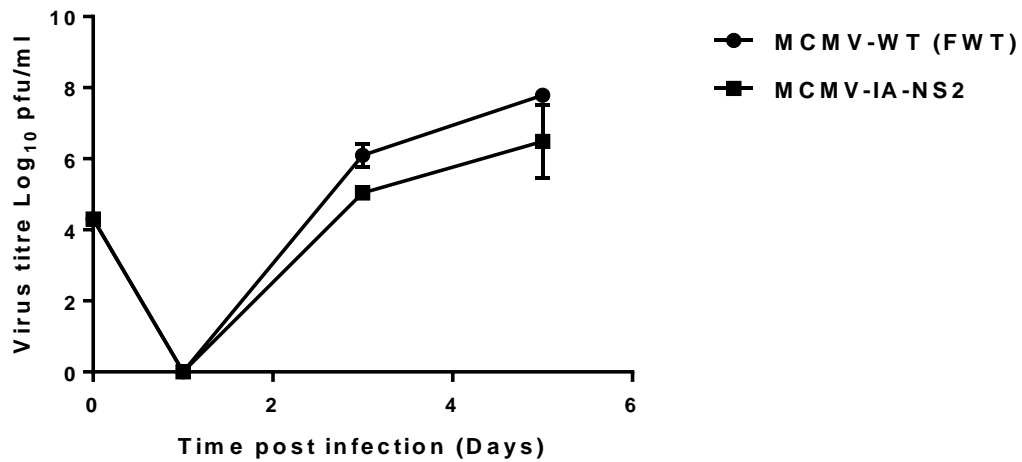


Figure 4.11 Replication of recombinant MCMV-IA vectors compared to its parental MCMV-WT (FWT) virus. MEF cells were infected with: (A) MCMV-IA-NP, (B) MCMV-IA-PA, (C) AMCMV-IA-NS2 or MCMV-WT at an MOI of 0.1 PFU/cell. At the time points indicated, supernatants were collected and virus levels were determined by TCID₅₀ assay on MEF cells. Results are the mean of two separate experiments, with samples measured in triplicate. Error bars show the standard deviations (Note: each recombinant is compared to the same MCMV-WT titration).

4.2.2 Induction of CD8⁺ T cell responses using recombinant MCMV-IA virus vectors

Recombinant MCMV-IA (NP, PA, or NS2) vectors were tested in a mouse model for their ability to induce specific CD8⁺T cell immune responses against the respective IA epitopes. Immunogenicity studies were performed in H2^b-restricted mice (C57BL/6, 6-8 week old, female). Mice were inoculated intraperitoneally with a single dose of 1×10^5 PFU of a mixture of the three recombinant MCMV-IA (NP, PA, and NS2) vectors combined as a single bolus for a total of 3×10^5 PFU (1×10^5 PFU of each virus). Control groups received 3×10^5 PFU of MCMV-WT, 1×10^5 PFU of formalin-inactivated H5N1 IA virus or diluent (mock).

After 7/8 and 12 weeks, splenocytes were harvested for analysis of T cell responses by using ICS (Section 2.8.1) with a 6 hr *in vitro* stimulation by incubation with the different IA and MCMV (control) peptides (Table 4.5). Importantly, peptides used for the *in vitro* stimulation were both those homologous to the PR8 (A/Puerto Rico/8/1934 H1N1) epitope present within the recombinant MCMV-IA viruses, as well as peptides representing the heterologous versions from an additional two different IA virus subtypes H3N1 (A/Swine/Minnesota/00395/2004) and H5N1 (A/Vietnam/1194/2004). In some cases, (for example PA₂₂₄₋₂₃₃) the epitope sequence is conserved across all three IA subtypes, such that measurement of T cell responses against a single peptide also represents the heterosubtypic response to this epitope for all three IA viruses. However, where sequences are divergent between different IA virus subtypes, this approach enables assessment of cross-reactive responses induced by the MCMV-IA virus encoding the PR8 epitope to the non-identical peptide of the heterologous virus. Together, this approach thereby enables both homo- as well as heterosubtypic IA virus T cell responses to be determined. A schematic of the vaccination and T cell characterization is shown in Figure 4.12.

Table 4.5 Influenza A and MCMV H2^b- restricted peptides, used in ICS assay for induction of T cell responses. (Source: Influenza Research Database (IRD))

H2 ^b - Restricted Peptides	Sequence	MHC specificity
IA NP ₃₆₆₋₃₇₄ (PR8+X31)	ASNENMETM	H-2D ^b
IA NP ₃₆₆₋₃₇₄ (H5N1Viet)	ASNENMEAM	H-2D ^b
IA PA ₂₂₄₋₂₃₃ (PR8+ X31+ H5N1Viet)	SSLENFRAYV	H-2D ^b & H-2K ^b
IA NS ₂₁₁₄₋₁₂₁ (PR8+X31)	RTFSFQLI	H-2D ^b & H-2K ^b
IA NS ₂₁₁₄₋₁₂₁ (H5N1Viet)	RAFSFQLI	H-2D ^b & H-2K ^b
IA PB ₁₇₀₃₋₇₁₁ (PR8+ X31+ H5N1Viet)*	SSYRRPVGI	H-2K ^b
MCMV M38**	HGIRNASFI	H-2K ^b
MCMV M45***	SSPPMFRV	H-2D ^b

* PB: Not present in MCMV-IAV vaccine construct

** M38: Endogenous MCMV peptide-inflationary

***M45: Endogenous MCMV peptide-non-inflationary

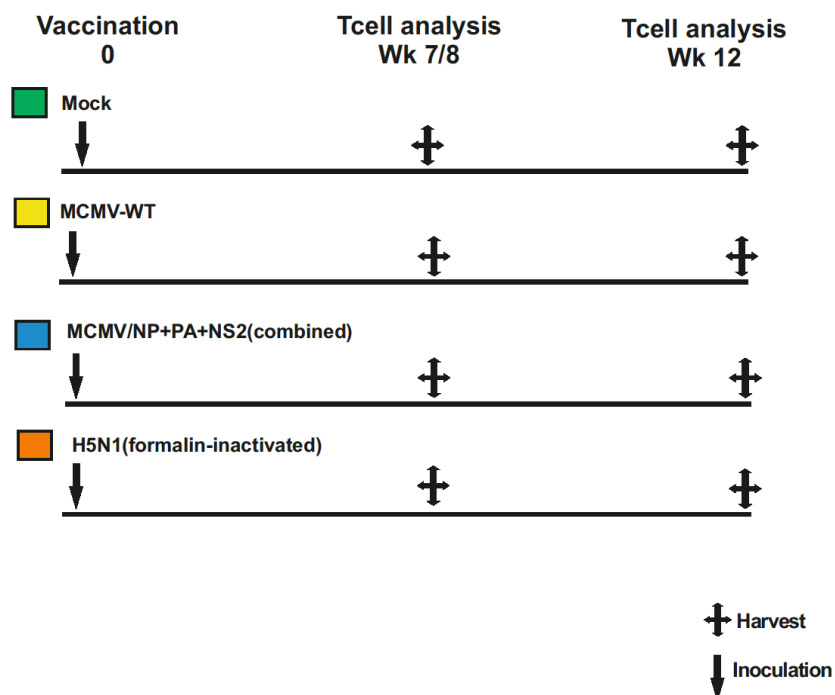


Figure 4.12 Schematic showing MCV-IA vaccinated mouse groups. C57BL/6 ($H2^b$ -restricted, 6-8 weeks old female mice) were inoculated intraperitoneally with a single dose of 1×10^5 PFU of each of the three recombinant MCMV-IA-(NP, PA and NS2) vectors combined for a total of 3×10^5 PFU (1×10^5 PFU of each virus). Control groups received 3×10^5 PFU of MCMV-WT, 1×10^5 PFU of diluent (Mock) or formalin-inactivated H5N1 IA. At weeks 8 and 12 splenocytes together with lungs for week 12 only were harvested for analysis of T cell responses.

Results are shown in Figure 4.13 through Figure 4.18. By week 7/8 post-inoculation, IA-specific T cell responses were observed against all homosubtypic IA epitopes in MCMV-IA vaccinated mice (Figures 4.13 - 4.14). Average homosubtypic responses against the PR8 peptides were as follows (n=4 group): NP 0.09 (+/- 0.08), PA 0.11 (+/- 0.05) and NS2 0.03 (+/- 0.01). We have determined a cut-off value for a positive response as 0.02 and above, which is based on the mean of all responses against the IA epitopes observed for MCMV-WT mice + 3 SD. These responses were shown to be statistically significant (t-test, 2-tailed)

when compared against either Mock or MCMV-WT control mouse groups (n=4) for PA (0.003) and NS2 (0.002), and trending towards significance for NP (p=0.056) (p-values presented are those compared against MCMV-WT). Statistically significant cross-reactive heterosubtypic responses were observed against PA (where the epitope is completely conserved across the three IA subtypes, and therefore is identical to homosubtypic, PR8 responses), as well as NP, which differs between IA subtypes by a single amino acid residue (see Table 4.5).

In contrast to earlier published studies, responses directed against the IA epitopes were an order of 10-fold lower than had been seen using comparable recombinant MCMV viruses expressing the IA virus NP₃₆₆ epitope (Karrer *et al.*, 2004), as well as other H2b-restricted CTL epitopes from either Ebola virus or human prostate specific antigen (PSA) fused to the IE2 carboxyl-terminus (Tsuda *et al.*, 2011; Tsuda *et al.*, 2015); (Figures 4.13- 4.14). Immune responses against H2b-restricted epitopes from endogenous MCMV proteins (M38 and M45) were present in mouse groups receiving either the MCMV-IAV (M38 1.9 +/- 0.65) or MCMV-WT (2.4 +/- 1.004) viruses, where levels were high and comparable to those presented in previous published studies. M38 responses were statistically identical between MCMV-IAV and MCMV-WT groups. M45 responses although at levels comparable to those seen in studies were indicated to be significantly lower in the MCMV-IAV compared to MCMV-WT group.

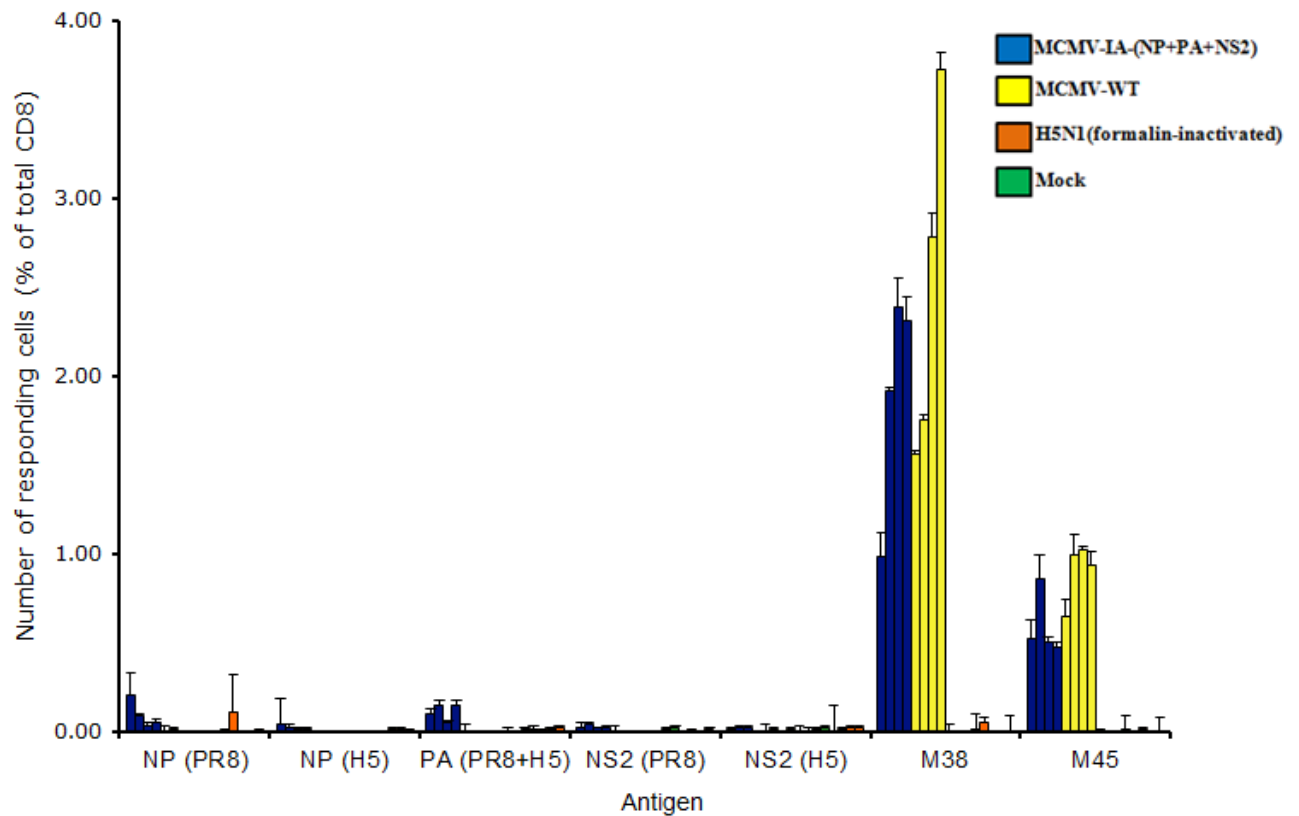


Figure 4.13 T cells responses at week 7/8 following vaccination with MCMV-IA (NP+PA+NS2) vector. C57BL/6 ($H2^b$ -restricted, 6-8 weeks old) female mice were immunized using a single i.p. dose of 1×10^5 PFU of the indicated MCMV-IA vector(s). Mice receiving the combination of the 3 MCMV IA vectors were inoculated with 1×10^5 PFU of each vector as a single i.p. bolus for a total of 3×10^5 PFU. Control groups received MCMV-WT (3×10^5 PFU), diluent (Mock) or formalin-inactivated H5N1. At weeks 7/8, splenocytes were harvested for analysis of T cell responses. T cells were analysed via using ICS with a 6 hour incubation in the presence of BFA with peptides. All MCMV-IA-(NP+NS2+PA) immunised mice ($n=4$) showed diminished T cell responses against flu target antigen when administrated as a mixture. Error bars show the s.d.

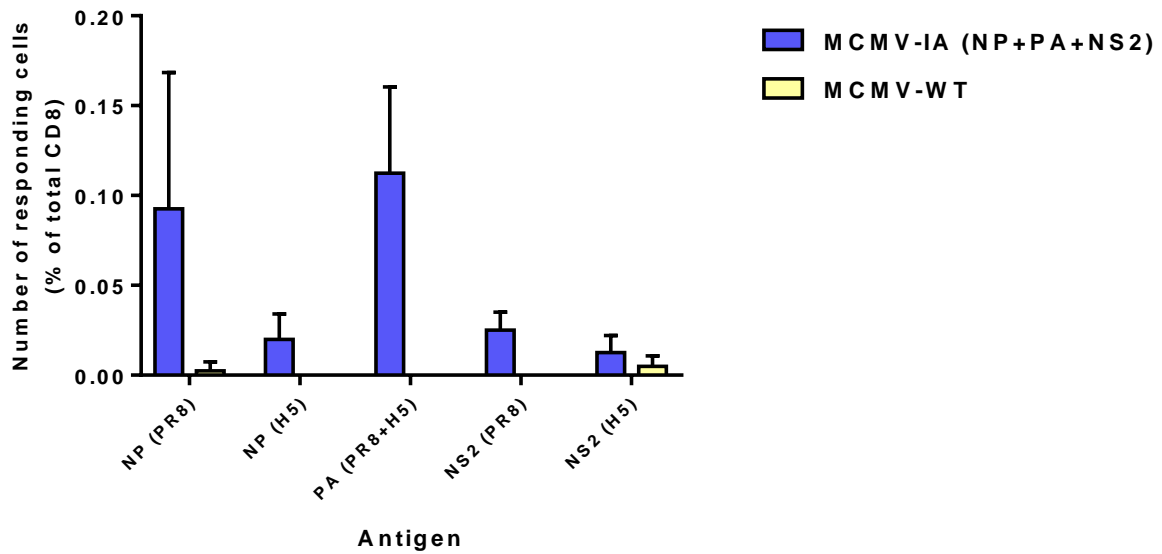


Figure 4.14 Kinetic analysis of T cells responses to MCMV-IA-(NP+PA+NS2) at week 7/8. C57BL/6 H2^b-restricted mice (N=4) were immunized using a single i.p. dose of 1×10^5 PFU of the indicated MCMV-IAV vector(s). Mice receiving the combination of the 3 MCMV IA vectors were inoculated with 1×10^5 PFU of each vector combined in a single i.p. bolus for a total of 3×10^5 PFU. Control group received MCMV-WT (3×10^5 PFU). At time indicated, splenocytes were harvested for analysis of T cell responses, ICS with a 6 hour incubation in the presence of BFA with the flu peptides. All MCMV-IA-(NP+NS2+PA) immunised mice (n= 4) showed diminished T cell responses against flu target antigen when administrated as a mixture. Error bars show the s.d.

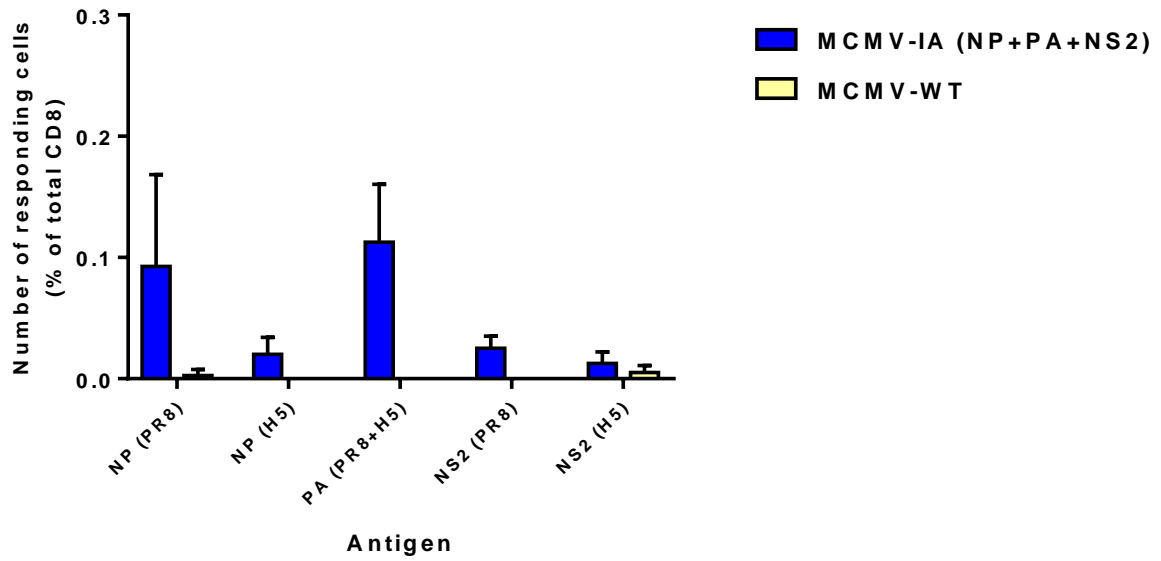


Figure 4.15 MCMV-IA-(NP+PA+NS2) induce low level of IA-specific T cell response in C57BL/6 mice at week 7/8. C57BL/6 H2^b-restricted mice (N=4) were immunized i.p.using a combination of the 3 MCMV IA vectors (each 1×10^5 PFU) for a total of 3×10^5 PFU as a single bolus. Control group (MCMV-WT) received 3×10^5 PFU. At time indicated, splenocytes were harvested for analysis of T cell responses, using ICS with a 6 hour incubation in the presence of BFA with the flu peptides. The average of all MCMV-IA-(NP+NS2+PA) immunised mice showed diminished T cell responses against flu target antigen when administrated as a mixture. Error bars show the s.d.

At week 12, T cell responses were analyzed in the different mouse groups (n=6) in both spleen as well as lung. Due to the lower level of T cells, lungs from groups of 3 mice were pooled for analysis of this organ site. The results are shown in Figures 4.16 through 4.18. IA-specific T cell responses were observed against homosubtypic IA NP (0.05 +/- 0.02) and PA (0.08 +/- 0.02) epitopes in MCMV-IAV vaccinated mice (Figures 4.16 and 4.18). Responses were no longer detected against the NS2 epitope, which had fallen below the detection cut-off (0.01 +/- 0.01). These responses were shown to be statistically significant (t-test, 2-tailed) when compared against either Mock or MCMV-WT control mouse groups (n=6) for PA ($p < 0.000001$) and NS2 (0.01).

Responses against NP were now shown to be statistically significant ($p < 0.0001$) (p-values presented are those compared against MCMV-WT). Statistically significant cross-reactive heterosubtypic responses were observed against PA (where the epitope is completely conserved across the three IA subtypes, and therefore is identical to homosubtypic, PR8 responses). However, the statistically significant responses against NP and NS2, which had been observed at week 7/8 were no longer present. It is important to note that although responses against H2^b restricted epitope from endogenous MCMV protein (M38) which had been observed at week 7/8 was high and comparable to the MCMV-WT, at week 12 these responses had fallen in MCMV-IAV immunized mice (0.51 +/- 0.2) compared to the MCMV-WT group (1.24 +/- 0.52). These responses were statistically significant (t-test, 2-tail; $p < 0.01$) when compared to the MCMV-WT control group (Figures 4.16 and 4.18). At week 12, PB1 peptide (not present in MCMV-IA vaccine construct) was included as another control.

At week 12 post-inoculation, in lung tissue, IA specific T-cell responses to IA PA (0.025 +/- 0.007) epitope in MCMV-IA vaccinated mice (Figure 4.18) were shown to be statistically significant when compared to the Mock or MCMV-WT control mouse group ($P = 0.03$).

However T cell responses against both homo and heterosubtypic IA NP and NS2 were no longer detected against the NP and NS2 epitopes, all had fallen down below the detection cut-off (0.01 +/- 0.01; Figure 4.18).

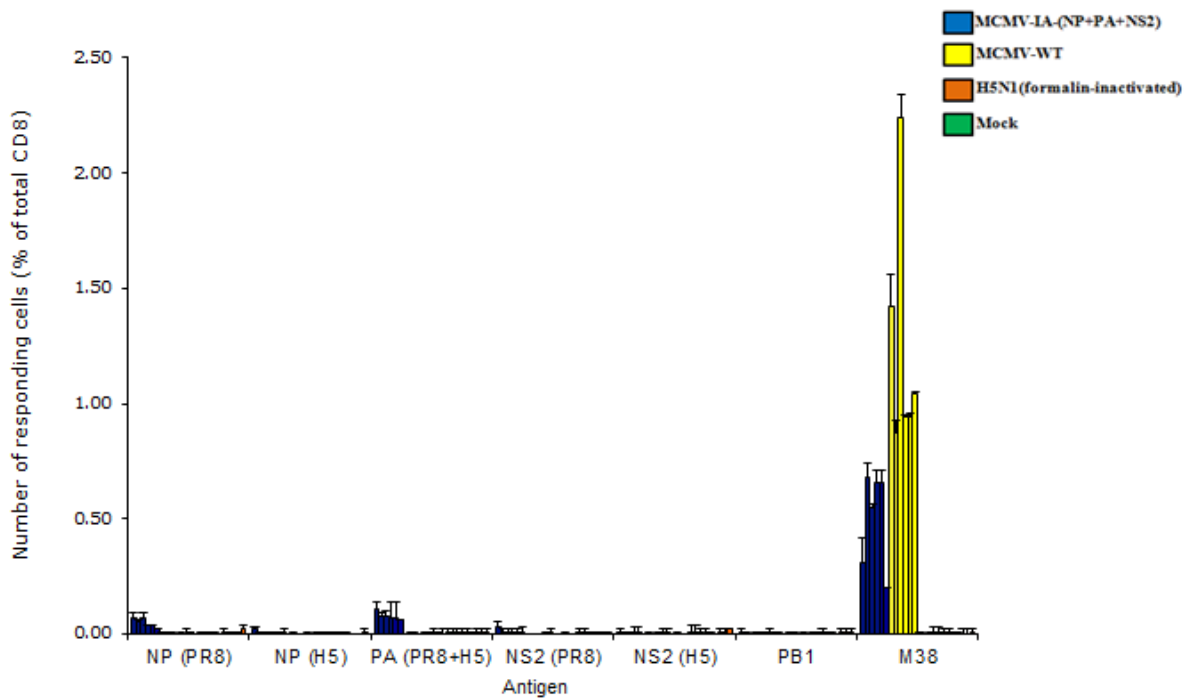


Figure 4.16 T cells responses at week 12 following vaccination with MCMV-IA (NP+PA+NS2) vector. C57BL/6 ($H2^b$ -restricted, 6-8 weeks old) female mice were immunized using a single i.p. dose of 1×10^5 PFU of the indicated MCMV-IA vector(s). Mice receiving the combination of the 3 MCMV IA vectors were inoculated with 1×10^5 PFU of each vector as a single i.p. bolus for a total of 3×10^5 PFU. Control groups received MCMV-WT (3×10^5 PFU), diluent (Mock) or formalin-inactivated H5N1. At weeks 12, splenocytes were harvested for analysis of T cell responses. T cells were analysed via using ICS with a 6 hour incubation in the presence of BFA with peptides. All MCMV-IA-(NP+NS2+PA) immunised mice (n= 6) showed diminished T cell responses against flu target antigen when administrated as a mixture. Error bars show the s.d.

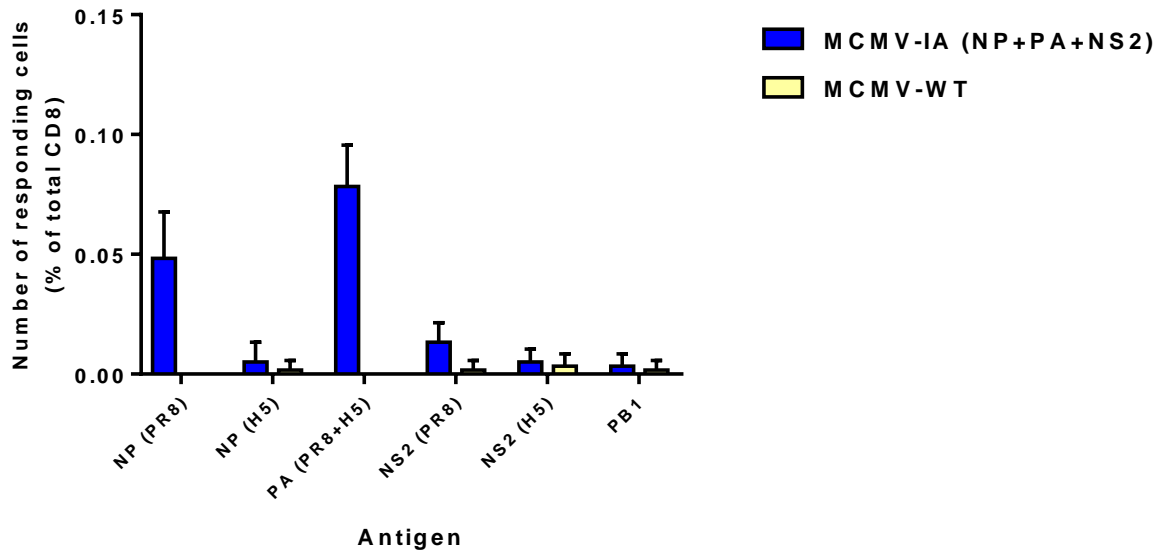


Figure 4.17 Kinetic analysis of T cells responses to MCMV-IA-(NP+PA+NS2) at week 12. C57BL/6 H2^b-restricted mice (N=4) were immunized using a single i.p. dose of 1×10^5 PFU of the indicated MCMV-IA vector(s). Mice receiving the combination of the 3 MCMV IA vectors were inoculated with 1×10^5 PFU of each vector as a single i.p. bolus for a total of 3×10^5 PFU. Control group received MCMV-WT (3×10^5 PFU). At time indicated, splenocytes were harvested for analysis of T cell responses, ICS with a 6 hour incubation in the presence of BFA with the flu peptides. All MCMV-IA-(NP+NS2+PA) immunised mice (n= 6) showed diminished T cell responses against flu target antigen when administrated as a mixture. Error bars show the s.d.

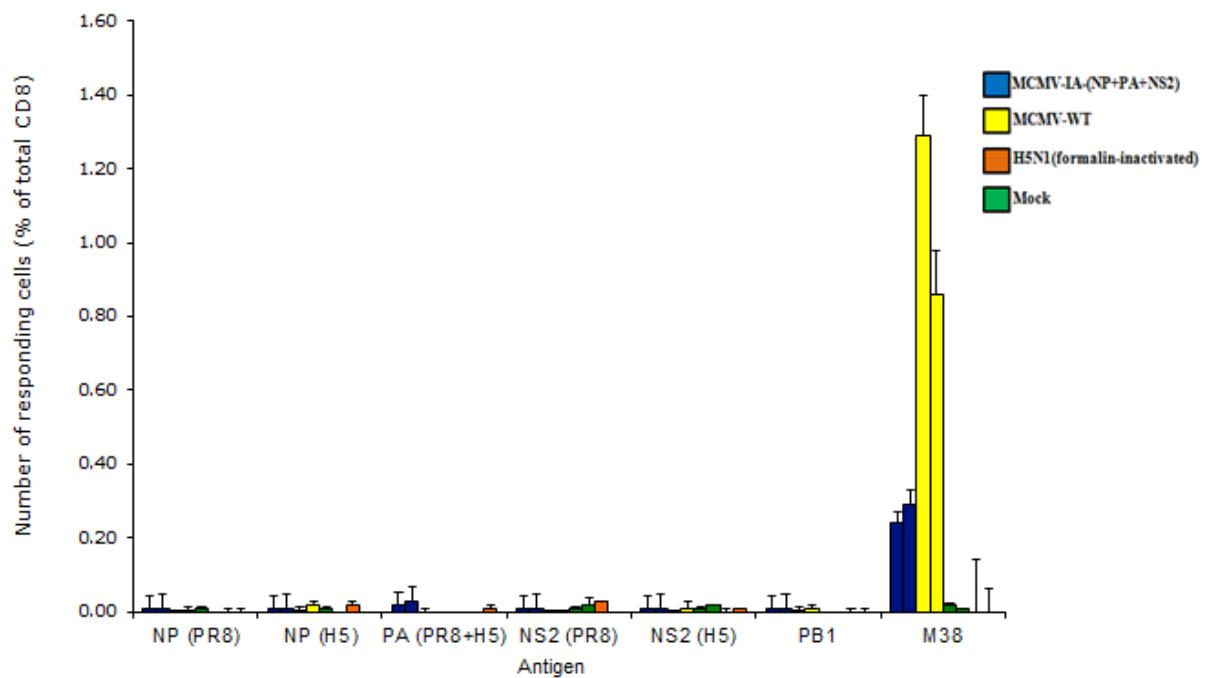


Figure 4.18 T cells responses at week 12 following vaccination with MCMV-IA (NP+PA+NS2) vector. C57BL/6 ($H2^b$ -restricted, 6-8 weeks old) female mice were immunized using a single i.p. dose of 1×10^5 PFU of the indicated MCMV-IA vector(s). Mice receiving the combination of the 3 MCMV IA vectors were inoculated with 1×10^5 PFU of each vector as a single i.p. bolus for a total of 3×10^5 PFU. Control groups received MCMV-WT (3×10^5 PFU), diluent (Mock) or formalin-inactivated H5N1. At week 12, lungs were harvested for analysis of T cell responses. T cells were analysed via using ICS with a 6 hour incubation in the presence of BFA with peptides. All MCMV-IA-(NP+NS2+PA) immunised mice showed diminished T cell responses against flu target antigen when administrated as a mixture. Error bars show the s.d.

4.2.3 Construction of recombinant MCMV-IA-NP within a different MCMV-WT background MCMV-WT (F5)

There are two possibilities to account for the lowered T cell response observed during the present studies using the MCMV-IA viruses. The first is a biological explanation, wherein the presence of CTL epitopes for presentation by MHC-I molecules of a limited number of APCs would result in competition between the individual CTL epitopes thereby diminishing responses when used as a mixture for vaccination. Such a phenomenon has been observed previously for recombinant MCMV vaccines, whereby ‘inflationary’ responses against the major endogenous T cell epitopes are diminished by inclusion of a second heterologous competing CTL epitope in a recombinant virus (Dekhtiarenko *et al.*, 2013; Farrington *et al.*, 2013). This is an extremely interesting biological phenomenon that also suggests that the APC involved in priming such responses are limiting when administered via the i.p. route. A second technical possibility, which would be less interesting from the biological context, is that an unexpected mutation in the MCMV genome may be responsible. However, this may not be the case since we get normal immune response against M38 in MCMV-WT control. These immune responses have been diminished in MCMV-IA- (NP+PA+NS2) version. This indicates that the competition is the more obvious reason behind low T cell responses as both viruses have the same genetic background.

To discriminate between these two hypotheses we constructed an additional recombinant MCMV-IAV vector that encodes the same NP epitope that we used for generation of the previous MCMV-IAV vectors with the exception of the parental genetic background. For generation of this vector we used the same genetic background as was used for development of recombinant MCMV-EBOV-NP (Tsuda *et al.*, 2011). In order to address this hypothesis, an additional recombinant MCMV-IAV vector expressing the H2^b-restricted T cell epitope from influenza A conserved structural proteins NP₃₆₆₋₃₇₄ (ASNENMETM), was generated in

this study. As described previously, MCMV-IAV vectors were constructed using MCMV (Smith strain) BAC pSMfr3 in which the natural killer cell activating m157 MCM gene has been deleted (pSMfr3Δ m157).

This MCMV-IA-NP (F5) was constructed exactly as described above (Section 4.2.1), using E/T homologous recombination to insert the NP epitope to the carboxyl terminus of IE2 locus of the MCMV-WT (FWT) BAC genome (Figure 4.19). The recombinant PCR fragment (containing the NP epitope and an FRT flanked Kan^R gene) was amplified from the pOriFRT (wt) plasmid using synthetic oligonucleotides IE2-NP-(FWT)-F and IE2-NP-(FWT)-R (Table 2.2). PCR products were separated on a 1% agarose gel and as expected, yielded a band of 1.5 kb in size. The PCR fragment was spin column purified (Section 2.3.7) to remove unwanted small molecular weight products. After purification, the PCR products were run on a 1% agarose gel again to confirm the small non-specific products had been removed (Figure 4.20).

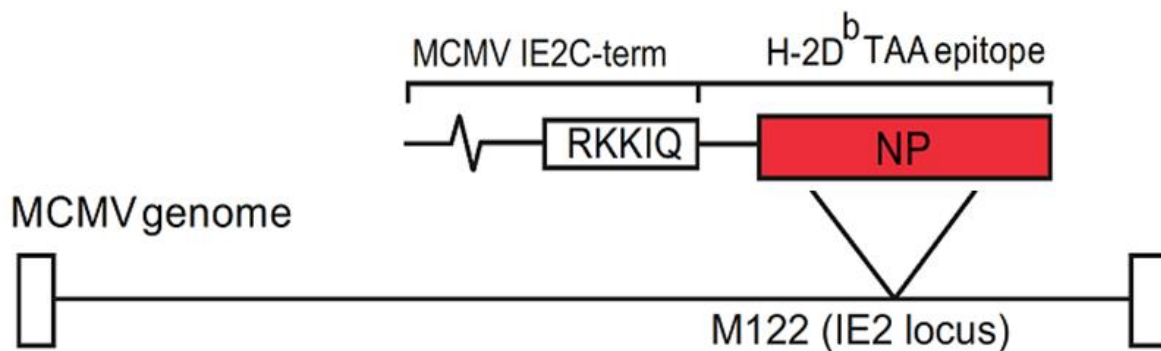
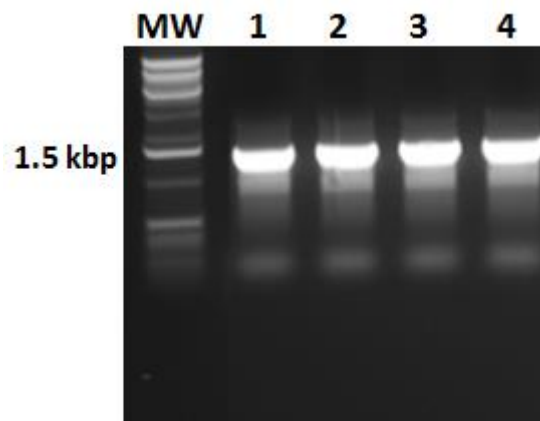


Figure 4.19 Schematic illustration of MCMV-IA-NP (F5) constructs expressing a single cytotoxic T cell (CTL) epitope. An H2^b-restricted T cell epitope from IA conserved structural proteins NP₃₆₆₋₃₇₄ (ASNENMETM) was fused in frame to the carboxyl terminus of MCMV IE2 generating the recombinant MCMV-IA-NP (F5) vaccine vectors.

(A)



(B)

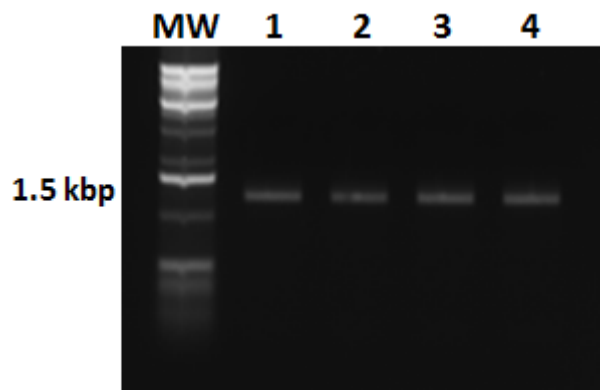


Figure 4.20 Recombination PCR fragments used for construction of MCMV-IA-NP (F5) vaccine vector. (A) DNA gel showing recombinant PCR generated fragments containing NP H2^b -restricted CD8⁺ T cell epitope from IA virus. The single DNA band at 1.5 kb shows amplification of the desired recombinant fragments. Two independent PCR reactions were prepared for each clone. (B) Gel purified PCR products confirming the extraction procedure was successful and the correct sized bands were purified. MW= 1kp molecular weight marker; lanes 1-4 = MCMV-IA-NP (F5).

The recombinant PCR products generated above were inserted into the IE2 locus of the MCMV BAC genome using E/T recombination, exactly as described above (Section 4.2.1.2) to generate MCMV-IA-NP(F5) recombinant BACs (in this alternate MCMV-WT genetic background). After the recombination procedure, the bacteria were plated out onto Kan/Cam plates to select clones that contained recombinant BACs. The colonies were counted (Table 4.6), and eight colonies were selected for further characterization by restriction digest (to confirm genomic integrity; Figure 4.21). After confirmation of genomic integrity, the Kan^R marker was excised as described above (Section 2.5.1.3), genomic integrity was confirmed and the presence of the NP epitope by PCR (Figure 4.22). Sanger sequencing of the amplified PCR product was used to confirm presence of the desired NP epitope (Figure 4.23), as described above (Section 2.3.8).

Table 4.6 Numbers of recombinat MCMV-IA-NP (F5) BAC clones

MCMV Construct	PCR fragment	Number of colonies
MCMV-IA-NP(F5)	1	200-250
	2	250-300

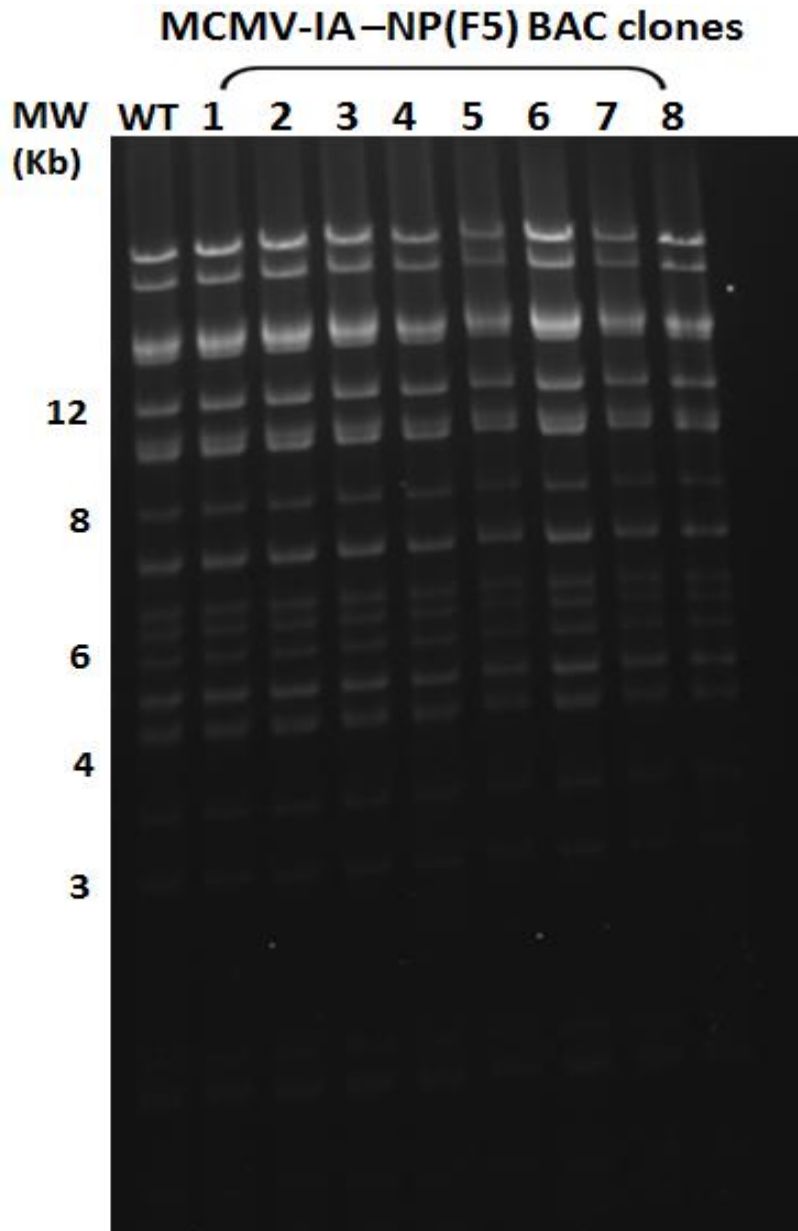


Figure 4.21 Characterization of recombinant MCMV-IA-NP (F5) BAC genome using *EcoRI* restriction enzyme digestion. MCMV-WT and eight independent clones of recombinant MCMV-IA-NP (F5) BACs were digested with *EcoRI* and the resulting fragments were separated on a 1% agarose gel for 18-20 h at 45 V, followed by visualization with 0.5 $\mu\text{g/ml}$ EtBr. Comparable restriction digestion pattern between the MCMV-IA clones and MCMV-WT (FRT F5) BAC shows the absence of any gross genomic rearrangements. Molecular size marker lane (MW) in kb is indicated.

Table 4.7 Analysis of MCMV BAC clones following excision of Kan cassette.

MCMV Construct	PCR	Clone	Selected colonies	Sensitivity to Kan
MCMV-IA-NP (F5)	1	4	25	All
	2	6	25	All

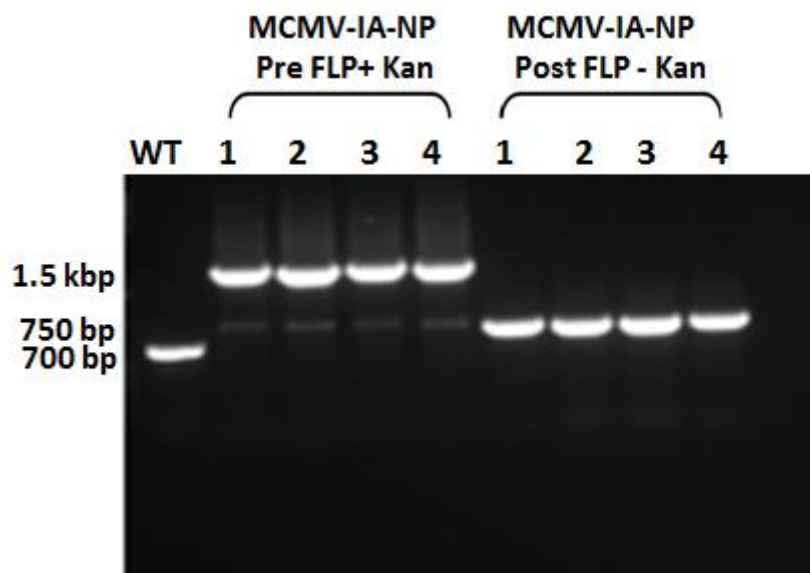


Figure 4.22 Confirming excision of Kan^R marker from MCMV-IA-NP(F5) BAC genome by PCR. BAC DNA from MCMV-WT (FRT F5) and four clones of each recombinant MCMV-IA-NP(F5) BAC (both pre and post-FLP) were screened by using PCR, using primers positioned 5` and 3`of the IE2 site targeted by recombination. PCR products were separated on a 1% agarose gel for 60-90 min at 75 V, and visualized by staining with 0.5 µg/ml EtBr. PCR of pre-FLP MCMV-IA-NP (F5), and post-FLP MCMV-IA-NP (F5) yield PCR products of 1.5 kb and 750bp, respectively. Molecular size marker (MW) in bp is indicated.

(A)

MCMV-IA-NP (F5) BAC clone (2-4)

```
CATCTCGGCGGGAAGGCGCTCCACCAGCAGATCTGTAAGATCAAGGGACACACCTGGTACCTG
AACGGTTGCCCGGCATGCTGAAGGACAGGGTGTTCGTCGCCACGCCGGACATCCCCCCTTC
GTCCGCCACGTGAACCTGGAACCTTTGGACATAGGTTTCTACCCATCGGTAGGGTGACCCGT
TCCCCGAGGATCCCGAGTGTGAGATGTTTATCATGGTGGACGCCGGGGGGCCATCTACGGG
CACATGTTAGATAGCGGGAAGGTGAGGAGGCTAGCTGATAACTTTGACCAGTTCATGCGGAT
GGGCACCCGGAGGGCTTATTTCAATTTCCAGATGGTTAAGGGAGATAGTCTCAACACCGAGT
ACGAGGAGACCTCGTTTGGGACCAAGAACCACGGGTTCTTTCTCTTGACCAGAGACCTGGTG
ACCGTCAGGAAGAAGATTCAGGGTGCCAGCAACGAGAACATGGAGACCATGTGA
```

(B)

MCMV-IA-NP (F5) BAC clone(4-16)

```
TCCTGCAGTCCTTCGGTAGGGAAGGACTCTGCAGGTGCGACAACGTCTACACCGAGGACGGCG
GCGCTCCGTACGCTACTCCCGAGGACCCCGTGCTCAAGAACATCGTGTTACGCCCATCTCG
GCGGGAAGGCGCTCCACCAGCAGATCTGTAAGATCAAGGGACACACCTGGTACCTGAACGGT
TGCCCCGGCATGCTGAAGGACAGGGTGTTCGTCGCCACGCCGGACATCCCCCCTTCGTCCGC
CACGTGAACCTGGAACCTTTGGACATAGGTTTCTACCCATCGGTAGGGTGACCCGTTCCCCC
GAGGATCCCGAGTGTGAGATGTTTATCATGGTGGACGCCGGGGGGCCATCTACGGGCACAT
GTTAGATAGCGGGAAGGTGAGGAGGCTAGCTGATAACTTTGACCAGTTCATGCGGATGGGCA
CCCGGAGGGCTTATTTCAATTTCCAGATGGTTAAGGGAGATAGTCTCAACACCGAGTACGAG
GAGACCTCGTTTGGGACCAAGAACCACGGGTTCTTTCTCTTGACCAGAGACCTGGTGACCGTC
AGGAAGAAGATTCAGGGTGCCAGCAACGAGAACATGGAGACCATGTGA
```

Figure 4.23 Confirmation of IA epitope within MCMV-IA-NP (F5) BACs via Sanger sequencing. PCR was performed on post-FLP BAC clones: (A) MCMV-AI-NP (F5) clone (2-4) and (B) MCMV-AI-NP (F5) clone (4-16). Blue text represents IE2 genome sequence, green represents represented NP epitope tag sequence and black text represents downstream MCMV genome sequence.

Two independent clones were selected for reconstitution. BAC DNA was electroporated into MEF cells as described above (Section 3.2.1.5 Table 3.5) and monolayers were monitored daily for signs of plaque development. Plaques were picked on day 5 post infection, and serially passaged five times in MEFs to allow excision of the BAC cassette from the viral genome (Section 2.6.2.3). Seed and concentrated high titre viral stocks were prepared as described above (Sections 2.6.2.4 and 2.6.2.5). PCR of viral DNA using IE2-Flank primers, was performed on recombinant viral DNA extracted from concentrated stocks (Section 2.6.2.5), to ensure that the MCMV-IA-NP (FRT WT) virus still contained the intact NP epitope (Figure 4.24) followed by sequencing of the PCR products to confirm that there were no point mutations in the epitope sequence (Figure 4.25). The titre of the recombinant MCMV-IA-NP (FRT WT) was measured and compared to both of the parental wild-type (MCMV-WT) and recombinant MCMV-EBOV-NP (5A1) using TCID50 assay (Section 2.6.2.6). Result indicated that the titre of the recombinant MCMV-IA-NP (FWT) virus was comparable to the parental wild-type virus and the recombinant MCMV-EBOV virus (Table 4.8).

Table 4.8 Reconstitution of recombinant MCMV-IA -NP BAC clones in the MEFs

MCMV-IA BAC vector	Clones	Plaque numbers
MCMV-IA-NP (FWT)	2-4	7
	4-16	8

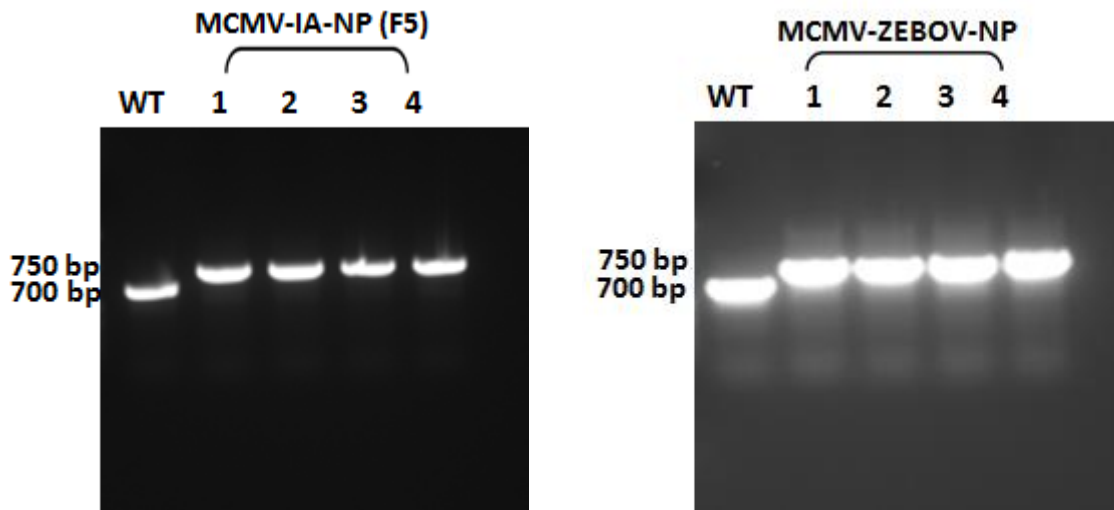


Figure 4.24 Confirming presence of NP epitope in MCMV-IA-NP (F5) virus genome by PCR. DNA was isolated from MCMV-IA-NP (F5) concentrated stock using a QIAmp kit and PCR was carried out using IE2-Flank-F and IE2-Flank-R primers. PCR products were separated on a 1% agarose gel. The presence of a 750 bp band in recombinant MCMV-IA-NP (F5) lanes (3-6) confirmed that the epitope was present, and the absence of the MCMV-WT sized band (700 bp) in the recombinant viruses lanes (1-2) confirmed the absence of WT contamination of recombinant stocks.

Table 4.9 Titres of MCMV-WT and the recombinant MCMV-IA virus vectors stocks.

Virus (MCMV)	Titre by TCID50 (PFU/cell)
MCMV-WT (F5)	1.22×10^8
MCMV-EBOV-NP (5A1)	1.10×10^8
MCMV-IA-NP (4-16)	1.08×10^8

(A)

MCMV-IA-NP (F5) PCR 1

```
CTGCAGGTGCGACAACGTCTACACCGAGGACGGCGGGCTCCGTACGCTACTCCCGAGGACCC
CGTGCTCAAGAACATCGTGTTCACGCCCATCTCGGCGGGAAGGCGCTCCACCAGCAGATCTG
TAAGATCAAGGGACACACCTGGTACCTGAACGGTTGCCCCGGCATGCTGAAGGACAGGGTGT
TCGTGCCCACGCCGGACATCCCCCCTTCGTCCGCCACGTGAACCTGGAACCTTTTGGACATA
GGTTTCTACCCATCGGTAGGGTGACCCGTTCCCCGAGGATCCCGAGTGTGAGATGTTTATCA
TGGTGGACGCCGGGGGGGCCATCTACGGGCACATGTTAGATAGCGGGAAGGTGAGGAGGCTA
GCTGATAACTTTGACCAGTTCATGCGGATGGGCACCCGGAGGGCTTATTTCAATTTCCAGAT
GGTTAAGGGAGATAGTCTCAACACCGAGTAGCGAGGAGACCTCGTTTGGGACCAAGAACCAC
GGTTCTTTCTCTTGACCAGAGACCTGGTGACCGTCAGGAAAAGATTCAGGGTGCCAGCAAC
GAGAACATGGAGACCATGTGA
```

(B)

MCMV-IA-NP (F5) PCR 2

```
AAGGCGCTCCACCAGCAGATCTGTAAGATCAAGGGACACACCTGGTACCTGAACGGTTGCCCC
GGCATGCTGAAGGACAGGGTGTTCGTGCCCACGCCGGACATCCCCCCTTCGTCCGCCACGTG
AACCTGGAACCTTTTGGACATAGGTTTCTACCCATCGGTAGGGTGACCCGTTCCCCGAGGAT
CCCGAGTGTGAGATGTTTATCATGGTGGACGCCGGGGGGGCCATCTACGGGCACATGTTAGA
TAGCGGGAAGGTGAGGAGGCTAGCTGATAACTTTGACCAGTTCATGCGGATGGGCACCCGGA
GGGCTTATTTCAATTTCCAGATGGTTAAGGGAGATAGTCTCAACACCGAGTACGAGGAGACC
TCGTTTGGGACCAAGAACCACGGGTTCTTTCTCTTGACCAGAGACCTGGTGACCGTCAGGAA
GAAGATTCAGGGTGCCAGCAACGAGAACATGGAGACCATGTGA
```

Figure 4.25 Confirmation of NP epitope within MCMV-IA-NP (F5) virus genome. PCR was performed on viral DNA isolated from concentrated viral stocks and two independent PCR products were Sanger sequenced. (A) PCR 1 and (B) PCR 2. Blue text represents IE2 genome sequence, green represents represented IA epitope tag sequence and black text represents downstream MCMV genome sequence.

Multistep growth curves were performed in a similar way as was described above (Section 4.2.1.9), to determine whether the insertion of NP into this MCMV-WT (F5) genetic background had any deleterious effects on virus replication. As described above, MEF cells were infected in triplicate at a multiplicity of infection (0.1 PFU/cell) with MCMV-WT (F5), MCMV-IA-NP (F5) or MCMV-ZEBOV-NP (5A1) virus. Supernatants were harvested at selected time points (day 0, 1, 3, and 5 post infection) and viral titres were quantified by TCID50 (Section 2.6.2.6). MCMV-ZEBOV-NP (5A1) recombinant virus (Tsuda *et al.*, 2011) was also included as an additional control. As observed previously, presence of IA-NP (F5) or ZEBOV-NP (5A1) did not affect virus replication in MEFs, with comparable levels of virus growth being observed for all strains at all time points (Figures 4.26 - 4.28). There were no significant differences in the growth of both recombinant MCMV-IA-NPs compared to the both parental wild type (MCMV-WT (FWT or F5) wild-type and recombinant MCMV-EBOV with respect to growth on MEFs ($P > 0.05$). Taken together, neither the introduction of NP epitope to the MCMV with the (F5), nor to the MCMV with the (FWT) impairs growth in fibroblast, as shown in Figure 4.28 and both mutants show both wild-type and recombinant MCMV-EBOV properties in MEF cells.

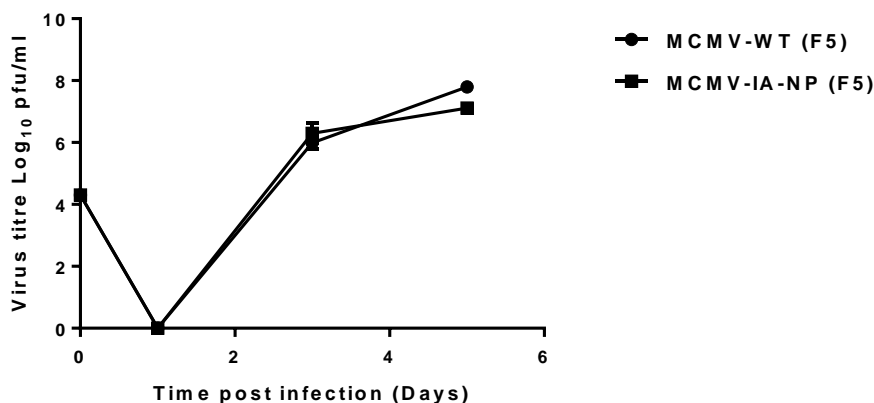


Figure 4.26 Replication of recombinant MCMV-IA-NP (F5) virus compared to its parental MCMV-WT (F5) virus. MEF cells were infected with the MCMV-IA-NP (F5) or MCMV-WT (F5) at an MOI of 0.1 PFU/cell. At the time points indicated, supernatants were collected and analysed for the presence of virus by TCID₅₀ assay on MEF cells. Results are the mean of two separate experiments, each in triplicate. Error bars representing the standard deviations. Some of the standard deviations are so small that the error bars are hidden behind the symbols representing the data points.

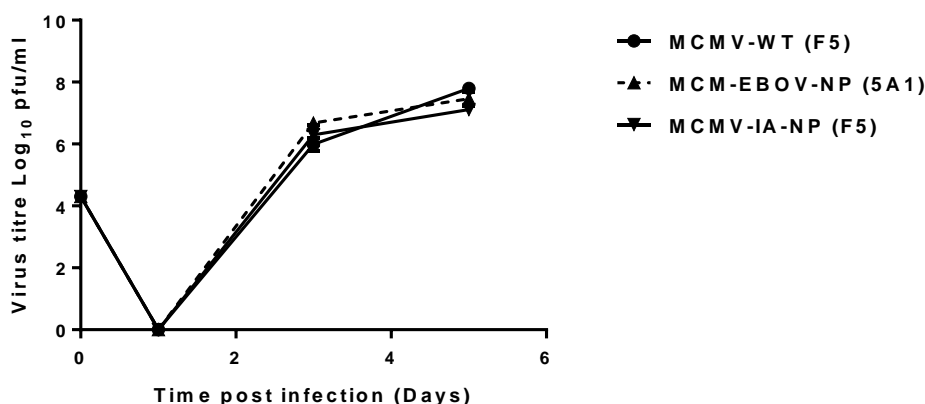


Figure 4.27 Replication of recombinant MCMV-IA-NP (F5) virus compared to its parental MCMV-WT (F5) and MCMV-EBOV-NP (5A1) virus. MEF cells were infected with the desired MCMV-IA-NP (F5), MCMV-EBOV-NP (5A1) or MCMV-WT (F5) at an MOI of 0.1 PFU/cell. At the time points indicated, supernatants were collected and analysed for the presence of virus by TCID₅₀ assay on MEF cells. Results are the mean of two separate experiments, each in triplicate. Error bars representing the standard deviations. Some of the standard deviations are so small that the error bars are hidden behind the symbols representing the data points.

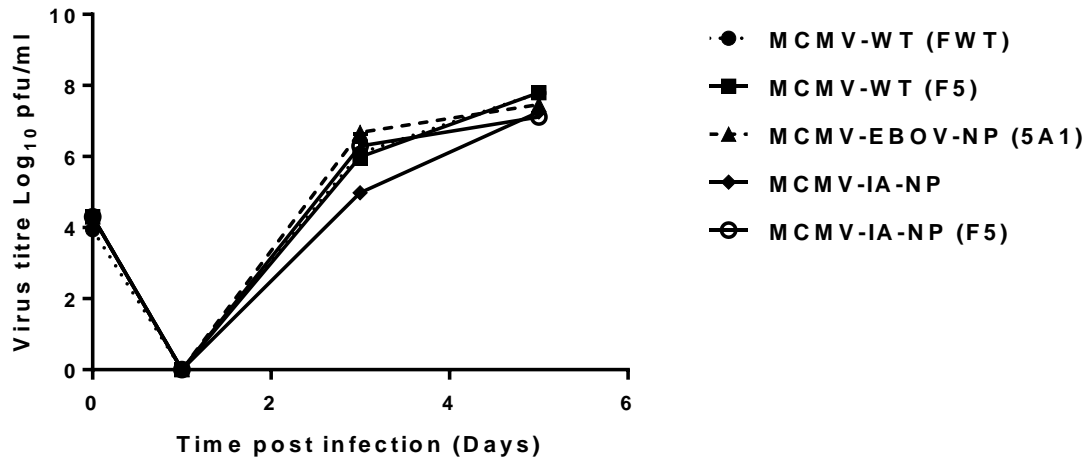


Figure 4.28 Replication of recombinant MCMV-IA-NP (F5) virus compared to its parental MCMV-WT (F5), MCMV-EBOV-NP (5A1), MCMV-WT (FWT), and the MCMV-IA-NP (FWT) virus. MEF cells were infected with the desired viruses at an MOI of 0.1 PFU/cell. At the time points indicated, supernatants were collected and analysed for the presence of virus by TCID50 assay on MEF cells. Results are the mean of two separate experiments, each in triplicate. Error bars representing the standard deviations. Some of the standard deviations are so small that the error bars are hidden behind the symbols representing the data points.

4.2.3.1 Expression of IE2 protein in the recombinant MCMV-IAV vectors

In order to explore and analyse the expression kinetics of the IE2 protein and whether fusion of the flu epitope affect the expression of the IE2 protein, MEF cells were infected with MCMV-IA-NP (F5), MCMV-IA-NP (FWT), MCMV-WT (F5), MCMV-WT (FWT) or MCMV-EBOV-NP (as a positive control). At various time post infection (8, 12, 24 and 36 hours), western blot analysis was performed as described in (Section 2.7.2). As shown in (Figure 4.29), results indicated that the expression kinetics of IE2 fused epitope in recombinant MCMV-IA-NP (F5/FWT) were comparable to those of parental MCMV-WT(F5/FWT) as well as recombinant MCMV-EBOV-NP virus. The IE2 protein with a molecular mass of 43 KDa, predominantly were produced between 0.5 and 3 hr post infection

(Messerle, Keil & Koszinowski, 1991). The 43KDa IE2 proteins were already highly expressed at 8 hr post infection and persistent throughout infection (Figure 4.29). The level of expression was monitored and no significant differences between viruses were found, indicating that the presence of the NP insertion did not affect the expression of the IE2 protein. Therefore, these results provided additional evidence for the absence of genome rearrangements during construction of recombinant MCMV-IAV vectors.

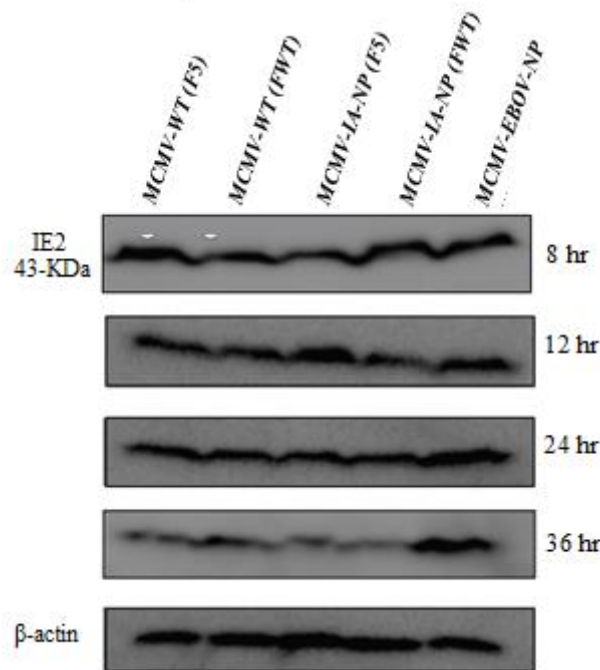


Figure 4.29 Analysis of IE2 expression of recombinant MCMV and parental wild-type via Western blot. MEF cells were infected with recombinant MCMV or wild-type viruses at MOI: 0.01. The infected cells were harvested at 8, 12, 24 and 36 hours post infection and processed for Western blotting analysis. The infected cell lysates showed that IE2 was expressed and that expression was stable over multiple time point. The number of the right panel represents the time point. While on the left hand panel represent the size of IE2 protein in kilo Daltons. Beta-actin served as a loading control.

An alternative approach to using the three MCMV/IA vectors in combination, will be to design an experiment to characterize MCMV-IA-NP (F5) immunogenicity and to determine protective efficacy against IA virus challenge. C57BL/6 mice (H2^b-restricted, 6-8 week old female; ten mice per group) will be immunized i.p. with the indicated MCMV-IA-NP (F5) vector or controls: Mock, UV-inactivated H1N1, MCMV-WT and MCMV-IA (NP+NS2+PA combined). Vaccination will consist of a single i.p. dose of 1×10^5 PFU of the indicated MCMV-IA-NP (F5) vector. Control groups will receive MCMV-WT (3×10^5 PFU), diluent (Mock), 1×10^7 PFU of UV- inactivated H1N1 (PR8) or a combination of the three MCMV/IA (NP+NS2+PA) vectors as a single i.p. bolus, giving a total of 3×10^5 PFU (1×10^5 PFU of each vector). At weeks 7-8, one mouse per each group and at week 12, four mice will be chosen for analysis of T cell responses by harvesting splenocytes. At week 14, C57BL/6 mice will be challenged with LD₅₀ of H1N1(A/Puerto Rico/8/1934) given intranasally as a 30 μ l dose (Kashima *et al.*, 2009). Following this challenge, the disease severity will be monitored on the basis of visual clinical signs (on a daily basis), as well as by rectal temperature and weight loss every other day post-IA challenge, followed by analysis of T cell responses one month post IA challenge.

4.3 Discussion

The unpredictable emergence of pandemic IA subtypes represents a constant major global health concern (Taubenberger & Morens, 2013; Zhang, Hirve & Kieny, 2017). One approach to prevent a pandemic IA strain is the development of vaccines that induce heterosubtypic immunity capable of protecting against all possible IA subtypes. Current seasonal inactivated vaccines work primarily by inducing antibodies that confer strain-specific immunity, rather than creating cross-protective (heterosubtypic) immunity against IA infection. When mismatched with circulating strains, these vaccines become less efficacious (Demicheli *et al.*, 2014). Thus, there is an urgent need to develop effective cross-protective vaccines. Evidence suggests that CD8⁺ cytotoxic T cells play a critical role in protective immunity against the influenza virus (Subbarao, Murphy & Fauci, 2006) and that a breadth of T cell immunity is essential for broad heterosubtypic protection (Gianfrani *et al.*, 2000).

An aim of the thesis was to provide initial studies in the mouse MCMV model towards development of a universal vaccine against all serotypes of IA by targeting internal structural proteins to enhance the strength of influenza virus specific ‘effector’ CD8⁺ T cell based immunity. The potential of CMV for development as such a vaccine against IA virus is supported by previous studies that have identified CMV-based vaccines as a unique vaccine platform capable of inducing high levels of ‘effector’ CD8⁺ T cells with immediate effector functions that accumulate at peripheral sites including the lungs (Hansen *et al.*, 2011; Marzi *et al.*, 2016; Tsuda *et al.*, 2011). This characteristic makes the CMV vector platform ideal for inducing immunity against IA virus, which infects the lung and can spread rapidly within the host.

We constructed a MCMV recombinant that expressed the epitope sequence of three conserved internal structural proteins (NP, NS2 and PA) of the IA virus that are less changeable than the surface glycoproteins hemagglutinin and neuraminidase (Townsend &

Skehel, 1984). The selection of conserved proteins is critical for dictating the breadth of immune response, through boosting cross-reactive immunity (Kwon *et al.*, 2014). It has been shown that about 90% of T cell responses that recognize cytotoxic T cell epitopes derived from the conserved internal proteins of IA were directed towards an NP₃₃₆ protein (Doherty *et al.*, 2006); heterosubtypic protection which is mediated by T cells can only be achieved when challenge viruses share the internal protein (NP) epitope (Zhong *et al.*, 2010). Therefore, to achieve heterosubtypic protection against distant strains of IA virus, the NP epitope was selected.

MCMV was used as an *in vivo* model for the assessment of CMV-based IA vaccines. CMVs are highly host specific with each mammalian host carrying its own species-specific CMV (Kern, 2006). However, all CMVs share common characteristic of growth, cytopathology and capacity to establish persist and latent infection. These similarities have enabled the use of MCMV infection of mice to address questions relating to human CMV (HCMV; (Krpmotic *et al.*, 2003). In addition, due to the extensive characterization of the mouse immune response, low cost of mice and the availability of reagents, the MCMV mouse model is the most extensively used *in vivo* model for HCMV. The mouse IA model is also extremely well characterized and enables extensive analysis of vaccine immunogenicity and efficacy against IA infection. Since CMV possess large-sized genomes and replicate slowly in the cell culture, in the past mutagenesis by homologous recombination was difficult and time consuming (Mocarski *et al.*, 1996). The propagation of CMV genomes as infectious BACs in *E.coli* has made the CMV genome accessible to manipulation (Messerle *et al.*, 1997).

MCMV-based IA vaccines (MCMV-IA) were designed, expressing a CD8⁺ CTL epitope from IA conserved proteins; NP₃₆₆₋₃₇₄ ASNENMETM (Andreansky *et al.*, 2005), NS₂₁₁₄₋₁₂₁ RTFSFQLI (Belz *et al.*, 2000), and PA₂₂₄₋₂₃₃ SSLENFRAYV (Belz *et al.*, 2000), all of which were fused to the IE2 protein of MCMV in separate vectors (Figure 4.1). IE2 is a

nonessential protein that has been used in a number of previous studies as a site for fusion for a variety of defined T cell epitopes for induction of T cell responses (Karrer *et al.*, 2004; Tsuda *et al.*, 2011). MCMV-IA (NP, NS2, and PA) were constructed by lambda-based E/T linear recombination (Tierney *et al.*, 2012; Tsuda *et al.*, 2011) using the pSMfr3 BAC containing the MCMV (Smith strain) genome (Messerle *et al.*, 1997). The strategy is outlined in (Figure 3.2). In order to avoid attenuation of MCMV replication by natural killer (NK) cells in the C57BL/6 mouse strain, the m157 gene of MCMV was deleted (pSMfr3Δm157). The deletion was necessary since the activation of NK cells is regulated by the cell surface receptor Ly49H, which encodes both activator and inhibitor receptors (Arase *et al.*, 2002). The m157 gene which has MHC class I molecule structure, is recognized by the Ly49H activate receptor. Binding of m157 to host Ly49H NK receptors delivers an activating signal to NK cells as a result limiting viral replication (Pyzik *et al.*, 2011).

Following identification of recombinant MCMV BACs, restriction enzyme digestion of the BAC DNA which was carried out in order to determine successful recombination as well as to confirm genome integrity prior to the reconstitution of mutant viral progeny, showed no gross genomic rearrangement compared to the WT parental BAC (Figures 4.4 and 4.6). Next, the biological properties of the mutant MCMV were analysed upon the reconstitution of the virus into the MEF cells. The virus reconstitution was achieved through direct transfection of MEFs by invasive bacteria carrying BAC DNA via electroporation. Since the presence of the BAC sequence in the viral genome interferes with biological properties of MCMV *in vitro* and potentially causes unpredictable effects *in vivo* (Wagner *et al.*, 1999) the BAC sequence was removed. The results of experiments performed to remove BAC sequence from the mutant MCMV-IA genome showed that removal of this sequence had no influence on the genomic integrity and stability of the recombinant viruses, with the continued stable expression of the IA epitope within mutant viral genome. Our data from the growth kinetics

assay *in vitro* indicated that this insertion of IA epitope has no effect on virus growth *in vitro* in MEF cells. Furthermore, recombinant MCMV-IA (NP, PA or NS2) vector showed similar growth kinetics to the MCMV-WT (FWT) *in vitro* (Figures 4.11 - 4.13).

Using this panel of MCMV-IAV viruses we then performed immunogenicity studies in C57BL/6 H2^b-restricted mice. It has previously been shown that CMV-based vaccine vectors have the ability to induce significant levels of CD8⁺ CTL responses against target pathogens (Dekhtiarenko *et al.*, 2013; Hansen *et al.*, 2011; Tsuda *et al.*, 2011). In addition, it has been shown in the case of C57BL/6 mice infected with the recombinant MCMV expressing the CD8⁺ T cell epitope from the nucleoprotein of the *Zaire Ebola* virus (fused into the IE2 protein comparable to the IA epitopes), that the recombinant MCMV successfully induced considerable levels of CD8⁺ T cells (1 to 2% of total CD8⁺ T cells); (Tsuda *et al.*, 2011). However, this high level of CD8⁺ T cell was not observed in this present study (Figure 4. 14), which showed an order of magnitude lower levels.

There are two possible explanations that would explain the low CD8⁺ T-cell responses in this present study. Firstly, there is possibility that the low responses may be due to unexpected mutation in the MCMV genome that then resulted in diminution of T cell response. The second possibility is associated with use of a combination of the three constructed vectors (MCMV-IA- NP, PA and NS2), which in the present study were used together as a mixture for the mice vaccination. In this model, the use of a mixture would result in competition between these three epitopes in terms of their presentation on the antigen presenting cells (APCs), consequently causing diminished CD8⁺ T cell responses as compared to responses when administered individually (Tsuda *et al.*, 2011). This is in agreement with a recent study by Dekhtiarenko and colleagues who used an MCMV recombinant containing a single CD8⁺ T cell epitope (gB) from HSV-1 (SSIEFARL, linked to the C terminus of either M45 or IE2 gene), to examine the role of gene expression and antigen competition in CMV T cell

immunity. They revealed that the mice that were infected with either recombinant MCMV (M45 or IE2) resulted in strong CD8⁺ T cell responses when the peptide was expressed in each case, while in case of multiple target antigens, expressed by the same recombinant MCMV/HSV-1, suboptimal immune responses to the target antigens resulted. This may have been due to competition between T cells for recognition of antigens, potentially limiting its protective capacity (Dekhtiarenko *et al.*, 2013).

Similarly, Farrington *et al.* (2013) showed that a recombinant MCMV encoding an immunodominant heterologous SIINFEKL peptide fused to the C terminus of IE2 resulted in the SIINFEKL epitope being a completely immunodominant epitope, which was associated with high CD8⁺ T cell responses. However, responses against endogenous MCMV-derived epitopes that were normally inflationary for WT-MCMV no longer exhibited an inflationary phenotype. Importantly, suppression of these inflationary responses against the endogenous epitopes was observed only when SIINFEKL was co-expressed within the same MCMV recombinant. Inhibition was not observed when mice were co-infected with separate MCMV-WT and recombinant MCMVs. This observation implies that when different cells in the same mice can present endogenous epitopes in the absence of the SIINFEKL epitope, the SIINFEKL epitope had no inhibitory influence on endogenous responses. Thus, MCMV-WT infected APCs have the ability to present MCMV epitopes which T cells can recognise and which are able to inflate with SIINFEKL response. However, when both SIINFEKL and endogenous epitopes were encoded by the same virus and therefore necessarily expressed on the same APC, induction of T cells to SIINFEKL out-competed induction of those against endogenous antigens. This may have been due to the cells possessing more available Ag or alternatively because they were able to access the Ag more efficiently (Farrington *et al.*, 2013).

Thus, this supports the hypothesis that competition between T cell clones for antigens at the level of the APC have a significant role in inflationary responses during MCMV infection, based on the possibility that the combined MCMV-IA (NP+PA+ NS2) vector dose is giving far lower CD8⁺ T cell responses than have been observed previously with other CMV recombinant vectors when used singly (Tsuda *et al.*, 2011).

To address the possible technical issue that probably are responsible for diminish T cell responses that observed using the MCMV-IAV vectors, new recombinant MCMV-IAV encoding NP epitope of NP protein were constructed. However this may not be the case, since our results indicated the normal T cell responses against M38 of the MCMV-WT (Figure 4.14) and then this T cell responses were diminished using the MCMV-IAV vector. Decrease T cell responses against M38 in the MCMV-IA virus compare to the MCMV-WT indicates that the MCMV-WT background is fine (Figure 4.14 & Tables 4.6 - 4.7). The low T cell responses probably not due to a defective background may be due to the competition of epitopes on the surface of APC.

In addition, binding peptides to the MHC molecules is important for the T cell activation. Peptides that are more abundantly presented, due to the processing, expression or binding affinity are more likely to succeed to induce T cell response (Yewdell, 2006). So another evidence to explain the low T cell responses is due to the competition between the epitopes is that IA epitopes (PA and NS2) and the MCMV-derived inflationary epitope (M38), all of which are presented by binding to H-2K^b alleli this probably caused the competition (Table 4.5),

To avoid the competing epitopes being recognized on the same APC (which may be caused by using three vectors combined in a single dose, administrating MCMV-IAV encoding NP epitope individually, since MHC binding affinity of NP₃₆₆ and inflationary M38 peptides are

different (H-2D^b or H-2K^b, respectively; Table 4.5). May results in presentation of IA internal protein individually on the surface of APCs, thus avoiding presentation on the same APCs consequently will avoid competition between them.

As described previously, the m157 gene of the parental MCMV that was used in this study has been deleted by homologous recombination using FRT sites (FWT) and for construction of recombinant MCMV-IA-(NP, PA, or NS2) vectors (F5; a different version of FRT sites) has been used, since they were two different version of FRT they cannot combine with each other.

For the generation of the new MCMV-IA-NP construct, we used a different genetic background using plasmid template that contain, (FRTWT) and from which the m157 has been deleted using FRT 5 (F5). This genetic background is the same that has been used for construction of recombinant MCMV-EBOV-NP (5A1) which was developed by other members of the Jarvis lab (Tsuda *et al.*, 2011).

The new MCMV-IA-NP was constructed as detailed in the generation of previous MCMV-IAV vectors. Only the NP epitope was assayed, since the research to date has tended to focus on the NP protein rather than other internal conserved proteins. It has been shown that heterosubtypic protection which is mediated by T cell responses can only be achieved when inoculum and challenge viruses contain the NP₃₆₆ epitope (Zhong *et al.*, 2010). It has also been shown that 90% of CD8⁺ T-cell responses are directed to an NP₃₆₆ epitope (Kwon *et al.*, 2014). In addition, NP is predominant during primary and secondary influenza infection (Flynn *et al.*, 1999). Moreover, as a result of using a recombinant MCMV expressing IA virus nucleoprotein (NP₃₆₆₋₃₇₄) epitope that was fused to the IE2 gene in C terminus showed that this recombinant virus was able to induce T cell response to the NP epitope and that after

IA virus infection, NP specific CD8⁺ T cells rapidly increased in number and have capability to provide protection against influenza virus challenge (Karrer *et al.*, 2004).

In order to assess the efficacy of recombinant MCMV-IAV vectors *in vivo*, an alternative approach to characterize immunogenicity and determine protective efficacy against IA virus challenge, by inoculation of C57BL/6 mice with the MCMV-IA-NP(F5) alone or controls Mock, UV-inactivated H1N1, MCMV-IA-(NP+PA+NS2) combined, MCMV-EBOV-NP and both parental MCMV-WT (F5 and FWT).

In summary, a MCMV-based IA vaccine expressing a CD8⁺ CTL epitope from three conserved proteins (NP, PA and NS2) was designed by using lambda-based linear recombination with a BAC contained within the MCMV genome. Characterization of MCMV vectors *in vitro* for genomic stability and IA epitope sequence integrity showed stability of the IA epitope expression within MCMV genome. Although the CD8⁺ T cell response were not as were expected, on the basis of the evidence presented above one can predict that low CD8⁺ T cell responses are likely to have occurred due to the competition between T cell clones for immune responses which would potentially limit their protective activity. Use of a single clone vector (MCMV-IA-NP) to present the NP epitope individually on the surface of APCs may avoid this competition.

Chapter Five

Conclusions And Future Direction

5. Conclusion and Future Direction

Vaccines are widely regarded as one of the most successful public health interventions to date. Many approaches have been used to design variant vaccines against pathogens, among them recombinant viral vectors. Various recombinant viral vectors were created and evaluated for vaccine and immunotherapeutic applications. Several studies have shown effectiveness of CMV vectors at inducing protective immunity against various pathogens. As such, recombinant MCMV vector has also been shown to induce protective immunity against various pathogens (i.e. express antigens from) like highly virulent Ebola virus and Mycobacterium tuberculosis (Tierney *et al.*, 2012; Tsuda *et al.*, 2011; Tsuda *et al.*, 2015). In this dissertation, the MCMV mouse model is used for initial investigation into development of CMV as a vaccine platform. MCMV, a natural pathogen isolated from mice, is a *Betaherpesvirus* and constitutes the most widely used animal model for studying HCMV infection.

Studies described in Chapter three of this dissertation explored use of MCMV to examine the ability of a destabilization domain strategy to generate a conditionally replication-defective MCMV vaccine vector that can be produced *in vitro*, but will be attenuated *in vivo*. Chapter four is concerned with the initial development of a MCMV-based vector expressing internal conserved proteins of IA virus towards development of a universal IA vaccine.

5.1 Development of a conditionally-attenuated CMV vaccine vector platform

CMV, a beta-herpesvirus represents a widespread pathogen that causes morbidity and mortality in both immunocompromised and immunocompetent individuals, depending on age as well as location and socioeconomic status (Mocarski *et al.*, 2013; Pass, 2001). Generally, HCMV infection in immunocompetent individuals is asymptomatic. However, it can cause life-threatening disease in immunocompromised individuals. Several studies have shown CMV vectors to be an attractive vaccine platform. It is also an important source of knowledge that despite their attractive immunological characteristics, fully replicating CMV vector have disadvantages. The important one is that associated with safety profile *in vivo* in immunocompromised individuals (Corona-Nakamura *et al.*, 2013). Several studies have revealed that replication of CMV is not required for priming immune responses by CMV (Mohr *et al.*, 2010; Snyder *et al.*, 2011).

There are several challenges that hamper the generation of an effective live attenuated virus as a vaccine vector. For instance, it is essential to have balance between safety and immunogenicity. Generation of a live HCMV vaccine based on the Towne strain, could not prevent infection in renal transplant individuals, but lowered severity of the CMV disease (Adler *et al.*, 1998). Suggesting that this vaccine was probably over attenuated. Subsequently, there is a need to develop a CMV vaccine that presents an excellent safety profile and at the same time is capable of inducing an immune response like natural infection. To generate recombinant viruses with mutated essential genes requires the complementing cell lines that express the missing viral gene product(s). For herpesviruses, the complementing cells that support mutant herpesviruses are difficult to obtain especially for β - and γ - subfamilies, since only a few complementing cell lines have been established for virus mutants, and because many of these vaccines can be propagated on primary cultures only (Borst *et al.*, 2008; Mocarski *et al.*, 1996; Silva *et al.*, 2003). An alternative approach to the use and development

of such cell lines, which is expensive, technically difficult and not suitable for use in low and middle-income countries, is using destabilization domain (DD) technology (Banaszynski *et al.*, 2006; Glaß *et al.*, 2009). DDs are conditionally unstable protein domains that genetically fuse to the protein of interest. The stability of fused proteins thus generated depends on the presence of a small molecule ligand (Banaszynski *et al.*, 2006).

In this regard, this work has aimed to propose that generation replication-defective version of MCMV vaccine vector targeting essential tegument proteins (pp150 and pp28) to determine whether is a suitable strategy for development of the conditional replication defective MCMV vaccine vector, for use in low and middle-income countries (LMICs). Although previous studies have shown the sufficient of the FKBP-based destabilization domain for targeting essential genes of CMV (Table 1.4) using shield-1 as a ligand, however the disadvantage is that the shield-1 must be maintained in the infected cells to maintain growth and replication of the mutant virus, this may become cost-prohibitive because this ligand is relatively expensive. Fortunately, similar effective DD-system such as dihydrofolate reductase (ecDHFR)-based destabilization domain which is stabilized by trimethoprim (TMP), an inexpensive ligand (Matthews *et al.*, 1985) has been developed. Characterization of the ecDHFR-based system is also revealed that this DD behave very similar to the FKBP-based system and both systems work orthogonally (Iwamoto *et al.*, 2010) would allow modulation of protein of interest. Another important advantage of using the ecDHFR-domain is that the TMP is commercially available, inexpensive, with excellent pharmacological properties. In addition, using DD strategy for the development of vaccines, the essential gene (tegument proteins in this project) was not expressed by a complementing cell line in *trans*. Instead, adding TMP ligand into Murine fibroblast cells to enable restoring of function of missing gene.

The products of pp150 and pp28 function to regulate the replication of MCMV directly that plays a role in virus pathogenesis and in supporting production and late infection (Figure 3.37). Mutation or deletion in these genes results in attenuation of virus replication in fibroblast cells *in vitro*. Our results indicated that reconstitution of recombinant MCMV-pp28-F140P in MEFs cultured in the absence of TMP did not result in any detectable viral infection. However when TMP was added, the ligand restored the fused protein consequently growth of the virus to levels approaching wild-type. This suggests a direct effect of the DD domain on stability of the pp28 protein, which is then stabilized by TMP at least partially restoring function (Figure 3.37). Our results are consistent with prior reports that pp28 of MCMV is essential for late stage of virus assembly and egress.

Notably, in the MCMV-pp28-F140P mutants analysed *in vitro* we did not observe any reversion to the wild type sequence this phenomenon is essential for development of replication defective vaccine vector. We did not see the similar behaviour of MCMV-pp150-F140P virus as the reconstitution of the virus resulted in production of viral plaques regardless presence or absence of TMP (Figure 3.36), however it is partially attenuated. Although the DD system has been successfully applied to regulate other proteins of CMV (Table 1.4), however this strategy may not be applicable to all proteins. Fehr and his colleague showed that the DD technique was not successful and failed to regulate protein (Fehr & Yu, 2011).

For future directions, it will be interesting to test these vectors *in vivo* in mice model. The DHFR-derived system may be a suitable strategy for *in vivo* regulation of proteins that are required for vaccine development. As another important advantage of using the ecDHFR-derived DD system *in vivo* is that the TMP possesses good pharmacological properties is commercially available inexpensive. The TMP can be administered orally, a more convenient and less invasive method of drug administration than both i.p. injection or i.v. administration.

It has been shown that TMP concentration in rat *in vivo* has no adverse effects, like diarrhea or body weight loss. TMP passes the placenta and the blood-brain barrier (Schulz, 1972; Barling & Selkont, 1978).

5.2 An initial investigation into use of MCMV as a vaccine against pandemic IA virus

IA virus is an infectious pathogen that causes significant respiratory illness in human populations worldwide (Duan & Thomas, 2016). From the Spanish flu in 1918 to the Asian flu 1957 and the Hong Kong flu 1963 to the Swine flu 2009, millions of people died from influenza pandemics (Li & Cao, 2016). IA viruses are a continuing threat to humans due to their naturally high mutation rate and their ability to undergo antigenic drift or shift in their evolution (Gaspar *et al.*, 2016). IA virus with antigenic shift has distinct surface antigens when compared to the recently circulating seasonal virus.

Currently, vaccinations are the most effective strategy used to prevent influenza infection (Schotsaert & García-Sastre, 2014). Since seasonal inactivated influenza vaccines work primarily by inducing antibodies that confer strain-specific immunity, rather than creating cross-protective (heterosubtypic) immunity against influenza infection, there has been a boost in research on vaccines that have the ability for inducing heterosubtypic immunity against multiple subtypes of influenza A virus. In the past years, many strategies have been developed targeting conserved parts of IA virus. Generally, these strategies can be divided into T cell inducing and antibody-inducing vaccines. Potential T cell inducing vaccines often aim to induce T-cell responses directed towards more conserved parts of the internal proteins of IA virus such as NP, M1 and PB1 (Assarsson *et al.*, 2008; Grant *et al.*, 2013). On the other hand, antibody inducing vaccines often aim to induce antibodies directed to HA, NA or M2e epitopes (Fiers *et al.*, 2004; Steel *et al.*, 2010). Although virus spread can be limited by

antibodies, T cells are responsible for elimination of the virus by killing virus infected cells mainly by CD8⁺ and CD4⁺ T cells. Even though, T cell inducing vaccines cannot prevent infection, they are critical for inducing clearance of infection and limiting virus transmission and disease severity (Duan & Thomas, 2016).

In this study, we attempted to develop a safe, inexpensive, single dose universal vaccine capable of inducing CD8⁺ T cell responses against conserved proteins and thus potentially providing a broad protection against all serotypes of IA virus. We decided to use an MCMV-based vaccine approach expressing epitopes of IA virus conserved proteins. In the first part of this study three MCMV-based influenza vaccines (MCMV-IAV) were generated and characterised *in vitro*, each expressing a single H2^b restricted CD8⁺ T cell epitope of a conserved IA structural protein; NP₃₆₆₋₃₇₄, PA₂₂₄₋₂₃₃ and NS2₁₁₄₋₁₂₁ were designed. These epitopes were fused to the non-essential gene (IE2) of MCMV using BAC technology and homologous recombination.

To assess the potential for development of MCMV as a vaccine vector against influenza A virus, we developed and characterised MCMV-IAV expressing a CD8⁺ T cell epitope from conserved proteins of IA virus (NP, PA and NS2) both in *in vitro* and *in vivo*. Epitopes were fused to the carboxyl terminus of a non-essential protein of MCMV (IE2; Figures 4.1 and 4.17). Two independent clones from each vector were selected for *in vitro* characterization. Restriction enzyme digestion analysis followed by electrophoresis showed no gross genomic rearrangements compared to the parental wild-type BAC and also following the removal of Kan^R marker consistent with previous studies that used MCMV as a vaccine vector. We concluded that insertion of the NP, PA or NS2 epitope of influenza A virus in the selected locus (IE2) of MCMV was stable and did not change the level of expression of IE2 gene and did not change the replication of recombinant MCMV *in vitro*. The growth kinetics of

recombinant MCMV was comparable to those of the parental virus (Tierney *et al.*, 2012; Tsuda *et al.*, 2011).

The main aim of construction of recombinant MCMV-IA vaccine vector was to induce flu specific CD8⁺ T cell responses, therefore, experiments were designed to find out whether these vectors were capable of inducing robust T cell responses. During influenza virus infection, CD8⁺ T cells have been shown to be involved in the reduction and control of viral load. The CD8⁺ precursor T cells mature into (CTL). Upon recognition of short peptides presented by MHC class I molecules on APCs they control virus replication by releasing high levels of cytokines such as IFN γ and TNF- α . Secondly, they can destroy infected cells through lytic action involving granzymes and perforin.

Previous studies have shown that CMV-based vaccine vectors have the ability to induce high levels of CD8⁺ T cell responses, followed by robust protection against different pathogen challenge (Dekhtiarenko *et al.*, 2013; Hansen *et al.*, 2011; Tsuda *et al.*, 2011). All of the vectors in the study here were able to induce CD8 T cells. However, this significant level of CD8⁺ T cell response was not observed in our study. Following vaccination, specific T cell responses were induced but were significantly lower than those previously reported. There are two possibilities to explain this low T cell response: (i) there may be unexpected mutations in the MCMV genome that may cause immune responses to be diminished, (ii) The second possibility to explain the low level of T cell responses and in agreement with a study by Dekhtiarenko and his colleagues (Dekhtiarenko *et al.*, 2013), is that the three constructed vectors (MCMV-IA-NP, PA and NS2) were used together for the mice vaccination, this combination could have caused competition between the three epitopes in terms of their presentation on the antigen presenting cells (APCs), consequently causing diminished CD8⁺ T cell responses as compared to the positive control (Tsuda *et al.*, 2011).

To avoid the competing epitopes being recognized on the same APC, using single MCMV-IAV vector is probably needed to obtain a protective response after vaccination. A recombinant MCMV-IAV encoding a single epitope from the NP protein was constructed to achieve presentation of an internal protein from the influenza virus individually on the surface of APCs, thus avoiding presentation on the same APCs. In future studies, since only low T cell responses were achieved, it will be of interest to repeat *in vivo* study. Comparing the single MCMV-IA-NP vector with the combine MCMV-IA-(NP+PA+NS2) vector despite of inducing robust CD8⁺ T cell responses. In order to avoid the competing epitopes being recognised on the same APC, using individual vector may result in presentation of influenza epitope individually on the surface of APCs. If successful, future and ongoing studies could be focused on the design of CMV vectors expressing IA epitopes using RhCMV-based vectors. To initially prove the ability of the IA epitopes to induce CD8⁺ T cell responses. A future study combining generation of replication defective MCMV model using DD system with epitope from internal influenza virus protein would be very interesting to generate safe and effective vaccine platform against pandemic IA virus in immunocompromised individuals.

APPENDIX I- Seeding densities, Staining and Fixative

Cell Seeding Densities

Dish Type	MEF cells
96 well plate	1×10^5
24 well plate	2×10^5
6 well plate	4×10^5

Cell culture solutions

2.5% Glutaraldehyde

1.5 ml of 50% glutaraldehyde stock was added to 28.5 ml DPBS buffer. The solution was aliquoted and stored at RT.

Freezing Solution

FCS	80 %
DMSO	20 %

1.2 Seaplaque agar

Sea Plaque agar	0.6 g
Sterile H ₂ O	50 ml

Microwave for two min until boiled and then sterilized by autoclaving.

20 % Sorbitol Cushion

D- sorbitol	100g
1M Tris pH 7.4	2.5 ml
1M MgCl ₂	1 ml

Distilled H₂O to 500 ml

1M MgCl₂

MgCl ₂ *6H ₂ O	101.65 g
--------------------------------------	----------

Distilled H₂O to 500 ml

2xDMEM

DMEM powder	13.38 g
NaHCO ₃	49.3 ml

Distilled H₂O to 500 ml. Mixed thoroughly and then added 10 ml PSG and 100 ml FBS.

Mixed by shaking and then sterilized by filtration.

10 × RBC buffer

NH ₄ Cl (0.155M)	45 g
KHCO ₃ (0.01M)	5 g
EDTA (0.1mM)	185 ml

Distilled H₂O to 500 ml.

Trypsin Diluent

Na ₂ HPO ₄ ·7 H ₂ O	245 g
Dextrose	2.5 g
KH ₂ PO ₄	0.015 g
KCl	1.0 g
NaCl	20.0 g
Phenol Red	0.05 g

All the reagents were dissolved in 2 L of double distilled H₂O. The pH was adjusted to 7.3 with 1N HCl. The volume was gradually brought to 2.5 L with double distilled H₂O.

Neutral red stain solution

Trypsin diluent	50 ml
Sodium bicarbonate (7.5%)	0.1 ml
Neutral red stock	4 ml

1X Methylcellulose (MTC)

4 g methylcellulose powder carefully weighed out and placed in 250 ml bottle. 110 ml molecular distilled H₂O was placed in 250 ml bottle. Next, the MTC and H₂O were autoclaved for 30 minutes. As soon as MTC and H₂O were removed from autoclave, the hot H₂O was poured into MTC in tissue culture hood. In a cold room the solution was continuously shaken for 20 min. In a tissue culture hood, 100 ml of 2 × DME was added to 100 ml MTC solution and stored at 4 °C.

APPENDIX II- PCR and Agarose Gel Electrophoresis

PCR Reaction

Ingredients	amount
PCR Reaction Buffer (10 x)	5 μ l
Forward primer (10 μ M)	1.25 μ l
Reverse primer (10 μ M)	1.25 μ l
Taq DNA polymerase (5 U)	0.2 μ l
Distilled H ₂ O	40.3 μ l
cDNA	2 μ l
Total	50 μ l

Standard PCR Conditions

	Temperature	Duration	Number of cycles
Initial denaturation	94°C	5 minutes	1 cycle
Denaturation	94°C	30 seconds	35 × cycles
Annealing	58°C	30 seconds	
Extension	68°C	5 minutes	
Final extension	68°C	10 minutes	1 cycle

- The annealing temperature depends on the melting temperatures TM of the primers.
- Extension time depends on the length of sequence to be amplified.

50 × Tris Acetate EDTA (TAE) Running Buffer

Tris Base (Sigma)	242 g
Glacial Acetic Acid (Sigma)	57.2 ml
0.5 M EDTA, pH 8	100 ml
Distilled H ₂ O to 1000 ml	

50 × TAE stock solutions were diluted to 1 × concentration using distilled H₂O.

1 g agarose was added to 100 ml 1 × TAE buffer and microwaved until dissolved completely. The agarose was allowed to cool slightly and 5 µl ethidium bromide (EtBr) was added to the flask and gently swirled to ensure adequate mixing. The gel was poured and allowed to set at room temperature for 20 min prior to use.

0.5 M EDTA

186 g disodium ethylene was added to 1000 ml distilled H₂O. The pH was adjusted to 8.0 with NaOH.

Molecular Ladder (1Kb)

Kb DNA Extension Ladder (Invitrogene)	80 µl
Loading Dye (5 ×)	133.2 µl
Distilled H ₂ O	586.41 µl

APPENDIX III- BAC Preparation Buffers and Reagents

Buffer P1

Tris base 6.055 g

EDTA 3.722 g

H₂O 80 ml

The pH was adjusted to 8.0 with HCl.

Buffer P2

5M NaOH 4 ml

10% SDS 10 ml

H₂O 86 ml

Buffer P3

KAc 294.45 g

H₂O 500 ml

The pH was adjusted to 5.5 with glacial acetic acid.

3M NaOAc

NaOAc 204.15 g

dH₂O 500 ml

The pH was adjusted to 5.5 with glacial acetic acid

APPENDIX IV-Culture Media

LB Broth

Tryptone	1 % (w/v)
Yeast extract	0.5 % (w/v)
NaCl	1 % (w/v)

5 g LB broth powder was added to 200 ml dH₂O. Sterilized by autoclaving at 15 lbs/in² for 15 min. LB medium was used for bacterial culture.

LB Agar Plates

Tryptone	1 % (w/v)
Yeast extract	0.5 % (w/v)
NaCl	1 % (w/v)

H₂O dye was added to a final volume of 500 ml. Sterilised by autoclaving at 20 lbs/in² for 15 min. LB plates were used for cultivation of bacteria.

SOC medium

Tryptane	2.0g
Yeast extract	0.5g
1M MgCl ₂	1 ml
1M MgSO ₄	1 ml
1M NaCl	1ml
1M KCl	250µl
20% Glucose	1.8 µl

In 100 ml dH₂O.

M9 Salts Medium (1×) for 1000 ml

Na ₂ HPO ₄	3 g
NH ₄ Cl	1 g
NaCl	0.5 g

The above ingredients were added to 1 liter dH₂O. Sterilized by autoclaving for 15 min at 121 °C. The M9 salt medium was used to wash transfected SW105 bacteria to remove any carbohydrates before plating on galactose or DOG selection plates.

M63 Salts (5X)

(NH ₄) ₂ SO ₄	10 g
KH ₂ PO ₄	68 g
Fe SO ₄ .7H ₂ O	2.5 g

The above ingredients were added to 1 liter dH₂O. Adjust the pH to 7 with KOH. Sterilized by autoclaving for 15 min at 121 °C. M63 salt solution was used for preparation of galactose and DOG selection plates

Others

d-biotin	0.2 mg/ml (1: 5000)
Galactose	20% in water (1:100)
2-deoxy-galactose	20% in water (1:100)
Glycerol	20% in water (1:100)
L-leucine	10 mg/ml (1%)
MgSO ₄ . 7H ₂ O	1 M in water (1:1000)
Chloramphenicol	25 mg/ml in EtOH (1:2000)

M63-Agar plates for 300 ml/1000 ml

Autoclave 4.5 g/15 g agar in 240/800 ml H₂O and then let cool down a little. Add 60 ml/200 ml of autoclaved 5 × M63 medium and 300 µl/ 1 ml MgSO₄. Adjust volume to 300 ml/ 1000 ml with H₂O. Let cool down to 50°C then add 3.3 ml/ 10 ml of carbon source, 1.5 ml/ 5 ml Biotin, 1.4 ml/ 4.5 ml L-leucine, and 150 µl/ 500 µl Chloramphenicol.

Galactose plates

Agar	15 g
dd H ₂ O	800 ml

Sterilized by autoclaving and then let cool down to 50 °C. Added sterile: 200 ml 5 × M63 medium, 1 ml MgSO₄, 10 ml 20% galactose, 5ml 0.2 mg/ml D-biotin, 4.5 ml/ 10mg/ ml L-leucine, and 368 µl 34 µg/ml Chloramphenicol. Galactose plates were used for positive selection of SW105 bacterial colonies that encode the galactokinase K (galK) gene.

MacConkey indicator plates

MacConkey agar	10 g
Dd H ₂ O	250 ml

Sterilized by autoclaving and then let cool down to 50 °C.

Add sterile 2.5 ml 20% galactose and 91.911µl chloramphenicol (12.5 µg /ml). MacConkey plates were used as indicator plate to verify expression of galK gene. Galk+ bacteria colonies turn pink/red while galK- bacteria colonies stay white.

DOG plates

Agar	15 g
Dd H ₂ O	250 ml

Sterilized by autoclaving and then let cool down to 50 °C. Added sterile: 200 ml 5 × M63 medium, 1 ml MgSO₄, 10 ml 20% glycerol, 10 ml 20% DOG, 5ml 0.2 mg/ml D-biotin, 4.5 ml/ 10 mg/ ml L-leucine, and 368 µl 34 µg/ml Chloramphenicol. DOG plates were used for negative selection of galk- SW105 bacterial colonies.

APPENDIX V-SDS-PAGE Gel Electrophoresis

Sodium Dodecyl Sulphate (SDS- Solution 10 %)

SDS stock (10 %) made in 100 ml volumes and stored at room temperature.

10 % Ammonium Persulphate (APS)

0.1 g APS was weighed out and dissolved in 1 ml sterile distilled H₂O immediately prior to use.

Resolving Gel

10 ml was sufficient for 1 mini gel.

	12%	15%
Sterile distilled H ₂ O	3.3 ml	2.3 ml
30 % Acrylamide	4.0 ml	5.0 ml
1.5 M Tris (pH 8.8)	2.5 ml	2.5 ml
10 % SDS	100 µl	100 µl
10 % APS	100 µl	100 µl
TEMED	8 µl	8 µl

Stacking Gel

4 ml of stacking gel was sufficient for 1 mini gel.

	4 ml 5% stacking gel
Sterile distilled H ₂ O	2.7 ml
30 % Acrylamide	670 µl
1.5 M Tris (pH 6.8)	500 µl
10 % SDS	40 µl
10 % APS	40 µl
TEMED	4 µl

5 × Sample Buffer

SDS Powder	2 g
1 M Tris/HCl, (pH 6.8)	6 ml
Bromophenol Blue	0.05 g
Glycerol	8 ml
Sterile distilled H ₂ O to 18.8 ml	

10 × Running Buffer

SDS Powder	20 g
Tris Base	30.3 g
Glycine	144.2 g
Sterile distilled H ₂ O to 1 L	

The 10 × stock solution was diluted to 1 × concentration using distilled H₂O prior to use.

1 × Transfer Buffer (pH 8.3)

SDS Powder	1 g
Tris Base	3 g
Glycine	14.42 g
Sterile distilled H ₂ O 800 ml	
Methanol	200 ml

APPENDIX X-Animal Study

Intracellular Cytokine Staining (ICS)

Reagents	Source	Comment
Brefeldin A Solution (BFA)	eBiosciences	Inhibit intracellular protein transport
Intracellular Fixation and Permeabilization Buffer set	eBiosciences	Use in intracellular staining
Comp Bead; Anti-rat and anti-hamster IgG kappa negative control compensation particle set.	BD Biosciences	Use to optimise fluorescence-compensation setting for multicolour Flow cytometric analysis.

Surface Staining Antibodies

Antibody	Clone	Source
CD3, APC-eFlour780	17A2	eBiosciences
CD4; Pacific Blue	RM4-5	BD Biosciences
CD8a; PerCP-Cy5.5	53-6.7	BD Biosciences

Intracellular Staining Antibodies

Antibody	Clone	Source
TNF α ; PE	MP6-XT22	BD Biosciences
IFN γ ; APC	XMG1.2	BD Biosciences

Peptides

H2^b- Restricted Peptides (Influenza A Peptides)

Peptides	Sequence
IA NP ₃₆₆₋₃₇₄ (PR8)	ASNENMETM
IA NP ₃₆₆₋₃₇₄ (H5N1 Viet)	ASNENMEAM
IA PA ₂₂₄₋₂₃₃ (PR8+ H5N1 Viet)	SSLENFRAYV
IA NS2 ₁₁₄₋₁₂₁ (PR8)	RTFSFQLI
IA NS2 ₁₁₄₋₁₂₁ (H5N1 Viet)	RAFSFQLI
IA PB ₁₇₀₃₋₇₁₁ (PR8+ H5N1 Viet) Not present in MCMV/IA vaccine construct	SSYRRPVGI

H2^b- Restricted Peptides (Control Peptides)

Antibody	Sequence
MCMV M38 (endogenous MCMV peptide-inflationary)	HGIRNASFI
MCMV M45 (endogenous MCMV peptide-non-inflationary)	SSPPMFRV

BIBLIOGRAPHY

Abate, D. A., Watanabe, S. & Mocarski, E. S. (2004) 'Major human cytomegalovirus structural protein pp65 (ppUL83) prevents interferon response factor 3 activation in the interferon response'. *Journal of Virology*, 78 (20), pp. 10995-11006.

Achdout, H., Arnon, T. I., Markel, G., Gonen-Gross, T., Katz, G., Lieberman, N., Gazit, R., Joseph, A., Kedar, E. & Mandelboim, O. (2003) 'Enhanced recognition of human NK receptors after influenza virus infection'. *The Journal of Immunology*, 171 (2), pp. 915-923.

Adams, S. & Sandrock, C. (2010) 'Avian influenza: update'. *Medical Principles and Practice*, 19 (6), pp. 421-432.

Adler, H., Messerle, M. & Koszinowski, U. H. (2003) 'Cloning of herpesviral genomes as bacterial artificial chromosomes'. *Reviews in Medical Virology*, 13 (2), pp. 111-121.

Adler, H., Messerle, M., Wagner, M. & Koszinowski, U. H. (2000) 'Cloning and mutagenesis of the murine gammaherpesvirus 68 genome as an infectious bacterial artificial chromosome'. *Journal of Virology*, 74 (15), pp. 6964-6974.

Adler, S.P., Hempfling, S.H., Starr, S.E., Plotkin, S.A. and Riddell, S., 1998. Safety and Immunogenicity of the Towne Strain Cytomegalovirus Vaccine. *The Pediatric infectious disease journal*, 17(3), pp.200-206.

Adler, S. P., Nigro, G. & Pereira, L. (2007) 'Recent advances in the prevention and treatment of congenital cytomegalovirus infections', *Seminars in Perinatology*. Elsevier, pp. 10-18.

Ahn, J.-H., Jang, W.-J. & Hayward, G. S. (1999) 'The human cytomegalovirus IE2 and UL112-113 proteins accumulate in viral DNA replication compartments that initiate from the periphery of promyelocytic leukemia protein-associated nuclear bodies (PODs or ND10)'. *Journal of Virology*, 73 (12), pp. 10458-10471.

Akel, H. & Sweet, C. (1993) 'Isolation and preliminary characterisation of twenty-five temperature-sensitive mutants of mouse cytomegalovirus'. *FEMS Microbiology Letters*, 113 (3), pp. 253-260.

Akkina, R. (1990) 'Antigenic reactivity and electrophoretic migrational heterogeneity of the three polymerase proteins of type A human and animal influenza viruses'. *Archives of Virology*, 111 (3-4), pp. 187-197.

Alexopoulou, L., Holt, A. C., Medzhitov, R. & Flavell, R. A. (2001) 'Recognition of double-stranded RNA and activation of NF- κ B by Toll-like receptor 3'. *Nature*, 413 (6857), pp. 732-738.

Altenburg, A. F., Rimmelzwaan, G. F. & de Vries, R. D. (2015) 'Virus-specific T cells as correlate of (cross-) protective immunity against influenza'. *Vaccine*, 33 (4), pp. 500-506.

Amemiya, C. T., Garnes, J., Kroisel, P. M., Shizuya, H., Chen, C., Batzer, M. A. & de Jong, P. J. (1994) 'A new bacteriophage P1-derived vector for the propagation of large human DNA fragments'. *Nature Genetics*, 6 (1), pp. 84-89.

Andrade, F. (2010) 'Non - cytotoxic antiviral activities of granzymes in the context of the immune antiviral state'. *Immunological Reviews*, 235 (1), pp. 128-146.

Andreansky, S. S., Stambas, J., Thomas, P. G., Xie, W., Webby, R. J. & Doherty, P. C. (2005) 'Consequences of immunodominant epitope deletion for minor influenza virus-specific CD8+-T-cell responses'. *Journal of Virology*, 79 (7), pp. 4329-4339.

Arase, H., Mocarski, E. S., Campbell, A. E., Hill, A. B. & Lanier, L. L. (2002) 'Direct recognition of cytomegalovirus by activating and inhibitory NK cell receptors'. *Science*, 296 (5571), pp. 1323-1326.

Arbuckle, J. H., Medveczky, M. M., Luka, J., Hadley, S. H., Luegmayr, A., Ablashi, D., Lund, T. C., Tolar, J., De Meirleir, K. & Montoya, J. G. (2010) 'The latent human herpesvirus-6A genome specifically integrates in telomeres of human chromosomes in vivo and in vitro'. *Proceedings of the National Academy of Sciences*, 107 (12), pp. 5563-5568.

Armas, J. G., Morello, C. S., Cranmer, L. D. & Spector, D. H. (1996) 'DNA immunization confers protection against murine cytomegalovirus infection'. *Journal of Virology*, 70 (11), pp. 7921-7928.

Arnon, T. I., Achdout, H., Levi, O., Markel, G., Saleh, N., Katz, G., Gazit, R., Gonen-Gross, T., Hanna, J. & Nahari, E. (2005) 'Inhibition of the NKp30 activating receptor by pp65 of human cytomegalovirus'. *Nature Immunology*, 6 (5), pp. 515-523.

Arnon, T. I., Lev, M., Katz, G., Chernobrov, Y., Porgador, A. & Mandelboim, O. (2001) 'Recognition of viral hemagglutinins by NKp44 but not by NKp30'. *European Journal of Immunology*, 31 (9), pp. 2680-2689.

Arnon, T. I., Markel, G. & Mandelboim, O. (2006) 'Tumor and viral recognition by natural killer cells receptors', *Seminars in Cancer Biology*. Elsevier, pp. 348-358.

Assarsson, E., Bui, H.-H., Sidney, J., Zhang, Q., Glenn, J., Oseroff, C., Mbawuikie, I. N., Alexander, J., Newman, M. J. & Grey, H. (2008) 'Immunomic analysis of the repertoire of T-cell specificities for influenza A virus in humans'. *Journal of Virology*, 82 (24), pp. 12241-12251.

AuCoin, D. P., Smith, G. B., Meiering, C. D. & Mocarski, E. S. (2006) 'Betaherpesvirus-conserved cytomegalovirus tegument protein ppUL32 (pp150) controls cytoplasmic events during virion maturation'. *Journal of Virology*, 80 (16), pp. 8199-8210.

Avalos, R. T., Yu, Z. & Nayak, D. P. (1997) 'Association of influenza virus NP and M1 proteins with cellular cytoskeletal elements in influenza virus-infected cells'. *Journal of Virology*, 71 (4), pp. 2947-2958.

Baer, A. & Kehn-Hall, K. (2014) 'Viral concentration determination through plaque assays: using traditional and novel overlay systems'. *Journal of Visualized Experiments: JoVE*, (93), pp. e52065.

Baigent, S. J., Petherbridge, L. J., Smith, L. P., Zhao, Y., Chesters, P. M. & Nair, V. K. (2006) 'Herpesvirus of turkey reconstituted from bacterial artificial chromosome clones induces protection against Marek's disease'. *Journal of General Virology*, 87 (4), pp. 769-776.

Baldick, C., Marchini, A., Patterson, C. E. & Shenk, T. (1997) 'Human cytomegalovirus tegument protein pp71 (ppUL82) enhances the infectivity of viral DNA and accelerates the infectious cycle'. *Journal of Virology*, 71 (6), pp. 4400-4408.

Banaszynski, L. A., Chen, L.-c., Maynard-Smith, L. A., Ooi, A. & Wandless, T. J. (2006) 'A rapid, reversible, and tunable method to regulate protein function in living cells using synthetic small molecules'. *Cell*, 126 (5), pp. 995-1004.

Banaszynski, L. A., Sellmyer, M. A., Contag, C. H., Wandless, T. J. & Thorne, S. H. (2008) 'Chemical control of protein stability and function in living mice'. *Nature Medicine*, 14 (10), pp. 1123-1127.

Banchereau, J. & Steinman, R. M. (1998) 'Dendritic cells and the control of immunity'. *Nature*, 392 (6673), pp. 245-252.

Barling, R. & Selkont, J. (1978) 'The penetration of antibiotics into cerebrospinal fluid and brain tissue'. *Journal of Antimicrobial Chemotherapy*, 4 (3), pp. 203-227.

Baxter, M. K. & Gibson, W. (2001) 'Cytomegalovirus basic phosphoprotein (pUL32) binds to capsids in vitro through its amino one-third'. *Journal of Virology*, 75 (15), pp. 6865-6873.

Beale, R., Wise, H., Stuart, A., Ravenhill, B. J., Digard, P. & Randow, F. (2014) 'A LC3-interacting motif in the influenza A virus M2 protein is required to subvert autophagy and maintain virion stability'. *Cell Host & Microbe*, 15 (2), pp. 239-247.

Belshe, R., Lee, M.-S., Walker, R. E., Stoddard, J. & Mendelman, P. M. (2004) 'Safety, immunogenicity and efficacy of intranasal, live attenuated influenza vaccine'. *Expert Review of Vaccines*, 3 (6), pp. 643-654.

Belz, G. T., Xie, W., Altman, J. D. & Doherty, P. C. (2000) 'A previously unrecognized H-2Db-restricted peptide prominent in the primary influenza A virus-specific CD8+ T-cell response is much less apparent following secondary challenge'. *Journal of Virology*, 74 (8), pp. 3486-3493.

Bender, B. S., Croghan, T., Zhang, L. & Small, P. (1992) 'Transgenic mice lacking class I major histocompatibility complex-restricted T cells have delayed viral clearance and increased mortality after influenza virus challenge'. *The Journal of Experimental Medicine*, 175 (4), pp. 1143-1145.

Berkhoff, E., Geelhoed-Mieras, M., Fouchier, R., Osterhaus, A. & Rimmelzwaan, G. (2007) 'Assessment of the extent of variation in influenza A virus cytotoxic T-lymphocyte epitopes by using virus-specific CD8+ T-cell clones'. *Journal of General Virology*, 88 (2), pp. 530-535.

Biswas, S. K., Boutz, P. L. & Nayak, D. P. (1998) 'Influenza virus nucleoprotein interacts with influenza virus polymerase proteins'. *Journal of Virology*, 72 (7), pp. 5493-5501.

Boehme, K. W., Singh, J., Perry, S. T. & Compton, T. (2004) 'Human cytomegalovirus elicits a coordinated cellular antiviral response via envelope glycoprotein B'. *Journal of Virology*, 78 (3), pp. 1202-1211.

Boon, A. C., de Mutsert, G., van Baarle, D., Smith, D. J., Lapedes, A. S., Fouchier, R. A., Sintnicolaas, K., Osterhaus, A. D. & Rimmelzwaan, G. F. (2004) 'Recognition of homo- and heterosubtypic variants of influenza A viruses by human CD8+ T lymphocytes'. *The Journal of Immunology*, 172 (4), pp. 2453-2460.

Borenstein, R. & Frenkel, N. (2009) 'Cloning human herpes virus 6A genome into bacterial artificial chromosomes and study of DNA replication intermediates'. *Proceedings of the National Academy of Sciences*, 106 (45), pp. 19138-19143.

Borst, E.-M., Hahn, G., Koszinowski, U. H. & Messerle, M. (1999) 'Cloning of the human cytomegalovirus (HCMV) genome as an infectious bacterial artificial chromosome in *Escherichia coli*: a new approach for construction of HCMV mutants'. *Journal of Virology*, 73 (10), pp. 8320-8329.

Borst, E. M., Kleine-Albers, J., Gabaev, I., Babić, M., Wagner, K., Binz, A., Degenhardt, I., Kalesse, M., Jonjić, S. & Bauerfeind, R. (2013) 'The human cytomegalovirus UL51 protein is essential for viral genome cleavage-packaging and interacts with the terminase subunits pUL56 and pUL89'. *Journal of Virology*, 87 (3), pp. 1720-1732.

Borst, E. M., Wagner, K., Binz, A., Sodeik, B. & Messerle, M. (2008) 'The essential human cytomegalovirus gene UL52 is required for cleavage-packaging of the viral genome'. *Journal of Virology*, 82 (5), pp. 2065-2078.

Bosch, F., Garten, W., Klenk, H.-D. & Rott, R. (1981) 'Proteolytic cleavage of influenza virus hemagglutinins: primary structure of the connecting peptide between HA1 and HA2 determines proteolytic cleavability and pathogenicity of Avian influenza viruses'. *Virology*, 113 (2), pp. 725-735.

Bosch, F., Orlich, M., Klenk, H.-D. & Rott, R. (1979) 'The structure of the hemagglutinin, a determinant for the pathogenicity of influenza viruses'. *Virology*, 95 (1), pp. 197-207.

Both, G. W., Sleight, M., Cox, N. & Kendal, A. (1983) 'Antigenic drift in influenza virus H3 hemagglutinin from 1968 to 1980: multiple evolutionary pathways and sequential amino acid changes at key antigenic sites'. *Journal of Virology*, 48 (1), pp. 52-60.

Bouvier, N. M. & Palese, P. (2008) 'The biology of influenza viruses'. *Vaccine*, 26 pp. D49-D53.

Braciale, T. J., Sun, J. & Kim, T. S. (2012) 'Regulating the adaptive immune response to respiratory virus infection'. *Nature Reviews Immunology*, 12 (4), pp. 295-305.

Bramucci, M. G. & Nagarajan, V. (1996) 'Direct selection of cloned DNA in *Bacillus subtilis* based on sucrose-induced lethality'. *Applied and Environmental Microbiology*, 62 (11), pp. 3948-3953.

Britt, W. J., Jarvis, M., Seo, J.-Y., Drummond, D. & Nelson, J. (2004) 'Rapid genetic engineering of human cytomegalovirus by using a lambda phage linear recombination system: demonstration that pp28 (UL99) is essential for production of infectious virus'. *Journal of Virology*, 78 (1), pp. 539-543.

Brockman, M. A. & Knipe, D. M. (2002) 'Herpes simplex virus vectors elicit durable immune responses in the presence of preexisting host immunity'. *Journal of Virology*, 76 (8), pp. 3678-3687.

Brown, D. M. (2010) 'Cytolytic CD4 cells: Direct mediators in infectious disease and malignancy'. *Cellular Immunology*, 262 (2), pp. 89-95.

Brown, I. H. (2000) 'The epidemiology and evolution of influenza viruses in pigs'. *Veterinary Microbiology*, 74 (1), pp. 29-46.

Brown, L. E. & Kelso, A. (2009) 'Prospects for an influenza vaccine that induces cross-protective cytotoxic T lymphocytes'. *Immunology and Cell Biology*, 87 (4), pp. 300-308.

Brune, W., Ménard, C., Hobom, U., Odenbreit, S., Messerle, M. & Koszinowski, U. H. (1999) 'Rapid identification of essential and nonessential herpesvirus genes by direct transposon mutagenesis'. *Nature Biotechnology*, 17 (4), pp. 360-364.

Brune, W., Messerle, M. & Koszinowski, U. H. (2000) 'Forward with BACs: new tools for herpesvirus genomics'. *Trends in Genetics*, 16 (6), pp. 254-259.

Bubeck, A., Wagner, M., Ruzsics, Z., Lötzerich, M., Iglesias, M., Singh, I. R. & Koszinowski, U. H. (2004) 'Comprehensive mutational analysis of a herpesvirus gene in the viral genome context reveals a region essential for virus replication'. *Journal of Virology*, 78 (15), pp. 8026-8035.

Bui, M., Wills, E. G., Helenius, A. & Whittaker, G. R. (2000) 'Role of the influenza virus M1 protein in nuclear export of viral ribonucleoproteins'. *Journal of Virology*, 74 (4), pp. 1781-1786.

Burke, D. T., Carle, G. F. & Olson, M. V. (1987) 'Cloning of large segments of exogenous DNA into yeast by means of artificial chromosome vectors'. *Science*, 236 pp. 806-813.

Butcher, S., Aitken, J., Mitchell, J., Gowen, B. & Dargan, D. (1998) 'Structure of the human cytomegalovirus B capsid by electron cryomicroscopy and image reconstruction'. *Journal of Structural Biology*, 124 (1), pp. 70-76.

Carragher, D. M., Kaminski, D. A., Moquin, A., Hartson, L. & Randall, T. D. (2008) 'A novel role for non-neutralizing antibodies against nucleoprotein in facilitating resistance to influenza virus'. *The Journal of Immunology*, 181 (6), pp. 4168-4176.

Cha, T.-a., Tom, E., Kemble, G. W., Duke, G. M., Mocarski, E. S. & Spaete, R. R. (1996) 'Human cytomegalovirus clinical isolates carry at least 19 genes not found in laboratory strains'. *Journal of Virology*, 70 (1), pp. 78-83.

Chang, W. W. & Barry, P. A. (2003) 'Cloning of the full-length rhesus cytomegalovirus genome as an infectious and self-excisable bacterial artificial chromosome for analysis of viral pathogenesis'. *Journal of Virology*, 77 (9), pp. 5073-5083.

Chee, M., Bankier, A., Beck, S., Bohni, R., Brown, C., Cerny, R., Horsnell, T., Hutchison III, C., Kouzarides, T. & Martignetti, J. (1990) 'Analysis of the protein-coding content of the sequence of human cytomegalovirus strain AD169', *Cytomegaloviruses*. Springer, pp. 125-169.

Chen, D. H., Jiang, H., Lee, M., Liu, F. & Zhou, Z. H. (1999) 'Three-dimensional visualization of tegument/capsid interactions in the intact human cytomegalovirus'. *Virology*, 260 (1), pp. 10-16.

Chen, J. & Deng, Y.-M. (2009) 'Influenza virus antigenic variation, host antibody production and new approach to control epidemics'. *Virology Journal*, 6 (1), pp. 1.

Chen, L., Zanker, D., Xiao, K., Wu, C., Zou, Q. & Chen, W. (2014) 'Immunodominant CD4+ T-cell responses to influenza A virus in healthy individuals focus on matrix 1 and nucleoprotein'. *Journal of Virology*, 88 (20), pp. 11760-11773.

Chen, W., Calvo, P. A., Malide, D., Gibbs, J., Schubert, U., Bacik, I., Basta, S., O'Neill, R., Schickli, J. & Palese, P. (2001) 'A novel influenza A virus mitochondrial protein that induces cell death'. *Nature Medicine*, 7 (12), pp. 1306-1312.

Cherepanov, P. P. & Wackernagel, W. (1995) 'Gene disruption in Escherichia coli: Tc R and Km R cassettes with the option of Flp-catalyzed excision of the antibiotic-resistance determinant'. *Gene*, 158 (1), pp. 9-14.

Cheung, T. K. & Poon, L. L. (2007) 'Biology of influenza a virus'. *Annals of the New York Academy of Sciences*, 1102 (1), pp. 1-25.

Chien, C.-y., Xu, Y., Xiao, R., Aramini, J. M., Sahasrabudhe, P. V., Krug, R. M. & Montelione, G. T. (2004) 'Biophysical characterization of the complex between double-stranded RNA and the N-terminal domain of the NS1 protein from influenza A virus: evidence for a novel RNA-binding mode'. *Biochemistry*, 43 (7), pp. 1950-1962.

Childs, R. A., Palma, A. S., Wharton, S., Matrosovich, T., Liu, Y., Chai, W., Campanero-Rhodes, M. A., Zhang, Y., Eickmann, M. & Kiso, M. (2009) 'Receptor-binding specificity of pandemic influenza A (H1N1) 2009 virus determined by carbohydrate microarray'. *Nature Biotechnology*, 27 (9), pp. 797-799.

Cho, U., Zimmerman, S. M., Chen, L.-c., Owen, E., Kim, J. V., Kim, S. K. & Wandless, T. J. (2013) 'Rapid and tunable control of protein stability in *Caenorhabditis elegans* using a small molecule'. *PLoS One*, 8 (8), pp. e72393.

Chu, C., Dawson, I. & Elford, W. (1949) 'Filamentous forms associated with newly isolated influenza virus'. *The Lancet*, 253 (6554), pp. 602-603.

Collins, J. & Hohn, B. (1978) 'Cosmids: a type of plasmid gene-cloning vector that is packageable in vitro in bacteriophage lambda heads'. *Proceedings of the National Academy of Sciences*, 75 (9), pp. 4242-4246.

Compton, T., Kurt-Jones, E. A., Boehme, K. W., Belko, J., Latz, E., Golenbock, D. T. & Finberg, R. W. (2003) 'Human cytomegalovirus activates inflammatory cytokine responses via CD14 and Toll-like receptor 2'. *Journal of Virology*, 77 (8), pp. 4588-4596.

Compton, T., Nepomuceno, R. R. & Nowlin, D. M. (1992) 'Human cytomegalovirus penetrates host cells by pH-independent fusion at the cell surface'. *Virology*, 191 (1), pp. 387-395.

Compton, T., Nowlin, D. M. & Cooper, N. R. (1993) 'Initiation of human cytomegalovirus infection requires initial interaction with cell surface heparan sulfate'. *Virology*, 193 (2), pp. 834-841.

Corona-Nakamura, A., Arias-Merino, M., Price, P., Makwana, N. & Brunt, S. (2013) 'Management of CMV-associated diseases in immunocompromised patients'. *Manifestations of Cytomegalovirus Infection*,

Costes, B., Fournier, G., Michel, B., Delforge, C., Raj, V. S., Dewals, B., Gillet, L., Drion, P., Body, A. & Schynts, F. (2008) 'Cloning of the koi herpesvirus genome as an infectious bacterial artificial chromosome demonstrates that disruption of the thymidine kinase locus induces partial attenuation in *Cyprinus carpio koi*'. *Journal of Virology*, 82 (10), pp. 4955-4964.

Cox, M. M. (1988) 'FLP site-specific recombination system of *Saccharomyces cerevisiae*'. *Genetic Recombination*, pp. 429-443.

Cox, R., Brokstad, K. & Ogra, P. (2004) 'Influenza virus: immunity and vaccination strategies. Comparison of the immune response to inactivated and live, attenuated influenza vaccines'. *Scandinavian journal of Immunology*, 59 (1), pp. 1-15.

Crough, T. & Khanna, R. (2009) 'Immunobiology of human cytomegalovirus: from bench to bedside'. *Clinical Microbiology Reviews*, 22 (1), pp. 76-98.

Dai, W., Jia, Q., Bortz, E., Shah, S., Liu, J., Atanasov, I., Li, X., Taylor, K. A., Sun, R. & Zhou, Z. H. (2008) 'Unique structures in a tumor herpesvirus revealed by cryo-electron tomography and microscopy'. *Journal of Structural Biology*, 161 (3), pp. 428-438.

Dai, X., Yu, X., Gong, H., Jiang, X., Abenes, G., Liu, H., Shivakoti, S., Britt, W. J., Zhu, H. & Liu, F. (2013) 'The smallest capsid protein mediates binding of the essential tegument protein pp150 to stabilize DNA-containing capsids in human cytomegalovirus'. *PLoS Pathog*, 9 (8), pp. e1003525.

Das, S., Ortiz, D. A., Gurczynski, S. J., Khan, F. & Pellett, P. E. (2014) 'Identification of human cytomegalovirus genes important for biogenesis of the cytoplasmic virion assembly complex'. *Journal of Virology*, 88 (16), pp. 9086-9099.

Davison, A. (1993) 'Herpesvirus genes'. *Reviews in Medical Virology*, 3 (4), pp. 237-244.

Davison, A. J. (2002) 'Evolution of the herpesviruses'. *Veterinary Microbiology*, 86 (1), pp. 69-88.

Davison, A. J., Dolan, A., Akter, P., Addison, C., Dargan, D. J., Alcendor, D. J., McGeoch, D. J. & Hayward, G. S. (2003) 'The human cytomegalovirus genome revisited: comparison with the chimpanzee cytomegalovirus genome FN1'. *Journal of General Virology*, 84 (1), pp. 17-28.

Dekhtiarenko, I., Jarvis, M. A., Ruzsics, Z. & Čičin-Šain, L. (2013) 'The context of gene expression defines the immunodominance hierarchy of cytomegalovirus antigens'. *The Journal of Immunology*, 190 (7), pp. 3399-3409.

Delecluse, H.-J., Hilsendegen, T., Pich, D., Zeidler, R. & Hammerschmidt, W. (1998) 'Propagation and recovery of intact, infectious Epstein-Barr virus from prokaryotic to human cells'. *Proceedings of the National Academy of Sciences*, 95 (14), pp. 8245-8250.

DeLuca, N. A., McCARTHY, A. M. & Schaffer, P. A. (1985) 'Isolation and characterization of deletion mutants of herpes simplex virus type 1 in the gene encoding immediate-early regulatory protein ICP4'. *Journal of Virology*, 56 (2), pp. 558-570.

Demicheli, V., Rivetti, D., Deeks, J. & Jefferson, T. (2014) 'Vaccines for preventing influenza in healthy adults'. *voir commentaire*][Update of Cochrane Database Systematic Reviews 2001, 4

Dias, A., Bouvier, D., Crépin, T., McCarthy, A. A., Hart, D. J., Baudin, F., Cusack, S. & Ruigrok, R. W. (2009) 'The cap-snatching endonuclease of influenza virus polymerase resides in the PA subunit'. *Nature*, 458 (7240), pp. 914-918.

Digard, P., Blok, V. C. & Inglis, S. C. (1989) 'Complex formation between influenza virus polymerase proteins expressed in *Xenopus* oocytes'. *Virology*, 171 (1), pp. 162-169.

Digard, P., Elton, D., Bishop, K., Medcalf, E., Weeds, A. & Pope, B. (1999) 'Modulation of nuclear localization of the influenza virus nucleoprotein through interaction with actin filaments'. *Journal of Virology*, 73 (3), pp. 2222-2231.

Doherty, P. C., Turner, S. J., Webby, R. G. & Thomas, P. G. (2006) 'Influenza and the challenge for immunology'. *Nature Immunology*, 7 (5), pp. 449-455.

Dolin, R., Murphy, B. & Caplan, E. (1978) 'Lymphocyte blastogenic responses to influenza virus antigens after influenza infection and vaccination in humans'. *Infection and Immunity*, 19 (3), pp. 867-874.

Drape, R. J., Macklin, M. D., Barr, L. J., Jones, S., Haynes, J. R. & Dean, H. J. (2006) 'Epidermal DNA vaccine for influenza is immunogenic in humans'. *Vaccine*, 24 (21), pp. 4475-4481.

Duan, S. & Thomas, P. G. (2016) 'Balancing immune protection and immune pathology by CD8+ T-Cell responses to influenza infection'. *Frontiers in Immunology*, 7

Dudek, T. & Knipe, D. M. (2006) 'Replication-defective viruses as vaccines and vaccine vectors'. *Virology*, 344 (1), pp. 230-239.

Dulbecco, R. (1952) 'Production of plaques in monolayer tissue cultures by single particles of an animal virus'. *Proceedings of the National Academy of Sciences*, 38 (8), pp. 747-752.

Dunn, W., Chou, C., Li, H., Hai, R., Patterson, D., Stolc, V., Zhu, H. & Liu, F. (2003) 'Functional profiling of a human cytomegalovirus genome'. *Proceedings of the National Academy of Sciences*, 100 (24), pp. 14223-14228.

Dvorin, J. D., Martyn, D. C., Patel, S. D., Grimley, J. S., Collins, C. R., Hopp, C. S., Bright, A. T., Westenberger, S., Winzeler, E. & Blackman, M. J. (2010) 'A plant-like kinase in *Plasmodium falciparum* regulates parasite egress from erythrocytes'. *Science*, 328 (5980), pp. 910-912.

Eggers, M., Bogner, E., Kern, H. & Radsak, K. (1992) 'Inhibition of human cytomegalovirus maturation by brefeldin A'. *Journal of General Virology*, 73 (10), pp. 2679-2692.

Eizuru, Y., Inagawa, S. & Minamishima, Y. (1984) 'Application of " Hirt supernatant" DNA to the molecular epidemiology of cytomegalovirus infections'. *Journal of Clinical Microbiology*, 20 (5), pp. 1012-1014.

Elkington, R., Walker, S., Crough, T., Menzies, M., Tellam, J., Bharadwaj, M. & Khanna, R. (2003) 'Ex vivo profiling of CD8+-T-cell responses to human cytomegalovirus reveals broad and multispecific reactivities in healthy virus carriers'. *Journal of Virology*, 77 (9), pp. 5226-5240.

Ellebedy, A. H. & Ahmed, R. (2012) 'Re-engaging cross-reactive memory B cells: the influenza puzzle'. *Frontiers in Immunology*, 3 pp. 53.

Elton, D., Medcalf, E., Bishop, K. & Digard, P. (1999) 'Oligomerization of the influenza virus nucleoprotein: identification of positive and negative sequence elements'. *Virology*, 260 (1), pp. 190-200.

Elton, D., Simpson-Holley, M., Archer, K., Medcalf, L., Hallam, R., McCauley, J. & Digard, P. (2001) 'Interaction of the influenza virus nucleoprotein with the cellular CRM1-mediated nuclear export pathway'. *Journal of Virology*, 75 (1), pp. 408-419.

Enami, M. & Enami, K. (1996) 'Influenza virus hemagglutinin and neuraminidase glycoproteins stimulate the membrane association of the matrix protein'. *Journal of Virology*, 70 (10), pp. 6653-6657.

Ennis, F., Yi-Hua, Q., Riley, D., Rook, A., Schild, G., Pratt, R. & Potter, C. (1981) 'HLA-restricted virus-specific cytotoxic T-lymphocyte responses to live and inactivated influenza vaccines'. *The Lancet*, 318 (8252), pp. 887-891.

Epstein, S. L. (2006) 'Prior H1N1 influenza infection and susceptibility of Cleveland Family Study participants during the H2N2 pandemic of 1957: an experiment of nature'. *Journal of Infectious Diseases*, 193 (1), pp. 49-53.

Estep, R. D., Powers, M. F., Yen, B. K., Li, H. & Wong, S. W. (2007) 'Construction of an infectious rhesus rhadinovirus bacterial artificial chromosome for the analysis of Kaposi's sarcoma-associated herpesvirus-related disease development'. *Journal of Virology*, 81 (6), pp. 2957-2969.

Estes, J. E. & Huang, E.-S. (1977) 'Stimulation of cellular thymidine kinases by human cytomegalovirus'. *Journal of Virology*, 24 (1), pp. 13-21.

Farrington, L. A., Smith, T. A., Grey, F., Hill, A. B. & Snyder, C. M. (2013) 'Competition for antigen at the level of the APC is a major determinant of immunodominance during memory inflation in murine cytomegalovirus infection'. *The Journal of Immunology*, 190 (7), pp. 3410-3416.

Fehr, A. R. & Yu, D. (2011) 'Human cytomegalovirus early protein pUL21a promotes efficient viral DNA synthesis and the late accumulation of immediate-early transcripts'. *Journal of Virology*, 85 (2), pp. 663-674.

Fiers, W., De Filette, M., Birkett, A., Neiryneck, S. & Jou, W. M. (2004) 'A "universal" human influenza A vaccine'. *Virus Research*, 103 (1), pp. 173-176.

Flynn, K. J., Riberdy, J. M., Christensen, J. P., Altman, J. D. & Doherty, P. C. (1999) 'In vivo proliferation of naive and memory influenza-specific CD8+ T cells'. *Proceedings of the National Academy of Sciences*, 96 (15), pp. 8597-8602.

Fodor, E., Crow, M., Mingay, L. J., Deng, T., Sharps, J., Fechter, P. & Brownlee, G. G. (2002) 'A single amino acid mutation in the PA subunit of the influenza virus RNA polymerase inhibits endonucleolytic cleavage of capped RNAs'. *Journal of Virology*, 76 (18), pp. 8989-9001.

Fodor, E. & Smith, M. (2004) 'The PA subunit is required for efficient nuclear accumulation of the PB1 subunit of the influenza A virus RNA polymerase complex'. *Journal of Virology*, 78 (17), pp. 9144-9153.

Fons, M., Graves, K., Cavallo, T., Pollard, R. & Albrecht, T. (1986) 'Human cytomegalovirus: development and progression of nuclear inclusions by primary clinical isolates and laboratory-adapted strains'. *Experimental Biology and Medicine*, 181 (3), pp. 416-422.

Fortes, P., Beloso, A. & Ortin, J. (1994) 'Influenza virus NS1 protein inhibits pre-mRNA splicing and blocks mRNA nucleocytoplasmic transport'. *The EMBO journal*, 13 (3), pp. 704.

Fortunato, E. A., McElroy, A. K., Sanchez, V. & Spector, D. H. (2000) 'Exploitation of cellular signaling and regulatory pathways by human cytomegalovirus'. *Trends in Microbiology*, 8 (3), pp. 111-119.

Fouchier, R. A., Munster, V., Wallensten, A., Bestebroer, T. M., Herfst, S., Smith, D., Rimmelzwaan, G. F., Olsen, B. & Osterhaus, A. D. (2005) 'Characterization of a novel influenza A virus hemagglutinin subtype (H16) obtained from black-headed gulls'. *Journal of Virology*, 79 (5), pp. 2814-2822.

Fowler, K. B., Stagno, S., Pass, R. F., Britt, W. J., Boll, T. J. & Alford, C. A. (1992) 'The outcome of congenital cytomegalovirus infection in relation to maternal antibody status'. *New England Journal of Medicine*, 326 (10), pp. 663-667.

Furth, P. A., St Onge, L., Böger, H., Gruss, P., Gossen, M., Kistner, A., Bujard, H. & Hennighausen, L. (1994) 'Temporal control of gene expression in transgenic mice by a tetracycline-responsive promoter'. *Proceedings of the National Academy of Sciences*, 91 (20), pp. 9302-9306.

Garfinkel, M. S. & Katze, M. G. (1993) 'Translational control by influenza virus. Selective translation is mediated by sequences within the viral mRNA 5'-untranslated region'. *Journal of Biological Chemistry*, 268 (30), pp. 22223-22226.

Gasper, D. J., Neldner, B., Plisch, E. H., Rustom, H., Carrow, E., Imai, H., Kawaoka, Y. & Suresh, M. (2016) 'Effective Respiratory CD8 T-Cell Immunity to Influenza Virus Induced by Intranasal Carbomer-Lecithin-Adjuvanted Non-replicating Vaccines'. *PLoS Pathogens*, 12 (12), pp. e1006064.

Gazit, R., Gruda, R., Elboim, M., Arnon, T. I., Katz, G., Achdout, H., Hanna, J., Qimron, U., Landau, G. & Greenbaum, E. (2006) 'Lethal influenza infection in the absence of the natural killer cell receptor gene *Ncr1*'. *Nature Immunology*, 7 (5), pp. 517-523.

Ghanem, A., Mayer, D., Chase, G., Tegge, W., Frank, R., Kochs, G., García-Sastre, A. & Schwemmle, M. (2007) 'Peptide-mediated interference with influenza A virus polymerase'. *Journal of Virology*, 81 (14), pp. 7801-7804.

Gianfrani, C., Oseroff, C., Sidney, J., Chesnut, R. W. & Sette, A. (2000) 'Human memory CTL response specific for influenza A virus is broad and multispecific'. *Human Immunology*, 61 (5), pp. 438-452.

Gibson, W. (1996) 'Structure and assembly of the virion'. *Intervirology*, 39 (5-6), pp. 389-400.

Gibson, W., Clopper, K. S., Britt, W. J. & Baxter, M. K. (1996) 'Human cytomegalovirus (HCMV) smallest capsid protein identified as product of short open reading frame located between HCMV UL48 and UL49'. *Journal of Virology*, 70 (8), pp. 5680-5683.

Gibson, W. & Irmieri, A. (1983) 'Selection of particles and proteins for use as human cytomegalovirus subunit vaccines'. *Birth Defects Original Article Series*, 20 (1), pp. 305-324.

Gilbert, M. J., Riddell, S. R., Plachter, B. & Greenberg, P. D. (1996) 'Cytomegalovirus selectively blocks antigen processing and presentation of its immediate-early gene product'. *Nature*, 383 (6602), pp. 720-722.

Gillet, L., Daix, V., Donofrio, G., Wagner, M., Koszinowski, U., China, B., Ackermann, M., Markine-Goriaynoff, N. & Vanderplasschen, A. (2005) 'Development of bovine herpesvirus 4 as an expression vector using bacterial artificial chromosome cloning'. *Journal of General Virology*, 86 (4), pp. 907-917.

Gioia, C., Castilletti, C., Tempestilli, M., Piacentini, P., Bordi, L., Chiappini, R., Agrati, C., Squarcione, S., Ippolito, G. & Puro, V. (2008) 'Cross-subtype immunity against avian influenza in persons recently vaccinated for influenza'. *Emerging Infectious Diseases*, 14 (1), pp. 121.

Girard, M. P., Tam, J. S., Assossou, O. M. & Kieny, M. P. (2010) 'The 2009 A (H1N1) influenza virus pandemic: A review'. *Vaccine*, 28 (31), pp. 4895-4902.

Glaß, M., Busche, A., Wagner, K., Messerle, M. & Borst, E. M. (2009) 'Conditional and reversible disruption of essential herpesvirus proteins'. *Nature Methods*, 6 (8), pp. 577-579.

Goldrick, B. A. & Goetz, A. M. (2007) 'Pandemic influenza: what infection control professionals should know'. *American Journal of Infection Control*, 35 (1), pp. 7-13.

Gorai, T., Goto, H., Noda, T., Watanabe, T., Kozuka-Hata, H., Oyama, M., Takano, R., Neumann, G., Watanabe, S. & Kawaoka, Y. (2012) 'F1Fo-ATPase, F-type proton-translocating ATPase, at the plasma membrane is critical for efficient influenza virus budding'. *Proceedings of the National Academy of Sciences*, 109 (12), pp. 4615-4620.

Gottschalk, A. (1957) 'Neuraminidase: the specific enzyme of influenza virus and *Vibrio cholerae*'. *Biochimica et Biophysica Acta*, 23 pp. 645-646.

Grant, E., Wu, C., Chan, K.-F., Eckle, S., Bharadwaj, M., Zou, Q. M., Kedzierska, K. & Chen, W. (2013) 'Nucleoprotein of influenza A virus is a major target of immunodominant CD8⁺ T-cell responses'. *Immunology and Cell Biology*, 91 (2), pp. 184-194.

Green, E. D., Riethman, H. C., Dutchik, J. E. & Olson, M. V. (1991) 'Detection and characterization of chimeric yeast artificial-chromosome clones'. *Genomics*, 11 (3), pp. 658-669.

Greijer, A. E., van de Crommert, J. M., Stevens, S. J. & Middeldorp, J. M. (1999) 'Molecular fine-specificity analysis of antibody responses to human cytomegalovirus and design of novel synthetic-peptide-based serodiagnostic assays'. *Journal of Clinical Microbiology*, 37 (1), pp. 179-188.

Greis, K. D., Gibson, W. & Hart, G. W. (1994) 'Site-specific glycosylation of the human cytomegalovirus tegument basic phosphoprotein (UL32) at serine 921 and serine 952'. *Journal of Virology*, 68 (12), pp. 8339-8349.

Grundy, J. E., McKEATING, J. A. & Griffiths, P. D. (1987) 'Cytomegalovirus strain AD169 binds β 2 microglobulin in vitro after release from cells'. *Journal of General Virology*, 68 (3), pp. 777-784.

Grundy, J. E., McKEATING, J. A., Ward, P., Sanderson, A. & Griffiths, P. (1987) ' β 2 microglobulin enhances the infectivity of cytomegalovirus and when bound to the virus enables class I HLA molecules to be used as a virus receptor'. *Journal of General Virology*, 68 (3), pp. 793-803.

Gustafsson, C. M., Hammarsten, O., Falkenberg, M. & Elias, P. (1994) 'Herpes simplex virus DNA replication: a spacer sequence directs the ATP-dependent formation of a nucleoprotein complex at oriS'. *Proceedings of the National Academy of Sciences*, 91 (11), pp. 4629-4633.

Gyulai, Z., Endresz, V., Burian, K., Pincus, S., Toldy, J., Cox, W. I., Meric, C., Plotkin, S., Gönczöl, E. & Berencsi, K. (2000) 'Cytotoxic T lymphocyte (CTL) responses to human cytomegalovirus pp65, IE1-

Exon4, gB, pp150, and pp28 in healthy individuals: reevaluation of prevalence of IE1-specific CTLs'. *Journal of Infectious Diseases*, 181 (5), pp. 1537-1546.

Hahn, G., Rose, D., Wagner, M., Rhiel, S. & McVoy, M. A. (2003) 'Cloning of the genomes of human cytomegalovirus strains Toledo, TownevarRIT3, and Towne long as BACs and site-directed mutagenesis using a PCR-based technique'. *Virology*, 307 (1), pp. 164-177.

Hampson, A. W. & Mackenzie, J. S. (2006) 'The influenza viruses'. *Medical Journal of Australia*, 185 (10), pp. S39.

Hansen, S. G., Ford, J. C., Lewis, M. S., Ventura, A. B., Hughes, C. M., Coyne-Johnson, L., Whizin, N., Oswald, K., Shoemaker, R. & Swanson, T. (2011) 'Profound early control of highly pathogenic SIV by an effector memory T-cell vaccine'. *Nature*, 473 (7348), pp. 523-527.

Hansen, S. G., Vieville, C., Whizin, N., Coyne-Johnson, L., Siess, D. C., Drummond, D. D., Legasse, A. W., Axthelm, M. K., Oswald, K. & Trubey, C. M. (2009) 'Effector memory T cell responses are associated with protection of rhesus monkeys from mucosal simian immunodeficiency virus challenge'. *Nature Medicine*, 15 (3), pp. 293-299.

Harrington, J. J., Van Bokkelen, G., Mays, R. W., Gustashaw, K. & Willard, H. F. (1997) 'Formation of de novo centromeres and construction of first-generation human artificial microchromosomes'. *Nature Genetics*, 15 (4), pp. 345-355.

Hashimoto, Y., Moki, T., Takizawa, T., Shiratsuchi, A. & Nakanishi, Y. (2007) 'Evidence for phagocytosis of influenza virus-infected, apoptotic cells by neutrophils and macrophages in mice'. *The Journal of Immunology*, 178 (4), pp. 2448-2457.

Heider, J. A., Bresnahan, W. A. & Shenk, T. E. (2002) 'Construction of a rationally designed human cytomegalovirus variant encoding a temperature-sensitive immediate-early 2 protein'. *Proceedings of the National Academy of Sciences*, 99 (5), pp. 3141-3146.

Herm-Götz, A., Agop-Nersesian, C., Münter, S., Grimley, J. S., Wandless, T. J., Frischknecht, F. & Meissner, M. (2007) 'Rapid control of protein level in the apicomplexan *Toxoplasma gondii*'. *Nature Methods*, 4 (12), pp. 1003-1005.

Hertel, L. & Mocarski, E. S. (2004) 'Global analysis of host cell gene expression late during cytomegalovirus infection reveals extensive dysregulation of cell cycle gene expression and induction of Pseudomitosis independent of US28 function'. *Journal of Virology*, 78 (21), pp. 11988-12011.

Heyer, W.-D. (2006) 'Biochemistry of eukaryotic homologous recombination', *Molecular Genetics of Recombination*. Springer, pp. 95-133.

Hirt, B. (1967) 'Selective extraction of polyoma DNA from infected mouse cell cultures'. *Journal of Molecular Biology*, 26 (2), pp. 365-369.

Holland, J., Spindler, K., Horodyski, F., Grabau, E., Nichol, S. & VandePol, S. (1982) 'Rapid evolution of RNA genomes'. *Science*, 215 (4540), pp. 1577-1585.

Holsinger, L. J., Nichani, D., Pinto, L. H. & Lamb, R. A. (1994) 'Influenza A virus M2 ion channel protein: a structure-function analysis'. *Journal of Virology*, 68 (3), pp. 1551-1563.

Horimoto, T. & Kawaoka, Y. (1994) 'Reverse genetics provides direct evidence for a correlation of hemagglutinin cleavability and virulence of an avian influenza A virus'. *Journal of Virology*, 68 (5), pp. 3120-3128.

Horsburgh, B., Hubinette, M., Qiang, D., MacDonald, M. & Tufaro, F. (1999) 'Allele replacement: an application that permits rapid manipulation of herpes simplex virus type 1 genomes'. *Gene Therapy*, 6 (5), pp. 922-930.

Huber, M. T. & Compton, T. (1998) 'The human cytomegalovirus UL74 gene encodes the third component of the glycoprotein H-glycoprotein L-containing envelope complex'. *Journal of Virology*, 72 (10), pp. 8191-8197.

Huber, M. T. & Compton, T. (1999) 'Intracellular formation and processing of the heterotrimeric gH-gL-gO (gCIII) glycoprotein envelope complex of human cytomegalovirus'. *Journal of Virology*, 73 (5), pp. 3886-3892.

Hunter, N. (2007) 'Meiotic recombination', *Molecular genetics of recombination*. Springer, pp. 381-442.

Irmiere, A. & Gibson, W. (1983) 'Isolation and characterization of a noninfectious virion-like particle released from cells infected with human strains of cytomegalovirus'. *Virology*, 130 (1), pp. 118-133.

Ish-Horowicz, D. & Burke, J. (1981) 'Rapid and efficient cosmid cloning'. *Nucleic Acids Research*, 9 (13), pp. 2989-2898.

Ito, T., Couceiro, J. N. S., Kelm, S., Baum, L. G., Krauss, S., Castrucci, M. R., Donatelli, I., Kida, H., Paulson, J. C. & Webster, R. G. (1998) 'Molecular basis for the generation in pigs of influenza A viruses with pandemic potential'. *Journal of Virology*, 72 (9), pp. 7367-7373.

Iwamoto, M., Björklund, T., Lundberg, C., Kirik, D. & Wandless, T. J. (2010) 'A general chemical method to regulate protein stability in the mammalian central nervous system'. *Chemistry & Biology*, 17 (9), pp. 981-988.

Jagger, B., Wise, H., Kash, J., Walters, K.-A., Wills, N., Xiao, Y.-L., Dunfee, R., Schwartzman, L., Ozinsky, A. & Bell, G. (2012) 'An overlapping protein-coding region in influenza A virus segment 3 modulates the host response'. *Science*, 337 (6091), pp. 199-204.

Jahn, G., Kouzarides, T., Mach, M., Scholl, B., Plachter, B., Traupe, B., Preddie, E., Satchwell, S., Fleckenstein, B. & Barrell, B. (1987) 'Map position and nucleotide sequence of the gene for the large structural phosphoprotein of human cytomegalovirus'. *Journal of Virology*, 61 (5), pp. 1358-1367.

Jameson, J., Cruz, J., Terajima, M. & Ennis, F. A. (1999) 'Human CD8+ and CD4+ T lymphocyte memory to influenza A viruses of swine and avian species'. *The Journal of Immunology*, 162 (12), pp. 7578-7583.

Jarvis, M. A., Hansen, S. G., Nelson, J. A., Picker, L. J. & Früh, K. (2013) 'Vaccine vectors using the unique biology and immunology of cytomegalovirus'. *Cytomegaloviruses: from molecular pathogenesis to intervention*, 2

Jarvis, M. A. & Nelson, J. A. (2007) 'Human cytomegalovirus tropism for endothelial cells: not all endothelial cells are created equal'. *Journal of Virology*, 81 (5), pp. 2095-2101.

Joffre, O. P., Segura, E., Savina, A. & Amigorena, S. (2012) 'Cross-presentation by dendritic cells'. *Nature Reviews Immunology*, 12 (8), pp. 557-569.

Jones, T. R. & Lee, S.-W. (2004) 'An acidic cluster of human cytomegalovirus UL99 tegument protein is required for trafficking and function'. *Journal of Virology*, 78 (3), pp. 1488-1502.

Jones, T. R. & Sun, L. (1997) 'Human cytomegalovirus US2 destabilizes major histocompatibility complex class I heavy chains'. *Journal of Virology*, 71 (4), pp. 2970-2979.

Kalejta, R. F. (2008) 'Tegument proteins of human cytomegalovirus'. *Microbiology and Molecular Biology Reviews*, 72 (2), pp. 249-265.

Kari, B. & Gehrz, R. (1992) 'A human cytomegalovirus glycoprotein complex designated gC-II is a major heparin-binding component of the envelope'. *Journal of Virology*, 66 (3), pp. 1761-1764.

Karrer, U., Wagner, M., Sierro, S., Oxenius, A., Hengel, H., Dumrese, T., Freigang, S., Koszinowski, U. H., Phillips, R. E. & Klenerman, P. (2004) 'Expansion of protective CD8+ T-cell responses driven by recombinant cytomegaloviruses'. *Journal of Virology*, 78 (5), pp. 2255-2264.

Karzon, D. T. (1996) 'Cytotoxic T cells in influenza immunity', *Seminars in Virology*. Elsevier, pp. 265-271.

Kashima, Y., Ikeda, M., Itoh, Y., Sakoda, Y., Nagata, T., Miyake, T., Soda, K., Ozaki, H., Nakayama, M. & Shibuya, H. (2009) 'Intranasal administration of a live non-pathogenic avian H5N1 influenza virus

from a virus library confers protective immunity against H5N1 highly pathogenic avian influenza virus infection in mice: comparison of formulations and administration routes of vaccines'. *Vaccine*, 27 (52), pp. 7402-7408.

Kasowski, E. J., Garten, R. J. & Bridges, C. B. (2011) 'Influenza pandemic epidemiologic and virologic diversity: reminding ourselves of the possibilities'. *Clinical Infectious Diseases*, 52 (suppl 1), pp. S44-S49.

Kern, E. R. (2006) 'Pivotal role of animal models in the development of new therapies for cytomegalovirus infections'. *Antiviral research*, 71 (2), pp. 164-171.

Kilbourne, E. D. (2006) 'Influenza pandemics of the 20th century'. *Emerging infectious diseases*, 12 (1), pp. 9.

Kilpatrick, B. A. & Huang, E.-S. (1977) 'Human cytomegalovirus genome: partial denaturation map and organization of genome sequences'. *Journal of Virology*, 24 (1), pp. 261-276.

Kim, H. M., Lee, Y.-W., Lee, K.-J., Kim, H. S., Cho, S. W., Van Rooijen, N., Guan, Y. & Seo, S. H. (2008) 'Alveolar macrophages are indispensable for controlling influenza viruses in lungs of pigs'. *Journal of Virology*, 82 (9), pp. 4265-4274.

Kim, K. S. & Carp, R. I. (1971) 'Growth of murine cytomegalovirus in various cell lines'. *Journal of Virology*, 7 (6), pp. 720-725.

Kim, U.-J., Shizuya, H., de Jong, P. J., Birren, B. & Simon, M. I. (1992) 'Stable propagation of cosmid sized human DNA inserts in an F factor based vector'. *Nucleic Acids Research*, 20 (5), pp. 1083-1085.

Klyushnenkova, E. N., Kouivaskaia, D. V., Parkins, C. J., Caposio, P., Botto, S., Alexander, R. B. & Jarvis, M. A. (2012) 'A cytomegalovirus-based vaccine expressing a single tumor-specific CD8+ T cell epitope delays tumor growth in a murine model of prostate cancer'. *Journal of Immunotherapy (Hagerstown, Md.: 1997)*, 35 (5), pp. 390.

Kobasa, D., Takada, A., Shinya, K., Hatta, M., Halfmann, P., Theriault, S., Suzuki, H., Nishimura, H., Mitamura, K. & Sugaya, N. (2004) 'Enhanced virulence of influenza A viruses with the haemagglutinin of the 1918 pandemic virus'. *Nature*, 431 (7009), pp. 703-707.

Kondo, K. & Mocarski, E. S. (1994) 'Cytomegalovirus latency and latency-specific transcription in hematopoietic progenitors'. *Scandinavian journal of infectious diseases. Supplementum*, 99 pp. 63-67.

Kovall, R. & Matthews, B. W. (1997) 'Toroidal structure of λ -exonuclease'. *Science*, 277 (5333), pp. 1824-1827.

Krause, J. C., Tumpey, T. M., Huffman, C. J., McGraw, P. A., Pearce, M. B., Tsibane, T., Hai, R., Basler, C. F. & Crowe, J. E. (2010) 'Naturally occurring human monoclonal antibodies neutralize both 1918 and 2009 pandemic influenza A (H1N1) viruses'. *Journal of Virology*, 84 (6), pp. 3127-3130.

Kreijtz, J., de Mutsert, G., Van Baalen, C., Fouchier, R., Osterhaus, A. & Rimmelzwaan, G. (2008) 'Cross-recognition of avian H5N1 influenza virus by human cytotoxic T-lymphocyte populations directed to human influenza A virus'. *Journal of Virology*, 82 (11), pp. 5161-5166.

Kreijtz, J., Fouchier, R. & Rimmelzwaan, G. (2011) 'Immune responses to influenza virus infection'. *Virus Research*, 162 (1), pp. 19-30.

Krmpotic, A., Bubic, I., Polic, B., Lucin, P. & Jonjic, S. (2003) 'Pathogenesis of murine cytomegalovirus infection'. *Microbes and Infection*, 5 (13), pp. 1263-1277.

Krug, R. M., Alonso-Caplen, F. V., Julkunen, I. & Katze, M. G. (1989) 'Expression and replication of the influenza virus genome', *The influenza Viruses*. Springer, pp. 89-152.

Kwon, J. S., Yoon, J., Kim, Y. J., Kang, K., Woo, S., Jung, D. I., Song, M. K., Kim, E. H., Kwon, H. i. & Choi, Y. K. (2014) 'Vaccinia - based influenza vaccine overcomes previously induced immunodominance hierarchy for heterosubtypic protection'. *European Journal of Immunology*,

La Gruta, N. L., Turner, S. J. & Doherty, P. C. (2004) 'Hierarchies in cytokine expression profiles for acute and resolving influenza virus-specific CD8+ T cell responses: correlation of cytokine profile and TCR avidity'. *The Journal of Immunology*, 172 (9), pp. 5553-5560.

Laemmli, U. (1970) 'Most commonly used discontinuous buffer system for SDS electrophoresis'. *Nature*, 227 pp. 680-685.

Lamb, R. A., Krug, R. & Knipe, D. (2001) 'Fields Virology'. *Fields virology*, 1

Lamb, R. A., Zebedee, S. L. & Richardson, C. D. (1985) 'Influenza virus M 2 protein is an integral membrane protein expressed on the infected-cell surface'. *Cell*, 40 (3), pp. 627-633.

LaMere, M. W., Lam, H.-T., Moquin, A., Haynes, L., Lund, F. E., Randall, T. D. & Kaminski, D. A. (2011a) 'Contributions of antinucleoprotein IgG to heterosubtypic immunity against influenza virus'. *The Journal of Immunology*, 186 (7), pp. 4331-4339.

LaMere, M. W., Moquin, A., Lee, F. E.-H., Misra, R. S., Blair, P. J., Haynes, L., Randall, T. D., Lund, F. E. & Kaminski, D. A. (2011b) 'Regulation of antinucleoprotein IgG by systemic vaccination and its effect on influenza virus clearance'. *Journal of Virology*, 85 (10), pp. 5027-5035.

Landini, M. P., Ripalti, A., Sra, K. & Pouletty, P. (1991) 'Human cytomegalovirus structural proteins: immune reaction against pp150 synthetic peptides'. *Journal of Clinical Microbiology*, 29 (9), pp. 1868-1872.

Lauring, A. S., Jones, J. O. & Andino, R. (2010) 'Rationalizing the development of live attenuated virus vaccines'. *Nature Biotechnology*, 28 (6), pp. 573-579.

Laver, W. & Valentine, R. (1969) 'Morphology of the isolated hemagglutinin and neuraminidase subunits of influenza virus'. *Virology*, 38 (1), pp. 105-119.

Lee, C.-W. & Saif, Y. M. (2009) 'Avian influenza virus'. *Comparative Immunology, Microbiology and Infectious Diseases*, 32 (4), pp. 301-310.

Lee, E.-C., Yu, D., De Velasco, J. M., Tessarollo, L., Swing, D. A., Court, D. L., Jenkins, N. A. & Copeland, N. G. (2001) 'A highly efficient Escherichia coli-based chromosome engineering system adapted for recombinogenic targeting and subcloning of BAC DNA'. *Genomics*, 73 (1), pp. 56-65.

Lee, Y.-T., Kim, K.-H., Ko, E.-J., Lee, Y.-N., Kim, M.-C., Kwon, Y.-M., Tang, Y., Cho, M.-K., Lee, Y.-J. & Kang, S.-M. (2014) 'New vaccines against influenza virus'. *Clinical and Experimental Vaccine Research*, 3 (1), pp. 12-28.

Lepesant, J.-A., Kunst, F., Lepesant-Kejzlarová, J. & Dedonder, R. (1972) 'Chromosomal location of mutations affecting sucrose metabolism in Bacillus subtilis Marburg'. *Molecular and General Genetics MGG*, 118 (2), pp. 135-160.

Leung, G. M. & Nicoll, A. (2010) 'Reflections on pandemic (H1N1) 2009 and the international response'. *PLoS Med*, 7 (10), pp. e1000346.

Li, H. & Cao, B. (2016) 'Pandemic and Avian Influenza A Viruses in Humans: Epidemiology, Virology, Clinical Characteristics, and Treatment Strategy'. *Clinics in Chest Medicine*,

Li, M. L., Rao, P. & Krug, R. M. (2001) 'The active sites of the influenza cap - dependent endonuclease are on different polymerase subunits'. *The EMBO journal*, 20 (8), pp. 2078-2086.

Liu, B. & Stinski, M. F. (1992) 'Human cytomegalovirus contains a tegument protein that enhances transcription from promoters with upstream ATF and AP-1 cis-acting elements'. *Journal of Virology*, 66 (7), pp. 4434-4444.

Liu, C., Eichelberger, M. C., Compans, R. W. & Air, G. M. (1995) 'Influenza type A virus neuraminidase does not play a role in viral entry, replication, assembly, or budding'. *Journal of Virology*, 69 (2), pp. 1099-1106.

Liu, J., Wu, B., Zhang, S., Tan, S., Sun, Y., Chen, Z., Qin, Y., Sun, M., Shi, G. & Wu, Y. (2013) 'Conserved epitopes dominate cross - CD8+ T - cell responses against influenza A H1N1 virus among Asian populations'. *European Journal of Immunology*, 43 (8), pp. 2055-2069.

Liu, M. A. (2010a) 'Gene-based vaccines: Recent developments'. *Current Opinion in Molecular Therapeutics*, 12 (1), pp. 86-93.

Liu, M. A. (2010b) 'Immunologic basis of vaccine vectors'. *Immunity*, 33 (4), pp. 504-515.

Lötzerich, M., Ruzsics, Z. & Koszinowski, U. H. (2006) 'Functional domains of murine cytomegalovirus nuclear egress protein M53/p38'. *Journal of Virology*, 80 (1), pp. 73-84.

Lu, X., Pinto, A. K., Kelly, A. M., Cho, K. S. & Hill, A. B. (2006) 'Murine cytomegalovirus interference with antigen presentation contributes to the inability of CD8 T cells to control virus in the salivary gland'. *Journal of Virology*, 80 (8), pp. 4200-4202.

Lund, J. M., Alexopoulou, L., Sato, A., Karow, M., Adams, N. C., Gale, N. W., Iwasaki, A. & Flavell, R. A. (2004) 'Recognition of single-stranded RNA viruses by Toll-like receptor 7'. *Proceedings of the National Academy of Sciences of the United States of America*, 101 (15), pp. 5598-5603.

Ma, W., Kahn, R. E. & Richt, J. A. (2009) 'The pig as a mixing vessel for influenza viruses: human and veterinary implications'. *Journal of Molecular and Genetic Medicine: an International Journal of Biomedical Research*, 3 (1), pp. 158.

Ma, Y., Galluzzi, L., Zitvogel, L. & Kroemer, G. (2013) 'Autophagy and cellular immune responses'. *Immunity*, 39 (2), pp. 211-227.

Mach, M., Kropff, B., Dal Monte, P. & Britt, W. (2000) 'Complex formation by human cytomegalovirus glycoproteins M (gpUL100) and N (gpUL73)'. *Journal of Virology*, 74 (24), pp. 11881-11892.

Mahony, T. J., McCarthy, F. M., Gravel, J. L., West, L. & Young, P. L. (2002) 'Construction and manipulation of an infectious clone of the bovine herpesvirus 1 genome maintained as a bacterial artificial chromosome'. *Journal of Virology*, 76 (13), pp. 6660-6668.

Manning, W. C. & Mocarski, E. S. (1988) 'Insertional mutagenesis of the murine cytomegalovirus genome: one prominent α gene (ie2) is dispensable for growth'. *Virology*, 167 (2), pp. 477-484.

Marzi, A., Murphy, A. A., Feldmann, F., Parkins, C. J., Haddock, E., Hanley, P. W., Emery, M. J., Engelmann, F., Messaoudi, I. & Feldmann, H. (2016) 'Cytomegalovirus-based vaccine expressing Ebola virus glycoprotein protects nonhuman primates from Ebola virus infection'. *Scientific Reports*, 6

- Matrosovich, M. N., Matrosovich, T. Y., Gray, T., Roberts, N. A. & Klenk, H.-D. (2004) 'Human and avian influenza viruses target different cell types in cultures of human airway epithelium'. *Proceedings of the National Academy of Sciences of the United States of America*, 101 (13), pp. 4620-4624.
- Matthews, D., Bolin, J., Burrige, J., Filman, D., Volz, K. W. & Kraut, J. (1985) 'Dihydrofolate reductase. The stereochemistry of inhibitor selectivity'. *Journal of Biological Chemistry*, 260 (1), pp. 392-399.
- McAuley, J. L., Hornung, F., Boyd, K. L., Smith, A. M., McKeon, R., Bennink, J., Yewdell, J. W. & McCullers, J. A. (2007) 'Expression of the 1918 influenza A virus PB1-F2 enhances the pathogenesis of viral and secondary bacterial pneumonia'. *Cell Host & Microbe*, 2 (4), pp. 240-249.
- McCormick, A. L. & Mocarski, E. S. (2015) 'The immunological underpinnings of vaccinations to prevent cytomegalovirus disease'. *Cellular & Molecular Immunology*, 12 (2), pp. 170-179.
- McElhaney, J. E., Xie, D., Hager, W. D., Barry, M. B., Wang, Y., Kleppinger, A., Ewen, C., Kane, K. P. & Bleackley, R. C. (2006) 'T cell responses are better correlates of vaccine protection in the elderly'. *The Journal of Immunology*, 176 (10), pp. 6333-6339.
- McGeoch, D. J., Cook, S., Dolan, A., Jamieson, F. E. & Telford, E. A. (1995) 'Molecular phylogeny and evolutionary timescale for the family of mammalian herpesviruses'. *Journal of Molecular Biology*, 247 (3), pp. 443-458.
- McGill, J., Heusel, J. W. & Legge, K. L. (2009) 'Innate immune control and regulation of influenza virus infections'. *Journal of Leukocyte Biology*, 86 (4), pp. 803-812.
- McGregor, A. & Schleiss, M. R. (2001) 'Molecular cloning of the guinea pig cytomegalovirus (GPCMV) genome as an infectious bacterial artificial chromosome (BAC) in Escherichia coli'. *Molecular Genetics and Metabolism*, 72 (1), pp. 15-26.
- McHardy, A. C. & Adams, B. (2009) 'The role of genomics in tracking the evolution of influenza A virus'. *PLoS Pathogens*, 5 (10), pp. e1000566.
- McMahon, T. P. & Anders, D. G. (2002) 'Interactions between human cytomegalovirus helicase-primase proteins'. *Virus Research*, 86 (1), pp. 39-52.
- McMichael, A. J., Gotch, F. M., Noble, G. R. & Beare, P. A. (1983) 'Cytotoxic T-cell immunity to influenza'. *New England Journal of Medicine*, 309 (1), pp. 13-17.
- Mead, D. A., Pey, N. K., Herrnstadt, C., Marcil, R. A. & Smith, L. M. (1991) 'A universal method for the direct cloning of PCR amplified nucleic acid'. *Nature Biotechnology*, 9 (7), pp. 657-663.

Medina, R. A., Manicassamy, B., Stertz, S., Seibert, C. W., Hai, R., Belshe, R. B., Frey, S. E., Basler, C. F., Palese, P. & García-Sastre, A. (2010) 'Pandemic 2009 H1N1 vaccine protects against 1918 Spanish influenza virus'. *Nature Communications*, 1 pp. 28.

Meseda, C. A., Schmeisser, F., Pedersen, R., Woerner, A. & Weir, J. P. (2004) 'DNA immunization with a herpes simplex virus 2 bacterial artificial chromosome'. *Virology*, 318 (1), pp. 420-428.

Messerle, M., Crnkovic, I., Hammerschmidt, W., Ziegler, H. & Koszinowski, U. H. (1997) 'Cloning and mutagenesis of a herpesvirus genome as an infectious bacterial artificial chromosome'. *Proceedings of the National Academy of Sciences*, 94 (26), pp. 14759-14763.

Messerle, M., Keil, G. M. & Koszinowski, U. H. (1991) 'Structure and expression of murine cytomegalovirus immediate-early gene 2'. *Journal of Virology*, 65 (3), pp. 1638-1643.

Meyer, H. H., Ripalti, A., Landini, M. P., Radsak, K., Kern, H. F. & Hensel, G. M. (1997) 'Human cytomegalovirus late-phase maturation is blocked by stably expressed UL32 antisense mRNA in astrocytoma cells'. *Journal of General Virology*, 78 (10), pp. 2621-2631.

Michaelis, M., Doerr, H. W. & Cinatl Jr, J. (2009) 'Novel swine-origin influenza A virus in humans: another pandemic knocking at the door'. *Medical Microbiology and Immunology*, 198 (3), pp. 175-183.

Min, J.-Y. & Krug, R. M. (2006) 'The primary function of RNA binding by the influenza A virus NS1 protein in infected cells: Inhibiting the 2' -5' oligo (A) synthetase/RNase L pathway'. *Proceedings of the National Academy of Sciences*, 103 (18), pp. 7100-7105.

Mitchell, D. B., Ruggli, N. & Tratschin, J.-D. (1992) 'An improved method for cloning PCR fragments'. *Genome Research*, 2 (1), pp. 81-82.

Mocarski, E., Shenk, T., Griffiths, P. & Pass, R. (2013) 'Cytomegaloviruses, p 1960–2014'. *Fields virology, 6th ed. Lippincott Williams & Wilkins, Philadelphia, PA*,

Mocarski, E. S. (2002) 'Immunomodulation by cytomegaloviruses: manipulative strategies beyond evasion'. *Trends in Microbiology*, 10 (7), pp. 332-339.

Mocarski, E. S., Kemble, G. W., Lyle, J. M. & Greaves, R. F. (1996) 'A deletion mutant in the human cytomegalovirus gene encoding IE1 (491aa) is replication defective due to a failure in autoregulation'. *Proceedings of the National Academy of Sciences*, 93 (21), pp. 11321-11326.

Mocarski, E. S., Post, L. E. & Roizman, B. (1980) 'Molecular engineering of the herpes simplex virus genome: insertion of a second LS junction into the genome causes additional genome inversions'. *Cell*, 22 (1), pp. 243-255.

Mohr, C. A., Arapovic, J., Mühlbach, H., Panzer, M., Weyn, A., Dölken, L., Krmptotic, A., Voehringer, D., Ruzsics, Z. & Koszinowski, U. (2010) 'A spread-deficient cytomegalovirus for assessment of first-target cells in vaccination'. *Journal of Virology*, 84 (15), pp. 7730-7742.

Momose, F., Basler, C. F., O'Neill, R. E., Iwamatsu, A., Palese, P. & Nagata, K. (2001) 'Cellular splicing factor RAF-2p48/NPI-5/BAT1/UAP56 interacts with the influenza virus nucleoprotein and enhances viral RNA synthesis'. *Journal of Virology*, 75 (4), pp. 1899-1908.

Monaco, A. P. & Larin, Z. (1994) 'YACs, BACs, PACs and MACs: artificial chromosomes as research tools'. *Trends in Biotechnology*, 12 (7), pp. 280-286.

Morello, C. S., Ye, M. & Spector, D. H. (2002) 'Development of a vaccine against murine cytomegalovirus (MCMV), consisting of plasmid DNA and formalin-inactivated MCMV, that provides long-term, complete protection against viral replication'. *Journal of Virology*, 76 (10), pp. 4822-4835.

Morens, D. M., Taubenberger, J. K. & Fauci, A. S. (2009) 'The persistent legacy of the 1918 influenza virus'. *New England Journal of Medicine*, 361 (3), pp. 225-229.

Morley, P. J., Ertl, P. & Sweet, C. (2002) 'Immunisation of Balb/c mice with severely attenuated murine cytomegalovirus mutants induces protective cellular and humoral immunity'. *Journal of Medical Virology*, 67 (2), pp. 187-199.

Morrison, L. A. & Knipe, D. M. (1996) 'Mechanisms of immunization with a replication-defective mutant of herpes simplex virus 1'. *Virology*, 220 (2), pp. 402-413.

Munks, M. W., Cho, K. S., Pinto, A. K., Siervo, S., Klenerman, P. & Hill, A. B. (2006) 'Four distinct patterns of memory CD8 T cell responses to chronic murine cytomegalovirus infection'. *The Journal of Immunology*, 177 (1), pp. 450-458.

Muralidharan, V., Oksman, A., Iwamoto, M., Wandless, T. J. & Goldberg, D. E. (2011) 'Asparagine repeat function in a Plasmodium falciparum protein assessed via a regulatable fluorescent affinity tag'. *Proceedings of the National Academy of Sciences*, 108 (11), pp. 4411-4416.

Murphy, E., Yu, D., Grimwood, J., Schmutz, J., Dickson, M., Jarvis, M. A., Hahn, G., Nelson, J. A., Myers, R. M. & Shenk, T. E. (2003) 'Coding potential of laboratory and clinical strains of human cytomegalovirus'. *Proceedings of the National Academy of Sciences*, 100 (25), pp. 14976-14981.

Muyrers, J. P., Zhang, Y., Buchholz, F. & Stewart, A. F. (2000) 'RecE/RecT and Red α /Red β initiate double-stranded break repair by specifically interacting with their respective partners'. *Genes & Development*, 14 (15), pp. 1971-1982.

Muyrers, J. P., Zhang, Y., Testa, G. & Stewart, A. F. (1999) 'Rapid modification of bacterial artificial chromosomes by ET-recombination'. *Nucleic Acids Research*, 27 (6), pp. 1555-1557.

Nagaike, K., Mori, Y., Gomi, Y., Yoshii, H., Takahashi, M., Wagner, M., Koszinowski, U. & Yamanishi, K. (2004) 'Cloning of the varicella-zoster virus genome as an infectious bacterial artificial chromosome in *Escherichia coli*'. *Vaccine*, 22 (29), pp. 4069-4074.

Nakagawa, Y., Oda, K. & Nakada, S. (1996) 'The PB1 subunit alone can catalyze cRNA synthesis, and the PA subunit in addition to the PB1 subunit is required for viral RNA synthesis in replication of the influenza virus genome'. *Journal of Virology*, 70 (9), pp. 6390-6394.

Nassetta, L., Kimberlin, D. & Whitley, R. (2009) 'Treatment of congenital cytomegalovirus infection: implications for future therapeutic strategies'. *Journal of Antimicrobial Chemotherapy*, 63 (5), pp. 862-867.

Neumann, G., Noda, T. & Kawaoka, Y. (2009) 'Emergence and pandemic potential of swine-origin H1N1 influenza virus'. *Nature*, 459 (7249), pp. 931-939.

Nguyen, L. H., Knipe, D. M. & Finberg, R. W. (1992) 'Replication-defective mutants of herpes simplex virus (HSV) induce cellular immunity and protect against lethal HSV infection'. *Journal of Virology*, 66 (12), pp. 7067-7072.

Noda, T. & Kawaoka, Y. (2010) 'Structure of influenza virus ribonucleoprotein complexes and their packaging into virions'. *Reviews in Medical Virology*, 20 (6), pp. 380-391.

O'Neill, R. E. & Palese, P. (1995) 'NPI-1, the human homolog of SRP-1, interacts with influenza virus nucleoprotein'. *Virology*, 206 (1), pp. 116-125.

Odeberg, J., Plachter, B., Brandén, L. & Söderberg-Nauclér, C. (2003) 'Human cytomegalovirus protein pp65 mediates accumulation of HLA-DR in lysosomes and destruction of the HLA-DR α -chain'. *Blood*, 101 (12), pp. 4870-4877.

Ogawa-Goto, K., Tanaka, K., Gibson, W., Moriishi, E., Miura, Y., Kurata, T., Irie, S. & Sata, T. (2003) 'Microtubule network facilitates nuclear targeting of human cytomegalovirus capsid'. *Journal of Virology*, 77 (15), pp. 8541-8547.

Oien, N. L., Thomsen, D. R., Wathen, M. W., Newcomb, W. W., Brown, J. C. & Homa, F. L. (1997) 'Assembly of herpes simplex virus capsids using the human cytomegalovirus scaffold protein: critical role of the C terminus'. *Journal of Virology*, 71 (2), pp. 1281-1291.

Osterhaus, A., Fouchier, R. & Rimmelzwaan, G. (2011) 'Towards universal influenza vaccines?'. *Philosophical Transactions of the Royal Society B: Biological Sciences*, 366 (1579), pp. 2766-2773.

Oxford, J. (2000) 'Influenza A pandemics of the 20th century with special reference to 1918: virology, pathology and epidemiology'. *Reviews in Medical Virology*, 10 (2), pp. 119-133.

Palese, P. & Shaw, M. L. (2007) 'Orthomyxoviridae: the viruses and their replication'. *Fields Virology*, 2 pp. 1647-1689.

Palese, P., Tobita, K., Ueda, M. & Compans, R. W. (1974) 'Characterization of temperature sensitive influenza virus mutants defective in neuraminidase'. *Virology*, 61 (2), pp. 397-410.

Pan, D., Xuan, B., Sun, Y., Huang, S., Xie, M., Bai, Y., Xu, W. & Qian, Z. (2016) 'An intein-mediated modulation of protein stability system and its application to study human cytomegalovirus essential gene function'. *Scientific Reports*, 6

Pang, I. K. & Iwasaki, A. (2011) 'Inflammasomes as mediators of immunity against influenza virus'. *Trends in Immunology*, 32 (1), pp. 34-41.

Pappas, C., Aguilar, P. V., Basler, C. F., Solórzano, A., Zeng, H., Perrone, L. A., Palese, P., García-Sastre, A., Katz, J. M. & Tumpey, T. M. (2008) 'Single gene reassortants identify a critical role for PB1, HA, and NA in the high virulence of the 1918 pandemic influenza virus'. *Proceedings of the National Academy of Sciences*, 105 (8), pp. 3064-3069.

Paragas, J., Talon, J., O'Neill, R. E., Anderson, D. K., García-Sastre, A. & Palese, P. (2001) 'Influenza B and C virus NEP (NS2) proteins possess nuclear export activities'. *Journal of Virology*, 75 (16), pp. 7375-7383.

Paredes, A. M. & Yu, D. (2012) 'Human cytomegalovirus: bacterial artificial chromosome (BAC) cloning and genetic manipulation'. *Current Protocols in Microbiology*, pp. 14E. 14.11-14E. 14.33.

Pass, R. (2001) 'Cytomegalovirus, p 2675–2706'. *Fields Virology, 4th ed. Lippincott Williams & Wilkins, Philadelphia, PA*,

Paterson, D. & Fodor, E. (2012) 'Emerging roles for the influenza A virus nuclear export protein (NEP)'. *PLoS Pathogens*, 8 (12), pp. e1003019.

Patrone, M., Percivalle, E., Secchi, M., Fiorina, L., Pedrali-Noy, G., Zoppe, M., Baldanti, F., Hahn, G., Koszinowski, U. H. & Milanesi, G. (2003) 'The human cytomegalovirus UL45 gene product is a late, virion-associated protein and influences virus growth at low multiplicities of infection'. *Journal of General Virology*, 84 (12), pp. 3359-3370.

Peiris, J., Tu, W. w. & Yen, H. I. (2009) 'A novel H1N1 virus causes the first pandemic of the 21st century'. *European Journal of Immunology*, 39 (11), pp. 2946-2954.

Peiris, J. M., De Jong, M. D. & Guan, Y. (2007) 'Avian influenza virus (H5N1): a threat to human health'. *Clinical Microbiology Reviews*, 20 (2), pp. 243-267.

Pellet, P. & Roizman, B. (2007) 'Fields Virology, eds Knipe DM, Howley PM'. [in Lippincott Williams and Wilkins, New York. (Accessed: Pellet, P. & Roizman, B.

Peng, L., Ryazantsev, S., Sun, R. & Zhou, Z. H. (2010) 'Three-dimensional visualization of gammaherpesvirus life cycle in host cells by electron tomography'. *Structure*, 18 (1), pp. 47-58.

Perng, Y.-C., Qian, Z., Fehr, A. R., Xuan, B. & Yu, D. (2011) 'The human cytomegalovirus gene UL79 is required for the accumulation of late viral transcripts'. *Journal of Virology*, 85 (10), pp. 4841-4852.

Phillips, S. L. & Bresnahan, W. A. (2012) 'The human cytomegalovirus (HCMV) tegument protein UL94 is essential for secondary envelopment of HCMV virions'. *Journal of Virology*, 86 (5), pp. 2523-2532.

Pittet, L. A., Hall-Stoodley, L., Rutkowski, M. R. & Harmsen, A. G. (2010) 'Influenza virus infection decreases tracheal mucociliary velocity and clearance of *Streptococcus pneumoniae*'. *American Journal of Respiratory Cell and Molecular Biology*, 42 (4), pp. 450-460.

Plachter, B., Sinzger, C. & Jahn, G. (1996) 'Cell types involved in replication and distribution of human cytomegalovirus'. *Advances in Virus Research*, 46 pp. 195-261.

Portela, A. n. & Digard, P. (2002) 'The influenza virus nucleoprotein: a multifunctional RNA-binding protein pivotal to virus replication'. *Journal of General Virology*, 83 (4), pp. 723-734.

Potter, C. & Oxford, J. (1979) 'Determinants of immunity to influenza infection in man'. *British Medical Bulletin*, 35 (1), pp. 69-75.

Price, G. E., Soboleski, M. R., Lo, C.-Y., Misplon, J. A., Quirion, M. R., Houser, K. V., Pearce, M. B., Pappas, C., Tumpey, T. M. & Epstein, S. L. (2010) 'Single-dose mucosal immunization with a candidate universal influenza vaccine provides rapid protection from virulent H5N1, H3N2 and H1N1 viruses'. *PLoS One*, 5 (10), pp. e13162.

Pyzik, M., Charbonneau, B., Gendron-Pontbriand, E.-M., Babić, M., Krmpotić, A., Jonjić, S. & Vidal, S. M. (2011) 'Distinct MHC class I-dependent NK cell-activating receptors control cytomegalovirus infection in different mouse strains'. *The Journal of Experimental Medicine*, 208 (5), pp. 1105-1117.

Qian, X., Chien, C., Lu, Y., Montelione, G. & Krug, R. (1995) 'An amino-terminal polypeptide fragment of the influenza virus NS1 protein possesses specific RNA-binding activity and largely helical backbone structure'. *Rna*, 1 (9), pp. 948.

Qian, Z., Leung-Pineda, V., Xuan, B., Piwnica-Worms, H. & Yu, D. (2010) 'Human cytomegalovirus protein pUL117 targets the mini-chromosome maintenance complex and suppresses cellular DNA synthesis'. *PLoS Pathog*, 6 (3), pp. e1000814.

Qiu, Y., Nemeroff, M. & Krug, R. M. (1995) 'The influenza virus NS1 protein binds to a specific region in human U6 snRNA and inhibits U6-U2 and U6-U4 snRNA interactions during splicing'. *Rna*, 1 (3), pp. 304-316.

Ramsay, M. (1994) 'Yeast artificial chromosome cloning'. *Molecular Biotechnology*, 1 (2), pp. 181-201.

Rawlinson, W. D., Farrell, H. E. & Barrell, B. G. (1996) 'Analysis of the complete DNA sequence of murine cytomegalovirus'. *Journal of Virology*, 70 (12), pp. 8833-8849.

Razuri, H., Romero, C., Tinoco, Y., Guezala, M. C., Ortiz, E., Silva, M., Reaves, E., Williams, M., Laguna-Torres, V. A. & Halsey, E. S. (2012) 'Population-based active surveillance cohort studies for influenza: lessons from Peru'. *Bulletin of the World Health Organization*, 90 (4), pp. 318-320.

Redwood, A. J., Harvey, N. L., Lloyd, M., Lawson, M. A., Hardy, C. M. & Shellam, G. R. (2007) 'Viral vectored immunocontraception: screening of multiple fertility antigens using murine cytomegalovirus as a vaccine vector'. *Vaccine*, 25 (4), pp. 698-708.

Redwood, A. J., Messerle, M., Harvey, N. L., Hardy, C. M., Koszinowski, U. H., Lawson, M. A. & Shellam, G. R. (2005) 'Use of a murine cytomegalovirus K181-derived bacterial artificial chromosome as a vaccine vector for immunocontraception'. *Journal of Virology*, 79 (5), pp. 2998-3008.

Regner, M., Pavlinovic, L., Koskinen, A., Young, N., Trapani, J. A. & Müllbacher, A. (2009) 'Cutting edge: rapid and efficient in vivo cytotoxicity by cytotoxic T cells is independent of granzymes A and B'. *The Journal of Immunology*, 183 (1), pp. 37-40.

Reed, Lowell Jacob, and Hugo Muench. "A simple method of estimating fifty per cent endpoints 1 2 ." *American Journal of Epidemiology* 27, no. 3 (1938): 493-497.

Richardson, J. & Akkina, R. (1991) 'NS2 protein of influenza virus is found in purified virus and phosphorylated in infected cells'. *Archives of Virology*, 116 (1-4), pp. 69-80.

Riddell, S. R., Rabin, M., Geballe, A. P., Britt, W. J. & Greenberg, P. D. (1991) 'Class I MHC-restricted cytotoxic T lymphocyte recognition of cells infected with human cytomegalovirus does not require endogenous viral gene expression'. *The Journal of Immunology*, 146 (8), pp. 2795-2804.

Robb, N. C., Smith, M., Vreede, F. T. & Fodor, E. (2009) 'NS2/NEP protein regulates transcription and replication of the influenza virus RNA genome'. *Journal of General Virology*, 90 (6), pp. 1398-1407.

Roberts, A. D., Ely, K. H. & Woodland, D. L. (2005) 'Differential contributions of central and effector memory T cells to recall responses'. *The Journal of Experimental Medicine*, 202 (1), pp. 123-133.

Roberts, K. L., Leser, G. P., Ma, C. & Lamb, R. A. (2013) 'The amphipathic helix of influenza A virus M2 protein is required for filamentous bud formation and scission of filamentous and spherical particles'. *Journal of Virology*, 87 (18), pp. 9973-9982.

- Roby, C. & Gibson, W. (1986) 'Characterization of phosphoproteins and protein kinase activity of virions, noninfectious enveloped particles, and dense bodies of human cytomegalovirus'. *Journal of Virology*, 59 (3), pp. 714-727.
- Roizman, B. & Pellett, P. (2001) 'The family Herpesviridae: a brief introduction'. *Fields Virology*, 2 pp. 2381-2397.
- Roizman, B. & Sears, A. (2001) 'Herpes simplex viruses and their replication'. *Fields Virology*, 2 pp. 2399-2459.
- Roose, K., Fiers, W. & Saelens, X. (2009) 'Pandemic preparedness: toward a universal influenza vaccine'. *Drug News Perspect*, 22 (2), pp. 80-92.
- Rossman, J. S. & Lamb, R. A. (2011) 'Influenza virus assembly and budding'. *Virology*, 411 (2), pp. 229-236.
- Rubin, B. K. (2014) 'Secretion properties, clearance, and therapy in airway disease'. *Translational Respiratory Medicine*, 2 (1), pp. 6.
- Rudolph, J., O'CALLAGHAN, D. & Osterrieder, N. (2002) 'Cloning of the Genomes of Equine Herpesvirus Type 1 (EHV - 1) Strains KyA and RaCL11 as Bacterial Artificial Chromosomes (BAC)'. *Journal of Veterinary Medicine, Series B*, 49 (1), pp. 31-36.
- Rupp, B., Ruzsics, Z., Sacher, T. & Koszinowski, U. H. (2005) 'Conditional cytomegalovirus replication in vitro and in vivo'. *Journal of Virology*, 79 (1), pp. 486-494.
- Russo, I., Oksman, A., Vaupel, B. & Goldberg, D. E. (2009) 'A calpain unique to alveolates is essential in Plasmodium falciparum and its knockdown reveals an involvement in pre-S-phase development'. *Proceedings of the National Academy of Sciences*, 106 (5), pp. 1554-1559.
- Ruzsics, Z. & Koszinowski, U. (2008) 'Mutagenesis of the cytomegalovirus genome', *Human Cytomegalovirus*. Springer, pp. 41-61.
- Ryckman, B. J., Jarvis, M. A., Drummond, D. D., Nelson, J. A. & Johnson, D. C. (2006) 'Human cytomegalovirus entry into epithelial and endothelial cells depends on genes UL128 to UL150 and occurs by endocytosis and low-pH fusion'. *Journal of Virology*, 80 (2), pp. 710-722.
- Sakaki, Y., Karu, A. E., Linn, S. & Echols, H. (1973) 'Purification and properties of the γ -protein specified by bacteriophage λ : an inhibitor of the host recBC recombination enzyme'. *Proceedings of the National Academy of Sciences*, 70 (8), pp. 2215-2219.

Salvatore, M., García-Sastre, A., Ruchala, P., Lehrer, R. I., Chang, T. & Klotman, M. E. (2007) ' β -defensin inhibits influenza virus replication by cell-mediated mechanism (s)'. *Journal of Infectious Diseases*, 196 (6), pp. 835-843.

Sambrook, J. & Russell, D. (2001) 'Molecular Cloning: A Laboratory Manual,(pp3. 17-3.32)'. [in Cold Spring Harbor: Cold Spring Harbor Laboratory Press. (Accessed:Sambrook, J. & Russell, D.

Samji, T. (2009) 'Influenza A: understanding the viral life cycle'. *The Yale Journal of Biology and Medicine*, 82 (4), pp. 153.

Sampaio, K. L., Cavignac, Y., Stierhof, Y.-D. & Sinzger, C. (2005) 'Human cytomegalovirus labeled with green fluorescent protein for live analysis of intracellular particle movements'. *Journal of Virology*, 79 (5), pp. 2754-2767.

Sanchez, V., Angeletti, P. C., Engler, J. & Britt, W. (1998) 'Localization of human cytomegalovirus structural proteins to the nuclear matrix of infected human fibroblasts'. *Journal of Virology*, 72 (4), pp. 3321-3329.

Sanchez, V., Greis, K. D., Sztul, E. & Britt, W. J. (2000) 'Accumulation of virion tegument and envelope proteins in a stable cytoplasmic compartment during human cytomegalovirus replication: characterization of a potential site of virus assembly'. *Journal of Virology*, 74 (2), pp. 975-986.

Sanchez, V., Sztul, E. & Britt, W. J. (2000) 'Human cytomegalovirus pp28 (UL99) localizes to a cytoplasmic compartment which overlaps the endoplasmic reticulum-Golgi-intermediate compartment'. *Journal of Virology*, 74 (8), pp. 3842-3851.

Sandbulte, M. R., Westgeest, K. B., Gao, J., Xu, X., Klimov, A. I., Russell, C. A., Burke, D. F., Smith, D. J., Fouchier, R. A. & Eichelberger, M. C. (2011) 'Discordant antigenic drift of neuraminidase and hemagglutinin in H1N1 and H3N2 influenza viruses'. *Proceedings of the National Academy of Sciences*, 108 (51), pp. 20748-20753.

Sanz-Ezquerro, J. J., De La Luna, S., Ortín, J. & Nieto, A. (1995) 'Individual expression of influenza virus PA protein induces degradation of coexpressed proteins'. *Journal of Virology*, 69 (4), pp. 2420-2426.

Schaffer, P. A., Aron, G. M., Biswal, N. & Benyesh-Melnick, M. (1973) 'Temperature-sensitive mutants of herpes simplex virus type 1: isolation, complementation and partial characterization'. *Virology*, 52 (1), pp. 57-71.

Schmolke, S., Kern, H. F., Drescher, P., Jahn, G. & Plachter, B. (1995) 'The dominant phosphoprotein pp65 (UL83) of human cytomegalovirus is dispensable for growth in cell culture'. *Journal of Virology*, 69 (10), pp. 5959-5968.

Schnell, J. R., Dyson, H. J. & Wright, P. E. (2004) 'Structure, dynamics, and catalytic function of dihydrofolate reductase'. *Annu. Rev. Biophys. Biomol. Struct.*, 33 pp. 119-140.

Schotsaert, M. & García-Sastre, A. (2014) 'Influenza vaccines: a moving interdisciplinary field'. *Viruses*, 6 (10), pp. 3809-3826.

Schumacher, D., Tischer, B. K., Fuchs, W. & Osterrieder, N. (2000) 'Reconstitution of Marek's disease virus serotype 1 (MDV-1) from DNA cloned as a bacterial artificial chromosome and characterization of a glycoprotein B-negative MDV-1 mutant'. *Journal of Virology*, 74 (23), pp. 11088-11098.

Sedarati, F. & Rosenthal, L. (1988) 'Isolation and Partial Characterization of Nucleocapsid Forms from Cells Infected with Human Cytomegalovirus Strains AD 169 and Towne'. *Intervirology*, 29 (2), pp. 86-100.

Selik, R. M., Chu, S. Y. & Ward, J. W. (1995) 'Trends in infectious diseases and cancers among persons dying of HIV infection in the United States from 1987 to 1992'. *Annals of Internal Medicine*, 123 (12), pp. 933-936.

Selinsky, C., Luke, C., Wloch, M., Geall, A., Hermanson, G., Kaslow, D. & Evans, T. (2005) 'A DNA-based vaccine for the prevention of human cytomegalovirus-associated diseases'. *Human Vaccines*, 1 (1), pp. 16-23.

Seo, J.-Y. & Britt, W. J. (2006) 'Sequence requirements for localization of human cytomegalovirus tegument protein pp28 to the virus assembly compartment and for assembly of infectious virus'. *Journal of Virology*, 80 (11), pp. 5611-5626.

Seo, J.-Y. & Britt, W. J. (2007) 'Cytoplasmic envelopment of human cytomegalovirus requires the postlocalization function of tegument protein pp28 within the assembly compartment'. *Journal of Virology*, 81 (12), pp. 6536-6547.

Shen, Y., Utama, B., Wang, J., Raveendran, M., Senthil, D., Waldman, W., Belcher, J., Vercellotti, G., Martin, D. & Mitchell, B. (2004) 'Human cytomegalovirus causes endothelial injury through the ataxia telangiectasia mutant and p53 DNA damage signaling pathways'. *Circulation Research*, 94 (10), pp. 1310-1317.

Shizuya, H., Birren, B., Kim, U.-J., Mancino, V., Slepak, T., Tachiiri, Y. & Simon, M. (1992) 'Cloning and stable maintenance of 300-kilobase-pair fragments of human DNA in *Escherichia coli* using an F-factor-based vector'. *Proceedings of the National Academy of Sciences*, 89 (18), pp. 8794-8797.

Silva, M. C., Yu, Q.-C., Enquist, L. & Shenk, T. (2003) 'Human cytomegalovirus UL99-encoded pp28 is required for the cytoplasmic envelopment of tegument-associated capsids'. *Journal of Virology*, 77 (19), pp. 10594-10605.

Sinzger, C., Kahl, M., Laib, K., Klingel, K., Rieger, P., Plachter, B. & Jahn, G. (2000) 'Tropism of human cytomegalovirus for endothelial cells is determined by a post-entry step dependent on efficient translocation to the nucleus'. *Journal of General Virology*, 81 (12), pp. 3021-3035.

Skenderi, F. & Jonjić, S. (2012) 'Viral vaccines and vectors—some lessons from cytomegaloviruses'. *Periodicum Biologorum*, 114 (2), pp. 201-210.

Slater, J., Borchers, K., Thackray, A. & Field, H. (1994) 'The trigeminal ganglion is a location for equine herpesvirus 1 latency and reactivation in the horse'. *Journal of General Virology*, 75 (8), pp. 2007-2016.

Smith, G. A. & Enquist, L. W. (1999) 'Construction and Transposon Mutagenesis in *Escherichia coli* of a Full-Length Infectious Clone of Pseudorabies Virus, an Alphaherpesvirus'. *Journal of Virology*, 73 (8), pp. 6405-6414.

Smith, G. J., Vijaykrishna, D., Bahl, J., Lycett, S. J., Worobey, M., Pybus, O. G., Ma, S. K., Cheung, C. L., Raghwani, J. & Bhatt, S. (2009) 'Origins and evolutionary genomics of the 2009 swine-origin H1N1 influenza A epidemic'. *Nature*, 459 (7250), pp. 1122-1125.

Smith, J. D. & de Harven, E. (1974) 'Herpes simplex virus and human cytomegalovirus replication in WI-38 cells II. An ultrastructural study of viral penetration'. *Journal of Virology*, 14 (4), pp. 945-956.

Smith, L., McWhorter, A., Masters, L., Shellam, G. & Redwood, A. (2008) 'Laboratory strains of murine cytomegalovirus are genetically similar to but phenotypically distinct from wild strains of virus'. *Journal of Virology*, 82 (13), pp. 6689-6696.

Smith, R. M., Kosuri, S. & Kerry, J. A. (2014) 'Role of human cytomegalovirus tegument proteins in virion assembly'. *Viruses*, 6 (2), pp. 582-605.

Snyder, C. M., Cho, K. S., Bonnett, E. L., Allan, J. E. & Hill, A. B. (2011) 'Sustained CD8+ T cell memory inflation after infection with a single-cycle cytomegalovirus'. *PLoS Pathogens*, 7 (10), pp. e1002295.

Söderberg - Naucér, C. (2006) 'Does cytomegalovirus play a causative role in the development of various inflammatory diseases and cancer?'. *Journal of Internal Medicine*, 259 (3), pp. 219-246.

Song, Y.-J. & Stinski, M. F. (2002) 'Effect of the human cytomegalovirus IE86 protein on expression of E2F-responsive genes: a DNA microarray analysis'. *Proceedings of the National Academy of Sciences*, 99 (5), pp. 2836-2841.

Soroceanu, L., Akhavan, A. & Cobbs, C. S. (2008) 'Platelet-derived growth factor- α receptor activation is required for human cytomegalovirus infection'. *Nature*, 455 (7211), pp. 391-395.

Spaete, R. R. & Mocarski, E. S. (1987) 'Insertion and deletion mutagenesis of the human cytomegalovirus genome'. *Proceedings of the National Academy of Sciences*, 84 (20), pp. 7213-7217.

Spaete, R. R., Perot, K., Scott, P. I., Nelson, J. A., Stinski, M. F. & Pachl, C. (1993) 'Coexpression of truncated human cytomegalovirus gH with the UL115 gene product or the truncated human fibroblast growth factor receptor results in transport of gH to the cell surface'. *Virology*, 193 (2), pp. 853-861.

Sridhar, S., Begom, S., Bermingham, A., Hoschler, K., Adamson, W., Carman, W., Bean, T., Barclay, W., Deeks, J. J. & Lalvani, A. (2013) 'Cellular immune correlates of protection against symptomatic pandemic influenza'. *Nature Medicine*, 19 (10), pp. 1305-1312.

Stanecková, Z. & Vareckova, E. (2010) 'Conserved epitopes of influenza A virus inducing protective immunity and their prospects for universal vaccine development'. *Virology*, 7 pp. 351.

Steel, J., Lowen, A. C., Wang, T. T., Yondola, M., Gao, Q., Haye, K., García-Sastre, A. & Palese, P. (2010) 'Influenza virus vaccine based on the conserved hemagglutinin stalk domain'. *MBio*, 1 (1), pp. e00018-00010.

Steen, R. L., Martins, S. B., Taskén, K. & Collas, P. (2000) 'Recruitment of protein phosphatase 1 to the nuclear envelope by A-kinase anchoring protein AKAP149 is a prerequisite for nuclear lamina assembly'. *The Journal of Cell Biology*, 150 (6), pp. 1251-1262.

Stern-Ginossar, N., Weisburd, B., Michalski, A., Le, V. T. K., Hein, M. Y., Huang, S.-X., Ma, M., Shen, B., Qian, S.-B. & Hengel, H. (2012) 'Decoding human cytomegalovirus'. *Science*, 338 (6110), pp. 1088-1093.

Streblow, D. N., Varnum, S. M., Smith, R. D. & Nelson, J. A. (2006) 'A proteomics analysis of human cytomegalovirus particles'. *Cytomegaloviruses: molecular biology and immunology*. Caister Academic Press, Wymondham, Norfolk, United Kingdom, pp. 91-110.

Strutt, T. M., McKinstry, K. K., Marshall, N. B., Vong, A. M., Dutton, R. W. & Swain, S. L. (2013) 'Multipronged CD4+ T - cell effector and memory responses cooperate to provide potent immunity against respiratory virus'. *Immunological Reviews*, 255 (1), pp. 149-164.

Subbarao, K., Murphy, B. R. & Fauci, A. S. (2006) 'Development of effective vaccines against pandemic influenza'. *Immunity*, 24 (1), pp. 5-9.

Suda, T., Kawano, M., Nogi, Y., Ohno, N., Akatsuka, T. & Matsui, M. (2011) 'The route of immunization with adenoviral vaccine influences the recruitment of cytotoxic T lymphocytes in the lung that provide potent protection from influenza A virus'. *Antiviral Research*, 91 (3), pp. 252-258.

Sun, P. D. (2003) 'Structure and function of natural-killer-cell receptors'. *Immunologic Research*, 27 (2), pp. 539-548.

Sweet, C. (1999) 'The pathogenicity of cytomegalovirus'. *FEMS Microbiology Reviews*, 23 (4), pp. 457-482.

Sweet, C., Ball, K., Morley, P. J., Guilfoyle, K. & Kirby, M. (2007) 'Mutations in the temperature - sensitive murine cytomegalovirus (MCMV) mutants tsm5 and tsm30: A study of genes involved in immune evasion, DNA packaging and processing, and DNA replication'. *Journal of Medical Virology*, 79 (3), pp. 285-299.

Sylwester, A. W., Mitchell, B. L., Edgar, J. B., Taormina, C., Pelte, C., Ruchti, F., Sleath, P. R., Grabstein, K. H., Hosken, N. A. & Kern, F. (2005) 'Broadly targeted human cytomegalovirus-specific CD4+ and CD8+ T cells dominate the memory compartments of exposed subjects'. *The Journal of Experimental Medicine*, 202 (5), pp. 673-685.

Tai, S. S., Niikura, M., Cheng, H. H., Kruger, J. M., Wise, A. G. & Maes, R. K. (2010) 'Complete genomic sequence and an infectious BAC clone of feline herpesvirus-1 (FHV-1)'. *Virology*, 401 (2), pp. 215-227.

Tamashiro, J. C. & Spector, D. H. (1986) 'Terminal structure and heterogeneity in human cytomegalovirus strain AD169'. *Journal of Virology*, 59 (3), pp. 591-604.

Tamura, S.-i. & Kurata, T. (2004) 'Defense mechanisms against influenza virus infection in the respiratory tract mucosa'. *Jpn J Infect Dis*, 57 (6), pp. 236-247.

Tandon, R. & Mocarski, E. S. (2008) 'Control of cytoplasmic maturation events by cytomegalovirus tegument protein pp150'. *Journal of Virology*, 82 (19), pp. 9433-9444.

Tandon, R. & Mocarski, E. S. (2011) 'Cytomegalovirus pUL96 is critical for the stability of pp150-associated nucleocapsids'. *Journal of Virology*, 85 (14), pp. 7129-7141.

Taubenberger, J. K. & Morens, D. M. (2010) 'Influenza: the once and future pandemic'. *Public Health Reports*, pp. 16-26.

Taubenberger, J. K. & Morens, D. M. (2013) 'Influenza viruses: breaking all the rules'. *MBio*, 4 (4), pp. e00365-00313.

Tierney, R., Nakai, T., Parkins, C. J., Caposio, P., Fairweather, N. F., Sesardic, D. & Jarvis, M. A. (2012) 'A single-dose cytomegalovirus-based vaccine encoding tetanus toxin fragment C induces sustained levels of protective tetanus toxin antibodies in mice'. *Vaccine*, 30 (20), pp. 3047-3052.

Tong, S., Li, Y., Rivaller, P., Conrardy, C., Castillo, D. A. A., Chen, L.-M., Recuenco, S., Ellison, J. A., Davis, C. T. & York, I. A. (2012) 'A distinct lineage of influenza A virus from bats'. *Proceedings of the National Academy of Sciences*, 109 (11), pp. 4269-4274.

Tong, S., Zhu, X., Li, Y., Shi, M., Zhang, J., Bourgeois, M. & Yang, H. 'Recuenco 457 S, Gomez J, Chen LM, Johnson A, Tao Y, Dreyfus C, Yu W, McBride R, Carney 458 PJ, Gilbert AT, Chang J, Guo Z, Davis CT, Paulson JC, Stevens J, Rupprecht CE, 459 Holmes EC, Wilson IA, Donis RO. 2013'. *New world bats harbor diverse influenza A*, 460

Tooze, J., Hollinshead, M., Reis, B., Radsak, K. & Kern, H. (1993) 'Progeny vaccinia and human cytomegalovirus particles utilize early endosomal cisternae for their envelopes'. *European Journal of Cell Biology*, 60 (1), pp. 163-178.

Topham, D., Tripp, R. & Doherty, P. (1997) 'CD8+ T cells clear influenza virus by perforin or Fas-dependent processes'. *The Journal of Immunology*, 159 (11), pp. 5197-5200.

Towbin, H., Staehelin, T. & Gordon, J. (1979) 'Electrophoretic transfer of proteins from polyacrylamide gels to nitrocellulose sheets: procedure and some applications'. *Proceedings of the National Academy of Sciences*, 76 (9), pp. 4350-4354.

Townsend, A. & Skehel, J. (1984) 'The influenza A virus nucleoprotein gene controls the induction of both subtype specific and cross-reactive cytotoxic T cells'. *The Journal of Experimental Medicine*, 160 (2), pp. 552-563.

Trapp, S., Osterrieder, N., Keil, G. M. & Beer, M. (2003) 'Mutagenesis of a bovine herpesvirus type 1 genome cloned as an infectious bacterial artificial chromosome: analysis of glycoprotein E and G double deletion mutants'. *Journal of General Virology*, 84 (2), pp. 301-306.

Trgovcich, J., Cebulla, C., Zimmerman, P. & Sedmak, D. D. (2006) 'Human cytomegalovirus protein pp71 disrupts major histocompatibility complex class I cell surface expression'. *Journal of Virology*, 80 (2), pp. 951-963.

Trus, B. L., Gibson, W., Cheng, N. & Steven, A. C. (1999) 'Capsid structure of simian cytomegalovirus from cryoelectron microscopy: evidence for tegument attachment sites'. *Journal of Virology*, 73 (3), pp. 2181-2192.

Trus, B. L., Heymann, J. B., Nealon, K., Cheng, N., Newcomb, W. W., Brown, J. C., Kedes, D. H. & Steven, A. C. (2001) 'Capsid structure of Kaposi's sarcoma-associated herpesvirus, a gammaherpesvirus, compared to those of an alphaherpesvirus, herpes simplex virus type 1, and a betaherpesvirus, cytomegalovirus'. *Journal of Virology*, 75 (6), pp. 2879-2890.

Tsuda, Y., Caposio, P., Parkins, C. J., Botto, S., Messaoudi, I., Cicin-Sain, L., Feldmann, H. & Jarvis, M. A. (2011) 'A replicating cytomegalovirus-based vaccine encoding a single Ebola virus nucleoprotein CTL epitope confers protection against Ebola virus'. *PLoS Negl Trop Dis*, 5 (8), pp. e1275.

Tsuda, Y., Parkins, C. J., Caposio, P., Feldmann, F., Botto, S., Ball, S., Messaoudi, I., Cicin-Sain, L., Feldmann, H. & Jarvis, M. A. (2015) 'A cytomegalovirus-based vaccine provides long-lasting protection against lethal Ebola virus challenge after a single dose'. *Vaccine*, 33 (19), pp. 2261-2266.

Turan, K., Mibayashi, M., Sugiyama, K., Saito, S., Numajiri, A. & Nagata, K. (2004) 'Nuclear MxA proteins form a complex with influenza virus NP and inhibit the transcription of the engineered influenza virus genome'. *Nucleic Acids Research*, 32 (2), pp. 643-652.

Ulmanen, I., Broni, B. A. & Krug, R. M. (1981) 'Role of two of the influenza virus core P proteins in recognizing cap 1 structures (m7GpppNm) on RNAs and in initiating viral RNA transcription'. *Proceedings of the National Academy of Sciences*, 78 (12), pp. 7355-7359.

van de Sandt, C. E., Kreijtz, J. H. & Rimmelzwaan, G. F. (2012) 'Evasion of influenza A viruses from innate and adaptive immune responses'. *Viruses*, 4 (9), pp. 1438-1476.

Van Zijl, M., Quint, W., Briaire, J., De Rover, T., Gielkens, A. & Berns, A. (1988) 'Regeneration of herpesviruses from molecularly cloned subgenomic fragments'. *Journal of Virology*, 62 (6), pp. 2191-2195.

Varnum, S., Streblow, D., Monroe, M., Smith, P., Auberry, K., Pasa-Tolic, L. & Wang, D. (2004) 'Camp 2nd, DG, Rodland, K'. *Wiley S, Britt W, Shenk T, Smith RD, Nelson JA. Identification of proteins in human cytomegalovirus (HCMV) particles: the HCMV proteome. J Virol*, 78 (20), pp. 10960-10966.

Vink, C., Beuken, E. & Bruggeman, C. A. (1996) 'Structure of the rat cytomegalovirus genome termini'. *Journal of Virology*, 70 (8), pp. 5221-5229.

Virelizier, J.-L. (1975) 'Host defenses against influenza virus: the role of anti-hemagglutinin antibody'. *The Journal of Immunology*, 115 (2), pp. 434-439.

Wagner, M., Jonjić, S., Koszinowski, U. H. & Messerle, M. (1999) 'Systematic excision of vector sequences from the BAC-cloned herpesvirus genome during virus reconstitution'. *Journal of Virology*, 73 (8), pp. 7056-7060.

Wagner, M. & Koszinowski, U. H. (2004) 'Mutagenesis of viral BACs with linear PCR fragments (ET recombination)'. *Bacterial Artificial Chromosomes: Volume 2 Functional Studies*, pp. 257-268.

Wagner, M., Ruzsics, Z. & Koszinowski, U. H. (2002) 'Herpesvirus genetics has come of age'. *Trends in Microbiology*, 10 (7), pp. 318-324.

Wallace, P. R., Janet, W. H., Samuel, W., Horace, C. T. & Robert, J. H. (1956) 'Cytopathogenic agent resembling human salivary gland virus recovered from tissue cultures of human adenoids'. *Proceedings of the Society for Experimental Biology and Medicine*, 92 (2), pp. 418-424.

Wang, M., Lamberth, K., Harndahl, M., Røder, G., Stryhn, A., Larsen, M. V., Nielsen, M., Lundegaard, C., Tang, S. T. & Dziegiel, M. H. (2007) 'CTL epitopes for influenza A including the H5N1 bird flu; genome-, pathogen-, and HLA-wide screening'. *Vaccine*, 25 (15), pp. 2823-2831.

Wang, X., Basler, C. F., Williams, B. R., Silverman, R. H., Palese, P. & García-Sastre, A. (2002) 'Functional replacement of the carboxy-terminal two-thirds of the influenza A virus NS1 protein with short heterologous dimerization domains'. *Journal of Virology*, 76 (24), pp. 12951-12962.

Wang, X., Huang, D. Y., Huong, S.-M. & Huang, E.-S. (2005) 'Integrin $\alpha\beta 3$ is a coreceptor for human cytomegalovirus'. *Nature Medicine*, 11 (5), pp. 515-521.

Warden, C., Tang, Q. & Zhu, H. (2010) 'Herpesvirus BACs: past, present, and future'. *BioMed Research International*, 2011

Waring, P. & Müllbacher, A. (1999) 'Cell death induced by the Fas/Fas ligand pathway and its role in pathology'. *Immunology and Cell Biology*, 77 (4), pp. 312-317.

Warming, S., Costantino, N., Jenkins, N. A. & Copeland, N. G. (2005) 'Simple and highly efficient BAC recombineering using galk selection'. *Nucleic Acids Research*, 33 (4), pp. e36-e36.

Webster, R. & Laver, W. (1967) 'Preparation and properties of antibody directed specifically against the neuraminidase of influenza virus'. *The Journal of Immunology*, 99 (1), pp. 49-55.

Webster, R. G. (1998) 'Influenza: an emerging disease'. *Emerging Infectious Diseases*, 4 (3), pp. 436.

Webster, R. G., Bean, W. J., Gorman, O. T., Chambers, T. M. & Kawaoka, Y. (1992) 'Evolution and ecology of influenza A viruses'. *Microbiological Reviews*, 56 (1), pp. 152-179.

White, R. E., Calderwood, M. A. & Whitehouse, A. (2003) 'Generation and precise modification of a herpesvirus saimiri bacterial artificial chromosome demonstrates that the terminal repeats are required for both virus production and episomal persistence'. *Journal of General Virology*, 84 (12), pp. 3393-3403.

Whitley, R. J., Kimberlin, D. W. & Roizman, B. (1998) 'Herpes simplex viruses'. *Clinical Infectious Diseases*, pp. 541-553.

Wiertz, E. J., Jones, T. R., Sun, L., Bogyo, M., Geuze, H. J. & Ploegh, H. L. (1996) 'The human cytomegalovirus US11 gene product dislocates MHC class I heavy chains from the endoplasmic reticulum to the cytosol'. *Cell*, 84 (5), pp. 769-779.

Wilkinson, D. & Weller, S. (2003) 'The role of DNA recombination in herpes simplex virus DNA replication'. *IUBMB Life*, 55 (8), pp. 451-458.

Wilkinson, T. M., Li, C. K., Chui, C. S., Huang, A. K., Perkins, M., Liebner, J. C., Lambkin-Williams, R., Gilbert, A., Oxford, J. & Nicholas, B. (2012) 'Preexisting influenza-specific CD4+ T cells correlate with disease protection against influenza challenge in humans'. *Nature Medicine*, 18 (2), pp. 274-280.

Wing, B. A. & Huang, E.-S. (1995) 'Analysis and mapping of a family of 3'-coterminal transcripts containing coding sequences for human cytomegalovirus open reading frames UL93 through UL99'. *Journal of Virology*, 69 (3), pp. 1521-1531.

Wing, B. A., Lee, G. & Huang, E.-S. (1996) 'The human cytomegalovirus UL94 open reading frame encodes a conserved herpesvirus capsid/tegument-associated virion protein that is expressed with true late kinetics'. *Journal of Virology*, 70 (6), pp. 3339-3345.

Wise, H. M., Foeglein, A., Sun, J., Dalton, R. M., Patel, S., Howard, W., Anderson, E. C., Barclay, W. S. & Digard, P. (2009) 'A complicated message: Identification of a novel PB1-related protein translated from influenza A virus segment 2 mRNA'. *Journal of Virology*, 83 (16), pp. 8021-8031.

Wise, H. M., Hutchinson, E. C., Jagger, B. W., Stuart, A. D., Kang, Z. H., Robb, N., Schwartzman, L. M., Kash, J. C., Fodor, E. & Firth, A. E. (2012) 'Identification of a novel splice variant form of the influenza A virus M2 ion channel with an antigenically distinct ectodomain'. *PLoS Pathog*, 8 (11), pp. e1002998.

Wood, L. J., Baxter, M. K., Plafker, S. M. & Gibson, W. (1997) 'Human cytomegalovirus capsid assembly protein precursor (pUL80. 5) interacts with itself and with the major capsid protein (pUL86) through two different domains'. *Journal of Virology*, 71 (1), pp. 179-190.

Wright, J. F., Kurosky, A., Pryzdial, E. & Wasi, S. (1995) 'Host cellular annexin II is associated with cytomegalovirus particles isolated from cultured human fibroblasts'. *Journal of Virology*, 69 (8), pp. 4784-4791.

Wu, W. W., Sun, Y.-H. B. & Panté, N. (2007) 'Nuclear import of influenza A viral ribonucleoprotein complexes is mediated by two nuclear localization sequences on viral nucleoprotein'. *Virology Journal*, 4 (1), pp. 1.

Wu, Z., Xing, X., Bohl, C. E., Wisler, J. W., Dalton, J. T. & Bell, C. E. (2006) 'Domain structure and DNA binding regions of β protein from bacteriophage λ '. *Journal of Biological Chemistry*, 281 (35), pp. 25205-25214.

Xu, R., Ekiert, D. C., Krause, J. C., Hai, R., Crowe, J. E. & Wilson, I. A. (2010) 'Structural basis of preexisting immunity to the 2009 H1N1 pandemic influenza virus'. *Science*, 328 (5976), pp. 357-360.

Ye, M., Morello, C. S. & Spector, D. H. (2002) 'Strong CD8 T-cell responses following coimmunization with plasmids expressing the dominant pp89 and subdominant M84 antigens of murine cytomegalovirus correlate with long-term protection against subsequent viral challenge'. *Journal of Virology*, 76 (5), pp. 2100-2112.

Ye, Z., Pal, R., Fox, J. & Wagner, R. R. (1987) 'Functional and antigenic domains of the matrix (M1) protein of influenza A virus'. *Journal of Virology*, 61 (2), pp. 239-246.

Yewdell, J. W. (2006) 'Confronting complexity: real-world immunodominance in antiviral CD8+ T cell responses'. *Immunity*, 25 (4), pp. 533-543.

Yewdell, J. W., Bennink, J. R., Smith, G. L. & Moss, B. (1985) 'Influenza A virus nucleoprotein is a major target antigen for cross-reactive anti-influenza A virus cytotoxic T lymphocytes'. *Proceedings of the National Academy of Sciences*, 82 (6), pp. 1785-1789.

Young, L. S. & Murray, P. G. (2003) 'Epstein–Barr virus and oncogenesis: from latent genes to tumours'. *Oncogene*, 22 (33), pp. 5108-5121.

Yu, D., Ellis, H. M., Lee, E.-C., Jenkins, N. A. & Copeland, N. G. (2000) 'An efficient recombination system for chromosome engineering in *Escherichia coli*'. *Proceedings of the National Academy of Sciences*, 97 (11), pp. 5978-5983.

Yu, D., Silva, M. C. & Shenk, T. (2003) 'Functional map of human cytomegalovirus AD169 defined by global mutational analysis'. *Proceedings of the National Academy of Sciences*, 100 (21), pp. 12396-12401.

Yu, X., Shah, S., Lee, M., Dai, W., Lo, P., Britt, W., Zhu, H., Liu, F. & Zhou, Z. H. (2011) 'Biochemical and structural characterization of the capsid-bound tegument proteins of human cytomegalovirus'. *Journal of Structural Biology*, 174 (3), pp. 451-460.

Yuen, K., Chan, P., Peiris, M., Tsang, D., Que, T., Shortridge, K., Cheung, P., To, W., Ho, E. & Sung, R. (1998) 'Clinical features and rapid viral diagnosis of human disease associated with avian influenza A H5N1 virus'. *The Lancet*, 351 (9101), pp. 467-471.

Zambon, M. C. (1999) 'Epidemiology and pathogenesis of influenza'. *Journal of Antimicrobial Chemotherapy*, 44 (suppl 2), pp. 3-9.

Zhang, W., Hirve, S. & Kieny, M.-P. (2017) 'Seasonal vaccines—Critical path to pandemic influenza response'. *Vaccine*,

Zhang, Y., Buchholz, F., Muyrers, J. P. & Stewart, A. F. (1998) 'A new logic for DNA engineering using recombination in *Escherichia coli*'. *Nature Genetics*, 20 (2), pp. 123-128.

Zhong, W., Liu, F., Dong, L., Lu, X., Hancock, K., Reinherz, E. L., Katz, J. M. & Sambhara, S. (2010) 'Significant impact of sequence variations in the nucleoprotein on CD8 T cell-mediated cross-protection against influenza A virus infections'. *PLoS One*, 5 (5), pp. e10583.

Zhou, F.-C., Zhang, Y.-J., Deng, J.-H., Wang, X.-P., Pan, H.-Y., Hettler, E. & Gao, S.-J. (2002) 'Efficient infection by a recombinant Kaposi's sarcoma-associated herpesvirus cloned in a bacterial artificial chromosome: application for genetic analysis'. *Journal of Virology*, 76 (12), pp. 6185-6196.

Zhu, H., Cong, J.-P., Mamtora, G., Gingeras, T. & Shenk, T. (1998) 'Cellular gene expression altered by human cytomegalovirus: global monitoring with oligonucleotide arrays'. *Proceedings of the National Academy of Sciences*, 95 (24), pp. 14470-14475.

Zipeto, D., Baldanti, F., Percivalle, E., Gerna, G. & Milanesi, G. (1993) 'Identification of a human cytomegalovirus mutant in the pp150 matrix phosphoprotein gene with a growth-defective phenotype'. *Journal of General Virology*, 74 (8), pp. 1645-1648.